Employing an insect Sf9 cell model system of the fall armyworm, Spodoptera frugiperda, to investigate the role of transcription factors on the expression of detoxification genes in response to xenobiotics

Dries Amezian

▶ **To cite this version:**

Dries Amezian. Employing an insect Sf9 cell model system of the fall armyworm, Spodoptera frugiperda, to investigate the role of transcription factors on the expression of detoxification genes in response to xenobiotics. Molecular biology. Université Côte d'Azur, 2022. English. ⟨NNT : 2022COAZ6000⟩. ⟨tel-03847877⟩

HAL Id: tel-03847877

https://theses.hal.science/tel-03847877v1

Submitted on 10 Nov 2022

HAL is a multi-disciplinary open access archive for the deposit and dissemination of scientific research documents, whether they are published or not. The documents may come from teaching and research institutions in France or abroad, or from public or private research centers.

L'archive ouverte pluridisciplinaire **HAL**, est destinée au dépôt et à la diffusion de documents scientifiques de niveau recherche, publiés ou non, émanant des établissements d'enseignement et de recherche français ou étrangers, des laboratoires publics ou privés.

HAL Authorization

UNIVERSITÉ CÔTE D'AZUR

ÉCOLE DOCTORALE
SCIENCES DE LA VIE ET DE LA SANTÉ

THÈSE DE DOCTORAT

Utilisation du modèle cellulaire de la légionnaire d'automne, *Spodoptera frugiperda*, les cellules Sf9 pour étudier le rôle de facteurs de transcription sur l'expression des gènes de détoxification en réponse aux xénobiotiques

Dries AMEZIAN

Institut Sophia-Agrobiotech, UMR INRAE 1355, CNRS 7254, Université Côte d'Azur
Equipe « **Insect Defense** »

Présentée en vue de l'obtention du grade de docteur en
Interactions moléculaires et cellulaires
d'Université Côte d'Azur
Dirigée par :
Gaëlle LE GOFF et Ralf NAUEN
Soutenue le : 20/01/2022

Devant le jury, composé de :
Christine COUSTAU, DR CNRS, ISA, Présidente du Jury
Philip BATTERHAM, Professeur émérite, Université de Melbourne, Rapporteur
Jean-Philippe DAVID, CR CNRS, LECA, Rapporteur
Thomas VAN LEEUWEN, Professeur, Université de Gand, Examinateur
Ralf NAUEN, Distinguished Science Fellow, Bayer AG, Directeur de thèse
Gaëlle LE GOFF, CR INRAE, ISA, Directrice de thèse

BAYER

ANRT
ASSOCIATION NATIONALE RECHERCHE TECHNOLOGIE

Utilisation du modèle cellulaire de la légionnaire d'automne, *Spodoptera frugiperda*, les cellules Sf9 pour étudier le rôle de facteurs de transcription sur l'expression des gènes de détoxification en réponse aux xénobiotiques

Employing an insect Sf9 cell model system of the fall armyworm, *Spodoptera frugiperda*, to investigate the role of transcription factors on the expression of detoxification genes in response to xenobiotics

Jury :

Présidente du Jury

Christine COUSTAU, DR CNRS, Institut Sophia-Agrobiotech (ISA)

Rapporteurs

Philip BATTERHAM, Professeur émérite, Université de Melbourne
Jean-Philippe DAVID, CR CNRS, Laboratoire d'Écologie Alpine (LECA)

Examinateur
Thomas VAN LEEUWEN, Professeur, Université de Gand

Résumé

La légionnaire d'automne, *Spodoptera frugiperda* (Lepidoptera: Noctuidae), est un ravageur polyphage qui se nourrit de nombreuses plantes hôtes, dont des cultures importantes comme le maïs, le riz et le sorgho. Ce ravageur est responsable chaque année de milliards de dollars de pertes agricoles et n'a envahi que récemment l'hémisphère oriental, dont l'Asie. La lutte contre cet insecte se base principalement sur l'utilisation d'insecticides ce qui a entrainé l'apparition de résistance à de nombreuses classes chimiques d'insecticides. *S. frugiperda* a développé des mécanismes sophistiqués d'adaptation pour éliminer les composés toxiques (toxines de plantes ou insecticides) comme la surexpression et la duplication de gènes d'enzymes de détoxication. Souvent exprimées à un niveau basal, ces enzymes sont induites quand l'insecte est exposé à un xénobiotique. Si ces dernières sont bien connues chez plusieurs insectes ravageurs, les facteurs de transcription impliqués dans le contrôle de leur expression restent largement inexplorés. Le but de ma thèse a été de déterminer le rôle du facteur de transcription Cap'n'collar isoforme C (CncC) et musculoaponeurotic fibrosarcoma (Maf) dans l'adaptation de *S. frugiperda* aux xénobiotiques en utilisant le modèle cellulaire Sf9. J'ai montré que CncC et plusieurs gènes de détoxication sont induits par l'indole 3-carbinol (I3C), un glucosynolate présent dans les Brassicaceae comme le chou et le brocoli, et le méthoprène (Mtp), un insecticide qui imite l'hormone juvénile (JH). J'ai montré que la surexpression transitoire de CncC en cellules Sf9 est suivie d'une surexpression de certains de ces mêmes gènes de détoxication. Afin de caractériser le rôle des facteurs de transcription dans cette réponse j'ai établi deux types de lignées cellulaires transformées de manière stable. Le premier surexprime (OE) CncC, Maf ou les deux gènes et le second a été muté pour CncC (Knock-Out, KO) en utilisant la technique du CRISPR/Cas9. J'ai réalisé des tests de viabilité (MTT) et utilisé des sondes moléculaires en High Content Screening (HCS) pour tester si la modification de la voie de CncC:Maf affectait la capacité des cellules à faire face au stress toxique. Les lignées OE étaient plus tolérantes à l'I3C et au Mtp que le contrôle, tandis que les lignées KO étaient plus sensibles à ces composés. Les activités d'enzymes de détoxication, les carboxylesterases (CE) et les glutathion S-transférases (GST), à l'égard de substrats modèles étaient accrues dans les lignées OE, alors qu'elles étaient diminuées dans les lignées KO. Des études récentes ont montré que l'activation de la voie de CncC:Maf est médiée par la production d'espèces réactives de l'oxygène (ROS) lors d'un stress toxique. J'ai donc mesuré la production de ROS dans les cellules Sf9 traitées avec l'I3C et le Mtp. Les deux composés ont déclenché des pulses de ROS bien qu'à des niveaux limités dans les lignées OE, contrairement aux lignées KO pour lesquelles les niveaux de ROS étaient plus importants. L'utilisation d'un antioxydant a annulé les pulses de ROS et restauré la tolérance des cellules KO à l'I3C et au Mtp. Enfin, j'ai comparé les gènes différentiellement exprimés dans les lignées OE et KO lors une analyse transcriptomique (RNA-seq). Ceci m'a permis d'identifier les gènes potentiellement contrôlés par CncC et Maf, la plupart d'entre eux étant des gènes de détoxication dont le rôle dans la résistance aux insecticides et la métabolisation de composés de plantes a été démontrée dans plusieurs études. En conclusion, je présente ici de nouvelles données suggérant que la voie de signalisation CncC:Maf joue un rôle central dans l'adaptation des FAW aux composés environnementaux toxiques et aux insecticides. Ces connaissances aident à mieux comprendre les voies d'expression des gènes de détoxication et peuvent être utiles à la conception de nouveaux moyens de lutte contre les insectes en interférant avec ces voies et l'expression des gènes de détoxication.

Mots clés : Cap'n'collar isoform C (CncC), détoxication, résistance, adaptation aux plantes, régulation génétique

Abstract

The fall armyworm (FAW), *Spodoptera frugiperda* (Lepidoptera: Noctuidae) is a polyphagous pest feeding on numerous host-plants including important crops such as maize, rice and sorghum. It is one of the world's most destructive pests which only recently invaded the eastern hemisphere incl. Asia. It provides exceptional economic damage in many crops across continents each year. Controlling this insect pest largely relies on the application of insecticides resulting in the development of resistance to many classes of synthetic insecticides. FAW has developed sophisticated adaptive mechanisms to eliminate xenobiotics (plant secondary metabolites and insecticides), among them, upregulation and duplication of genes expressing detoxification enzymes. They are often expressed at low basal level and induced when the insect is exposed to xenobiotics. While the role of these enzymes is well characterized in several pest insects, the transcription factors controlling their expression remain largely unexplored. The aim of my thesis was to determine the role of Cap'n'collar isoform C (CncC) and musculoaponeurotic fibrosarcoma (Maf) in *S. frugiperda* adaptation to xenobiotics employing an Sf9 cell model.

I used the cell model of *S. frugiperda*, the Sf9 cells and showed that CncC, Maf and several detoxification enzymes are induced after exposure to indole 3-carbinol (I3C), a glucosinolate found in Brassicaceae such as cabbage and broccoli, and methoprene (Mtp), a juvenile hormone (JH) mimic insecticide. I showed that transient overexpression of CncC and Maf in Sf9 cells was followed by overexpression of several detoxification genes. In order to characterize the role of these transcription factors in response to xenobiotics two types of stably transformed cell lines were established. The first cell lines overexpress CncC, Maf or both genes while the second were mutated for CncC (Knock-Out, KO) using the CRISPR/Cas9 technique. I performed cell viability assays (MTT) and used molecular probes in High Content Screening (HCS) to test whether the modification of the CncC:Maf pathway affected the ability of Sf9 cells to cope with toxic stress. The OE cell lines were more tolerant to I3C and Mtp than the control (wildtype Sf9 cell line), whereas the KO cell lines were more sensitive to these xenobiotics. The activities of some detoxification enzymes, carboxylesterases (CEs) and glutathione S-transferases (GSTs) toward model substrates were also increased in OE cell lines, whereas they were decreased in KO cell lines. Recent studies have suggested that activation of the CncC:Maf pathway is mediated by the production of reactive oxygen species (ROS) upon toxic stress. I therefore measured ROS production in Sf9 cells treated with I3C and Mtp. Both xenobiotics triggered in-cell ROS pulses although at limited levels in OE lines, unlike to KO lines for which ROS levels were more prominent. The use of an antioxidant suppressed the ROS pulses and restored tolerance of KO cells to I3C and Mtp. Finally, I compared the differentially expressed genes in the OE and KO cell lines in a transcriptomic analysis using RNA-seq. This allowed me to identify genes potentially controlled by CncC and Maf, most of them being detoxification genes with a role in insecticide resistance and metabolism of plant compounds as demonstrated in several studies. In conclusion, I present here new data in designed model Sf9 cell lines suggesting that the CncC:Maf signaling pathway plays a central role in FAW adaptation to toxic environmental compounds and insecticides. This knowledge helps to better understand pathways in detoxification gene expression and can be helpful to design next-generation insect control measures by interfering with these pathways and detoxification gene expression.

Keywords: Cap'n'collar isoform C (CncC), detoxification, resistance, plant adaptation, gene regulation

À mes parents.

Remerciements

Acknowledgements

Gaëlle. Je ne saurais te remercier dûment ici, ou alors il faudrait rajouter 100 pages à ce manuscrit. On peut dire que « ça a matché ». J'en prends pour preuve les longues heures (tout mis bout-à-bout) qu'on a passées à rire ensemble. J'en prends pour preuve les mails délirants (faudra penser à brûler les serveurs... ne montrons jamais ça à personne !). J'en prends pour preuve la liste longue comme le bras des surnoms que tu auras pu me donner. Tu as été une directrice de thèse formidable et je t'en suis infiniment reconnaissant. Merci.

Ralf. I want to thank you from the bottom of my heart for having accepted to endorse me and even more for having flawlessly supported me during these three years. I really enjoyed working and discussing science with you. I hope that we will have more occasions to collaborate in the future.

L'obtention d'une thèse n'est jamais gagnée d'avance, et on peut dire que sans l'engagement et la ténacité de certaines personnes, je n'aurais sûrement pas eu la chance de pouvoir réaliser ce projet. Je remercie donc avec beaucoup de force **Gaëlle Le Goff**, **Thibaut Malausa**, **Cécillia Multeau**, **Frédéric Top**, **David Rouquie** et toutes celles et ceux qui ont fait monts et merveilles pour lancer cette thèse.

I sincerely thank the members of my jury for accepting to evaluate my work: **Philip Batterham**, **Jean-Philippe David**, **Thomas Van Leeuwen** and **Christine Coustau**.

Je tiens également à remercier les membres de mon comité de thèse : **Thomas Van Leeuwen** et **John Vontas**. **Thomas** and **John**, I want to thank you for having made time for me, first during Resistance'19 at Rothamsted and then later on via conference call. It was a pleasure to meet you and your insight was precious to my work. Many thanks.

During this project I had the opportunity to talk with other researchers, colleagues located all over the world, who gave me valuable advice to solve the scientific problems I was facing. I am thinking here in particular of **Dr. Shane Denecke**, who pointed me towards the right directions with my CRISPR experiments. After contacting **Dr. Jarvis** for CRISPR vectors, **Dr. Hideaki Mabashi-Asazuma** took from his time to advise me with technical aspects of CRISPR/Cas9 editing in my project, many thanks indeed.

Je remercie du fond du cœur toutes les personnes qui se sont investies dans mes travaux de thèse, qui m'ont aidé à réaliser certaines manipes, qui m'ont apporté leurs compétences scientifiques et techniques. Je pense bien sûr à **Thierry Fricaux** (mon maître !!), **Georges De Sousa**, un énorme merci pour tout le temps que tu as passé avec moi, et celui que tu as consacré à mes expériences. **Roxane Pichot**, qui m'a été d'un grand soutien pour supporter la charge de travail. **Frank Maiwald**, many thanks for your huge input in my project.

Je remercie également les stagiaires qui m'ont précédé. Ceux qui ont eu pour sujet de stage ce qui est plus tard devenu mon sujet de thèse. Merci à **Nicolas Soubeyran**, avec qui j'étais

en stage en 2017 dans l'équipe ID, lui travaillant sur la voie de détoxication (CncC) et moi sur la voie de l'immunité des insectes. Merci à **Calypso Vacher-Chicane** et **Hannah Isadora-Huditz** pour avoir poursuivi ces travaux et m'avoir donné une base solide pour continuer ce sujet en thèse.

Merci également à **Frédérique Hilliou**, **Martine Da Rocha** et **Corrine Rancurel** pour le soutien en génomique et bio-informatique !! Je remercie **Aurélie Seasseau** et **Marc Magliano** du Plateau de Biochimie Analytique pour l'analyse de bande par spectrométrie de masse, pour leur disponibilité et leur gentillesse.

Enfin je remercie toutes celles et ceux qui m'ont apporté leur aide, prêté voire donné (GEORGE ENCORE MERCIIIIIII) du matériel.

Trois ans de thèse ne se résument pas qu'à la science (eh non, heureusement !). J'ai passé trois années idéales avec l'équipe ID. On a pris l'apéro. Je repense notamment à cette « petite sauterie IDyllique » à l'orée du bois près d'entomopolis (*larme à l'œil*). Que de bons moments passés en votre compagnie, **Christine**, **Maëlle**, **Fred**, **Roxane** et bien sûr les deux autres loustics, lascards, trublions, bougres et j'en passe : **Thierry** et **Olivier**. Messieurs, je vais vous manquer je le sais. Vous faîtes les durs mais je vous vois déjà les yeux rouges alors que je suis à peine parti. Merci pour votre franche camaraderie ! On a vraiment bien ri. Quasi le seul étudiant permanent de l'équipe ID, j'ai quand même eu la chance et le grand plaisir de partager les paillasses du labo C314 avec deux (grands) complices de (petits) crimes : **Rakang** et **Hannah**. **Rakang** (what's uuuuuuuup) and **Hannah**, I am really grateful for sharing these months with you in the lab. You two are wonderful persons and I wish you both could have stayed longer. We could have started a band! Or anything else! "The triplets".

Un grand merci à tous mes amis de l'unité ! Ceux qui ont terminé leur thèse peu après que je sois arrivé : **Joffrey**, **Lucie**, **Danila**, **YongPan** et **Laïla**. Merci de m'avoir accueilli et intégré ☺ J'ai une belle pensée pour tous ceux de ma promotion : **Antoine**, **Yara**, **Salma**, **Rouba** et **Rahim**. On a trimé ensemble et ça créé des liens.

Enfin, last but not least, **Salomé** et **Mélina**, mes « gars sûres », mon squad agro à l'ISA ! Vous êtes incroyables toutes les deux, des amies loyales et attachantes. Merci de vous être occupé de moi ces dernières semaines, vous êtes super attentionnées et ça fait chaud au cœur ☺

Un grand merci à mes amis qui de loin m'ont soutenu : **Kevin**, **Martin**, **Gabriel** et tous les autres !

Valérie. Thank you for being there and being you.

Mon frère, **Omar**, ma sœur **Sofia**.

Mes **parents**. Je vous dois beaucoup. Je vous dois d'en être arrivé jusqu'ici. Merci merci merci merci merci !!

Contents

Résumé v
Abstract vi
Abbreviations xi
List of Tables xv
List of Figures xvi
General Introduction 17
CHAPTER 1 - Literature review 18
Part I – *Spodoptera frugiperda*, an invasive crop pest 18
1.1. Biology and ecology of FAW 19
1.2. FAW, a pest of cultured plants 20
1.3. Worldwide invasive pest status 20
1.4. Management strategies to control FAW 21
1.5. Resistance in *S. frugiperda* 25
1.6. Sf9 cells, the cellular model of *S. frugiperda* 27
Part II – Detoxification genes in *Spodoptera frugiperda* 28
2.1. The detoxification pathway 28
2.2. Responses of detoxification genes to xenobiotics in the *Spodoptera* genus 30
2.3. Gene expansion and detoxification capacity of *Spodoptera* species 52
Part III – Transcriptional regulation of detoxification genes in insects 55
3.1. The Keap1/CncC pathway 56
Objectives 65
CHAPTER 2 66
INTRODUCTION 66
MATERIALS & METHODS 68
Chemicals and products 68
Cells and cell culture 68
Cell viability assays 68
Transient overexpression of *CncC* and *Maf* transcription factors in Sf9 cells 69
RNA extractions, cDNA synthesis and RTqPCR 70
Statistical analyses 71
RESULTS 71
Toxicity of I3C and MTP on Sf9 cells 71
Selected detoxification genes are induced by I3C and MTP 72
CncC, *Maf* and *Keap1* are induced in Sf9 cells by I3C and MTP 72

Transient expression of *CncC* and *Maf* and their effect on detoxification genes 75
Discussion 77
CHAPTER 3 81
INTRODUCTION 81
MATERIALS & METHODS 82
Chemicals 82
Sf9 cells and cell culture 82
Stable overexpression of *CncC* and *Maf* transcription factors in Sf9 cells 82
Knock-Out of *CncC* and *Keap1* genes in Sf9 cells 84
RNA extractions, cDNA synthesis and RTqPCR 87
Cell viability assays 87
ROS measurements 88
Protein extractions and enzymatic activities 89
Statistical Analyses 90
RESULTS 91
Overexpression of *CncC* and *Maf* by a stable transformation of Sf9 cells 91
Stable overexpression of *CncC* and *Maf* genes increase Sf9 cells tolerance to xenobiotics 91
Knockout of *CncC* and *Keap1* using the CRISPR/Cas9 system 94
Viability assays with CRISPR/Cas9 mutated Sf9 cell lines 103
Enzymatic activity 104
The activation of the CncC:Maf pathway is modulated by ROS production 106
Effect of scavenging ROS on Sf9 transformants viability. 109
CHAPTER 4 119
INTRODUCTION 119
MATERIALS & METHODS 120
RNA extraction, library preparation and sequencing 120
RNA-seq transcriptomic analysis and differential expression 120
RESULTS 121
DISCUSSION 129
GENERAL DISCUSSION 139
Appendix A (Chapter 1 – Part II) 170
Appendix B (Chapter 2) 177
Appendix C (Chapter 3) 178
Appendix D (Chapter 4) 183
Appendix E - Result article 186
References 147

Abbreviations

20E	20-hydroxyecdysone
ABC	ATP-binding cassette
AC	Adenylate cyclase
AChE	Acetylcholinesterase
AhR	aryl hydrocarbon receptor
AITC	Allyl-isothiocyanate
ATI	Alternative translation initiation
approx.	Approximatively
ARE	Antioxidant response element
ARNT	AhR nuclear translocator
ATP	Adenosine-triphosphate
BDX	Benzoxazinoids
bHLH	basic helix–loop–helix
bp	Base pair
BSA	Bovine serum albumin
Bt	Bacillus thuringiensis
BTB	Broad-Complex, Tramtrack and Bric a brac
bZIP	basic leucine zipper
ca	Circa
CAR	Constitutive androstane receptor
Cas9	CRISPR associated protein 9
CAT	Catalase
CBP	CREB-binding protein
cDNA	Complementary deoxyribonucleic acid
CDNB	1-chloro-2,4-dinitrobenzene
CE/CCE	Carboxylesterase/carboxylcholineesterase
CHD6	chromo-ATPase/helicase DNA binding protein 6
CI	Confidence interval
CncC	Cap‘n’collar C isoform C
COE	Carboxylesterases
CPB	Colorado potato beetle
CPR	Cytochrome P450 reductase
CREB	cAMP-response element binding (protein)
CRISPR	Clustered Regularly Interspaced Short Palindromic Repeats
Cry	Crystalline
CUL3	Cullin3-based E3 ubiquitin ligase
CXE	Carboxylesterases
CYP	Cytochrome P450-dependent monooxygenase
DDT	Dichlorodiphenyltrichloroethane
DEG	Differentially expressed genes
DEM	Diethyl maleate
DGR	Double-glycine repeat
DIMBOA	2,4-dihydroxy-7-methoxy-1,4-benzoxazin-3-one
DIMBOA-glc	DIMBOA-glucosides
Dm	*Drosophila melanogaster*
DMSO	Dimethyl sulfoxide
DNA	Deoxyribonucleic acid
DPBS	Dulbecco’s Phosphate Buffered Saline
ds	Double stranded
DTT	Dithiothreitol
E	Esterase

e.g.	Exempli gratia
EB	Emamectin benzoate
EC	7-ethoxy coumarin
EcRE	Ecdysone response element
EDTA	Ethylenediaminetetraacetic acid
EF2	Elongation factor 2
EMSA	Electron mobility shift assays
EST	Expressed sequence tag
EU	European Union
FAO	Food and Agriculture Organization
FAW	Fall armyworm
FBS	Fetal bovine serum
Fig	Figure
g	Gram
x g	Relative centrifugation force (g-force)
GABA	Gamma-aminobutyric acid
GAPDH	Glyceraldehyde-3-phosphate dehydrogenase
GC-MS	Gas Chromatography-Mass spectrometry
gDNA	Genomic deoxyribonucleic acid
GluCl	Glutamate-gated chloride
GO	Gene Ontology
GPCR	G-protein coupled receptors (GPCRs)
GR	glucocorticoid receptor
Gs	G-protein subunit
GSH	Glutathione
GST	Glutathione S-transferase
h	Hour
HCS	High Content Screening
HO-1	Hemoxygenase-1
HPLC	High Performance Liquid Chromatography
HR96	hormone receptor-like in 96
HRD1	HMG-CoA reductase degradation protein 1
Hz	Hertz
I3C	Indole 3-carbinol
ICE	Inference of CRISPR Edits
i.e.	id est
IPM	Integrated Pest Management
IRAC	Insecticide Resistance Action Committee
IX	Insect XPRESS
JH	Juvenile hormone
JHA	Juvenile hormone analog
kdr	Knock-down resistance
Keap1	Kelch-like ECH associated protein 1
Kg	Kilogram
km	Kilometers
Km	Michaelis constant
KO	knockout
L	Liter
L10	Ribosomal Protein L10
L17	Ribosomal Protein L17
L18	Ribosomal Protein L18
LC	Lethal concentration
LDH	Lactate dehydrogenase
µg	Microgram

µL	Microliter
M	Molar
Maf	Muscle aponeurosis fibromatosis
mALP	Membrane-bound alkaline phosphatase
MAPK	Mitogen-activated protein kinase
MBOA	6-methoxy-2-benzoxazolinone
MCB	Monochlorobimane
MFO	Mixed-function oxidases
mg	Milligram
min	Minute
mito	Mitochondrial
mL	Milliliter
mM	Millimolar
MoA	Mode of action
mRNA	Messenger ribonucleic acid
MTP	Methoprene
MY	Million years
n	Number of replicates
nb	Number
NA	1-and 2-naphthyl acetate
NAC	N-acetylcysteine
nAChR	Nicotinic acetylcholine receptor
NADPH	Nicotinamide adenine dinucleotide hydrogen phosphate
NBD	Nucleotide-binding domain
NCBI	National Center for Biotechnology Information
ND	Not determined
Neh	NRF2-ECH (erythroid-derived cap'n'collar homology)
ng	Nanogram
nm	Nanometer
NMR	Nuclear magnetic resonance
nM	Nanomolar
Nrf2	NF-E2-Related Factor 2
nt	Nucleotide
OD	Optical density
OE	Over-expression
OP	Organophosphate
ORF	Open reading frame
P450(s)	Cytochrome P450-dependent monooxygenase(s)
PBO	Piperonyl butoxide
PBS	Phosphate-buffered saline
PCR	Polymerase chain reaction
P-gp	P-glycoprotein
PKA	Protein kinase A
PMS	Positional matrix screening
POD	Peroxidase
PSM	Plant secondary metabolites
PXR	Pregnane X receptor
RAC3	receptor-associated co-activator 3
RFU	Relative fluorescence units
RH	Relative humidity
RNA	Ribonucleic acid
RNAi	RNA interference
RNA-seq	RNA-sequencing
ROS	Reactive oxygen species

RR	Resistance ratio
RT	Room temperature
RT-qPCR	Reverse transcription quantitative real-time polymerase chain reaction
RyR	Ryanodine receptor
RXR α	retinoic X receptor α
s	Seconds
SD	Standard deviation
SE	Standard error
Se	Spodoptera exigua
SEM	Standard error of the mean
SF	Synergistic factor
Sf	Spodoptera frugiperda
sgRNA	single-guide RNA
skdr	super kdr
Sl	Spodoptera litura
SfMNPV	Sf multiple nucleopolyhedrovirus
skdr	Super knockdown resistance
SNP(s)	Single nucleotide polymorphism(s)
SOD	Superoxide dismutase
SP	Sodium pyruvate
SRS1	Substrate recognition site 1
Ta	Annealing temperature
t-BHP	tert-butyl hydroperoxide
TE	Transposable elements
TFBS	Transcription Factor Binding Sites
TMD	Transmembrane domains
UbcM2	ubiquitin-conjugating enzyme M2
UGT	Uridine 5'-diphospho-glucuronosyltransferase
US	United States
USA	United States of America
US$	US dollars
VGSC	Voltage-gated sodium channel
V	Volume
vs	Versus
XRE	Xenobiotic response element
XRE-xan	XRE to xanthotoxin
XRE-fla	XRE to flavone
β-TrCP	β-transducin repeat-containing protein
µg	Microgram
λem	Emission wavelength
λex	Excitation wavelength

List of Tables

Table 1 List of selected insecticides 23
Table 2 Selected transcription Factor Binding Sites (TFBS) in insect detoxification genes promoters. 61
Table 3 IC_{50} values of i3C and MTP towards stably transformed cell lines. 93
Table 4 IC_{50} values of i3C and MTP towards stably transformed cell lines 94
Table 5 Total number of CRISPR/Cas9 cell lines isolated and Sanger sequenced. 97
Table 6 Results of the ICE analysis of CRISPR/Cas9-mutated Sf9 cell lines. 100
Table 7 IC_{50} values of i3C and MTP towards CRISPR mutated cell lines. 103
Table 8 Effect of sodium pyruvate on cells tolerance to xenobiotics. 110

List of Figures

Fig. 1 *Spodoptera frugiperda* 18
Fig. 2 Distribution of *S. frugiperda* as of November 2021 21
Fig. 3 General scheme highlighting different pathways of xenobiotic elimination. 29
Fig. 4 Overview of expression levels data collected in the literature for detoxification genes in *Spodoptera*. 31
Fig. 5 State of play of detoxification gene studies in *Spodoptera* species. 33
Fig. 6 Characteristics of P450 response to xenobiotics in *Spodoptera* species. 35
Fig. 7 Expression prevalence of clustered detoxification genes from the literature. 43
Fig. 8 Pathways of transcriptional regulation of insect detoxification gene expression 56
Fig. 9 Structures of Nrf2 and Keap1 proteins in mammals – Source: Sanchez-Ortega et al. 2021 (Figure 2). 57
Fig. 10 Regulations of Nrf2 by several factors. Source: Bazak et al. 2017 (Figure 2). 59
Fig. 11 Dose-response curves of I3C and MTP in MTT bioassays. 72
Fig. 12 Induction of detoxification genes, *CncC*, *Maf* and *Keap1* in Sf9 cells. 74
Fig. 13 Transcript levels of *CncC* and *Maf* in transiently transformed Sf9 cells. 75
Fig. 14 Transcript levels of detoxification genes in transiently transformed Sf9 cells. 76
Fig. 15 Overexpression of *CncC* and *Maf* genes in Sf9 cells by stable transformation. 83
Fig. 16 Procedure for CRISPR/Cas9-induced mutations in Sf9 cells. 86
Fig. 17 Transcript levels of *CncC* and *Maf* in stably transformed Sf9 cells. 92
Fig. 18 Dose-response curves of I3C and MTP in MTT bioassays. 93
Fig. 19 Dose-response curves of I3C and MTP in HCS bioassays. 94
Fig. 20 CRISPR/Cas9 protocol development to silence *CncC* and *Keap1* 96
Fig. 21 Comparative analysis of CRISPR/Cas9 mutations in $Sf9^{CncC\text{-}08}$ using ICE and amplicon sequencing 99
Fig. 22 Transcript levels of *CncC* and *Keap1* in CRISPCR/Cas9-edited cells. 102
Fig. 23 Dose-response curves of I3C and MTP in MTT bioassays. 104
Fig. 24 Carboxylesterases enzymatic activity. 105
Fig. 25 Glutathione S-transferases enzymatic activity. 106
Fig. 26 ROS content in Sf9 cells under xenobiotic treatment and anti-oxidant treatment. 107
Fig. 27 ROS content in Sf9 cells under xenobiotic and antioxidant treatment. 108
Fig. 28 Effect of sodium pyruvate on dose-response curves of I3C in Sf9. 110
Fig. 29 PCA analysis of gene expression. 122
Fig. 30 GO terms enrichment from “biological processes” in the over-expressed genes. 123
Fig. 31 Summary of genes that are differentially expressed between the cell lines. 124
Fig. 32 Heatmaps summarizing the RNA-seq data of over-expressed detoxification genes in OE cell lines. 125
Fig. 33 Heatmaps summarizing the RNA-seq data of over-expressed detoxification genes in $Sf9^{Keap1\text{-}01}$. 126
Fig. 34 Heatmaps summarizing the RNA-seq data of under-expressed detoxification genes in $Sf9^{CncC\text{-}13}$. 127

General Introduction

A large majority of the complex trophic interactions occurring between plants and arthropods, two groups encompassing about half of all macroscopic organisms (Strong, 1988), is believed by many scientists to have yielded much of the biological diversity on Earth (Rausher, 2001). In the course of their co-evolution, plants and herbivorous arthropods have engaged in an arms race for survival (Ehrlich and Raven, 1964). On one hand, plants have evolved a myriad of specialized toxic metabolites directed towards phytophagous arthropods to defend themselves from herbivory (Li et al., 2020), while the latter have found means to detour these chemical innovations to use plants as a food source (Vogel et al., 2018). In this process more insects have become specialized feeders of a small number of plant families and develop sophisticated means to thwart plant defenses (Heckel, 2018). However, some generalist arthropods are able to feed on a large number of plant families and the way they manage to cope at the molecular level with the tremendous diversity of plant chemicals is still poorly understood (Vogel et al., 2018). In that respect, some generalist species, such as the fall armyworm (FAW), *Spodoptera frugiperda* (J.E. Smith) (Lepidoptera: Noctuidae), have become massive pests of cultured plants. The ability of *S. frugiperda* to cope and adapt to toxic molecules, including insecticides, is outstanding and poses serious problems for sustainable crop management and food production. Moreover, FAW recently appeared at the top rank of emerging pests causing significant losses in crop yields worldwide. Yet, the genetic and molecular grounds allowing quick and efficient detection and deployment of insect defenses are largely unknown.

This thesis is part of the search for a better understanding of the mechanisms that allow *S. frugiperda* to adapt to its diverse toxic environment, which includes plant allelochemicals and insecticides.

CHAPTER 1 - Literature review

Part I – *Spodoptera frugiperda*, an invasive crop pest

The genus *Spodoptera* Guinée (Lepidoptera), also known as the armyworms, is a group of roughly 30 species of noctuid moths present on 6 continents (Pogue, 2002). The fall armyworm (FAW), *Spodoptera frugiperda* (JE Smith), is native to tropical and subtropical regions of the Americas but has since 2016 invaded other parts of the globe. The FAW is a highly polyphagous insect that feeds on many plants and causes major damage to economically important crops. The difficulty to control this insect associated to its invasive behavior makes it one of the most serious threat to livelihoods and the environment worldwide. The Food and Agriculture Organization of the United Nations (FAO) proclaimed it in 2021 as "one of the most destructive pests jeopardizing food security across vast regions of the globe". In this first section, I review biological, ecological and agronomical aspects of this species.

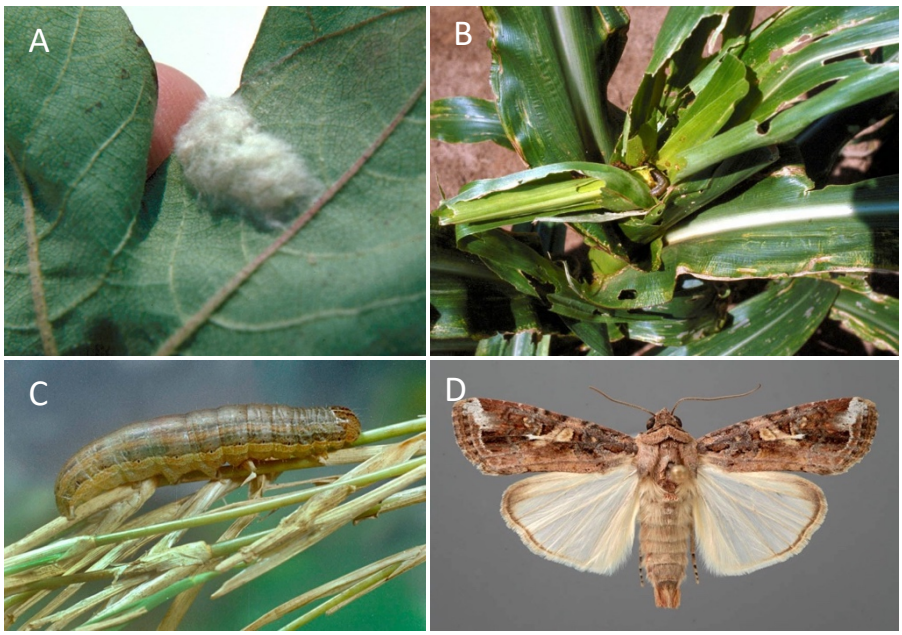

Fig. 1 *Spodoptera frugiperda*
(A) *S. frugiperda* egg mass[1] (B) damage caused by a lava in a whorl of maize (Zea mays)[2] (C) larvae[3] and (D) Adult[4] of *S. frugiperda*

[1] ©Ronald Smith/Auburn University/Bugwood.org - CC BY 3.0 US
[2] ©University of Georgia/Bugwood.org - CC BY 3.0 US
[3] ©Clemson University/USDA Cooperative Extension Slide Series/Bugwood.org - CC BY 3.0 US
[4] ©Lyle J. Buss/University of Florida/Bugwood.org - CC BY 3.0 US

1.1. Biology and ecology of FAW

FAW is a nocturnal species and most of its late larval and adult activity takes place at night. Eggs are laid on the leaves of the host located close to the soil surface, in clusters of 100-300 eggs (Fig. 1A, Nalim, 1991). After 3-5 days, newly hatched larvae will migrate to the whorl[5] and feed gregariously on leaves until reaching the third instar (Luginbill, 1928). FAW larvae are highly voracious and were reported on 353 plant hosts representing 76 plant families (Fig. 1B,C) (Montezano et al., 2018). Larval development through the six instars usually takes place within 14-21 days. In cases of high population density, larger larvae enter an armyworm phase whereby they swarm and disperse, seeking other food sources. Pupation then happens in an earthen cell and lasts 9 to 13 days (Luginbill, 1928). On average, adults live for 12-14 days during which females can migrate up to 500 kilometers (km) before laying over 1000 eggs on average (Fig. 1D)(Ferry et al., 2004; Montezano et al., 2018; Silva et al., 2017; Silva-Brandão et al., 2017). *S. frugiperda* is not able to enter diapause and does not survive at low temperatures, therefore adults are restricted to tropical and sub-tropical regions for overwintering. Adults are well adapted for long-distance flights and benefit from high wind currents to cover thousands of kilometers during seasonal migration (Westbrook et al., 2016). In warmer tropical regions, FAW can complete from eight to 11 generations per year (Busato et al., 2005).

FAW occurs in two morphologically identical but genetically distinct strains, the “rice strain” (R strain) found preferentially on rice and various pasture grasses and the “corn strain” (C strain) mainly found on maize, cotton and sorghum (Nagoshi et al., 2007; Pashley, 1986). Although several incompatibilities are known for the two strains (for a review, see Groot et al., 2010) cross-hybridization in the field has been observed although at a relatively low frequency (Kost et al., 2016; Nagoshi et al., 2017a). Therefore, the development of robust methods for determining population structure and genetic diversity of FAW invasive populations become crucial for taming further spread (Withers et al., 2021). Monitoring the gene flow in FAW strains and hybrid populations has also important implications for the development of pest management strategies. Indeed, while substantial genomic differences were reported between laboratory R and C strains by genome sequencing (Gouin et al., 2017)

[5] In botany, a whorl or verticil is an arrangement of leaves, sepals or petals that radiate from a single point and surround or wrap around the stem or stalk (Lindley, 1848)

recent studies have shown that genetic mixing in African invasive populations happens more often than expected before (Withers et al., 2021) and that new haplotypes seem to emerge (Nagoshi et al., 2019).

1.2. FAW, a pest of cultured plants

FAW thrive on a wide range of crops from various plant families including Poaceae like maize (*Zea mays*), sorghum (*Sorghum bicolor*), barley (*Hordeum vulgare*), and wheat (*Triticum aestivum*), but also Fabaceae like soybean (*Glycine max*) and Malvaceae like cotton (*Gossypium hirsutum*) (Bueno et al., 2011; Hardke et al., 2015; Marenco et al., 1992; Montezano et al., 2018; Pitre and Hogg, 1983). Damage can become substantial and result in serious yield losses when population outbreaks occur (for a review, see Overton et al., 2021). In large agricultural countries from the American continent, such as the USA and Brazil, annual yield losses were estimated at around US$300 to US$500 million or more in major outbreak years while the expenses for controlling the pest were in about the same range in Brazil (Wild, 2017). In African countries, reports mainly based on farmer surveys estimated yield losses and resulting economic damage to be very high (Chimweta et al., 2020; Day et al., 2017; De Groote et al., 2020). For example, maize yield losses in Ghana and Zambia were evaluated at 22 % and 67 %, respectively, resulting in close to US$200 million of loss (Day et al., 2017), yet these numbers may be overestimated as studies are so far mostly based on socio-economic surveys (Baudron et al.).

1.3. Worldwide invasive pest status

The FAW has recently made its way outside of its native range and has gone global at a lighting-speed hardly ever witnessed before in a pest species (Richardson et al., 2020; Stokstad, 2017). Despite many interceptions at quarantine in Europe (Day et al., 2017; Rwomushana et al., 2018) it was introduced in West Africa for the first time in early 2016 (Nagoshi et al., 2017b). Soon after FAW broke across the continent at a pace of at least 500 km per generation (Westbrook et al., 2016). After only 16 months the moth was detected in at least 21 African countries (Stokstad, 2017) and in 44 countries after two years. In 2018 it reached the Asian continent through India (Kalleshwaraswamy et al., 2018) and pursued its infestation at the same pace: by the end of 2019 FAW was present in China, Thailand and

Japan (Li et al., 2020a; Ma et al., 2019; Sun et al., 2019a). In 2020 it was reported for the first time in Australia in 2020 and detected on the Canary Islands (Spain) in July 2020 (Fig. 2).

Despite the colossal efforts made by intergovernmental plant protection agencies to limit the spread of these insects across borders (Goergen et al., 2016; Nagoshi et al., 2011; Van de Vossenberg and Van der Straten, 2014), FAW has unfolded the worrying scenario projected by migration models (Westbrook et al., 2016) and its invasion of Europe is now only a matter of time.

Fig. 2 Distribution of *S. frugiperda* as of November 2021
Source: www.fao.org/fall-armyworm (consulted on 29.11.21).

1.4. Management strategies to control FAW

Many strategies exist to efficiently contain FAW damage (for a review, see Wan et al. 2021). The choice and efficiency of each of these methods depend on several factors including insecticides availability and registration, presence of natural enemies, climate, size of crops and state of FAW resistance to insecticides.

1.4.1. Agricultural control

Agricultural approaches are implemented by using some biological and ecological aspects of FAW to control its reproduction, spread and to minimize the damage to crops. For example, in regions where FAW is seasonally invasive, pre-planting can be efficient to increase fitness cost for young larvae to develop on bigger plants. Deep ploughing allows to expose pupae to sunlight and predatory birds (Prasanna et al., 2018). The use of transgenic crops like *Bt* insect-resistant maize varieties has proven to be a very successful strategy as it influences

oviposition preference (Tellez-Rodriguez et al., 2014) and fitness costs (Jakka et al.). Countries such as Brazil and the USA heavily rely on these methods (Fatoretto et al., 2017; Siebert et al., 2008). The Food and Agricultural Organization (FAO) has issued a few recommendations for smallholders that have proven efficient in controlling FAW like handpicking and crushing the egg masses and larvae, or scatter ash, sand, sawdust or dirt into whorls to desiccate young larvae (FAO, 2021).

1.4.2. Biological control

Biological control mostly relies on the use of predators and parasitoids to control insect crop pests. A wide diversity of natural enemies of *S. frugiperda* has been reported in the Americas, Africa, and Asia (Molina-Ochoa et al., 2003; Prasanna et al., 2018; Shylesha et al., 2018). The Americas, where the FAW is native, have the most abundant parasitoids: approx. 150 taxa from 13 families including nine in Hymenoptera, and four in Diptera (Molina-Ochoa et al., 2003). Since its invasion in Africa and South-Eastern Asia many studies have investigated the presence of local natural enemies of FAW and several have since been reported. These include eight parasitoids from three families in West, Central and East Africa, with for instance *Chelonus curvimaculatus*, *Coccygidium luteum* and *Cotesia icipe*, five species of larval parasitoids, recorded in India (Sharanabasappa et al., 2019) and several *Telomnus* species in China (Jing et al., 2021).

Biological control also uses entomopathogens such as bacteria and viruses (for a review of their biopesticide potential and application status, see Bateman et al., 2018). *Bacillus thuringiensis* (Bt) is most widely used entomopathogenic bacteria used against lepidoptera and exerts high toxicity towards FAW (Singh et al., 2010). In addition, the *Spodoptera frugiperda* multiple nucleopolyhedrovirus (SfMNPV) was reported to cause FAW larval mortality rates of more than 90 % (Castillejos et al., 2002; Simon et al., 2012), however its efficacy is hindered by a number of factors including virulence of different isolates, larval instars, the amount of feeding viral occlusion bodies, formulation applied, and environmental conditions (Behle and Popham, 2012; Castillejos et al., 2002).

1.4.3. Chemical control

In agriculture, pest control essentially relies on the use of synthetic insecticides. In 2018 the sales market was estimated at ca 19.8 billion dollars (Sparks et al., 2020). Among

insect pests, *Spodoptera* is unquestionably one of the most destructive crop genus, and the control of FAW inevitably relies massively on the use of synthetic insecticides (Pogue, 2002).

Table 1 List of selected insecticides
Major modes of action and chemical classes commercialized globally for *S. frugiperda* control. Information adapted from "IRAC" (2020).

IRAC classification	Chemical class	Mode of Action (MoA) ‡	Example‡
1A	Carbamate	AChE[1] inhibitors	indoxacarb
1B	Organophosphate	AChE[1] inhibitors	chlorpyrifos
3A	Pyrethroids	VGSC[2] modulators	cypermethrin
5	Spinosyns	nAChR[3] allosteric modulators	spinosad
6	Avermectins	GluCl[4] allosteric modulators	emamectin benzoate
28	Diamides	RyR[5] modulators	chlorantraniliprole

[1] AChE: acetylcholinesterase
[2] VGSC: voltage-gated sodium channel
[3] nAChR: nicotinic acetylcholine receptor
[4] GluCl: glutamate-gated chloride
[5] RyR: ryanodine receptor
‡ Registrations of individual modes of action or products may differ regionally.

1.4.3.1. Carbamates and Organophosphates

Carbamates and organophosphates (OPs) act on the insect nervous system by irreversibly inhibiting acetylcholinesterase (AChE) which hydrolyses the neurotransmitter acetylcholine (Fournier et al., 1993) and are thus both classified in Group 1 according to IRAC (Table 1). Inhibition of the AChE leads to an accumulation of acetylcholine in the synaptic cleft and as a consequence to hyperexcitation of post-synaptic acetylcholine receptors (AChR) resulting in tremors, paralysis and death (Gunning and Moores, 2001). To date, there are 165 OPs and 43 carbamate insecticides available in the global market (Sparks et al., 2020) out of which indoxacarb and chlorpyrifos are two examples used to control FAW (Table 1).

1.4.3.2. Pyrethroids

Pyrethroids belong to group 3A, according to the IRAC classification scheme (Table 1). These insecticides disrupt nerve function by preventing the rapid kinetic closure of the voltage-gated sodium channel (VGSC) and hence trigger the generation of nerve action potentials leading to paralysis and death (Soderlund, 2012). Pyrethroids are acting quite fast on different developmental stages of lepidopteran pests (adult, larvae, and egg) (Elliott et al., 1978). Synthetic pyrethroid insecticides are structurally derived from natural pyrethrin

isolated from *Pyrethrum* flowers, with improvements made in photostability and residual activity, which allows effective use under field conditions (Casida, 1980; Elliott et al., 1978).

1.4.3.3. Spinosyns

Spinosyns (Group 5, IRAC) are targeting the insect nervous system by modulating the allosteric conformation of nicotinic acetylcholine receptors (nAChRs) which results in prolongated acetylcholine responses (Nauen and Bretschneider, 2002). Spinosad is an example of a spinosyn insecticide currently used in the control of *S. frugiperda* (Table 1). It consists of a mixture of two macrocyclic lactones, spinosyn A (85 %) and spinosyn D (15 %), derived from the actinobacteria *Saccharopolyspora spinosa*. Spinosad is highly effective against pests in the lepidopteran family Noctuidae (Nauen and Bretschneider, 2002).

1.4.3.4. Avermectins

Avermectins are another example of natural products (macrocyclic lactones) produced by actinomycete *Streptomyces avermitilis* exerting excellent acaricidal and less insecticidal properties (Argentine and Clark, 1990; Nauen and Bretschneider, 2002). However, structural modifications of avermectin result in products, such as emamectin benzoate (EB), having excellent lepidopteran activity (Argentine and Clark, 1990; Nauen and Bretschneider, 2002). EB (Group 6, IRAC) acts on the insect nervous system as an agonist of gamma-aminobutyric acid (GABA) and glutamate-gated chloride (GluCl) channels (Table 1) the binding of which induces a strong chloride ion influx and results in disruption of nerve impulses, paralysis, and death (Nauen and Bretschneider, 2002).

1.4.3.5. Diamides

Diamides (IRAC, Group 28) is one of the newest major class of insecticides and yet represents approx. 12 % of the insecticide market, with a global turnover of > 2.3 billion dollars (Sparks et al., 2020). Diamides are plant-derived insecticides from the alkaloid ryanodine which act on the ryanodine receptor (RyR). RyR is a large (homo)tetrameric calcium channel located in the sarco- and endoplasmic reticulum of neuromuscular tissues (Ebbinghaus-Kintscher et al., 2007; Lahm et al., 2005; Sattelle et al., 2008). By binding to RyR, diamides trigger the release and depletion of cellular calcium stores which leads to uncontrolled muscle contraction, paralysis, and finally death (Ebbinghaus-Kintscher et al., 2007; Lahm et al., 2005;

Masaki et al., 2006). Chlorantraniliprole is one of diamide insecticides used to control FAW (Table 1).

1.5. Resistance in *S. frugiperda*

Over the years, due to intensive selection pressure associated with the extensive use of synthetic insecticides, it has become very difficult to control *S. frugiperda* as it has developed resistance to a wide variety of insecticide classes. Resistance can be defined as the ability of some individuals or populations to survive doses of a compound that would normally kill the majority of specimens from the same species. Insects can develop resistance through different mechanisms, generally classified into four main categories: behavioral changes, reduced penetration or absorption, a reduction in the sensitivity of the target by mutations, as well as biochemical detoxification mediated by metabolic enzymes (Feyereisen, 1995). For *S. frugiperda*, high levels of resistance were reported to 42 insecticides, including Bt toxins (Mota-Sanchez and Wise, 2020).

1.5.1. Target site resistance in S. frugiperda

Target-site resistance typically emerges when non-synonymous mutations happen near or within the insecticide binding region of the target receptor. These mutations result in a change the amino acid sequence and consequently the binding affinity of the insecticide may be modified and lead to high levels of resistance (Somers et al., 2018). In FAW, target-site resistance has been described for many insecticide classes, including pyrethroids (Carvalho et al., 2013), OPs (Russell et al., 2004), neonicotinoids (Liu et al., 2006), and diamides (Boaventura et al., 2020a; Troczka et al., 2012). For example, point mutations A201S, G227A, and F290V in the AChE was responsible for strong resistance to chlorpyrifos in FAW from Brazil (Carvalho et al., 2013). Similarly, A201S and F290V in FAW collected in China led to carbamates and OPs resistance (Troczka et al., 2019). A recent study elucidated the mechanism of diamide resistance in *S. frugiperda* from Brazil (Boaventura et al., 2020a). FAW showed 237-fold resistance to chlorantraniliprole which was conferred by a point mutation in the RyR C-terminal transmembrane domain at position 4734. In another population from Brazil, three mutations including T929I, L932F and L1014F in the VGSC were reported to confer knockdown (kd)/super knockdown(skd)-type resistance to pyrethroids (Carvalho et al., 2013).

1.5.2. Metabolic resistance

Metabolic resistance can commonly be described as the ability to overcome pesticide toxicity as a result of effective transformation of the toxicant to less-toxic, more hydrophilic metabolites and more easily excretable from the insect's body. This process, takes place throughout a detoxification pathway involving mainly four enzyme families: microsomal cytochrome P450-dependent monooxygenases (CYPs or P450s), carboxylesterases (CEs), glutathione S-transferases (GSTs), and uridine diphosphate (UDP)-glucuronosyltransferases (UGTs). Overexpression, enhanced activity or a broader substrate range of enzymes are indicators pointing towards metabolic resistance. The monitoring of resistant populations of *S. frugiperda* across the world has allowed to document countless cases of enhanced activities in these major detoxification enzyme families. A substantial body of data has also accumulated on detoxification genes induced upon xenobiotic exposure or in insecticide resistant populations of FAW species, providing many potential candidate enzymes or transporters involved in resistance phenotypes. However, very few of these candidate detoxification enzymes were shown to metabolize insecticides *per se*. In the next Part of this chapter, I will specifically review those detoxification genes candidates in *S. frugiperda* and exemplify the outstanding metabolic capabilities they may provide towards both plant secondary metabolites and insecticides in this insect.

1.6. Sf9 cells, the cellular model of *S. frugiperda*

Sf9 cells were originally derived from the IPLB-SF21 cell line (Sf21 cells) which was isolated from *S. frugiperda* pupal ovarian tissue (Summers and Smith, 1987; Vaughn et al., 1977). It is since then one of the most widely used insect cell lines for it presents many advantages for studying the role of mammalian and insect enzymes and receptors pharmacology. First, Sf9 cell benefited from the establishment of the Sf9/baculovirus expression toolkit which uses infection of cells by genetically modified baculoviruses (*Autographa californica*) to drive the expression of high quantities of protein, often with the purpose of purification (Jarvis, 2009; Kost et al., 2005). Second, Sf9 cells also carry out conserved insect, and most of the described mammalian, post-translational modifications which are key for protein function (Asmann et al., 2004). This second feature makes it possible to functionally express and study receptors in the defined Sf9 environment. For example, Sf9 cells have been widely used to functionally express mammalian G-protein coupled receptors (GPCRs) in combination with different G-proteins (Schneider and Seifert, 2010).

S. frugiperda cells further proved to be an excellent cellular model to study insecticide resistance mechanisms is various insect species such *Nilaparvata lugens* (Zimmer et al., 2018), *Apis mellifera* (Manjon et al., 2018), *Leptinotarsa decemlineata* (Kalsi and Palli, 2017b) and *Culex quinquefasciatus* (Li and Liu, 2019). For example, biochemical studies of candidate detoxification enzymes such as P450s towards insecticides and model substrates are usually carried out with protein obtained by heterologous expression using the Sf9/baculovirus system (Nauen et al., 2021). In addition, Sf9 cells are well suited for gene reporter assays, such as the luciferase system. Many studies have used Sf9 cells to determine properties of gene promoters and to identify transcription factor binding sites (Kalsi and Palli, 2017b). Further, ectopic co-expression of proteins and receptors have proven to be robust methods to study gene function and interaction. Notable is the case of expression of mosquito GPCRs and downstream effectors such as G-protein subunits (Gs), adenylate cyclase (AC) and protein kinase A (PKA) in Sf9 cells which resulted in the overexpression of *SfCYP9A32* (Li and Liu, 2019).

More importantly, Sf9 cells are a cellular model to evaluate the molecular response of *S. frugiperda* to xenobiotics as well as to investigate potential resistance mechanisms (Cui et al., 2020; Giraudo et al., 2011; Giraudo et al., 2015). In addition, it has been extensively used to test the potential of certain molecules to act as insecticides in this species (Pereira et al., 2021; Ruttanaphan et al., 2020).

Part II – Detoxification genes in *Spodoptera frugiperda*

Large parts of this section have been published as Amezian D, Nauen R & Le Goff G (2021a) Comparative analysis of the detoxification gene inventory of four major *Spodoptera* pest species in response to xenobiotics. Insect Biochem Mol Biol 138: 103646. doi:10.1016/j.ibmb.2021.103646.

2.1. The detoxification pathway

The ability to metabolize, sequester and detoxify plant toxins is known as one of the central evolutionary solutions that arthropods have developed to feed on plants (Despres et al., 2007; Heidel-Fischer and Vogel, 2015). The detoxification pathway in insects allows the processing of toxicants present in their diet, including insecticides (Despres et al., 2007; Heckel, 2014). It is conventionally split into three phases (Fig. 3) that convert lipophilic substrates into hydrophilic products more easily excretable from the insect's body (Berenbaum and Johnson, 2015; Despres et al., 2007). In phase I (functionalization) cytochrome P450 monooxygenases (P450s) and carboxylesterases (CEs) render non-polar molecules "functional", *i.e.* with an active center by appending reactive groups suitable for subsequent conjugation. These intermediary metabolites may then fuel into phase II (conjugation) where glutathione S-transferases (GSTs) and (UDP)-glycosyl transferases (UGTs) catalyze the conjugation of target molecules, including phase I products, and facilitate their excretion. At last, phase III (transport) involves ATP-binding cassette (ABC) transporters that mediate efflux of the resulting product (Fig. 3).

The emergence of resistance to synthetic insecticides is presumed to reflect arthropods host-plant adaptation and their reliance on responses to similar chemical structures found among plant defense compounds (Gordon, 1961; McKenzie and Batterham, 1994). Approx. 400MY of plant-insect interactions has worked as an evolutionary driving force for diversification and sophistication of gene superfamilies such as those involved in detoxification (Feyereisen, 2011; Harari et al., 2020; Sezutsu et al., 2013). The increasing number of sequenced genomes has uncovered a genetic basis of resistance mechanisms that are thought to structurally and functionally overlap with host-plant adaptation (Dermauw et al., 2013; Despres et al., 2007; Grbić et al., 2011; Rane et al., 2019).

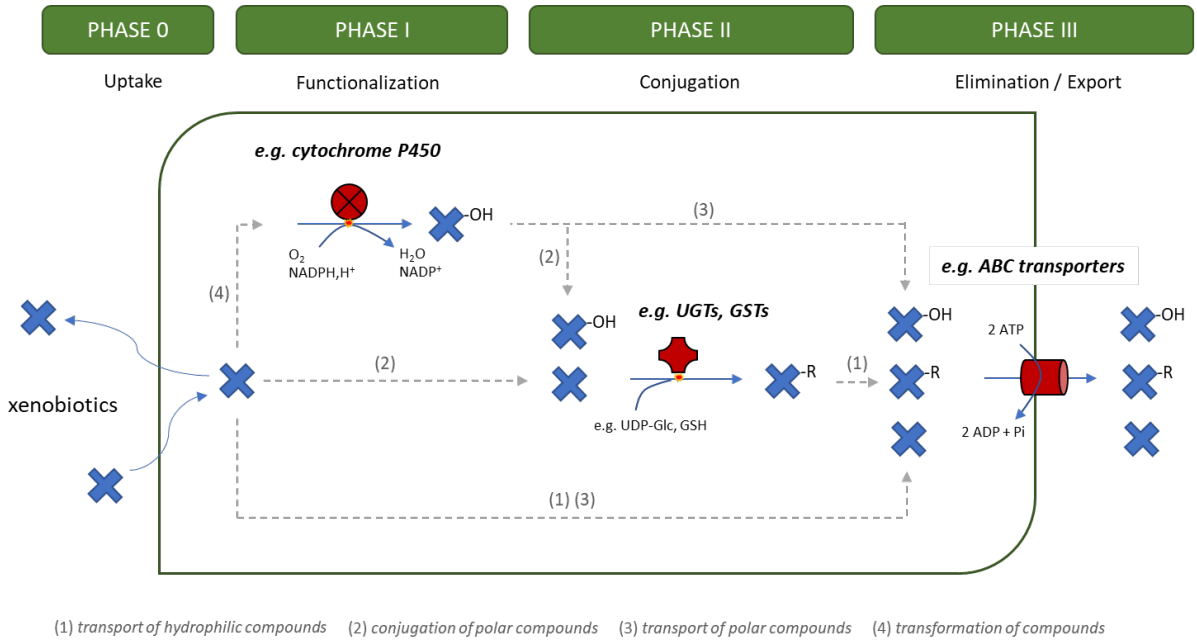

Fig. 3 General scheme highlighting different pathways of xenobiotic elimination.
Detoxification mediated by Phase I and Phase II enzymes are exemplified by reactions catalyzed by cytochrome P450 monooxygenases (P450s) and UDP-glycosyl transferases (UGTs), respectively. The elimination pathways shown can work simultaneously, but depending on the xenobiotic, individual pathways can dominate. Source: Amezian et al. (2021).

The genomes of *S. frugiperda* and *S. litura* are available since 2017 and revealed large expansions in most detoxification gene families as compared to the specialist *Bombyx mori* (Appendix A, Table S1) (Cheng et al., 2017b; Gouin et al., 2017). The genome of *S. exigua* was published last year (Zhang et al., 2020) and others are in progress, such as that of *S. littoralis.* The investigation of their detoxification gene families will help to understand to what extent these mechanisms allow species such as *S. frugiperda* to successfully feed on different host-plants and to develop resistance to insecticides. The role of the detoxification enzymes in insecticide resistance and host-plant adaptation is now well-acknowledged (Dermauw and Van Leeuwen, 2014; Feyereisen, 2005; Li et al., 2007; Pavlidi et al., 2018). Yet, while information accumulates on induction and overexpression of detoxification genes in *S. frugiperda*, very few of the enzymes they code for have been biochemically validated to be involved *per se* in the detoxification of xenobiotics.

In the following sections, I take a comprehensive look at responses of detoxification genes induced in *S. frugiperda,* as well as in close *Spodoptera* pest species, either from insecticide resistant populations or after exposure to xenobiotics, focusing on data published

during the past decade (the data can be found in Appendix A, Supplementary material). I further highlight the roles of these detoxification genes and discuss their implications for *S. frugiperda* host-plant adaptation and insecticide resistance.

2.2. Responses of detoxification genes to xenobiotics in the *Spodoptera* genus

I collected data from recently published studies (from 2010 to 2021) investigating the changes in expression of detoxification genes associated with insecticide resistance and host-plant adaptation in *Spodoptera* species. Data encompasses the nature of up- or downregulated genes assessed in real-time quantitative (RT-q)PCR, microarray, semi-quantitative assays or RNA sequencing (RNA-seq) when genes were duly annotated. A notice was added for significant validation of genes in genetic-functional approaches as well as from expression-based metabolic techniques in heterologous systems. It is important to note that gene induction is dependent on the dose, *i.e.* the concentration of inducers, and the time of exposure. While aware of these features, including this information was beyond scope of the present work. This makes comparisons between insects and xenobiotics difficult based on the data, which will be discussed below. Nevertheless, the data compiled here will provide useful information for those working in the field (Appendix A, Supplementary material). The transcriptomic responses of detoxification genes were obtained from resistant field or laboratory-raised *Spodoptera* populations or after exposure of insects to xenobiotics (in total 51 different compounds, Appendix A Fig. S1), including plant secondary metabolites (PSM, n=22), insecticides (n=21), herbicides (n=2), model inducers (n=2) and heavy metals (n=4). I excluded on purpose studies on *Bt* resistance mechanisms. Among all *Spodoptera* species described to date only four have been investigated post-2010 for their detoxification capability at gene expression level, namely *S. litura*, *S. frugiperda*, *S. exigua* and *S. littoralis*.

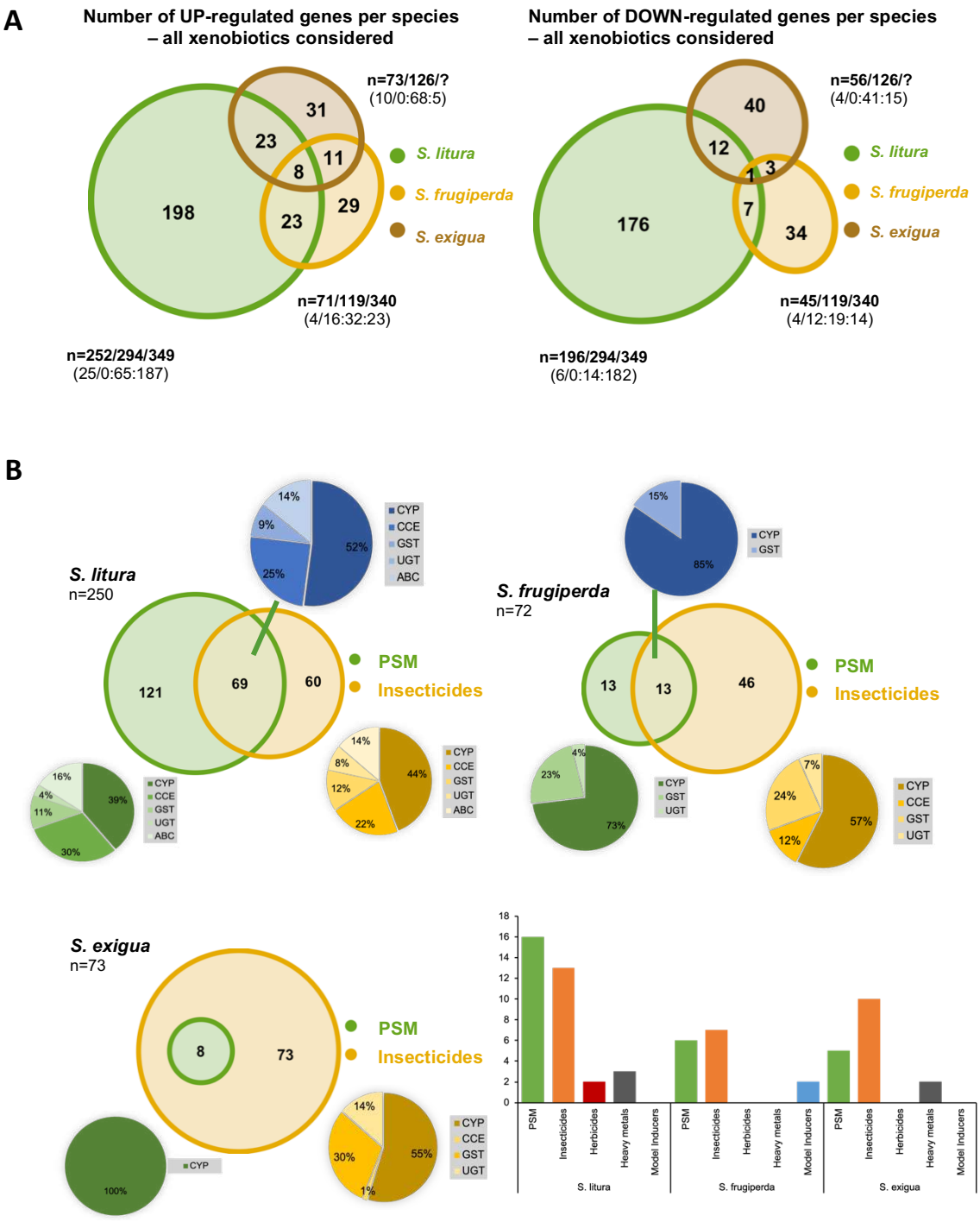

Fig. 4 Overview of expression levels data collected in the literature for detoxification genes in *Spodoptera*. Venn diagram displaying the number of unique or overlapping up- (left) and down- (right) regulated genes after exposure to xenobiotics or in resistant populations of *S. litura* (green), *S. frugiperda* (yellow) and *S. exigua* (brown). For each species "n =" indicates as follows: the number of total detoxification genes up- (or down-) regulated / number of detoxification genes gathered from the literature / number of detoxification genes manually curated in the reference genome. Similarly, the number of corresponding references and nature of expression data is given underneath as follows: (nb of references / microarrays: RT-qPCR: RNA-seq). Expression data from *S. littoralis* was purposely excluded from the diagram for only one UGT was upregulated after deltamethrin exposure (B) Venn diagram displaying the number of unique or overlapping detoxification genes upregulated after plant secondary metabolite (PSM, green) or insecticides (yellow) exposure. The proportion of detoxification gene types upregulated are given as pie charts in green (after PSM exposure), yellow (after insecticides exposure) or in blue (intersection). Methods for figures are detailed in Appendix A, Supplementary Information. Source: Amezian et al. 2021.

The number of genes found up- and downregulated per species are presented in Figure 4. Expression data of detoxification genes in *S. littoralis* is scarce: over the past decade a single gene, UGT46A6, was shown to be upregulated in the antennae after deltamethrin exposure (Bozzolan et al., 2014). Expression data of detoxification genes in *S. litura* exceeds the information available for both *S. frugiperda* and *S. exigua*, however the increasing numbers of studies being published in both species may shortly close this gap. The total and overlapping number of detoxification genes found upregulated in the three *Spodoptera* species was always higher than that of downregulated genes (Fig. 4A). The data altogether reflects the extent of the transcriptomic response generated by these four generalists *Spodoptera* species under xenobiotic challenges or intense insecticide pressure. This is also illustrated in Figure 4B by the relatively high share of overlapping genes between species for the two major xenobiotics types (PSM and insecticides). This revealed two findings: i) induction mechanisms of detoxification enzymes are overlapping with respect to inducing xenobiotics, ii) detoxification enzymes might have broad substrate specificities, for example encompassing both phytochemicals and synthetic pesticides.

This being said, the majority of up- and downregulated detoxification genes from the cited literature in *Spodoptera* lack respective validation studies (Fig. 5); therefore, it is premature to assume that the upregulated genes are involved in the detoxification of the xenobiotics. Indeed, detoxification enzymes may convert xenobiotics into more toxic metabolites. In that case, tolerance to insecticides or plant secondary metabolites can be conferred by downregulating these detoxification genes as it was shown in *Varroa destructor*. The suppression of *CYP4EP4* expression increased the tolerance of mites to coumaphos (Vlogiannitis et al., 2021). In addition, exposure to xenobiotics tend to induce a large number of genes and most enzymes that are upregulated by the presence of a putative toxin are not directly involved in the metabolization of that toxin. Host plant generalists in particular may induce a variety of defense mechanisms that eventually succeed in allowing the insect to feed on the plant. It has been suggested that both the overlapping spectrum and induction plasticity observed in detoxification enzymes of generalist species is a result of their feeding strategy (Vogel et al., 2014). It is possible that due to the diversity of toxic plant chemicals encountered in their diet, generalists are able to exhibit a larger inducible palette of enzymes. In that respect, the number of overlapping genes induced between PSM and insecticides presented in Figure 4B might be underestimated. For instance, although the pyrethroid

insecticide deltamethrin was the only xenobiotic exposed to all four species surveyed (Appendix A Fig. S2A), only 12 genes were reported to be upregulated and none of them was shared between species. Similarly, λ-cyhalothrin, chlorpyrifos and xanthotoxin were the sole xenobiotics used on three out of four species and yet, the lack of genes surveyed in *S. frugiperda* and *S. exigua* make conclusions difficult (Appendix A Fig. S2B,C,D). Extending both the number of detoxification genes assayed and compounds used in future studies would be of great interest to identify evolutionary conserved detoxification responses among close *Spodoptera* species.

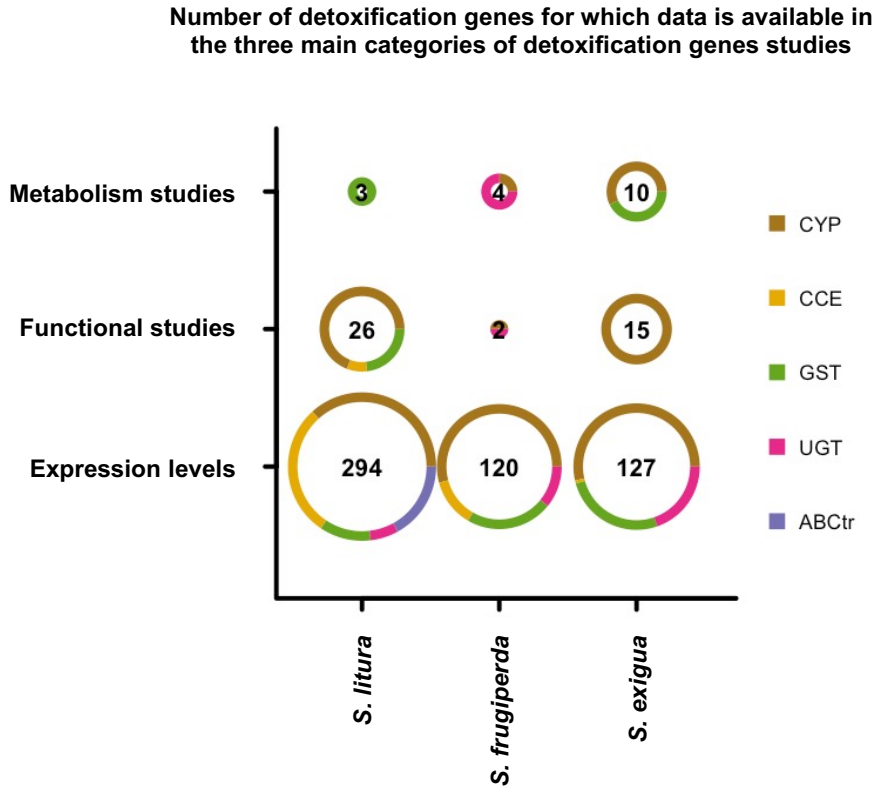

Fig. 5 State of play of detoxification gene studies in *Spodoptera* species.
Donutplot displaying for each species surveyed (x-axis) the number of detoxification genes for which data is available in three main categories of detoxification gene studies (y-axis): Expression levels, measurements of transcripts levels after xenobiotic exposure or in insecticide resistant populations (*i.e.*, data obtained through microarray, RT-qPCR or RNA-seq assays); Genetic validation, in vitro or in vivo functional genetic characterization of detoxification genes using molecular tools such as RNAi, CRISPR/Cas9; Biochemical studies, functional expression of recombinant detoxification enzymes and study of the interaction with xenobiotics. The donut rings show the corresponding share of CYP (brown), CCE (yellow), GST (green), UGT (magenta), ABC (purple). Methods for figures are detailed in Supplementary Information. Partly update from Amezian et al. 2021.

2.2.1. Phase I detoxification: functionalization of xenobiotics

2.2.1.1. P450 enzymes encoded by the CYP genes

P450 enzymes are heme thiolate proteins that catalyze a wide spectrum of reactions including oxidations involving C–C or C=N bond cleavage, hydrolysis, dehydration, dehydrogenation, dehalogenation and most notably monooxygenation of a variety of substrates (Mansuy, 1998) altogether encompassing 60 different types of chemical reactions (Feyereisen, 2011, 2012). They are known to play an important role in the interactions of insects with plants. They are usually considered as the first line of enzymatic defense against xenobiotics and have been studied in great detail (Dermauw et al., 2020; Nauen et al., 2022; Feyereisen, 2005, 2012). Beyond their major role in detoxification, P450s are also involved in pheromone, hormone biosynthesis and in cuticular hydrocarbon production (Petryk et al., 2003; Qiu et al., 2012; Reed et al., 1994; Rewitz et al., 2006; Warren et al., 2002). Insect P450s are classified into six clans: the mito (mitochondrial) clan, clan CYP2, clan CYP3, clan CYP4, clan CYP16 and clan CYP20 (Dermauw et al., 2020; Nelson, 1998). P450 sharing 40 % sequence identity belong to the same family while subfamilies are defined by a 55 % sequence identity cutoff (Fig. 6A). *S. frugiperda* and *S. litura* have large CYPomes (Appendix A Table S1). The number of manually curated CYP genes mounts to 138 in *S. litura* and 136 in *S. frugiperda* (Cheng et al., 2017b; Gouin et al., 2017). The size and structure of clans in these two species are quite different due to P450 blooms in clans CYP3 and CYP4 (Fig. 6A). The number of genes in clans CYP3 and CYP4 are four to six times higher than that in the two other clans and are unequally distributed in CYP subfamilies. For instance, subfamilies in the mitochondrial and CYP2 clan encompass no more than one or two genes whereas some CYP3 and CYP4 subfamilies have up to nine genes such as the *CYP6AEs* (9 genes in *S. litura* and 11 genes in *S. frugiperda*).

A

	Clan	Families and subfamilies	Total
S.litura	MITO	CYP49A(1), CYP301A(1), CYP301B(1), CYP302A(1), CYP314A(1), CYP315A(1), CYP333A(1), CYP333B(2), CYP339A(1), CYP428(1)	11
	CYP2	CYP15C(1), CYP18A(1), CYP18B(1), CYP303A(1), CYP305B(1), CYP306A(1), CYP307A(1)	7
	CYP3	CYP6AB(5), CYP6AE(9), CYP6AN(1), CYP6AW(1), CYP6B(6), CYP6CT(1), CYP9A(15), CYP9AJ(1), CYP9BS(1), CYP9G(1), CYP321A(5), CYP321B(5), CYP324A(3), CYP332A(2), CYP337B(1), CYP338A(1), CYP354A(1), CYP365A(1), CYP3097A(1)	60
	CYP4	CYP4AU(2), CYP4CG(2), CYP4G(4), CYP4L(3), CYP4M(4), CYP4S(2), CYP340AA(1), CYP340AB(1), CYP340AD(2), CYP340AQ(1), CYP340AX(5), CYP340G(1), CYP340K(1), CYP340L(5), CYP340Q(1), CYP341A(1), CYP341B(7), CYP366A(1), CYP367A(4), CYP367B(1), CYP421B(3)	52
S.frugiperda	MITO	CYP49A(1), CYP301A(1), CYP301B(1), CYP302A(1), CYP314A(1), CYP315A(2), CYP333A(1) CYP333B(3), CYP339A(1), CYP428A(1)	13
	CYP2	CYP15C(1), CYP18A(1), CYP18B(1), CYP303A(1), CYP304F(1), CYP305B(1), CYP306A(1), CYP307A(1)	8
	CYP3	CYP6AB(5), CYP6AE(11), CYP6AN(3), CYP6AW(1), CYP6B(7), CYP6CT(1), CYP9A(14), CYP9AJ(1), CYP9G(1), CYP321A(5), CYP321B(3), CYP324A(5), CYP332A(1), CYP337B(1), CYP338A(1), CYP354A(1), CYP365A(1), CYP3097A(1)	63
	CYP4	CYP4AU(3), CYP4CG(2), CYP4G(4), CYP4L(3), CYP4M(4), CYP4S(2), CYP340AD(1), CYP340K(1), CYP340L(9), CYP341A(1), CYP341B(4), CYP366A(1), CYP367A(1), CYP367B(1), CYP421B(1)	38

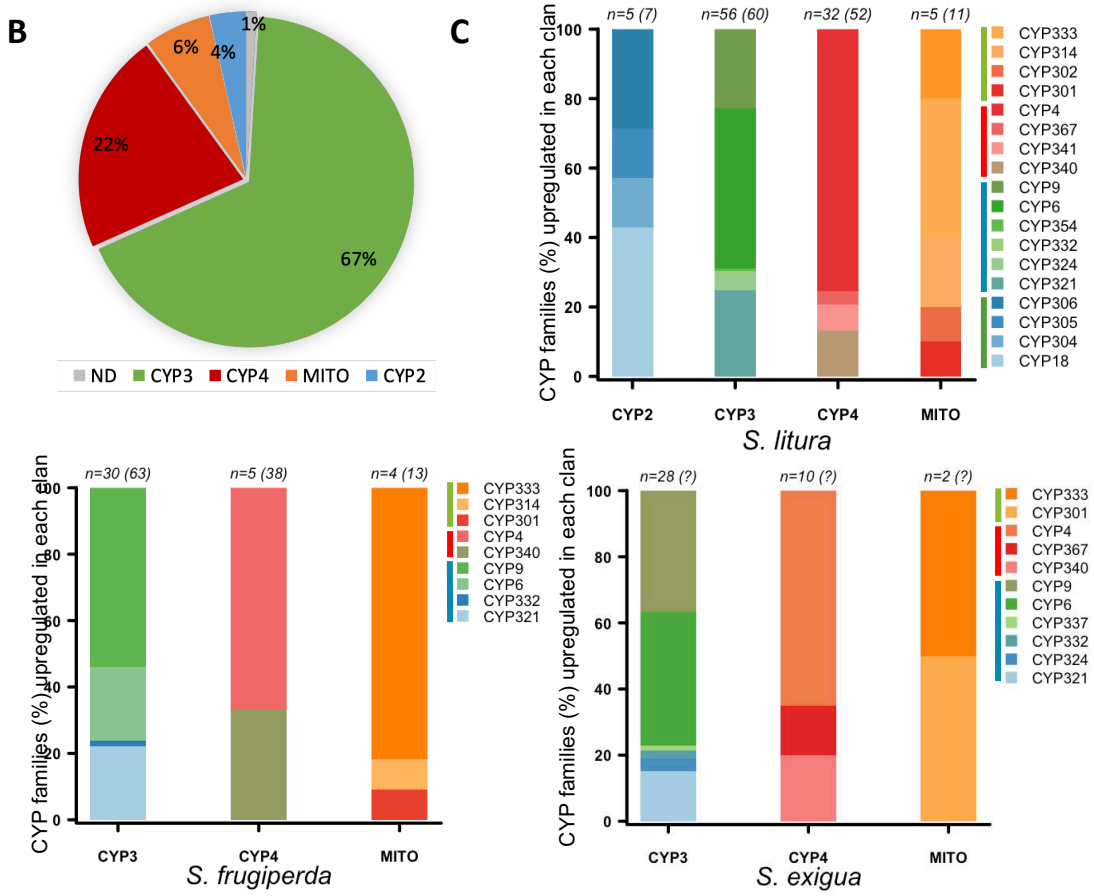

Fig. 6 Characteristics of P450 response to xenobiotics in *Spodoptera* species.
(A) Structure of CYPomes in *S. litura* and *S. frugiperda*. The number of family members is given in parenthesis. CYP3 and CYP4 clans have undergone large expansions and blooms through duplication of specific P450 families. **(B)** The proportion of CYP families accounting for upregulated P450 genes after xenobiotic exposure is depicted for each CYP clan in *S. litura* (top left), *S. frugiperda* (top right) and *S. exigua* (bottom left). On top of each stacked bar is given as follows: "n= 'number of genes from related clan involved' ('total number of genes belonging to related clan')". **(C)** CYP clan (%) origin of upregulated P450 across *Spodoptera* species (n=4). P450 with uncomplete annotation were marked as 'ND'. Methods for figures are detailed in Supplementary Information. Source: Amezian et al. 2021.

This distribution however follows a power-law pattern of many CYP families with few genes and few families with many genes widespread in arthropod CYPomes (Dermauw et al., 2020). P450 from clan CYP3 and CYP4 are commonly associated with detoxification, and this is reflected in the expression data collected in *Spodoptera* species: 67 % of all *CYPs* induced belonged to clan CYP3 while 22 % belonged to clan 4 (Fig. 6B).

2.2.1.1.1. Mitochondrial clan and CYP2 clan

P450 genes from the mitochondrial clan accounted for 6 % of all upregulated P450 genes across the literature (Fig. 6B). In line with what is known of the biological function of orthologous genes in other species, there were very few reports of mitochondrial and CYP2 P450s induced in *Spodoptera* within the limits outlined in this section (induced by xenobiotics or in resistant populations). The four ecdysteroidogenic genes *CYP302, CYP314, CYP315, CYP306*, involved in the biosynthesis of molting hormones (Dermauw et al., 2020; Rewitz et al., 2006), were mostly absent from the list of differentially expressed genes (Appendix A Fig. S3). A few other P450 genes from the mitochondrial clan including *CYP339, CYP428* and *CYP49* were not found differentially regulated in response to xenobiotics and there is very limited evidence as to the role they play in other species. In *S. frugiperda* the most induced mitochondrial P450s belonged to the *CYP333* family, representing approx. 80 % of all induced P450s from this clan (Fig. 6C). *CYP333B4* was induced by seven out of 11 different treatments applied to larvae and Sf9 cells, and fipronil was the sole treatment that induced the expression of *CYP333B4* in both larval midgut and Sf9 cells (Giraudo et al., 2015). This makes *CYP333B4* the most frequently induced P450 in *S. frugiperda.* In *S. litura CYP333B3* was induced by four different chemicals including xanthotoxin, imidacloprid, fluralaner and indoxacarb (Cheng et al., 2017b; Jia et al., 2020; Shi et al., 2019). More recently, a study analyzed the metabolic capacity of 18 mito and CYP2 enzymes from *H. armigera* against two model substrates, esfenvalerate and 2-tridecanonne (Shi et al., 2021c). The authors exemplified that *Ha*CYP333B3 could metabolize ethoxycoumarin and aldrin into their 4'-hydroxy metabolites with high efficiency. In this respect, upregulation of *CYP333B3* and *CYP333B4* in both *S. frugiperda* and *S. litura* to PSM and insecticide exposure is consistent with what was previously found for this P450s family in other insect species and points toward a general role in xenobiotic metabolism.

2.2.1.1.2. CYP3 clan

CYP321 genes. CYP321 family members accounted for ca. 20 % of all CYP3 P450s upregulated in *S. exigua*, *S. litura* and *S. frugiperda* (Fig. 6C) (Carvalho et al., 2013; Cheng et al., 2017b; Giraudo et al., 2015; Hu et al., 2019c; Jia et al., 2020; Liu et al., 2019; Nascimento et al., 2015; Shi et al., 2019; Wang et al., 2017b; Wang et al., 2017c). In particular *CYP321A7*, *CYP321A8* and *CYP321A9* were among those most often upregulated from this family (Cheng et al., 2017b; Giraudo et al., 2015; Hu et al., 2019c; Jia et al., 2020; Wang et al., 2017b). The role of CYP321 genes in insecticide resistance and plant toxin metabolism was confirmed in *S. litura*. For example, *CYP321A7* was by far the most often overexpressed P450 in *S. litura* and shown to be involved in larval susceptibility to imidacloprid using RNAi-mediated knock-down experiments (Cheng et al., 2017b). Hu and coworkers (2019c) assessed the expression patterns of 68 CYP genes in response to five different insecticides in *S. exigua* fat body cells. Among them *CYP321A16* and *CYP332A1* were found strongly upregulated. In a follow-up study, transgenic *D. melanogaster* flies expressing these genes were significantly more tolerant to chlorpyrifos treatments than wildtype flies (Hu et al., 2020a). In addition, recombinant *Se*CYP321A16 and *Se*CYP332A1 expressed in Sf9 cells were shown to metabolize chlorpyrifos *in vitro* demonstrating that these P450s likely contribute to the resistance of *S. exigua* to this insecticide. Furthermore, the overexpression of *S. exigua CYP321A8*, which is responsible for resistance to chlorpyrifos, cypermethrin, and deltamethrin in a strain from China, is due to two distinct mechanisms: the overexpression of transcription factors Cap'n'collar isorform C (CncC) and Muscle aponeurosis fibromatosis (Maf) as well as a mutation in the promoter region resulting in a new predicted *cis*-acting element that putatively facilitates the binding of the nuclear receptor Knirps (Hu et al., 2021). Furthermore, Chen and Palli (2021a) successfully transformed FAW to obtain constitutive *CYP321A8*-overexpressing transgenic insects. P450 activity and deltamethrin tolerance of transgenic larvae were greatly increased providing evidence that CYP321A8 contributes to deltamethrin resistance in this species.

CYP6 genes. In *S. frugiperda*, CYP6 genes accounted for approx. 20 % of induced CYP3s while accounting for *ca* 50 % and 40 % in *S. litura* and *S. exigua, respectively* (Fig. 6C). In *Spodoptera* this family is divided into six subfamilies including CYP6AB, CYP6B and CYP6AE, which are the most represented and both quantitatively and qualitatively involved in the

detoxification of xenobiotics. Others include CYP6AN, CYP6AW and CYP6CT genes of which very little is known to date (Fig. 6A).

CYP6AB genes were reported to be induced in nine different studies (Carvalho et al., 2013; Cheng et al., 2017b; Hafeez et al., 2019a; Hu et al., 2019c; Jia et al., 2020; Lu et al., 2020; Lu et al., 2019b; Sun et al., 2019b; Wang et al., 2015c), and *CYP6AB12*, *CYP6AB60* and *CYP6AB31* are among those most often upregulated (Cheng et al., 2017b; Hu et al., 2019c; Jia et al., 2020; Lu et al., 2020; Lu et al., 2019b; Sun et al., 2019b). *CYP6AB12* was only induced in *S. litura* and overexpressed upon imidacloprid and ricin exposure in an RNA-seq study, but was also downregulated by xanthotoxin (Cheng et al., 2017b). Lu et al. (2020) nicely linked increased levels of *CYP6AB12* transcripts to ROS (reactive oxygen species) bursts triggered by pyrethroid insecticide exposure and mediated by the CncC/Maf transcription pathway. The role of two additional *Sl*CYP6AB genes (*CYP6AB14* and *CYP6AB60*) was functionally confirmed in insecticide tolerance and upon exposure to various phytochemicals including coumarin, flavone, tomatine and xanthotoxin and by increased larval sensitivity to these toxins after RNAi-mediated silencing of respective P450 genes (Sun et al., 2019b; Wang et al., 2015c). Noteworthy, the deltamethrin-inducible *SeCYP6AB14* was similarly validated in an RNAi-mediated silencing assay which resulted in enhanced deltamethrin sensitivity of exposed larvae (Hafeez et al., 2019a).

The CYP6B subfamily is one of the major groups of CYP6s involved in PSM and insecticide metabolism and has been extensively studied (reviewed in Heckel, 2014; Li et al., 2007). Members of this subfamily were overexpressed to a high extent in *Spodoptera* (Carvalho et al., 2013; Cheng et al., 2017b; Giraudo et al., 2015; Jia et al., 2020; Li et al., 2019; Liu et al., 2018a; Liu et al., 2019; Lu et al., 2019a; Shi et al., 2019; Wang et al., 2015a; Wang et al., 2018c; Wang et al., 2016; Zhou et al., 2012a; Zhou et al., 2012b). In *S. litura* larvae, *CYP6B48* (Cheng et al., 2017b; Liu et al., 2018a; Liu et al., 2019; Wang et al., 2015a), *CYP6B58* (Cheng et al., 2017b; Liu et al., 2018a; Wang et al., 2015a), and *CYP6B47* (Cheng et al., 2017b; Liu et al., 2018a; Zhou et al., 2012a; Zhou et al., 2012b) were highly responsive to xenobiotic challenges and the most recurrent genes induced. Inducers were as diverse as flavones, ricin, imidacloprid, fenvalerate and α-cypermethrin. The furanocoumarin xanthotoxin significantly enhanced the transcripts of all three *S. litura* CYP genes as well as those of *SfCYP6B39* (Giraudo et al., 2015). *SfCYP6B39* was moreover recently found overexpressed 257-fold in a Brazilian population showing resistance to deltamethrin and chlorpyrifos (Boaventura et al., 2020b).

Insect CYP6B enzymes are known for their ability to detoxify furanocoumarins in specialists of the *Papilio* genus feeding on plants producing these toxic metabolites (Cohen et al., 1992; Hung et al., 1995; Li et al., 2002; Ma et al., 1994; Petersen et al., 2001). Investigating the metabolizing activity of CYP6Bs belonging to generalist Lepidoptera species including *Papilio glaucus* and *Helicoverpa zea* has shown that CYP6B enzymes were also capable of metabolizing furanocoumarins, but with less efficiency. Subsequent metabolic assays showed that the generalist *Hz*CYP6B8 exhibited substantial catalytic activity against other plant allelochemicals (quercetin, flavone, chlorogenic acid, indole-3-carbinol, rutin, etc.) as well as insecticides (cypermethrin, aldrin and diazinon) but with lower efficiency (Rupasinghe et al., 2007).

CYP6AE is a third CYP6 subfamily with an increasing body of evidence for its involvement in the metabolism of plant phytochemicals in Lepidoptera as most notably documented in *H. armigera* (Celorio-Mancera Mde et al., 2011; Krempl et al., 2016a; Krempl et al., 2016b; Liu et al., 2015; Shi et al., 2018; Tao et al., 2012; Wang et al., 2018a; Zhou et al., 2010). In *Spodoptera* the accumulation of CYP6AE transcripts was reported in several studies (Carvalho et al., 2013; Cheng et al., 2017b; Cui et al., 2020; Hafeez et al., 2020; Hou et al., 2021; Hu et al., 2019c; Shi et al., 2019). Hafeez et al. (2020) investigated the effect of quercetin exposure on tolerance of *S. exigua* larvae to λ-cyhalothrin. They showed that exposing larvae to quercetin, λ-cyhalothrin and their combination, resulted in higher transcript levels of *CYP6AE10*. RNAi to silence this P450 in larvae led to increased mortality suggesting that CYP6AE10 might take part in the detoxification of these xenobiotics. *CYP6AE10* and *CYP6AE47*, were found highly upregulated in *S. exigua* after larvae were exposed to various insecticides such as λ-cyhalothrin, chlorantraniliprole, metaflumizone and indoxacarb (Hu et al., 2019c) confirming the results of Hafeez et al. (2020). In *S. frugiperda*, *CYP6AE44* was upregulated in two different studies. Carvalho et al. (2013) used EST sequences from SPODOBASE (Negre et al., 2006) to analyze the gene expression in two *S. frugiperda* populations, resistant to OPs and pyrethroids, in a microarray-based study. Identification of the EST sequences by BLAST searches against the reference genome (LepidoDB, www.genouest.fr) revealed the overexpression of, among others, *CYP6AE44* in the OP resistant strain (Carvalho et al., 2013). In a more recent study, *CYP6AE44* was also found upregulated in Sf9 cells previously challenged with the alkaloid harmine, a monoamine oxidase inhibitor (Cui et al., 2020).

CYP9 genes. In *S. litura* CYP9s are subdivided into four subfamilies: CYP9A with 15 genes and CYP9AJ, CYP9BS and CYP9G encompassing one gene each. *S. frugiperda* has three CYP9 subfamilies: CYP9A with 14 genes, CYP9G and CYP9AJ with a single gene each (Fig. 6A). Of these subfamilies, CYP9As have undergone recent CYP blooms and are organized in clusters on chromosome 29 and chromosome 6 in *S. litura* and *S. frugiperda,* respectively (Cheng et al., 2017b; Xiao et al., 2020) (Fig. 7). As noted earlier, *Spodoptera* species did not have genes reported to be commonly responding to deltamethrin exposure in the literature (Appendix A Fig. S2). However, most of the genes found upregulated by deltamethrin belonged to the CYP9A subfamily. Similarly, a closer look at genes that were induced by PSM and insecticides shows that three out the four found in both *S. litura* and *S. frugiperda* overlaps are CYP9As (Figure S4) *CYP9A40* was upregulated in *S. litura* (Wang et al., 2015b), *CYP9A30*, *CYP9A31*, *CYP9A32* and *CYP9A59* were upregulated in *S. frugiperda* (Boaventura et al., 2020b; Giraudo et al., 2015), while *CYP9A105*, *CYP9A12*, *CYP9A98* were upregulated in *S. exigua* (Hafeez et al., 2019a; Hu et al., 2019c; Wang et al., 2018b). These observations in *Spodoptera* are somewhat consistent with additional reports on the CYP9As associated with pyrethroid resistance in other insect pests such as *H. armigera* and *Locusta migratoria* (Brun-Barale et al., 2010; Guo et al., 2015; Zhu et al., 2016b).

Although organized in clusters (Fig. 7) and sharing high sequence homology – only three pairs of clustered CYP9As can be considered as 1:1 orthologues, while *CYP9A28-31* share 76-90 % amino acid sequence identity (Sezutsu et al., 2013) – the expression patterns of CYP9As in *Spodoptera* are quite diverse in response to PSMs and insecticides (Carvalho et al., 2013; Cheng et al., 2017b; Giraudo et al., 2015; Hafeez et al., 2019a; Hafeez et al., 2019b; Hu et al., 2019c; Nascimento et al., 2015; Wang et al., 2018b; Wang et al., 2015b; Wang et al., 2018c; Wang et al., 2016; Zhou et al., 2012a) suggesting mechanisms of differential regulation of gene expression. This is exemplified in *S. litura* by an RNA-seq study showing complex expression profiles of the CYP9A clustered genes in the midgut, Malpighian tubules and fat bodies of larvae exposed to two PSMs (xanthotoxin and ricin) and imidacloprid (Cheng et al., 2017b). Altogether, CYP9 genes accounted for roughly 50 % of all upregulated CYPs from clan CYP3 in *S. frugiperda* (Fig. 6C). The share of upregulated genes belonging to the CYP9 family was also high in *S. exigua* (ca. 40 %) and less so in *S. litura* (*ca.* 20 %) (Fig. 6C). Although somewhat biased by the methodology used to assess transcript levels (RNA-seq *vs* RT-qPCR and microarrays) the data highlights the frequency at which *CYP9A30*, *CYP9A31* and *CYP9A32*

are upregulated in *Spodoptera* (*e.g.* in 4, 7 and 5 different conditions respectively in *S. frugiperda* mainly reported by Giraudo et al. (2015)). Recently, Boaventura et al. (2020b) also reported overexpression of *CYP9A59* and a CYP9A-like gene (by 267-fold) in a deltamethrin and chlorpyrifos resistant *S. frugiperda* strain from Brazil. Currently, only two CYP9A genes from *S. litura* have been confirmed to play a role in detoxification of xenobiotics by RNAi-based silencing: *dsCYP9A40* injection into larvae resulted in increased susceptibility to quercetin, cinnamic acid, deltamethrin and methoxyfenozide (Wang et al., 2015b) and *dsCYP9A31* injections were associated with increased mortality of larvae to imidacloprid (Cheng et al., 2017b). In *S. exigua*, four CYP9As were linked to metabolic detoxification of xenobiotics in similar RNAi experiments: *SeCYP9A10* to α-cypermethrin (Hafeez et al., 2019b), *SeCYP9A21v3* in a chlorantraniliprole-resistant field population from China (Wang et al., 2018c), *SeCYP9A105* in α-cypermethrin, deltamethrin and fenvalerate treated larvae (Wang et al., 2018b) and *SeCYP9A98*, in tolerance of larvae to deltamethrin exposure (Hafeez et al., 2019a). Very recently, the use of CRISPR/Cas9 to knockout *CYP9A186* provided evidence that CYP9A186 conferred emamectin benzoate (EB) and abamectin resistance in *S. exigua* (Zuo et al., 2021). *CYP9A186* was found overexpressed 10-fold in the EB-resistant population, however, the heterologous expression of CYP9A186 from both susceptible and resistant insects combined with *in vitro* metabolic bioassays showed that a single substitution (F116V) in the P450 substrate recognition site 1 (SRS1) enabled enhanced metabolism of EB and abamectin and also contributed to resistance seen in *S. exigua*.

CYP9As stand out for being metabolizing enzymes of xenobiotics and are notorious for their alleged and sometimes confirmed role in insecticide resistance phenotypes. For instance, *CYP9A3, CYP9A14, CYP9A15, CYP9A16, CYP9A12/17, CYP9A23* were associated with resistance to pyrethroids in *H. armigera*, as functional expression of recombinant proteins in either yeast or Sf9 cells showed clearance activity against the pyrethroid esfenvalerate, providing strong evidence that enhanced expression of pyrethroid-detoxifying enzymes can confer a resistance phenotype (Yang et al., 2008b).

2.2.1.1.3. CYP4 clan

P450s from clan CYP4 accounted for 22 % of all CYPs upregulated in the *Spodoptera* literature compiled in this chapter (Fig. 6B). Clan CYP4 comprises 52 P450 genes in *S. litura* and 38 in *S. frugiperda* (Fig. 6A). They were found upregulated in *S. litura* (32 genes), *S. frugiperda* (5) and

S. exigua (10) (Fig. 6C). The CYP4 family accounted for approximately 70 % of clan CYP4 P450s upregulated in *S. frugiperda*, 65 % in *S. exigua* and 75 % in *S. litura*, suggesting that they might have a crucial role in xenobiotic response (Cheng et al., 2017b; Cui et al., 2020; Giraudo et al., 2015; Hu et al., 2019c; Jia et al., 2020; Li et al., 2019; Liu et al., 2018a; Shi et al., 2019; Wang et al., 2018c; Wang et al., 2016; Yi et al., 2018).

CYP4G75 was found upregulated under several conditions in *S. litura*, and is hence the one most often upregulated in this species (Cheng et al., 2017b; Li et al., 2019). It was moderately upregulated by exposure to imidacloprid and ricin in the midgut and Malpighian tubules of larvae but repressed by xanthotoxin treatments as well as in fat bodies of all treatments considered (Cheng et al., 2017b). In another study where larvae were challenged with tomatine, *CYP4G75* was also induced in the midgut and repressed in fat bodies (Li et al., 2019). The remainder CYP4G genes induced in *Spodoptera* were limited to *SlCYP4G106*, *SlCYP4G109*, *SlCYP4G74* and *SeCYP4G37* genes (Wang et al., 2016). The CYP4G family is well-described for its involvement in cuticular hydrocarbon synthesis in several insect species (Balabanidou et al., 2016; Feyereisen, 2020; Kefi et al., 2019; Qiu et al., 2012; Wang et al., 2019). *S. litura* and *S. frugiperda* CYP4G family encompasses 4 genes, but whether these genes are involved in cuticular hydrocarbon synthesis and capable of providing a tolerance phenotype to sustained insecticide exposure is still uncertain and needs to be investigated yet.

Very few expression data were available for clan CYP4 P450s in *S. frugiperda* (Appendix A Supplementary material). Only five genes out of 38 were reported upregulated in the literature, most of them were found induced in one single situation except for *CYP4M14* which was moderately upregulated by exposure to xanthotoxin in larval midguts and by 2-tridecanone and methoprene in Sf9 cells (Giraudo et al., 2015).

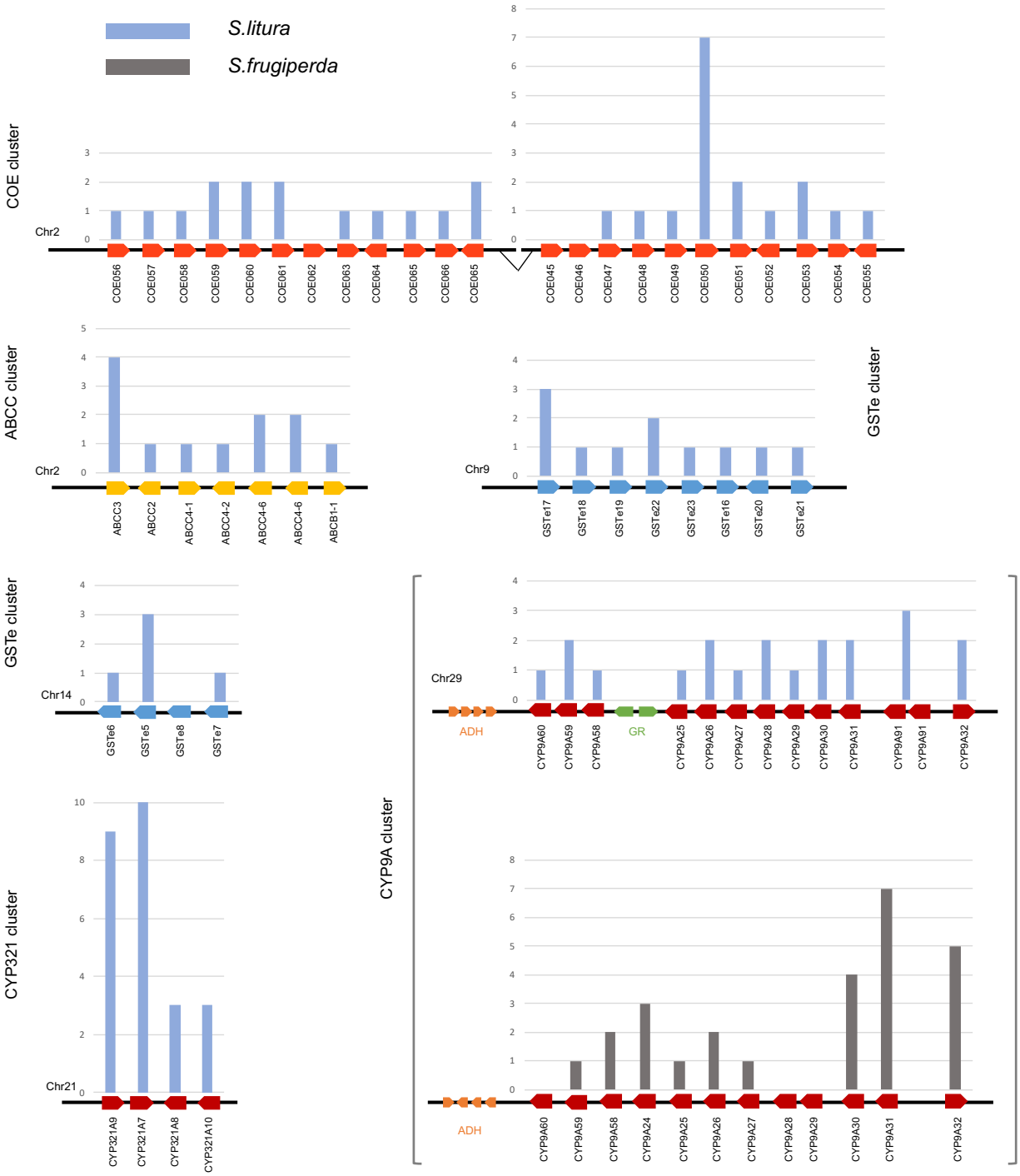

Fig. 7 Expression prevalence of clustered detoxification genes from the literature.
The number of upregulation occurrences of genes in selected clusters are shown in *S. litura* (blue) and *S. frugiperda* (grey). Caution should be taken when comparing the inducibility of genes presented above as the data was collected from various studies with different experimental procedures. For example, gene expression in *S. frugiperda* has been assessed by RT-qPCR (Giraudo et al., 2015), microarray (Carvalho et al., 2013) and RNA-seq (do Nascimento et al., 2015) which produces a biased picture of reality. ADH: alcohol dehydrogenase GR: gustative receptor. Methods for figures are detailed in Supplementary Information. Source: Amezian et al. 2021.

2.2.1.2. Carboxylesterases

The carboxylesterase (CE) gene superfamily is the second group of enzymes to participate in the functionalization of lipophilic exo- and endogenous compounds. It encompasses enzymes hydrolyzing diverse carboxylic, thio-, phospho-, and other ester substrates into their alcohol and acid components by relying on a catalytic triad of amino acid residues including a reactive serine nucleophile (Oakeshott et al., 2005). Similar to P450s, CEs are widespread in prokaryotes and eukaryotes (Oakeshott et al., 2005). The CE gene family classification is based on phylogenetic analyses and substrate specificities resulting in 3 classes and 33 clades (Ranson et al., 2002; Teese et al., 2010). The first class contains proteins considered to be non-catalytically active (with the exception of acetylcholinesterases) and involved in neuro/developmental functions (Biswas et al., 2010). The second class encompasses catalytically active, excreted enzymes involved in insect hormone and pheromone processing, found mostly expressed in the antennae and insect olfactory organs (Vogt et al., 1985). The third class contains active enzymes usually expressed in the midgut with intracellular localization to microsomes, cytosol and mitochondria and are predicted to have digestion or detoxification functions based on their expression in the midgut (Oakeshott et al., 2005; Small and Hemingway, 2000; Teese et al., 2010). Some esterases were shown to be involved in insecticide resistance and most of these are linked to the third class, with also a few that belong to the second class (Claudianos et al., 2006; Cui et al., 2011; Teese et al., 2010).

The CE gene family is, just as P450s, very consistent in *Spodoptera* genomes. The genome of *S. litura* contains 110 CE genes (Cheng et al., 2017b) (Appendix A Table S1). Over the past decade, 70 different CEs were reported upregulated *in S. litura* upon xenobiotics exposures or in insecticide resistant populations (Appendix A Supplementary material). Although *S. frugiperda* possesses 93 CE genes (Gouin et al., 2017), little information on their expression is available in the literature - only seven genes were reported upregulated to date (see below for more details). In *S. exigua*, only one predicted CE gene was found upregulated in a chlorantraniliprole-selected resistant laboratory strain (Unigene0045545, orthologous to carboxylesterase ae17 [*B. mori*]) as revealed by RNA-seq (Wang et al., 2018c). Similarly, the amount of expression data gathered in *S. frugiperda* and *S. exigua* over the past decade is very limited, which is mostly due to the lack of RNA-seq datasets (Fig. 4A). The lack of a reference genome for *S. littoralis* makes it difficult to thoroughly analyze the CE gene family in this

species. However, a recent transcriptome assembly provided a well-curated set of annotated gene transcripts of 56 CE genes from different chemosensory and non-chemosensory organs (Walker et al., 2019), including the 30 previously described genes (Durand et al., 2010; Durand et al., 2012; Merlin et al., 2007).

CEs are found under various denominations across the literature (e.g. CXE, COE or CarE) which makes comparisons between studies difficult. Nonetheless, I below refer to the nomenclature used by the authors in the cited literature. CEs were associated with the detoxification of xenobiotics in *S. litura* larvae, as shown by their inducibility after ricin, xanthotoxin and imidacloprid treatments in an RNA-seq study (Cheng et al., 2017b). The involvement of these CEs in metabolic resistance was further exemplified when *dsCOE057* and *dsCOE058*-injected larvae showed increased susceptibility compared to the control after imidacloprid exposure. This RNA-seq study revealed that *COE050* was primarily induced in the midgut by all three treatments, in Malpighian tubules after imidacloprid and ricin exposure as well as in fat bodies by xanthotoxin. In another study, high levels of *COE50* transcripts were detected in two indoxacarb resistant laboratory and field populations (Shi et al., 2019). Besides *COE050*, three additional CEs were shown to be overexpressed multiple times in the presence of a xenobiotic: *COE024*, *COE030* and *COE037* were similarly induced by ricin, imidacloprid and xanthotoxin (Cheng et al., 2017b) and *COE030* (gene5053) was also shown to be induced by fluralaner (Jia et al., 2020).

In *S. frugiperda*, the five CEs differentially expressed in a lufenuron-resistant population when compared to a susceptible population were all upregulated (Nascimento et al., 2015). The microarray analysis carried out by Carvalho et al. (2013) revealed that *CXE13* and *CXE001c* were overexpressed 21-fold and 3-fold in chlorpyrifos and λ-cyhalothrin resistant *S. frugiperda* populations, respectively, when compared to a susceptible population. *CXE13* was characterized in *S. litura* and *S. exigua* for its ability to metabolize plant volatiles and sex pheromones (He et al., 2014). *Se*CXE13 and *Sl*CXE13 were functionally expressed in High Five cells and purified. Recombinant enzymes were used in enzyme activity and kinetic studies with 20 different sex pheromones and other acetates. The two homologous esterases displayed a broad substrate spectrum and a highly similar hydrolysis pattern. Among the 20 acetate derivatives tested, 18 were hydrolyzed to different degrees. However, forward genetic-based functional studies are still necessary to confirm the ability of these enzymes to metabolize insecticides.

CEs are one of the three major types of proteins commonly accepted to be involved in arthropods olfaction process (Vogt, 2005). Several CEs are odorant-degrading enzymes and are hence often excreted into the cellular interspace or in cuticular wax layers to clear olfactory and gustatory receptors from environmental cues (Ferkovich et al., 1982; Vogt and Riddiford, 1986). *SlCXE10* (sic) was found highly expressed in adults' antennae and shown to hydrolyze a green leaf ester (Z3-6:Ac) produced by host-plants with high efficiency in kinetic studies combined with GC-MS analyses (Durand et al., 2010). The sequence analysis of *SlCXE10* predicted it to belong to the third class of CEs, known to be implicated in detoxification. Similarly, a recent study identified and amplified the cuticular *SeCXE11*. Its purified recombinant protein showed high hydrolytic activity towards two plant volatiles, *i.e.* (Z)-3-hexenyl caproate and pentyl acetate with >50 % degradation (He et al., 2020).

2.2.2. Phase II detoxification: conjugation of xenobiotics or metabolites

2.2.2.1. Glutathione S-transferases

Although detoxification mediated by glutathione S-transferases (GSTs) can principally fall into phase I (Ranson et al., 2001), they are best known for conjugating the thiol group of glutathione (GSH) to molecules possessing an electrophilic center (Enayati et al., 2005). The target molecules, endogenous metabolites or reactive products formed by phase I P450s or CEs, are thus rendered more water soluble which facilitates their elimination from the insect body (Enayati et al., 2005). The role of GSTs in protecting insects from adverse effects of plant chemicals is well-known, but most studies have focused on their involvement in insecticide resistance (Pavlidi et al., 2018). GSTs have been classified into two major groups according to their location within the cells, *i.e.* cytosolic or microsomal. The cytosolic GSTs are subdivided into six different classes: sigma (s), zeta (z), theta (t) and omega (o) classes are found ubiquitously across taxa and are believed to play roles in conserved endogenous functions, while two additional classes restricted to insects form multigene families and are involved in xenobiotic detoxification: epsilon (e) and delta (d) (Chelvanayagam et al., 2001; Ranson et al., 2002). Some GSTs were not assigned to any existing class and were hence designated as "unclassified".

The genome of *S. litura* contains 47 GST genes (Appendix A Table S1) out of which the epsilon class counts 20 members of two clusters of recently duplicated genes on chromosome 9 and 14 (Cheng et al., 2017b). The theta, sigma, delta, zeta and omega classes encompass

one, seven, five, two and three genes, respectively. The remaining ones are split between five microsomal and four "unclassified" GSTs. The GST repertoire of *S. frugiperda* includes 46 genes, as reported in the manually annotated reference genome (Gouin et al., 2017). These numbers are quite similar to those found in the genomes of *H. armigera* (42) and *H. zea* (40) (Pearce et al., 2017).

GSTs were ubiquitously overexpressed in *Spodoptera* in response to all kinds of xenobiotics and stressors, with the notable exception of clofibrate and phenobarbital, two model inducers (Appendix A Supplementary material). In *S. litura*, a total of 31 GSTs were reported upregulated, 19 of those belonged to the epsilon class, some being relatively frequently overexpressed such as *GSTe2* (Deng et al., 2009; Li et al., 2019; Liu et al., 2019), *GSTe3* (Deng et al., 2009; Huang et al., 2011; Liu et al., 2019; Zhang et al., 2016a) and *GSTe6* (Cheng et al., 2017b). In *S. exigua*, 21 GST genes were found induced, from which nine, four, four and three belonged to the GSTe, GSTo, GSTs and GSTd classes, respectively (Hu et al., 2019a; Hu et al., 2019b; Wang et al., 2018c; Xu et al., 2016).

GSTe1 was one of the most upregulated GSTs in *S. exigua* (Hu et al., 2019a; Hu et al., 2019b) and by far the most frequently upregulated in *S. litura*, but not in *S. frugiperda* (Chen et al., 2018a; Huang et al., 2011; Ling et al., 2019; Liu et al., 2018a; Xu et al., 2015; Zhang et al., 2016a; Zou et al., 2016). *SlGSTe1* was, among other GSTs including *GSTe3*, *GTSe4* and *GSTe5*, upregulated between 3-fold and 5-fold at 48h, 72h and 96h after treatment of sublethal doses of fluralaner (Liu et al., 2018a). However, synergist assays using dimethyl maleate (DEM) showed no difference in susceptibility of fluralaner treated insects. A total of four independent studies reported the induction of *SlGSTe1* after chlorpyrifos exposure or in a chlorpyrifos resistance phenotype (Chen et al., 2018a; Huang et al., 2011; Xu et al., 2015; Zhang et al., 2016a). *SlGSTe1* mRNA transcript levels were 5.51-fold increased after chlorpyrifos exposure in a chlorpyrifos-selected population compared to a susceptible population (Zhang et al., 2016a). Other GSTs were also highly inducible in this laboratory-selected population including *SlGSTe3*, *SlGSTe10*, *SlGSTe15*, *SlGSTt1*, *SlGSTo2*, *SlGSTs5*, *SlMGST1-2* and *SlMGST1-3*. Interestingly, *SlGSTe13*, *SlMGST1-1*, *SlGSTt1* and *SlGSTz1* were specifically upregulated in the selected population, but not inducible when larvae were exposed to chlorpyrifos. Xu et al. (2015) analyzed the detoxification activity of *SlGSTe1* in *S. litura* for several insecticides and heavy metals. They showed that *Sl*GSTe1 protein level was upregulated in the gut of insects after feeding on chlorpyrifos and cadmium. Although *Sl*GSTe1

was demonstrated to bind to some heavy metals with high affinity, further research is necessary to determine whether GSTs are able to detoxify toxic metals by directly sequestering them. Recombinantly expressed GSTe1 enzymes exerted high activity towards 1-chloro-2,4-dinitrobenzene (CDNB), a GST model substrate (Deng et al., 2009). *SlGSTe1* expression was modulated by additional PSMs such as asatone, isoasatone A, allyl-isothiocyanate (AITC) and indole-3-carbinol (I3C) (Ling et al., 2019; Zou et al., 2016). It was overexpressed at the mRNA and protein level in the midgut of *S. litura* larvae fed on *Brassica juncea* or on I3C-/AITC-supplemented diets (Zou et al., 2016). In the same study, a two-dimensional electrophoresis revealed that *Sl*GSTe1 was the only detoxification enzyme overexpressed in the midgut in a dose-dependent manner. The enzyme was shown to catalyze the conjugation of I3C and xanthotoxin in the presence of reduced glutathione with high efficiency. The authors further functionally validated the role of *SlGSTe1 in vivo* by RNAi-based silencing of the gene, inhibiting larval growth and feeding rates. Additional *S. litura* GSTs were confirmed to play a role in xenobiotics detoxification in RNAi-based knock-down experiments, such as *SlGSTs1* to tomatine (Li et al., 2019), *SlGSTe20* and *SlGSTe07* to imidacloprid (Cheng et al., 2017b). The confirmation of catalytic activity of candidate GSTs against phytochemicals and insecticides is limited in *S. exigua* and only *Se*GSTe6, *Se*GSTd3, *Se*GSTo2 were investigated for their ability to clear chlorpyrifos and cypermethrin insecticides in the presence of GSH using high performance liquid chromatography (HPLC) analysis (Hu et al., 2019b).

2.2.2.2. (UDP)-glycosyl transferases

UDP-glycosyltransferases (UGTs) constitute an enzyme superfamily found in all kingdoms of life and responsible for conjugating lipophilic endo- and xenobiotic substrates into more water-soluble glycosylated compounds (Bock, 2016). UGTs are membrane-bound proteins divided into two main domains: the N-terminal domain binds to aglycone substrates while the C-terminal domain is responsible for binding the sugar donor and anchoring the protein to lipid membranes. The C-terminal domain encompasses a signature motif of 44 amino-acids highly conserved across all organisms that catalyzes the linking of activated UDP-glucose moieties to specific substrates (Ahn et al., 2012; Krempl et al., 2016b). UGTs are named and classified in accordance with the nomenclature guidelines of the UGT Nomenclature Committee (Mackenzie et al., 1997), which groups them into families designated by a number including sequences that share ~45 % or more amino acid sequence

identity; subfamilies are designated by a capital letter and group sequences with more than ~60 % amino acid sequence identity. In this international nomenclature, families numbered 31 to 50 and 301 to 351 have been assigned to arthropods. UDP-glycosyltransferases are given multiple roles in insects such as olfaction, cuticle formation, endobiotic modulation, sequestration and detoxification of xenobiotics (Ahn et al., 2012; Despres et al., 2007; Heidel-Fischer and Vogel, 2015; Hopkins and Kramer, 1992; Wang et al., 1999).

The genome of the specialist silkworm *B. mori* contains 44 UGT genes, in comparison the generalists *H. armigera* and *H. zea* possess 46 and 42 UGT genes, respectively (Appendix A Table S1). In the *Spodoptera* genus, the reference genome of *S. frugiperda* contains 47 UGTs (Gouin et al., 2017). No information is available on the exact number of UGT genes in *S. litura* and *S. exigua* although a few selected genes have been investigated (Hu et al., 2019c; Li et al., 2019; Shi et al., 2019). However, *SlittUGT46A6* (*S. littoralis* UGT46A6) was reported to be induced after topical deltamethrin application onto antennae, suggesting a role in clearance of xenobiotics and involvement in olfaction (Bozzolan et al., 2014). In contrast, 17 UGTs were reported upregulated in *S. litura* by two different studies (Appendix A Supplementary material). The first study demonstrated in a *S. litura* population resistant to the oxadiazine indoxacarb that 10 UGT genes were significantly overexpressed as compared to a susceptible strain, however functional expression studies confirming their involvement in resistance were lacking (Shi et al., 2019). The second study revealed that exposing larvae to tomatine-supplemented artificial diet induced the expression of seven UGT genes mostly belonging to UGT33 and UGT40 families (Li et al., 2019). UGT33 was by far the most represented family throughout the literature of all surveyed *Spodoptera* species, documented by a total of 16 independent experimental proofs in *S. litura* (at least four UGT genes out of 17), *S. exigua* (four UGT genes out of nine) and *S. frugiperda* (two UGT genes out of five). In *S. exigua* most notably, multiple UGTs were shown to respond in a very similar manner to λ-cyhalothrin, chlorantraniliprole, metaflumizone and indoxacarb, but not abamectin (Hu et al., 2019c). Indeed, out of 32 UGTs tested, only two were significantly upregulated by abamectin (13-fold for *UGT40D5* and 7-fold for *UGT33T3*) whereas most of the remaining UGTs were significantly downregulated. In contrast, λ-cyhalothrin, chlorantraniliprole, metaflumizone and indoxacarb treatments induced most UGTs in similar expression profiles. For example, *UGT33J3* was found upregulated *ca.* 10-fold after treatment with all aforementioned insecticides. Additional members of UGT40 family were reported to be induced including *SfUGT40D5* (Cui et al., 2020),

SlUGT40Q1 (Li et al., 2019) *SfUGT40-07* (Carvalho et al., 2013), and *SeUGT40R4* (Cui et al., 2020; Hu et al., 2019c).

Benzoxazinoids (BXDs) are known defensive components of grasses such as maize and rye. DIMBOA (2,4-dihydroxy-7-methoxy-1,4-benzoxazin-3-one) the main BXD in maize and is stored as the inert glucosides (*2R*)-DIMBOA-Glc. When plant tissues are ingested by chewing insects, (*2R*)-DIMBOA-Glc is hydrolyzed by plant specific β-glucosidases, hence releasing the toxic aglycone DIMBOA (Wouters et al., 2014). It was demonstrated that *Spodoptera* species use stereoselective re-glycosylation of activated DIMBOA in their midgut as a detoxification strategy (Wouters et al., 2014). Analyses of larval frass using LC-MS/MS and nuclear magnetic resonance (NMR) showed that the main BDXs found in feces was (*2S*)-DIMBOA-Glc, the non-toxic enantiomer of the naturally occurring (*2R*)-DIMBOA-Glc (Glauser et al., 2011; Vassao et al., 2018; Wouters et al., 2014). The molecular work carried out by Israni et al. (2020) recently identified the genes responsible for DIMBOA detoxification in *S. frugiperda*. BDX-metabolizing *SfUGT33F28* and *SfUGT40L8* were highly expressed in the midgut and fat bodies, respectively, and *SfUGT33F28* was inducible when larvae were transferred from bean-based artificial diet to maize plants. Gene silencing *in vivo* of *SfUGT33F28* was strongly correlated with the reduction of (*2S*)-DIMBOA-Glc accumulation in frass, gut DIMBOA-UGT activity and larval growth rate. In addition, *N*-glucosylation of 6-methoxy-2-benzoxazolinone (MBOA), a toxic breakdown product of DIMBOA, was also reported in *S. frugiperda* and *S. littoralis* (Maag et al., 2014).

2.2.3. Phase III: transport and excretion

2.2.3.1. ATP-binding cassette (ABC) transporter

The ATP-binding cassette (ABC) transporter superfamily is the largest membrane transporter family across all kingdoms of life; however, they are still poorly described in insects, although a recent review analyzed ABCs from more than 150 arthropod species and highlighted specific expansions of ABC transporter families which suggest evolutionary adaptation (Denecke et al., 2021). ABC transporters are subdivided into eight subfamilies indicated by the letters A-H. They have been linked to insecticide resistance to at least 27 different chemistries by facilitating efflux of insecticides and acaricides [for a comprehensive review see Dermauw and Van Leeuwen (2014)]. Several recently published papers demonstrate an increasing interest on studying the significance of this gene family in

xenobiotic resistant phenotypes (He et al., 2019a; He et al., 2019b; Jin et al., 2019; Li et al., 2020b; Meng et al., 2020; Rosner and Merzendorfer, 2020), particularly since an ABC transporter was identified as a crucial receptor for Bt Cry1 toxin binding (Heckel, 2012; Jurat-Fuentes et al., 2021). With the extension of powerful genetic methods and high-throughput sequencing, a clearer picture of gene numbers, sequences and expression profiles of members belonging to this gene superfamily is starting to emerge.

Despite the known role of ABCs in detoxification, the information gathered thus far in *Spodoptera* is limited. Elevated transcript levels of ABC transporters in the presence of PSMs or insecticides are only documented in *S. litura*: 38 out of 54 ABC annotated genes were reported upregulated by three different studies in response to xanthotoxin, tomatine, ricin, imidacloprid as well as in an indoxacarb resistant field strain (Cheng et al., 2017b; Li et al., 2019; Shi et al., 2019; Supplementary material). ABC transporters were highly induced in larval midgut by ricin treatments (Cheng et al., 2017b), and in another study *ABCG1*, *ABCC4*, *ABCG4* were found strongly expressed (>9-fold) in the midgut after larvae fed on tomatine, while *ABCF4*, *ABCA2*, *ABCB6* were only moderately induced (>2-fold) (Li et al., 2019). In addition, ABC genes might be associated with indoxacarb resistance in an indoxacarb resistant strain of *S. litura*, as nine of them were differentially expressed in a resistant population. Most reports on upregulated ABC genes in *S. litura* were individual findings based on a single condition or tissue, however, *ABCC3*, *ABCB3-1*, *ABCB3-2* and *ABCH1* were independently reported to be induced 4, 3, 3 and 3 times (Cheng et al., 2017b; Shi et al., 2019). In accordance with what is known about ABC subfamilies involved in transport of metabolites and conjugates, genes of ABCC and ABCG were most represented among those upregulated by PSMs or insecticides. More precisely, 10 and 11 different ABCCs and ABCGs were found induced in different studies (Cheng et al., 2017b; Li et al., 2019; Shi et al., 2019; Supplementary material). Zuo et al. (2017) used CRISPR/Cas9 technology to introduce a four-nucleotide deletion in *S. exigua* P-glycoprotein (*ABCB1*) generating a truncated peptide in a *Se*P-gp (-/-) knockout strain. The susceptibility of mutated larvae to 12 insecticides were tested and showed that deletion of P-gp increased insecticide susceptibility against emamectin EB and abamectin, but not spinosad, chlorfenapyr, beta-cypermethrin, carbosulfan indoxacarb, chlorpyrifos, phoxim, diafenthiuron, chlorfluazuron and chlorantraniliprole, suggesting that P-gp might contribute to abamectin and EB excretion in *S. exigua*.

2.3. Gene expansion and detoxification capacity of *Spodoptera* species

It has been proposed that generalist herbivores exposed to a wide diversity of phytochemicals have expanded their palette of detoxification enzymes as an evolutionary requirement, allowing them to tolerate novel xenobiotics when expanding to newly colonized ecosystems (Heidel-Fischer and Vogel, 2015). This genomic plasticity is in most cases, if not always, embedded in the structural organizations of detoxification genes as many were shown to have expanded and originated from recent tandem duplications forming gene clusters. Although the underlying mechanisms triggering such blooms are still obscure, transposable elements (TE) have been shown to often arise in close proximity of clustered genes (Le Goff and Hilliou, 2017; Rostant et al., 2012) and evidence accumulates suggesting that increasing episodes of TE activity could have been an important source for gene duplication in hexapods (Roelofs et al., 2020).

Detoxification gene families have undergone prominent blooms over the course of evolution (Feyereisen, 2011; Ranson et al., 2002). The sequencing of both *S. litura* and *S. frugiperda* genomes have revealed large families of detoxification genes in comparison to the monophagous Lepidoptera *B. mori*, CYP genes for example are estimated twice as numerous in both *Spodoptera* species (Appendix A Table S1). Quite remarkable P450 blooms have occurred in this genus for a few families and seem to be restricted to CYP3 and CYP4 clans. Although P450 blooms are not restricted to a particular CYP clan (Dermauw et al., 2020) no P450 expansions were yet seen in the mitochondrial clan and CYP2 clan. In clan CYP3, the CYP6, CYP9, CYP321 and CYP324 families have seen expansions in both genomes compared to *B. mori* (Cheng et al., 2017b; Gouin et al., 2017) and the CYP6AE, CYP6B and CYP321 conserve their synteny across noctuid lineages. In FAW, the family *Sf*CYP340 of clan CYP4 encompasses 39 genes recently reported to be organized in one large cluster on chromosome 14 (Xiao et al., 2020) was also expanded in the genome of *S. litura* (Cheng et al., 2017b) and *Helicoverpa* species (Pearce et al., 2017). Xiao et al. (2020) further analyzed cluster organizations of P450s in the fall armyworm and found that a total of 163 P450 genes were mapped to its 23 chromosomes. Gene clusters can be dated by looking at their distribution in extinct species and conservation across closely related species or clades. The CYP6AE cluster is widespread in noctuid moths and has conserved its head to tail organization. The role of CYP6AE genes in detoxification has been extensively studied in *H. armigera*. Genome editing to knockout the *Ha*CYP6AE cluster resulted in increased susceptibility of insects to both plant toxins and

synthetic insecticides (Wang et al., 2018a). Individually expressing CYP6AEs in heterologous systems helped to identify candidate genes involved in xenobiotic metabolism. CYP6AEs showed distinct enzymatic activities towards tested compounds in particular: xanthotoxin was metabolized by CYP6AE19; 2-tridecanone by CYP6AE11, CYP6AE14, CYP6AE19 and indoxacarb by CYP6AE17 and CYP6AE18 (Wang et al., 2018a). As pointed out by Dermauw et al. (2020) there was no pattern between the catalytic activity, the phylogeny and the position on the cluster of these P450s suggesting that "there is a selective advantage to keep clusters as heritable units". The conserved CYP9A gene cluster in *Spodoptera* has been linked to PSM and insecticide tolerance (Boaventura et al., 2020b; Gimenez et al., 2020b; Giraudo et al., 2015). In *S. frugiperda* Giraudo et al. (2015) showed complex induction patterns of those P450s to 11 different xenobiotics implying the involvement of a complex regulation network. Figure 7 presents the number of induction occurrences across the literature from selected gene clusters in *S. litura* and *S. frugiperda*. The data collected here suggests that most CYP9A genes are inducible by xenobiotics. Although functional evidence for their role in insecticide and plant toxin metabolism is still scarce, a recent report demonstrated that CYP9A transcriptomic responses can match their metabolic capacity (Zuo et al., 2021). Induction patterns of clustered genes highlight the role of detoxification genes in xenobiotic response as heritable units advantageous when selected as functional units. Gimenez et al. (2020b) surprisingly found that the whole CYP9A cluster was present in two copies in a resistant Puerto Rico (PR) fall armyworm population, providing enhanced detoxification capability in this specific haplotype.

In *S. litura* 23 members from the large CEs gene family are split in two clusters on the chromosome 2 (Fig. 7). The genome of *S. frugiperda* was reported to contain 96 CEs, which is 24 more than in *B. mori*, with the notable expansion of clade 001, also found clustered (Gouin et al., 2017). *Spodoptera's* expanded gene families were enriched not only in phase I enzymes but also in phase II and transport systems, such as GSTs, UGTs and ABC transporters (Gouin et al., 2017). Huang et al. (2011) identified that three genes of the highly expanded *Sl*GST epsilon class were intronless, namely *GSTe1*, *GSTe2* and *GSTe3*, suggesting that these genes have duplicated by retrotransposition. Analysis of exon-intron relationships between interspecific lineages are of importance when it comes to establish gene evolution at specific loci (Gouin et al., 2017). Gouin et al. (2017) found patterns supporting lineage-specific expansions through tandem duplications of *Sf*UGT genes such as those of the UGT33 and UGT40 families.

A handful of these expansions were shown to be specific to Lepidoptera (Wang et al., 2014). For the CYP9As, the expansion specificity might even be stronger as it seems to be restricted to the Noctuid lineage only *i.e.,* there are 15 CYP9A genes in *S. frugiperda*, eight in *H. armigera* and *H. zea* compared to four in monophagous *B. mori*, while none were found in the cruciferous specialist *P. xylostella*. The size of the detoxification gene families in that respect has been argued to be linked to polyphagia and the ability of insects to easily develop insecticide resistance, although this is still debated (Dermauw et al., 2018; Feyereisen, 2011; Rane et al., 2019; Rane et al., 2016). The data gathered in this work shows that genes organized in clusters respond, to a great extent, frequently to xenobiotic exposures which may indicate an adaptation of *Spodoptera* species to common ecological and metabolic challenges, with a particular emphasis on their ability to cope with plant metabolites and probably to insecticides as well (Fig. 7). In that prospect it would be of great interest to analyze xenobiotic responses of more specialized *Spodoptera* species and sequence their genomes in order to compare detoxification gene family organizations, promoter regions and introns for transcription factor binding sites.

Part III – Transcriptional regulation of detoxification genes in insects

Large parts of this section have been published as Amezian D, Nauen R & Le Goff G (2021b) Transcriptional regulation of xenobiotic detoxification genes in insects - An overview. Pestic Biochem Physiol 174: 104822. doi:10.1016/j.pestbp.2021.104822.

Possessing an arsenal of detoxification tools is of little use if an adverse effect mediated by a chemical cannot be detected and addressed by appropriately deploying the enzymes that will circumvent the adverse effects of xenobiotics. As exemplified by the expression data presented in the previous section, *S. frugiperda* genes encoding for enzymes and transporters involved in detoxification are coordinately induced upon exposures to toxicants or sometimes even constitutively overexpressed in populations under continuous insecticide pressure, which implies the existence of pathways of gene regulation finely tuned to ensure an adequate response. The potency and duration of gene induction depends on xenobiotic concentration and time of exposure. Xenobiotics as inducing agents and/or substrates tend to trigger particularly the upregulation of large sets of genes remotely involved in their detoxification. Transcriptional regulation is commonly driven by *cis*-regulatory elements (*cis*-acting), short sequences located within the promoter region, onto which specific transcription factors bind (*trans*-acting) and further recruit the transcriptional machinery (Guo et al., 2018). In mammals, induction of detoxification and oxidative stress response genes is mediated by three main transcription factor superfamilies: the nuclear receptor superfamily such as pregnane X receptor (PXR), the constitutive androstane receptor (CAR); the basic helix–loop–helix (bHLH)-PAS domain transcription factors superfamily including aryl hydrocarbon receptor (AhR)/AhR nuclear translocator (ARNT) and the NF-E2-related factor family belonging to the wider group of basic leucine zipper (bZIP) transcription factors comprising a conserved CNC domain (e.g. NF-E2-related factor 2 - Nrf2) (Basak et al., 2017; Hankinson, 1995; Higgins and Hayes, 2011; Nakata et al., 2006; Pascussi et al., 2008; Sykiotis and Bohmann, 2010; Vorrink and Domann, 2014). In arthropods however, the mechanisms underlying the regulation of enhanced enzymatic metabolism of plant secondary metabolites (PSM) or insecticides are still poorly understood and most of what is known has been elucidated only recently (Fig. 8). Indeed, recent work using advanced genetic methods in insecticide-resistant

arthropod species is starting to close this gap. To date, five main pathways have been described from various insect species to lead to transcriptional activation of detoxification genes, including the G protein-coupled receptors (GPCRs), AhR/ARNT, the hormone receptor-like in 96 (HR96), the CncC/Maf and the mitogen-activated protein kinase (MAPK) and cAMP-response element binding protein (CREB protein) pathway (Fig. 8) (reviewed in Amezian et al. 2021). In this Part, I will further focus on the CncC/Maf pathway.

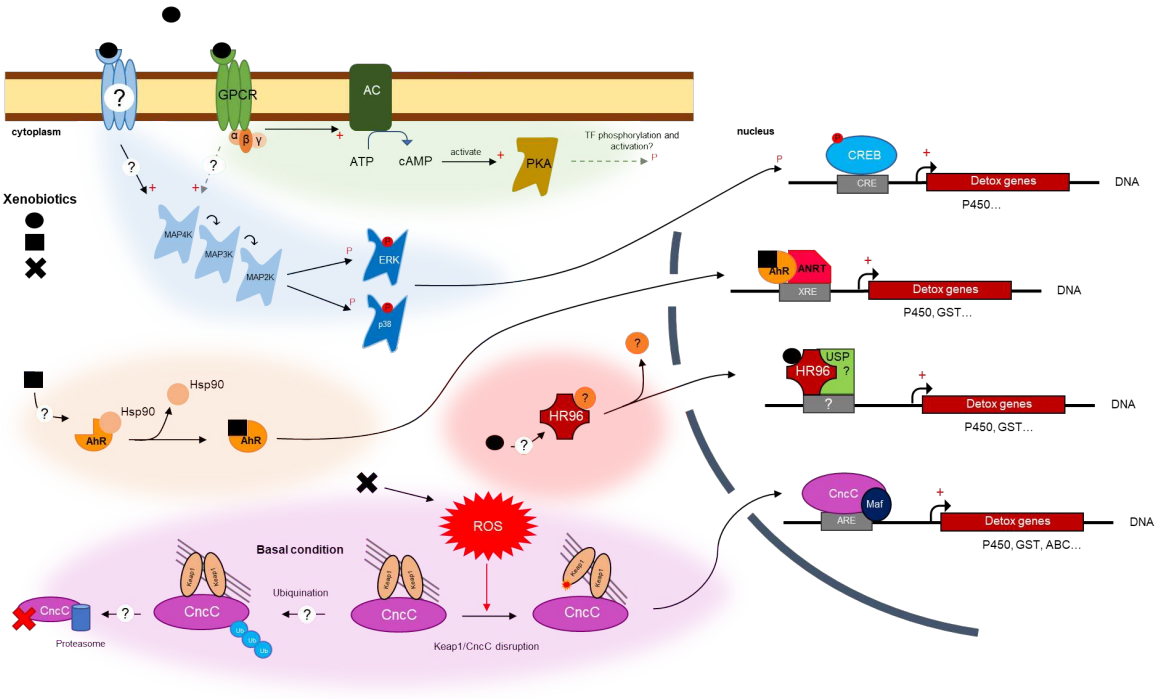

Fig. 8 Pathways of transcriptional regulation of insect detoxification gene expression.
To date, five signaling pathways leading to the transcriptional regulation of detoxification genes involved in plant compounds metabolism and insecticide resistance have been described to various degrees: the GPCR signaling pathway (green), the MAPKs-CREB pathway (blue), the AhR/ARNT pathway (orange), the HR96 pathway (red) and the CncC/Keap1 pathway (purple). Source: Amezian et al. 2021.

3.1. The Keap1/CncC pathway

Among all pathways recently revealed to be involved in the regulation of detoxification genes, the Cap´n´collar isoform C/Kelch-like ECH associated protein 1 (CncC/Keap1) pathway is the one that has sparked most interest within the scientific community over the past few years. An increasing body of work in multiple insect species has identified and clarified the role of CncC as the “master regulator” of gene transcription coding for enzymes involved in xenobiotic and oxidative stress response (Fig. 8). CncC has been linked to resistance phenotypes observed in field populations of insect pests and disease vectors as well as shown

to be specifically involved in the induction of detoxification and resistance-associated genes (Palli, 2020; Wilding, 2018).

CncC is the orthologue of the mammalian NF-E2-Related Factor 2 (Nrf2) which belongs to the basic leucine zipper (bZIP) family of transcription factors. It is part of a major signaling pathway that plays a central role in regulation of cytoprotective genes addressing xenobiotic and oxidative stresses (Hirotsu et al., 2012; Nguyen et al., 2009; Suzuki and Yamamoto, 2015).

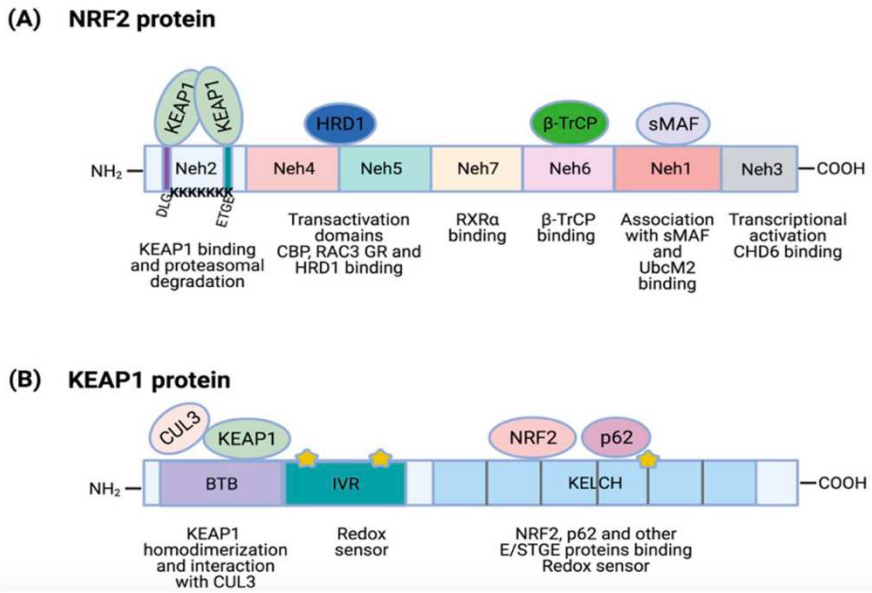

Fig. 9 Structures of Nrf2 and Keap1 proteins in mammals – Source: Sanchez-Ortega et al. 2021 (Figure 2).
(**A**) Nrf2 contains 7 highly conserved domains called Neh domains. Neh1 is required for complex formation with transcription factor sMaf, DNA binding and for binding to the ubiquitin-conjugating enzyme M2 (UbcM2). Neh2 contains ETGE and DLG sequences that are required for Keap1 binding and 7 ubiquitin-lysine residues for targeting Nrf2 for proteasomal degradation. Neh3 is needed for transcriptional activation (binding with CHD6, a chromo-ATPase/helicase DNA binding protein). Neh4 and Neh5 are transactivation domains that bind activators (CREB-binding protein (CBP), receptor-associated co-activator 3 (RAC3)) or repressors (glucocorticoid receptor (GR), HMG-CoA reductase degradation protein 1 (HRD1)). Neh6 regulates Nrf2 stability by binding to β-transducin repeat-containing protein (β-TrCP) that promote Nrf2 poly-ubiquitination. Finally, Neh7 can interact with retinoic X receptor α (RXRα), a Nrf2 repressor. (**B**) Keap1 protein contains 5 conserved regions: N-terminal region, BTB domain (Broad-Complex, Tramtrack and Bric a brac domain), intervening region (IVR) region, DGR domain and C-terminal regions form a Kelch motif. The BTB domain facilitates Keap1 homodimerization and binding with Cullin3-based E3 ubiquitin ligase (CUL3) which promotes the proteasomal degradation of Nrf2. The IVR possesses a cysteine-rich domain that acts as a direct redox sensor. Double-glycine repeat (DGR)/Kelch regions contains 6 repeats of a Kelch motif that mediate their interaction with Nrf2 and other proteins with E/STGE conserved motifs, such as p62 This region also contains additional cysteine residues for stress sensing. Stars represent several cysteine residues located in IVR and Kelch domains.

Under basal conditions Nrf2 is retained in the cytoplasm by its major repressor, the cytoskeletal Keap1. When binding selectively to Nrf2, Keap1 forms a protein complex with Cullin3-based E3 ubiquitin ligase which activity promotes the proteasomal degradation of Nrf2 (Fig. 8 and Fig. 9). In mammalian models Keap1 was identified as a sensor of electrophiles and reactive oxygen species (ROS), by means of specific cysteine residues (Fig. 9). ROS are highly

reactive dioxygen-derived molecules such as peroxide, superoxide and singlet-oxygen that play an important role in cell signaling and homeostasis (Pardini, 1995). Upon oxidative stress, electrophiles and ROS react with Keap1 cysteine sulfhydryl groups inducing conformational changes in Keap1 ultimately leading to the release of Nrf2. Nrf2 then quickly translocates to the nucleus where it dimerizes with its partner small Muscle aponeurosis fibromatosis (Maf, a bZIP transcription factor) to mediate both base-level and inducible expression of Antioxidant Response Element (ARE)-responsive genes (Kensler et al., 2007). The structure of Nrf2 and the role of each of its Neh domains in protein-protein and DNA-protein interaction is well studied in mammals (Fig. 9 and Fig. 10) (Sanchez-Ortega et al., 2021). In particular, *Nrf2* and *Keap1* have been heavily studied for their pro-oncogenic properties. Indeed, there is growing evidence indicating that altered *Nrf2* and *Keap1* genes, leading to the pathway activation are involved in the generation and progression of many tumor types as well as resistance to chemotherapy (Basak et al., 2017; Sanchez-Ortega et al., 2021).

In arthropods, CncC is suspected to have multiple roles and intervene in biological processes such as development, maintenance of proteostasis and stress response (Deng, 2014; Deng and Kerppola, 2013; Mao et al., 2020; Pitoniak and Bohmann, 2015). More importantly it has recently been shown to have a role in the constitutive activation of detoxification pathways leading to metabolic resistance (Hu et al., 2019b; Misra et al., 2013; Shi et al., 2017). However, the information available on the mechanisms underlying CncC/Keap1-mediated regulation of xenobiotic response in invertebrates is still scarce.

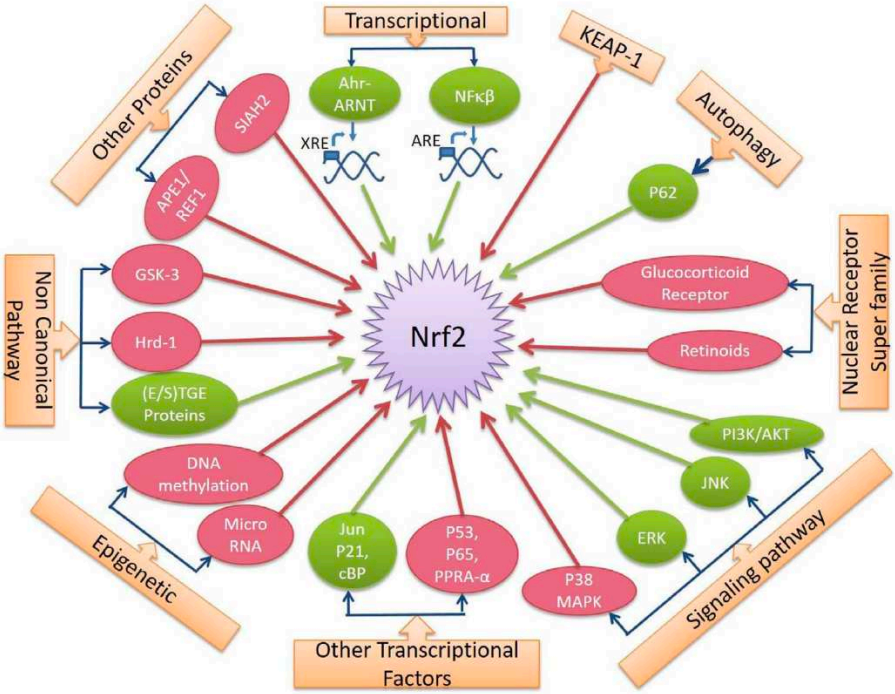

Fig. 10 Regulations of Nrf2 by several factors. Source: Bazak et al. 2017 (Figure 2).
The green color indicates upregulation of Nrf2 activity and the red color indicates downregulation of Nrf2 activity.

Earlier studies on the fruit fly showed that the CncC/Keap1 pathway regulates 70 % of the genes induced by PB including P450s and GSTs, and that its ectopic activation in mutant *Drosophila* flies was sufficient to confer resistance to the insecticide malathion (Misra et al., 2011). The same authors showed in another study that the CncC/Keap1 pathway was constitutively activated in two DDT-resistant *Drosophila* strains (RDDTR and 91R) along with the overexpression of genes coding for putative DDT-detoxifying enzymes such as *DmGSTd1*, *DmCYP6A2* and *DmCYP6A8* (Misra et al., 2013). This work paved the way to the discovery that the CncC/Keap1 pathway is indeed involved in mediating metabolic resistance to insecticides in several insect pest species. Wan et al. (2014) demonstrated that DDT resistance in strain 91R of *D. melanogaster* was genetically linked to a CncC:Maf binding site in the *DmCYP6A2* gene promoter region. The CncC/Keap1 pathway was shown to be involved in resistance to deltamethrin in *D. melanogaster* and *T. castaneum* (Kalsi and Palli, 2015, 2017a; Liu et al., 2020), to imidacloprid in the Colorado potato beetle (CPB) *Leptinotarsa decemlineata* and the brown planthopper *Nilaparvata lugens* (Gaddelapati et al., 2018; Kalsi and Palli, 2017b; Tang et al., 2020) as well as to chlorpyrifos and cypermethrin in *S. exigua* (Hu et al., 2019b; Hu et al., 2020a). CncC was also linked to abamectin resistance in olive fruit fly *Bactrocera dorsalis* (Tang et al., 2019), fenpropathrin resistance in the carmine spider mite *Tetranychus*

cinnabarinus (Shi et al., 2017) and indoxacarb resistance in *S. litura* (Shi et al., 2020). Studies on *Anopheles gambiae* showed that the transcription factor Maf-S regulates the expression of *CYP6M2* and *GSTd1*, conferring resistance to pyrethroids and DDT (Ingham et al., 2017). Upregulation of multiple P450s and GSTs in the silkworm *B. mori* were also reported to be mediated by the CncC/Keap1 pathway (Hu et al., 2018; Mao et al., 2019; Wang et al., 2020). Tolerance to the plant secondary metabolite gossypol was shown to be mediated by the activation of this pathway in the cotton aphid, *A. gossypii*, and resulted in overexpression of *CYP6DA2* (Peng et al., 2016).

Most studies mentioned above reported that subsets of P450- and GST-encoding genes when found upregulated in these resistant strains were observed downregulated after RNAi-mediated knockdown of *CncC* and/or *Maf*, suggesting that their overexpression is controlled by CncC (Chen et al., 2018a; Gaddelapati et al., 2018; Ingham et al., 2017; Kalsi and Palli, 2015, 2017a, b; Liu et al., 2020; Lu et al., 2020; Peng et al., 2016; Shi et al., 2020; Shi et al., 2017; Tang et al., 2020). Knockdown of the transcription factors lead to increased susceptibility to insecticides in treated insects, showing that CncC/Keap1-mediated constitutive activation of detoxification enzymes was involved in the resistant phenotypes. Kalsi and Palli (2017a) further investigated the role of six genes identified as CncC targets in the red flour beetle *T. castaneum*. RNAi-mediated knockdown of the detoxification genes coupled to bioassays using pyrethroids confirmed the role of *TcCYP4G7*, *TcCYP4G14*, *TcGST-1* and four ABC transporters, *TcABCA-UB*, *TcABCA-A1/L*, and *TcABCA-9B* in insecticide sensitivity. In another study conducted by the same group, but on *L. decemlineata*, three ABC transporters, *ABCH278B*, *ABCH278C*, and *ABCG1041A* supposed to be critical for its tolerance to imidacloprid were shown to have their expression driven by the CncC/Keap1 pathway (Gaddelapati et al., 2018). In addition to ABC transporters, four P450s were previously reported to be involved in imidacloprid resistance in CPB (Zhu et al., 2016a) and shown to be overexpressed under the control of the same transcription pathway (Kalsi and Palli, 2017b).

Table 2 Selected transcription Factor Binding Sites (TFBS) in insect detoxification genes promoters.

TF	Species	Sequence	Gene	Reference
CncC/Maf	*D. melanogaster*	5'-TGACcggGC-3'	GSTd1	Sykiotis and Bohmann, 2008
		5'-TCAgcATGACcggGCAaaaa-3' (extended ARE)	GSTd1	Sykiotis and Bohmann, 2008
		5'-TGCGTAGTCAT-3'	CYP6A2	Misra et al., 2011
		5'-TGCGTAGTCAT-3'	CYP6A2	Wan et al., 2013
		5'-nGCnnnnTCAn-3'	-	Lacher et al., 2015
	A. gossypii	*ND*	CYP6DA2	Peng et al. 2017
	S. litura	5'TGACAAGGC-3'	GSTE1	Chen et al., 2018
	S. exigua	5'-GATGACAATACAACA-3'	CYP321A16	Hu et al. 2020
		5'-AATGACAAGGCAAA-3'	GSTe6	Hu et al., 2019b
	L. decemlineata	5'-GCAGAAT-3'; 5'-GTACTGA-3'	CYP9Z25	Kalsi and Palli, 2017
	T. castaneum	5'-GCAGTAC-3'	CYP6BQ family	Kalsi and Palli, 2015
AhR/ARNT	*A. gossypii*	*ND*	CYP6DA2	Peng et al. 2017
	P. polyxenes	3'-CTCGCAAGCA-5'	CYP6B1v3	Hung et al., 1996; Petersen et al., 2001, 2003; Li et al., 2002; Brown et al., 2004, 2005; McDonnel et al., 2004
		5'-TGGCGTG-3' ; QTCGCAAGGCA-3'	CYP6B3v2	
	P. glaucus	5'-CACGCAAGCA-3'	CYP6B4v2	
		5'-CACCCAAGCA-3'	CYP6Bv51	
	H. armigera	5'-CATGACACCTG-3'	CYP6B6	Li et al., 2014a
	S. exigua	5'-CACGCGATG-3'	GSTe6	Hu et al., 2019b
	B. tabaci	5'-TGATTGATC-3'	CYP6CM1	Yang et al. 2020

The CncC:Maf heterodimer binds to ARE elements in the upstream region of target genes. AREs are required for CncC:Maf-mediated xenobiotic-induced increased expression of these genes. Although Transcription Factor Binding Sites (TFBS) are species-specific for transcription factors exhibiting conserved functions in different species, there was substantial conservation between the consensus sequence identified for Nrf2:Maf in mammals and CncC:Maf in insects (Clark et al., 2007). This similarity allows for computational-based TFBS discovery in different insect species, however functional identification of AREs needs experimental validation. Promoter constructs of detoxification genes in reporter assays have been used *in vitro* and *in vivo* to functionally link CncC:Maf transducing activity to binding with ARE motifs. Mutagenesis in the putative ARE or progressive truncation of promoters can help to characterize the transcriptional response of detoxification genes mediated by the CncC/Keap1 pathway. Kalsi and Palli (2015) identified ARE motifs in multiple *T. castaneum CYP6BQ* promoters that were necessary to mediate the CncC:Maf regulation of these genes. Using a luciferase reporter assay with truncated *L. decemlineata* (*Ld)CYP9Z25* promoter constructs and directed mutagenesis (Kalsi and Palli, 2017b) identified two binding sites (*i.e.* 5'-GCAGAAT-3' and 5'-GTACTGA-3') for CncC:Maf inducibility (Table 2).

The knowledge of the CncC:Maf binding sites in different species allows a retrospective look at unknown *cis*-acting elements found in earlier studies on allelochemical-responsive detoxification gene promoters. For instance, the promoters of *PpCYP6B1* and *PgCYP6B4* (see above) revealed an additional 18-bp region termed XRE-xan directly flanking an ecdysone response element (EcRE) and overlapping with an antioxidant response element (EcRE/ARE/XRE-xan; 5'-AAGACA/ATGACTGGCA/ATTTTTTTT-3'). It was found responsible for the induced expression of *PpCYP6B1* and *PgCYP6B4* upon xanthotoxin exposure (Brown et al., 2004; Brown et al., 2005; Petersen et al., 2003; McDonnell et al., 2004). Further deletion experiments showed that the EcRE/ARE/XRE-xan motif mediated induction by both xanthotoxin and benzo[α]pyrene and is needed to obtain the strongest expression (Brown et al., 2005). The identity of the transcription factor that bound this motif remains unknown although it might interact with the often-occurring AhR/ARNT element located downstream (Brown et al., 2005; McDonnell et al., 2004). It would be interesting to know whether the CncC/Keap1 regulation pathway is involved in the transcriptional response of *PpCYP6B1* and *PgCYP6B4* to naturally occurring plant allelochemical in the *Papilio* genus. Another study identified an allelochemical response element responsive to flavone, termed XRE-fla, in the promoter region of the insecticide- and phytotoxin-metabolizing *CYP321A1* from *Heliothis zea* (Zhang et al., 2010). This XRE-fla motif was composed of two reversely orientated, overlapping ARE-like motifs which the authors interpreted as potentially being the binding site of CncC:Maf. This hypothesis remains to be validated, although partially supported by an electron mobility shift assays (EMSA) performed on nuclear extracts prepared from flavone-induced *H. zea* fat body cells.

Although the precise mechanisms underlying the initiation of the CncC/Keap1 transcription pathway in insects is not fully understood, it seems that they are conserved with those determined in mammals. Indeed, recent work on *S. exigua* and *S. litura* has pointed out the role of ROS in activating the CncC/Keap1 pathway. In *S. litura*, *CYP6AB12* is a midgut-specific P450 enzyme involved in pyrethroid tolerance (Lu et al., 2020; Lu et al., 2019b). Exposing insects to λ-cyhalothrin induced the expression of *SlCYP6AB12*, CncC and Maf in the midgut as well as triggered H_2O_2 accumulation. Silencing *CncC* by RNAi suppressed *SlCYP6AB12* expression and reduced larval tolerance to λ-cyhalothrin. Similarly, the use of N-acetylcysteine (NAC), a ROS scavenger, reduced H_2O_2 accumulation, suppressed *CncC*, *Maf* and *SlCYP6AB12* overexpression while increasing the susceptibility of insects to λ-cyhalothrin

(Lu et al., 2020). *Sl*GSTe1 catalyzes the conjugation of a variety of xenobiotics including the plant secondary metabolites xanthotoxin, indole-3-carbinol and allyl-isothiocyanate and the insecticides chlorpyrifos, deltamethrin, malathion, phoxim and DDT (Huang et al., 2011; Xu et al., 2015; Zhang et al., 2016a; Zou et al., 2016). Chen et al. (2018a) demonstrated that *Sl*GSTe1-dependent metabolism of chlorpyrifos and indole-3-carbinol was mediated by ROS and the CncC/Keap1 pathway. Both xenobiotics induced an increase in ROS content as well as transcript levels of *GSTe1* and *CncC* of a *S. litura* cell line. *SlGSTe1* contains an ARE element in its promoter region suggesting it is one of CncC:Maf target genes. This suggested that the xenobiotics-induced ROS promoted the expression of *CncC* and *SlGSTe1*. This is supported by the fact that the use of NAC prevented ROS formation and suppressed the induction of *CncC* and *SlGSTe1*, thus suggesting that activation of the CncC/Keap1 pathway is mediated by ROS accumulation (Chen et al., 2018a). Likewise, in *S. exigua* λ-cyhalothrin, chlorpyrifos and chlorantraniliprole were responsible for ROS bursts and the induction of several GSTs, including *SeGSTe6*, *SeGSTo2*, and *SeGSTd3*. These GSTs were identified as detoxification genes involved in resistance to chlorpyrifos and cypermethrin in *S. exigua* (Hu et al., 2019b). The authors identified the CncC:Maf binding site in the promoters of all seven GST genes upregulated by insecticide treatments. Subsequent reporter assays showed that this motif was necessary to obtain the increased expression of the GSTs after exposure to insecticides. The promoter of *SeGSTe6* was cloned and shown to be responsive to CncC in a luciferase reporter assay. Several mutations in the promoter further identified the CncC:Maf binding site in *SeGSTe6* promoter region (Hu et al., 2019b). Co-treatments of insecticides and NAC decreased the insecticide-induced luciferase activity of the *SeGSTe6* promoter construct, indicating that ROS intervene in the CncC-mediated signaling response to insecticides resulting in *SeGSTe6* induction (Hu et al., 2019a). Hu et al. (2020a) also found a conserved CncC:Maf binding site in the promoter region of two chlorpyrifos-metabolizing P450s, *SeCYP321A16* and *SeCYP332A1*. Successive truncations of the promoter combined with a luciferase reporter assay demonstrated that it was responsible for their constitutive overexpression and the resistance to chlorpyrifos observed in the *S. exigua* strain. In a recent study investigating indoxacarb resistance in *S. litura*, an RNA-seq analysis performed after RNAi-mediated silencing of *CncC* revealed that 842 and 127 genes were down- and up-regulated, respectively (Shi et al., 2020). Out of those 842 downregulated genes, 18 genes were identified as detoxification enzymes. Among the latter, six were associated with indoxacarb resistance, *i.e.*

could be induced by the insecticide and contained the CncC:Maf binding site in their promoter region, as predicted by a computational analysis. Very much alike the experiments conducted by Misra et al. (2011, 2013) the RNA-seq study demonstrated that xenobiotics are able to induced a very large number of genes by activating the CncC/keap1 pathway, genes of which many have unknown functions and only a small fraction are involved in xenobiotic metabolism and transport. This questions the specificity of this pathway, partly supported by its reliance on ROS which are involved in both redox signaling, and thus responsible for mediating fundamental biological processes and in oxidative stress causing lipid degradation and DNA damage.

The CncC/Keap1 pathway is undoubtedly an important route driving detoxification gene expression in response to xenobiotics in insects, yet further work needs to be carried out to clarify the remaining aspects of this response.

Objectives

S. frugiperda has well adapted to the variety of toxic compounds found in its environment. Detoxification of toxicants is at the core of its adaptation to many host plants species as well as the development of insecticide resistance. CncC has recently emerged as a "master regulator" of detoxification genes in other insect pest species. This highlights the importance of investigating the role of CncC in xenobiotic response to better understand the mechanisms underlying adaptation to host plants in herbivorous insects and development of metabolic resistance in insects.

Therefore, the overall goal of my research project was to characterize the role of the CncC:Maf transcription pathway in the regulation of detoxification genes of *S. frugiperda* by using its cellular model, Sf9 cells.

The goal and objectives of my work are:

1) Characterize the mechanism involved in detoxification genes induction after exposure of Sf9 cells to xenobiotics, one plant secondary metabolite, and one insecticide.

In Chapter 1, I aimed at identifying detoxification the genes that are inducible by sublethal doses of xenobiotics and determining the involvement of the CncC:Maf pathway in this induction.

2) Development of a cell-based assay format using reverse genetic methods to i) characterize the role of the CncC:Maf pathway in oxidative stress and xenobiotic response and ii) to screen for CncC-mediated modulation of detoxification gene expression.

In Chapter 2, I aimed at establishing two antagonistic Sf9 phenotypes, respectively overexpressing and knockdown for the CncC transcription factor. I used these two types of cell lines to investigate the role of CncC in cell xenobiotic tolerance, enzymatic activity of main detoxification family enzymes and modulation of in-cell ROS content.

In Chapter 3, my goal was to identify the metabolizing genes (*i.e.* phase I, phase II and phase III genes) regulated by CncC:Maf transcription factors by using a transcriptomic analysis of the cell lines established in the previous chapter.

CHAPTER 2

This chapter has been submitted as “Amezian D.; Mehlhorn S., Vacher-Chicane C., Nauen R., Le Goff G. (2022). Using Sf9 cells to decipher the role of detoxification enzymes in xenobiotic adaptation in the pest Spodoptera frugiperda” to *Chemosphere*

INTRODUCTION

Spodoptera frugiperda is a polyphagous insect exposed to many toxic compounds due to its wide host plant range. It must develop and adapt a response to render these compounds less toxic and eliminate them from its body. Detoxification enzymes play a major role in these processes as well as in insecticide resistance. These enzymes are often expressed at a basal level and induced when the insect is exposed to xenobiotics, whether they are secondary plant metabolites or insecticides. To determine how *S. frugiperda* adapts to the xenobiotics it encounters in its environment, I used its cellular model, the Sf9 cells. The objective of this first chapter was to determine the detoxification response that the cells deploy using a representative molecule of plant secondary metabolites and one of insecticides. The transcription factor CncC was shown to be a “master regulator” of detoxification, initially in *Drosophila* (Misra et al., 2011) but since then in several other insect species (Hu et al., 2021; Kalsi and Palli, 2015, 2017b; Lu et al., 2021a). I sought to explore the role of this factor in the establishment of the detoxification response in Sf9 cells.

The choice of the inducer compounds was based on a previous study from our lab that analyzed the toxicity and xenobiotic response of plant allelochemicals and insecticides towards Sf9 cells (Giraudo et al., 2015). Indeed, while most insecticides and plant secondary metabolites are toxic to *S. frugiperda* insects, some molecules will have no effect on Sf9 cells as they are likely not expressing the targets. Pyrethroids such as cypermethrin and deltamethrin for example form a class of insecticides to which *S. frugiperda* has developed strong resistance (Boaventura et al., 2020b; Gimenez et al., 2020b; Gutierrez-Moreno et al., 2019). These insecticides target the voltage gated sodium channel (VGSC) which is probably

not expressed in Sf9 cells as deltamethrin has no toxicity on the cells and cypermethrin has an IC_{50} above 450 µM (Le Goff, personal communication).

In 2015, my colleagues found that three out of the five plant allelochemicals tested, *i.e.* indole, indole 3-carbinol and 2-tridecanone triggered a xenobiotic response in Sf9 cells as shown by the induction of one, two and seven CYPs genes, respectively. Although 2-tridecanone was the most potent inducer of P450 genes, it also exerted weaker toxicity than its two indole counterparts.

Indole and indole 3-carbinol (I3C) are naturally occurring glucosinolate break-down products found in cruciferous vegetables and are phytochemicals that prevent insect herbivory (Muller et al., 2010). Earlier studies reported that I3C had the ability to suppress the proliferation of various cancer cell lines by reducing oxidative stress and promoting the expression and activity of antioxidant enzymes such as hemoxygenase-1 (HO-1) and glutathione S-transferases (Trusov et al., 2010). In mammals, I3C was shown to target a wide spectrum of signaling pathways including the Nrf2/ARE pathway (Ahmad et al., 2013; Fuentes et al., 2015; Hajra et al., 2018).

On the other hand, methoprene (MTP) induced seven P450s and was the insecticide that exerted the most potent response in Sf9 cells (Giraudo et al., 2015). MTP is a juvenile hormone analog (JHA) which acts as a growth regulator, delaying the insect's growth and inhibiting pupation. Previous studies have linked the CncC:Maf pathway to the regulation of genes involved in 20-hydroxyecdysone (20E) synthesis (Deng and Kerppola, 2013) and shown MTP to downregulate genes involved in 20E action (Bai et al., 2010).

I therefore chose to further investigate the xenobiotic response of Sf9 cells towards I3C and MTP and whether this response is mediated by the CncC:Maf pathway.

I monitored the xenobiotic response of Sf9 cells by following the expression of selected detoxification genes. Among the CYP genes most often induced in Sf9 cells from Giraudo et al. (2015) were four CYP9As, including *CYP9A24*, *CYP9A30*, *CYP9A31* and *CYP9A32*. We have recently reviewed the occurrences of detoxification gene induction by xenobiotics in four *Spodoptera* species (Amezian et al., 2021a). CYP9A P450s were found over-expressed in several other studies (Carvalho et al., 2013; Cheng et al., 2017b; Hafeez et al., 2019a; Hu et al., 2019c; Wang et al., 2018b; Wang et al., 2016; Zhou et al., 2012a). We highlighted the

overexpression of *CYP321A9* (found 9 times) as well as *CYP4M14* and *CYP4M15*, differentially expressed after exposure to xenobiotics such as ricin, fluralaner and xanthotoxin. Finally, *GSTe1* was chosen as it was the glutathione S-transferase (GST) gene found most often upregulated across the literature (Amezian et al., 2021a). More importantly, GSTe1 in *Spodoptera litura* (*Sl*) was shown to catalyzes the conjugation of a variety of xenobiotics including the plant secondary metabolite I3C (Chen et al., 2018b; Zou et al., 2016). In addition, *SlGSTe1* contains an ARE element in its promoter region suggesting it is one of CncC:Maf target genes.

In this chapter we tested whether the selected detoxification genes, the transcription factors *CncC* and *Maf* as well as CncC's repressor *Keap1* are inducible by sublethal doses of I3C and MTP in Sf9 cells. To determine whether the detoxification genes were controlled by the CncC:Maf pathway we transiently expressed *CncC* and *Maf* and monitored their level of expression by RT-qPCR.

MATERIALS & METHODS

Chemicals and products

Ethanol, chloroform and isopropanol were purchased from VWR International (Rosny-sous-bois, France). Fetal Bovine Serum (FBS) was from Invitrogen (Villebon-sur-Yvette, France). All other products were from Sigma-Aldrich Chimie (Saint-Quentin Fallavier, France) unless stated otherwise.

Cells and cell culture

Sf9 cells were maintained as adherent cultures at 27°C in Insect-XPRESS serum free medium (Lonza, France) and passaged every third day. Cell density was determined by Malassez haemocytometer (Marienfeld, Germany) counts and cell viability was evaluated by Trypan blue (1 mg/ml, v/v) staining.

Cell viability assays

MTT

Viable cells were determined by measuring the conversion of the tetrazolium salt MTT to formazan induced by mitochondrial succinate dehydrogenase, as previously described (Fautrel et al., 1991). MTT assays were performed in serum-free Insect-XPRESS media (IX). Prior to experiments cells were seeded onto 96-well plates (Techno Plastic Products AG, Switzerland) at 2.10^5 cells/ml and incubated for 24 h at 27°C. Cells were then treated for 24 h with increasing concentrations of I3C (10, 50, 100, 200, 350, 500 µM) and MTP (25, 75, 100, 150, 300 µM) or DMSO as a control. Each concentration was applied in three wells. All MTT assays were done for three independent, biological replicates. After 24 h, the medium was removed and cells were loaded with MTT (5 mg/ml final concentration in IX) and incubated at 27 °C for 2 h. Formazan crystals from cell homogenates were solubilized in 100 µl DMSO and used to measure absorbance at 570 nm using a microplate reader (SpectraMax 382, Molecular Devices, USA). Viability was expressed as a percentage of the maximum viability obtained in DMSO treatment.

Transient overexpression of *CncC* and *Maf* transcription factors in Sf9 cells

Plasmid constructions

RNA extracted from *S. frugiperda* larvae midguts was used to synthesize cDNA which served as template for *CncC* and *Maf* amplification. Two primer pairs were designed to amplify *CncC*, and one pair to amplify *Maf*, using the genomic sequences retrieved from the genome (v3.0) on BIPAA (bipaa.genouest.org, (Gouin et al., 2017)) and customized to introduce restriction enzymes sites (PR1-6 Table 1). *CncC* was amplified with two successive runs using overlapping primers and a high fidelity PrimeSTAR® polymerase (Takara Bio Europe, France) on a MJ Research Tetrad PTC-225 Thermal Cycler (GMI, USA). PCR products were purified using the GenElute™ PCR Clean-Up kit (Sigma-Aldrich, France) and the purity was assessed using NanoDrop™. The BglII/NotI digested PCR amplicons of *CncC* and *Maf* were subcloned into the BglII/NotI linearized pBiEx™ Expression Vector (Novagen, Germany) at 20:1 and 3:1 (w/w) ratios using a T4 DNA Ligase (Roche, Germany). The pBiEx-Maf and pBiEx-CncC products were subsequently transformed into Subcloning Efficiency™ DH5α™ Competent Cells (Life Technologies, Germany) according to the supplier's instruction. Successfully transformed bacterial colonies were screened by direct PCR using GoTaq® DNA Polymerase (Promega, France) and PR7 and PR8 primers (Table 1). Finally, plasmids were isolated using the

GenElute™ Plasmid Miniprep Kit (Sigma-Aldrich, France). All recombinant constructs were confirmed by Sanger sequencing (GENEWIZ, Germany).

Transient expression of CncC and Maf in Sf9 cells

Transient expression of target genes was performed by transfection of the expression vector pBiEx-1™ using FUGENE® transfection reagent (Life Technologies, Germany) according to the manufacturer's instructions. Briefly, Sf9 cells were seeded onto six-well plates at 1.10^6 cells/ml and incubated at 27°C for 24h prior to transfection. In each well, adherent cells were transfected with 2 µg expression vector DNA. The plasmid DNA and 3 µl FUGENE® transfection reagent were incubated 15 min in 100 µl of Insect-XPRESS medium at room temperature prior to be diluted to a final volume of 1 ml of Insect-XPRESS medium supplemented with 10% FBS. Cells were transfected with either a single expression plasmid construct, *i.e.* pBiEx:CncC or pBiEx:Maf, or transfected with both expression vectors in equal proportions. An empty vector was used to transfect control cell lines. Each transformation condition was replicated three times, *i.e.* in three different wells. Cells were incubated for 24, 48 and 72 hours at 27°C after what cells were collected for RNA extraction.

RNA extractions, cDNA synthesis and RT-qPCR

For induction assays, cells were seeded onto six-well plates at 2.10^5 cells/ml and incubated 24 h at 27°C for adhesion. Plated Sf9 cells were then treated for 24 h with sublethal doses of I3C (40, 58 and 74 µM) and MTP (50, 65 and 74 µM) or the equal volume of DMSO, which served as control. Induction doses were chosen at the IC_{10}, IC_{20}, IC_{30} which represents the inhibition concentration to 10, 20 and 30 % of the cells, respectively, as established by cytotoxicity assays. 24 h post-treatment cells from each well were washed with 1 ml DPBS and total RNA was extracted using 1 ml TRIzol Reagent (Life Technologies, Germany) according to the manufacturer's protocol.

RNA from cells transiently expressing CncC and Maf was extracted 24, 48 and 72 h post-transfection. Transfected cells were washed twice in 1 ml DPBS and RNA was extracted using 1 ml TRIzol Reagent (Life Technologies, Germany) following manufacturer's instruction.

Total RNA (500 ng) was reverse transcribed using the iScript cDNA Synthesis kit (Bio-Rad, France) following the manufacturer's guidelines. Real-Time quantitative (RTq)-PCR reactions were carried out on an AriaMx Real-Time PCR system (Agilent technologies, USA) using qPCR

Mastermix plus for SYBR Green I no ROX (Eurogentec, Belgium). The PCR conditions were as follows: 10 min at 95 °C, 40 cycles of 5 s at 95 °C and 30 s at 60 °C and followed by a melting curve step, except for CncC for which conditions were slightly different: 40 cycles of 5 s at 95 °C and 30 s at 60 °C and 20 s at 72°C. Each reaction was performed in duplicate and the mean of three independent, biological replicates was calculated. All results were normalized using the mRNA level of three reference genes (ribosomal protein L4, ribosomal protein L10, ribosomal protein L17) and relative expression values were calculated using SATqPCR (Rancurel et al., 2019). Primers were designed using Primer3 (v0.4.0), sequences and efficiencies are listed in Appendix B Table S2.

Statistical analyses

Dose-response assays were analyzed in GraphPad Software (V9.2.0) using a nonlinear regression (four-parameters logistic (4PL) regression model).

RESULTS

Toxicity of I3C and MTP on Sf9 cells

I investigated the toxicity of I3C and MTP on Sf9 cells. I3C is a plant secondary metabolite from the glucosinolate family present in Brassicaceae, and MTP a juvenile hormone (JA) mimic insecticide. These xenobiotics were chosen based on previous reports of induction of detoxification genes in Sf9 cells (Giraudo et al., 2013; Giraudo et al., 2015). Exposure for 24 hours to increasing concentrations of xenobiotic was used to calculate half maximal inhibitory concentration (IC_{50}) which represents the dose of xenobiotics inhibiting cell viability by 50%. IC_{50} values of I3C and MTP were 112.7 µM and 89.4 µM respectively (Fig. 11). Resulting IC_{10}, IC_{20} and IC_{30} interpolated values were 39.7, 57.8 and 73.8 µM respectively for I3C and 50.7, 65.3 and 74 µM respectively for MTP.

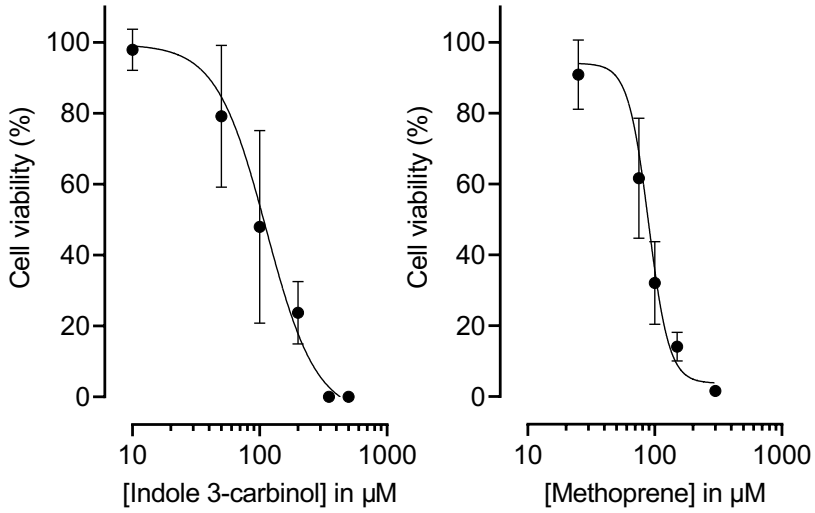

Xenobiotic	IC_{50} (µM)
Indole 3-carbinol	112.7
Methoprene	89.4

Fig. 11 Dose-response curves of I3C and MTP in MTT bioassays.
Toxicity of I3C (left) and MTP (right) towards Sf9 cells obtained by MTT bioassays. Each point was expressed as a percentage of the maximum viability (DMSO treatment). Curves were obtained by nonlinear regressions (sigmoidal, 4PL).

Selected detoxification genes are induced by I3C and MTP

To determine the response of the cells to these xenobiotics and whether this response is dose-dependent, Sf9 cells were treated with IC_{10}, IC_{20} and IC_{30} and the expression of detoxification genes were monitored by RT-qPCR (Fig. 12). The expression profiles of eight detoxification genes (*CYP4M14*, *CYP4M15*, *CYP9A24*, *CYP9A30*, *CYP9A31*, *CYP9A32*, *CYP321A9* and *GSTe1*) were dose-dependent and significantly induced at IC_{30} for both molecules. Some genes such as *CYP9A31* (28.74-FC, $p = 0.025$) were strongly expressed after I3C IC_{30} while other genes such as *CYP4M14* and *CYP4M15* were only weakly or even not induced (Fig. 12). MTP had overall a stronger effect on the expression of all detoxification genes although in the same order of magnitude as I3C, except for *CYP9A31* (expression fold-change 101.5 at MTP IC_{30}, $p = 0.0014$).

CncC, *Maf* and *Keap1* are induced in Sf9 cells by I3C and MTP

We tested whether *CncC* and *Maf* were also inducible in Sf9 cells by sublethal doses I3C and MTP (Fig. 12). Specific primers were designed on the genomic sequence of *CncC* specifically targeting the N-terminal end of the protein, corresponding to the isoform C of the Cnc gene

(Appendix B Table S2). The response of *CncC* and *Keap1* by I3C and MTP was dose-dependent, while the expression of *Maf* varied in a dose-independent manner. I3C had the least potent effect on the expression of *CncC* with a 3-fold increase at IC_{30} as compared to MTP (6.82-fold, n.s., $p = 0.069$). *Keap1* was strongly induced by both molecules. Exposure to MTP showed the most significant expression fold-change with 9.90-fold ($p = 0.012$) at IC_{30}.

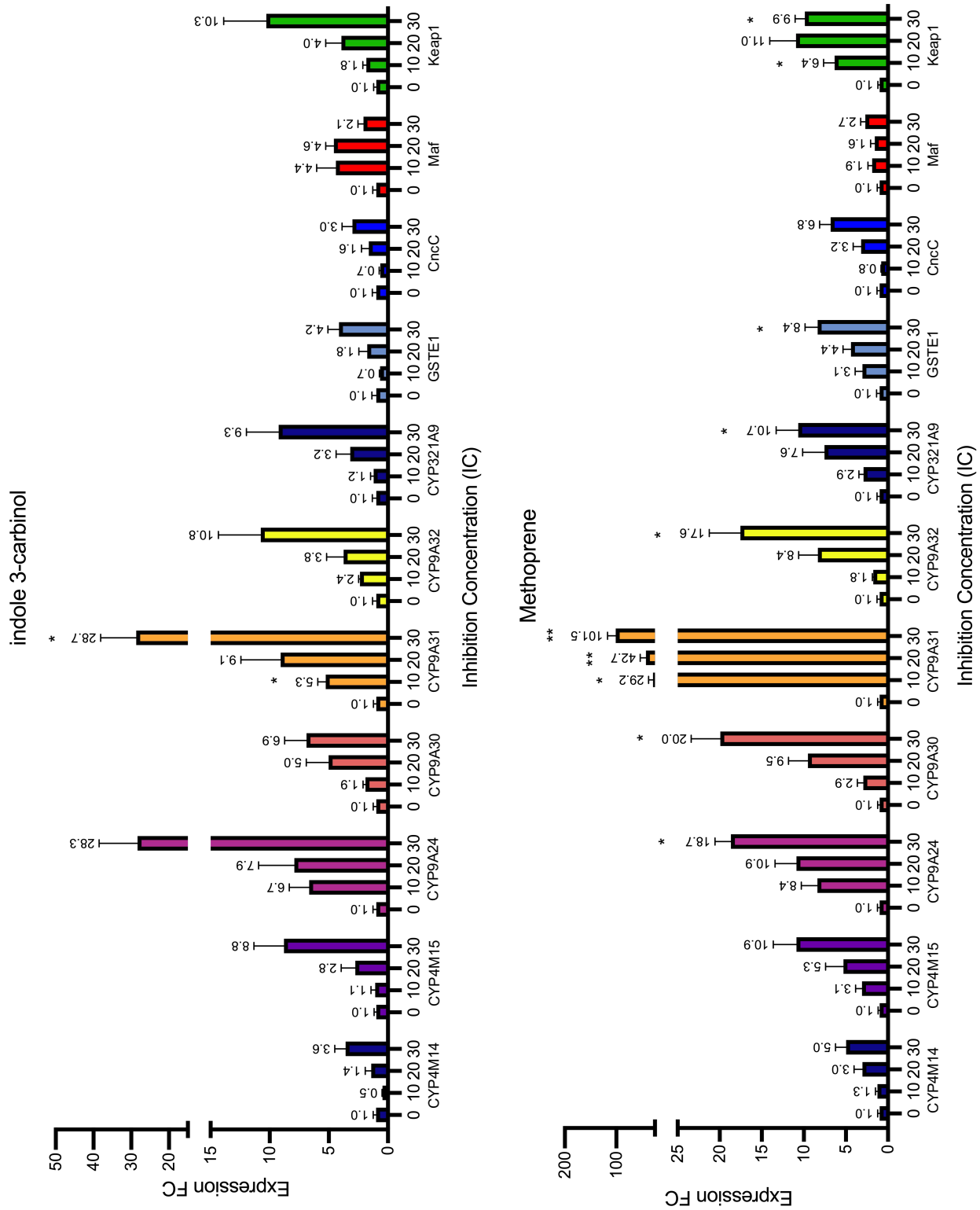

Fig. 12 Induction of detoxification genes, *CncC*, *Maf* and *Keap1* in Sf9 cells.
Expression levels of eight detoxification genes as well as *CncC*, *Maf* and *Keap1* were monitored in Sf9 cells exposed to IC_{10}, IC_{20} and IC_{30} I3C (top) and MTP (bottom). DMSO was used as control treatment (IC_0). Gene expression was normalized using the expression of the ribosomal protein L4, L10 and L17 reference genes and shown as fold-change relative to the expression of cell lines treated with DMSO. Data are mean values ± SEM.

Transient expression of *CncC* and *Maf* and their effect on detoxification genes

To test whether there is a causal link between the transcriptional upregulation of *CncC* and Maf and the activation of detoxification genes, the transcription factors were transiently overexpressed in Sf9 cells. The expression levels of *CncC* and *Maf* were monitored 24, 48 and 72 hours after transfection in each cell lines overexpressing *CncC*, *Maf* or both transcription factors.

CncC and *Maf* were strongly upregulated in transformants as compared with the control cells (Fig. 13). The highest expression fold-change was obtained at 48 hours post-transfection: 1012- and 1053-fold change respectively in *CncC* and *Maf* single-gene transformants and 1142- / 643-fold change in the double-gene transformants. The expression of detoxification genes was assessed 48 h post-transfection (Fig. 14). The overexpression of *CncC* and *Maf* genes led to significant upregulation of most detoxification genes monitored such as *CYP4M15*, *CYP9A24*, *CYP321A9* and *GSTe1* while the expression of *CYP9A30*, *CYP9A31* and *CYP9A31* were not affected. The co-transfection of *CncC* and *Maf* had a stronger impact on the induction of detoxification genes, for example the expression of *CYP4M15* was 2.5-fold higher in pCncC:Maf than in pCncC and pMaf.

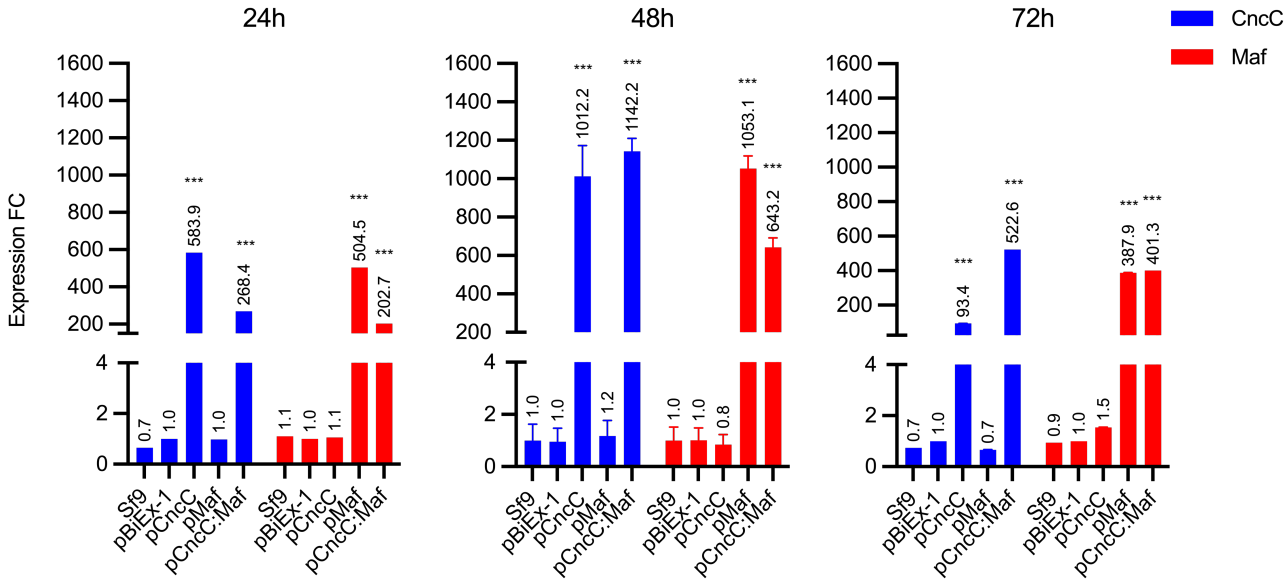

Fig. 13 Transcript levels of *CncC* and *Maf* in transiently transformed Sf9 cells.
Expression of *CncC* (blue) and *Maf* (red) were monitored in cell lines transfected with either *CncC* (pCncC), *Maf* (pMaf) or both transcription factors (pCncC:Maf). Gene expression was normalized using the expression of the ribosomal protein L4, L10 and L17 reference genes and shown as fold-change relative to the expression of cell lines transfected with an "empty" plasmid, pBiEx-1. Data are mean values ± SEM.

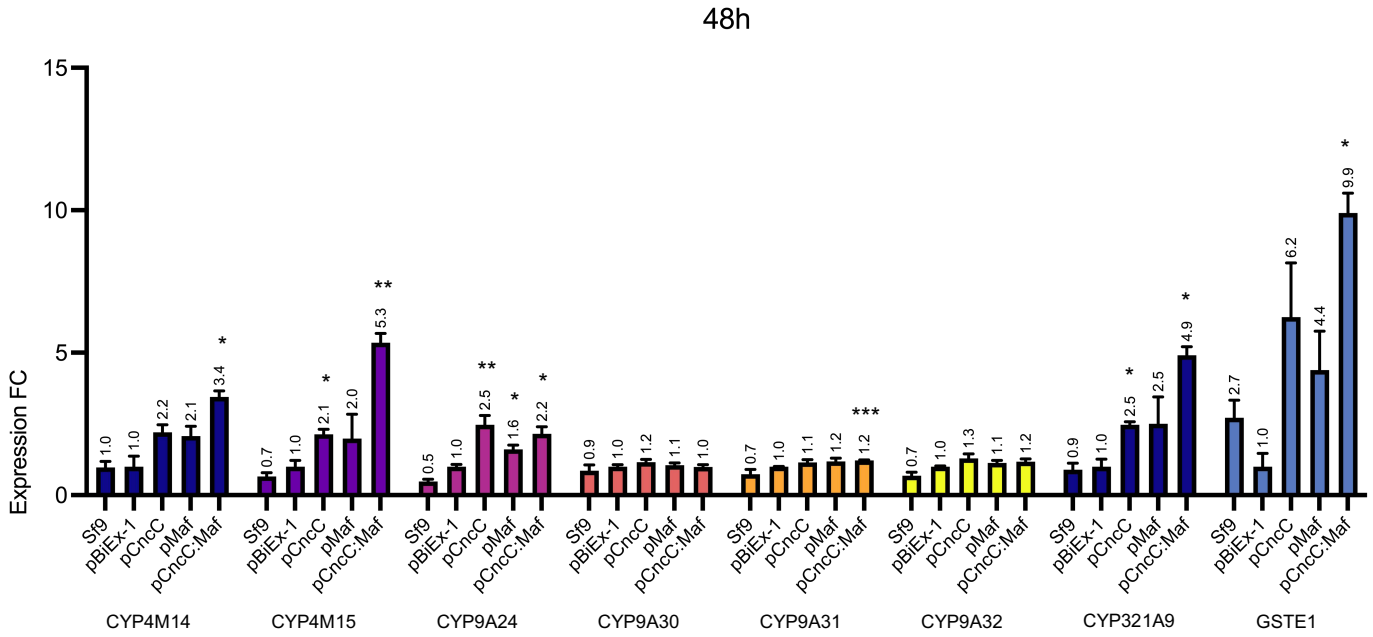

Fig. 14 Transcript levels of detoxification genes in transiently transformed Sf9 cells.
Expression of detoxification genes was monitored in cell lines transfected with either *CncC* (pCncC), *Maf* (pMaf) or both transcription factors (pCncC:Maf). Gene expression was normalized using the expression of the ribosomal protein L4, L10 and L17 reference genes and shown as fold-change relative to the expression of cell lines transfected with an "empty" plasmid, pBiEx-1. Data are mean values ± SEM.

Discussion

The inducibility of detoxifying enzymes upon exposure to xenobiotics allow insects to provide a timely and coordinated response to external stimuli that would otherwise be costly to implement permanently. In first chapter, we demonstrated that I3C and MTP are able to induce in a dose-dependent manner several detoxification genes as well as the transcription factor *CncC* in Sf9 cells. These induction profiles were obtained after exposure to sublethal concentrations of I3C and MTP in order to obtain specific adaptative responses of detoxification genes in *S. frugiperda* and avoid nonspecific general stress responses with higher doses. Transient overexpression of the transcription factors *CncC* and *Maf* induced the over-expression of *CYP4M14*, *CYP4M15*, *CYP9A24*, *CYP321A9* and *GSTEe1* while no effect was observed on *CYP9A30*, *CYP9A31* and *CYP9A32* expression, suggesting that another signaling pathway is involved in controlling their expression.

CYP9As were strongly induced by both xenobiotics (up to 100-fold for *CYP9A31* by MTP), which may suggest that they play a role in the metabolism of these compounds. CYP9As were reported inducible in the genus *Spodoptera* (*S. exigua*, *S. frugiperda* and *S. litura*) by plant secondary metabolites of various structures like terpenoids and glucosinolates, and insecticides (reviewed in (Amezian et al., 2021a). In *S. frugiperda*, their role in insecticide resistance is suggested by the fact that they are over-expressed in several field populations resistant to insecticides and in particular to pyrethroids (Boaventura et al., 2020b; Gimenez et al., 2020b). Their role in xenobiotic metabolism and resistance is strongly suggested by the over-expression of CYP9A in resistant population, however there is little evidence demonstrating the ability of these enzymes to metabolize insecticides in *S. frugiperda*. In *S. exigua*, one CYP9A, *CYP9A186* was shown to play a major role in resistance to abamectin and emamectin benzoate. Heterologous expression of this P450 in insect cells shows that it is able to metabolize these insecticides into hydroxy- and O-desmethyl-metabolites (Zuo et al., 2021). In a close lepidopteran, *Helicoverpa armigera,* heterologous expression of CYP9As including *CYP9A3, CYP9A14, CYP9A15, CYP9A16, CYP9A12/17 and CYP9A23* in yeast and Sf9 cells could also metabolize the pyrethroid esfenvalerate into its hydroxy-metabolites (Shi et al., 2021b; Yang et al., 2008a). These results show that there is functional redundancy among the six members of *H. armigera* CYP9A and raises the possibility that this functional redundancy may be linked to the conservation of the CYP9As as a gene cluster, six genes in *H. armigera* and

twelve in *S. frugiperda*. Induction of detoxification genes by xenobiotics is very common in clustered genes (Amezian et al., 2021a). Whether this catalytic redundancy can be found for *S. frugiperda* CYP9As and metabolize I3C and MTP remains to be elucidated.

Likewise, *CYP321A9* was inducible by both I3C and MTP suggesting it may be involved in the sensitivity of Sf9 cells to these compounds. This P450 is also part of a gene cluster of which the synteny (*CYP321A9-CYP321A7-CYP321A8-CYP321A10)* is conserved within the noctuid lineage (Cheng et al., 2017a). Although, *CYP321A9* is the only member of the CYP321A subfamily to be expressed in Sf9 cells (Giraudo et al., 2015) genes of this cluster were reported on several occasions to be induced and to metabolize xenobiotics in *S. litura* and *S. exigua* (Cheng et al., 2017a; Hu et al., 2021; Hu et al., 2019c; Jia et al., 2020; Wang et al., 2017b). For example, a recent study in *S. frugiperda* larvae showed that constitutive overexpression of *CYP321A8* increased tolerance of insects to deltamethrin by 10.3-fold based on LC_{50} values (Chen and Palli, 2021b). In *S. exigua CYP321A16* is able to metabolize the insecticide chlorpyrifos and *CYP321A8* chlorpyrifos, cypermethrin and deltamethrin (Hu et al., 2021; Hu et al., 2020b).

The data currently available show that both CYP9A and CYP321A have the ability to metabolize certain insecticides, but their action on plant secondary metabolites remains to be tested. Insecticides that CYP9A or CYP321A are able to metabolize include pyrethroids, avermectins and an organophosphate, however no studies have to our knowledge indicated their activity on the JHA methoprene. Yet microsomal CYPs have the ability to metabolize MTP when incubated with housefly microsomes (Terriere and Yu, 1973). In addition, it has been suggested that P450s could be involved in MTP resistance in the lesser grain borer, *Rhyzopertha dominica* (Sakka et al., 2021). The use of piperonyl butoxide, a P450 inhibitor, increased the susceptibility of the resistant strain. Thus, CYP9A and CYP321A could be potentially involved in MTP resistance and therefore deserve a more detailed analysis.

In our study, the induction of *CYP4M14*, *CYP4M15*, *CYP321A9* and *GSTe1* by xenobiotics correlated well with their upregulation after transient overexpression of *CncC* and *Maf*. For all these genes the expression was also higher when *CncC* and *Maf (Chen et al., 2018b)* were co-expressed, which supports the assumption that these two transcription factors act as heterodimers. These results corroborate those obtained in previous studies using ectopic expression of *CncC* and *Maf* in *T. castaneum* (Kalsi and Palli, 2015) and *S. exigua* (Hu et al., 2019b; Hu et al., 2020b). *GSTe1* was unsurprisingly upregulated by CncC and Maf.

Indeed it seems well established that this GST is a target gene of the CncC:Maf pathway in several species (*D. melanogaster:* (Deng and Kerppola, 2013); *S. exigua*: (Hu et al., 2019a; Hu et al., 2019b); *S. litura*: (Chen et al., 2018b) ; *Tribolium catsaneum*: (Kalsi and Palli, 2017a).

On the other hand, *CYP9A30*, *CYP9A31* and *CYP9A32* were not overexpressed in any of the *CncC* and *Maf* OE cell lines. This clearly demonstrates that MTP and I3C induction of these genes does not rely on the activation of the CncC/Maf pathway and is likely controlled by other actors and supports the idea of concomitant activation of several xenobiotic-responsive pathways upon xenobiotic exposure. While several of these pathways have been identified in recent years (for review see (Amezian et al., 2021b), we are still far from having a complete understanding of detoxification signaling in insects. One of the pathways potentially involved in the regulation of SfCYP9As could be the G-protein-coupled receptor (GPCR) pathway. Indeed, the work of Li and Liu on the mosquito *Culex quinquefasciatus* highlighted the role of these receptors and the intracellular effectors G-protein alpha subunit (Gs), adenylate cyclase (AC) and protein kinase A (PKA) in the development of insecticide resistance by regulating the expression of certain P450s. Most importantly, this work showed that heterologous expression of different of these mosquito effectors in Sf9 cells results in the over-expression of *SfCYP9A32* (Li and Liu, 2019). However, further experiments are needed to determine the role of the S*. frugiperda* GPCRs in the regulation of CYP9A, as Li and Liu further showed that the expression of *CYP9A30* and *CYP9A31* was not affected by the over-expression of GPCR effectors. Another possibility for the regulation of CYP9As is the aryl hydrocarbon receptor (AhR)/AHR nuclear translocator (ARNT) pathway. This pathway was initially shown to control the expression of *CYP6B1* and *CYP6B4* in *Papilio polyxenes* and *Papilio glaucus* and play a role in adaptation to furanocoumarins (Brown et al., 2005; Hung et al., 1996). In *S. frugiperda*, Giraudo et al (2015) have identified the possible presence of regulatory elements in CYP9A promoters, including a xenobiotic response element (XRE) from the aryl hydrocarbon receptor (AhR), suggesting the possible involvement of this nuclear receptor in the regulation of *CYP9A30*, and the XRE-Xan for xanthotoxin motifs in three of them (*CYP9A31*, *CYP9A30* and *CYP9A24*). Even though functional validation has yet to be provided, it is possible that different transcription factors and nuclear receptors are involved in the expression regulation of genes within the CYP9A cluster.

Although we identified putative detoxification genes regulated by the CncC:Maf pathway, the use of transient transformation has its pitfalls. First, the level of expression of

CncC and *Maf* ectopically expressed were very high, up to 1000-fold at 48 h post-transfection, as compared to the control. These levels are most likely not in the same order of magnitude than those seen within biological systems exposed to sublethal doses of xenobiotics. There has been reports of chlorpyrifos resistant *S. exigua* populations presenting transcript levels of *CncC* and *Maf* 8- and 3-times higher than those of susceptible populations, respectively (Hu et al., 2019b). More importantly, the genes induced by the activation of the CncC:Maf pathway following sublethal doses of xenobiotics might greatly differ from those regulated by a constitutive and potent overexpression of these transcription factors. Second, the ectopic expression by transient transformation of Sf9 cells does not allow the investigation of physiological effects of the CncC:Maf pathway activation. It would indeed be of great interest to test whether upregulation of *CncC* and *Maf* has an impact on cell viability, enzymatic activity and post-induction in-cell ROS levels.

CHAPTER 3

INTRODUCTION

In the previous chapter, I showed that the CncC:Maf pathway is likely controlling the expression of detoxification genes in Sf9 cells, including CYP and GST genes. The upregulation of detoxification genes in insects by ectopic expression of *CncC* was reported to result in enhanced enzymatic activity and lead to increased tolerance to xenobiotics exposure (reviewed inAmezian et al., 2021b; Misra et al., 2011). In addition, recent studies in *S. litura* and *S. exigua* suggested that CncC is involved in the transcriptional regulation of detoxifying enzymes and has a role in the development of metabolic resistance (Hu et al., 2019a; Hu et al., 2019b; Hu et al., 2020a; Shi et al., 2020). Here, I want to determine whether the CncC:Maf pathway is responsible for mediating xenobiotic and cytoprotective response in Sf9 cells and whether it is achieved by regulating detoxification genes. Work on *S. exigua* and *S. litura* has pointed out the role of reactive oxygen species (ROS) in activating the CncC/Keap1 pathway. Chen et al. (2018a) for instance demonstrated that GSTe1-dependent metabolism of chlorpyrifos and I3C was mediated by ROS and the CncC/Keap1 pathway in *S. litura*. Therefore, I sought to measure the production of ROS in Sf9 cells after treatment with I3C and MTP and test whether the use of antioxidant suppresses the CncC/Keap1-mediated response.

I opted for an over-expression (OE) *vs* knockout (KO) strategy in which two phenotypes, respectively enhanced and repressed for the CncC:Maf pathway, are monitored for their enzymatic activity and ability to cope with xenobiotic treatments. As I also want to identify the genes under the transcriptional control of *CncC* and *Maf* in S9 cells, the overarching goal of establishing OE *vs* KO cell lines is to carry out a comprehensive transcriptomic analysis using RNA-seq and identify the genes co-differentially regulated (Chapter 3).

Transient expression did not allow to test whether overexpression of *CncC* and *Maf* had an impact on tolerance of Sf9 cells to I3C and MTP. Here, I established stably transformed cell lines constitutively and permanently overexpressing *CncC*, *Maf* and both transcription factors. I established a second set of stable Sf9 cell transformants using the CRISPR/Cas9 system to knock out the *CncC* and *Keap1* genes. Suppressing the *Keap1* gene will presumably lead to *CncC* accumulation in the cytoplasm and its recruitment to the nuclear compartment.

In this chapter, I tested whether stable overexpression of the *CncC* and *Maf* had a significant impact on Sf9 cells tolerance to I3C and MTP. I then investigated if specific enzymatic activities of some of the main detoxification enzyme families were modified accordingly. Finally, I analyzed the production of ROS following xenobiotic exposures in each selected cell line and compared the effect of the antioxidant sodium pyruvate in viability assays.

MATERIALS & METHODS

Chemicals

Sodium chloride (NaCl), Triton X-100 as well as dipotassium hydrogen phosphate (K2HPO4) and Potassium dihydrogen phosphate (KH2PO4) to prepare potassium phosphate buffer (PBK) were purchased from VWR International (Rosny-sous-bois, France). Tris Amino was purchased from Euromedex France (Souffelweyersheim, France). Fetal Bovine Serum (FBS) was from Invitrogen (Villebon-sur-Yvette, France). Nuclear fluorescent probe Hoechst 33342 (Ex/Em: 350/461), propidium iodide (Ex/Em: 535⁄617), the membrane fluorescent probe calcein-AM (Ex/Em: 495⁄515) and 6-carboxy-2',7'-dichlorodihydrofluorescin diacetate (carboxy-H_2DCFDA, Ex/Em: 485/535) were purchased from Molecular Probes (Life Technologies, Saint Aubin, France). All other products were from Sigma–Aldrich Chimie (Saint-Quentin Fallavier, France) unless stated otherwise.

Sf9 cells and cell culture

Sf9 cells were maintained as adherent cultures at 27°C in Insect-XPRESS (IXP) serum free medium (Lonza, France) and passaged every third day. Sf9-eGFP cells are transgenic derivatives of Sf9 cells kindly provided by Dr. Don Jarvis (University of Wyoming, Laramie). Cell density was determined by Malassez haemocytometer (Marienfeld, Germany) counts and cell viability was evaluated by Trypan blue (1 mg/ml, v/v) staining.

Stable overexpression of *CncC* and *Maf* transcription factors in Sf9 cells

Stable transformation of Sf9 cells

Sf9 cells were seeded onto six-well plates at 2.10^5 cells/ml and incubated at 27°C for 24h prior transfection. To establish stable transformants, Sf9 cells were co-transfected with 2 µg of

pBiEx-1™ expression constructs (Chapter 1) and 0.2 µg of the pIE1-neo selection plasmid (Novagen, Germany) containing a resistance marker to neomycin (Fig. 1). Cells were transfected with either a single expression plasmid construct, *i.e.* pBiEx-CncC or pBiEx-Maf, or transfected with both expression vectors in equal proportions. An "empty vector" was used to transfect control cell lines. The plasmid DNA and 3 µl FuGENE® transfection reagent (Life Technologies, Germany) was incubated 15 min in 100 µl of IXP medium at room temperature prior to be diluted to a final volume of 1 ml of IXP medium supplemented with 10% FBS. Cells were incubated for 48 hours for at 27°C. After 48 hours, stable transformants were selected with 0.3 mg/ml G418 for three weeks. Single-cell colonies were carefully picked, isolated and expanded into independent cell lines and cryopreserved until further use (Fig. 15).

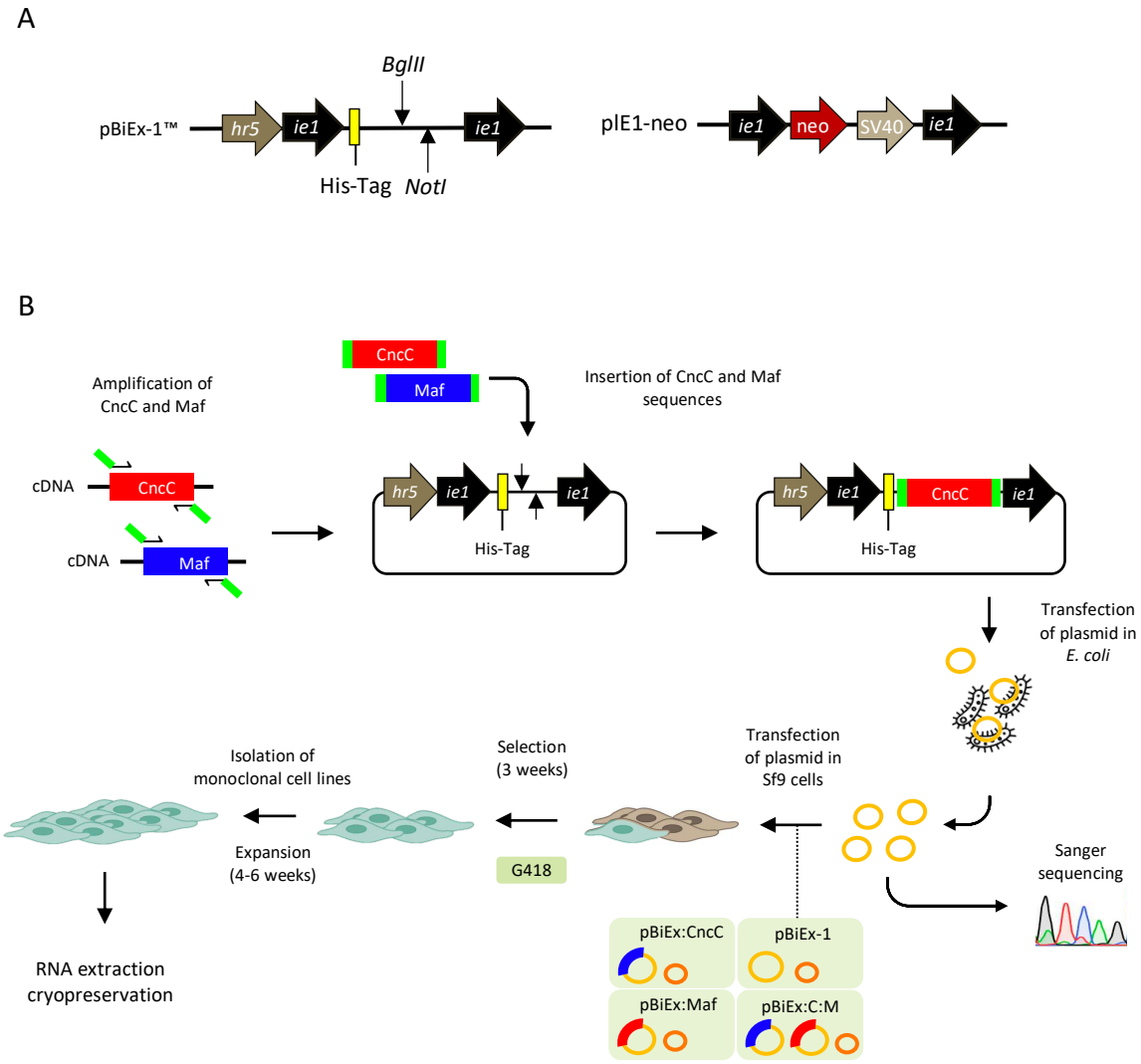

Fig. 15 Overexpression of *CncC* and *Maf* genes in Sf9 cells by stable transformation.
(**A**) Diagram showing the pBiEx-1™ plasmid (left), the *Spodoptera*-derived cells specific expression vector containing the *hr5* enhancer and the baculovirus *ie1* promoter and including an N-terminal His-Tag. When co-transfected with the pIE1-neo (right) encoding the neomycin-resistance marker, stable cell lines that constitutively express low levels of the target gene can be selected in the presence of the antibiotic G-418 (Jarvis

et al., 1996). (**B**) Stable transformation of Sf9 cells is a two-to-three-month process. The coding sequences of *CncC* and *Maf* genes were inserted into pBiEx-1™ and transfected to Sf9 cells for 48 hours before being selected for three weeks. Monoclonal cell lines were then isolated and expanded for four to six weeks before cryopreservation until further use.

Knock-Out of *CncC* and *Keap1* genes in Sf9 cells

Design of single-guide (sg)RNAs and construction of the Cas9 expression vector

Four guides were designed against exon 1 and exon 2 of the *CncC* and *Keap1* genes, respectively using the CRISPOR gRNA design tool (crispor.tefor.net) and the *SfCncC* and *SfKeap1* genomic DNA sequence as targets. The best scored guides were blasted onto the genome (v6.0) on BIPAA (bipaa.genouest.org, Gimenez et al., 2020b) to exclude those with off-targets in known CDS sequences and the best sgRNA candidates were chosen on least hits. The guide targeting *eGFP* (mock gene) was taken from Mabashi-Asazuma and Jarvis (2017). All guides are listed in Appendix C, Table S3.

To test the efficiency of the guides, those chosen to target *CncC* were first tried *in vitro.* The guides were ordered as synthetic sgRNAs (Sigma-Aldrich, France). A PCR amplicon spanning the target site (approx. 800 nt) was generated from Sf9 genomic DNA with Q5® High-Fidelity DNA Polymerase (New England Biolabs, France) and primers PR11-PR12 and PR13-PR14 (Appendix C, Table S1). The PCR cycle conditions were as follows: 1 min at 98°C, 35 cycles of 10 s at 98°C, 10 s at 67°C and 1 min at 72°C and a final step of 2 min at 72°C. The two resulting PCR products were purified using the GeneElute™ PCR Clean-Up Kit (Sigma-Aldrich, France) and used as templates for *in vitro* CRISPR/Cas9 edition. Cas9 enzyme (Sigma Aldrich, France) and sgRNAs were mixed together (1:1) in 10 µl of Cas9 enzyme reconstitution buffer and incubated 10 min at 25°C to allow complexing. 150 ng of the PCR product was added to the sgRNA:Cas9 complexes and incubated 10 min at 25°C. The resulting products were then migrated on a 1% agarose gel. The guides targeting the *Keap1* gene were not tested given the relatively high rate of edition efficiency obtained with *CncC*.

The guides were then ordered as pairs of complementary oligos with *Sap*I palindromic overhangs for subsequent insertion into the pIE1-Cas9-SfU6-sgRNA-Puro expression vector, which was a kind gift from Dr. Donald L. Jarvis (Fig. 2). The guides were annealed using 1 µl of 10 mM forward and reverse strands in 16 µl annealing buffer (9.5 mM Tris, 0.95 mM EDTA, 50 mM NaCl, pH 8) on a MJ Research Tetrad PTC-225 Thermal Cycler (GMI, USA). The program was as follows: an initiation step of 5’ at 95°C was followed by 3-min cycles at temperatures ranging from 90°C to 60°C (step: -5°C) and 3-min cycles at temperatures ranging from 57°C to

27°C (step: -3°C) and terminated with 10’ at 25°C. The annealed product was diluted 200 times in milliQ water and subcloned in *Sap*I linearized pIE1-Cas9-SfU6-sgRNA-puro using the T4 DNA ligase kit (Promega, France). Plasmid constructs were then transformed into Subcloning Efficiency™ DH5α™ Competent Cells (Life Technologies, Germany) according to the supplier's instruction. Bacterial colonies were verified by standard PCR using GoTaq® DNA Polymerase (Promega, France) and PR9 and PR10 primers (Appendix C, Table S2). Plasmids were then purified from positive cultured clones using the GenElute™ Plasmid Miniprep Kit (Sigma-Aldrich, France). All recombinant constructs were confirmed by Sanger sequencing (Genewiz, Germany).

CRISPR/Cas9 editing of Sf9 cells

Sf9 cells were seeded onto 96-well plates (Techno Plastic Products AG, Switzerland) at 1500 cells/well and incubated at 27°C for 24h prior to transfection. For each well, adherent cells were transfected with 100 ng plasmid DNA and 0.2 µl FUGENE® transfection reagent to a final volume of 100 µl IXP medium supplemented with 10% FBS and incubated 48 hours at 27°C. Cells from independent wells were transfected with a single plasmid construct. The plasmid containing the sgRNA targeting *eGFP* was used to produce control cell lines (mock-gene KO). After 48 hours, transfected cells were selected with 3 mg/ml puromycin in 10 % FBS IXP medium for 10 days. From 5 to 10 single-cell colonies were carefully picked, isolated and expanded into independent cell lines and cryopreserved until further use.

Sequence analysis of CRISPR/Cas9 modified cell lines

Genomic DNA was extracted from all isolated cell lines using the QuickExtract™ DNA Extraction Solution kit (Epicentre Biotechnologies, USA) according to manufacturer’s instructions. Each cell-line was seeded onto 6-well plates at 5.10^5 cells/ml and incubated at 27°C until reaching *ca.* 90% confluence. Adherent cell monolayers were washed in 1 ml DPBS and pelleted in 500 µl DPBS in a centrifuge for 1 min at 700 x g. The pellets were recovered in 20 µl of QuickExtract™ Solution and incubated 6 min at 65°C and 2 min at 98°C in a thermocycler. 3 µl of genomic DNA homogenate was directly used as template to amplify a *ca.* 800 nucleotides (nt) region spanning the CRISPR/Cas9 target sites with Q5® High-Fidelity DNA Polymerase (New England Biolabs, France) and primers PR11-PR12, PR13-PR14 and PR15-PR16 (Appendix C, Table S1, Fig. 2). The PCR cycle conditions were as follows: 1 min at

98°C, 35 cycles of 10 s at 98°C, 10 s at 67°C and 1 min at 72°C and a final step of 2 min at 72°C. The resulting PCR products were purified using the GeneElute™ PCR Clean-Up Kit (Sigma-Aldrich, France) and Sanger sequenced at Genewiz (Germany) to validate successful edits.

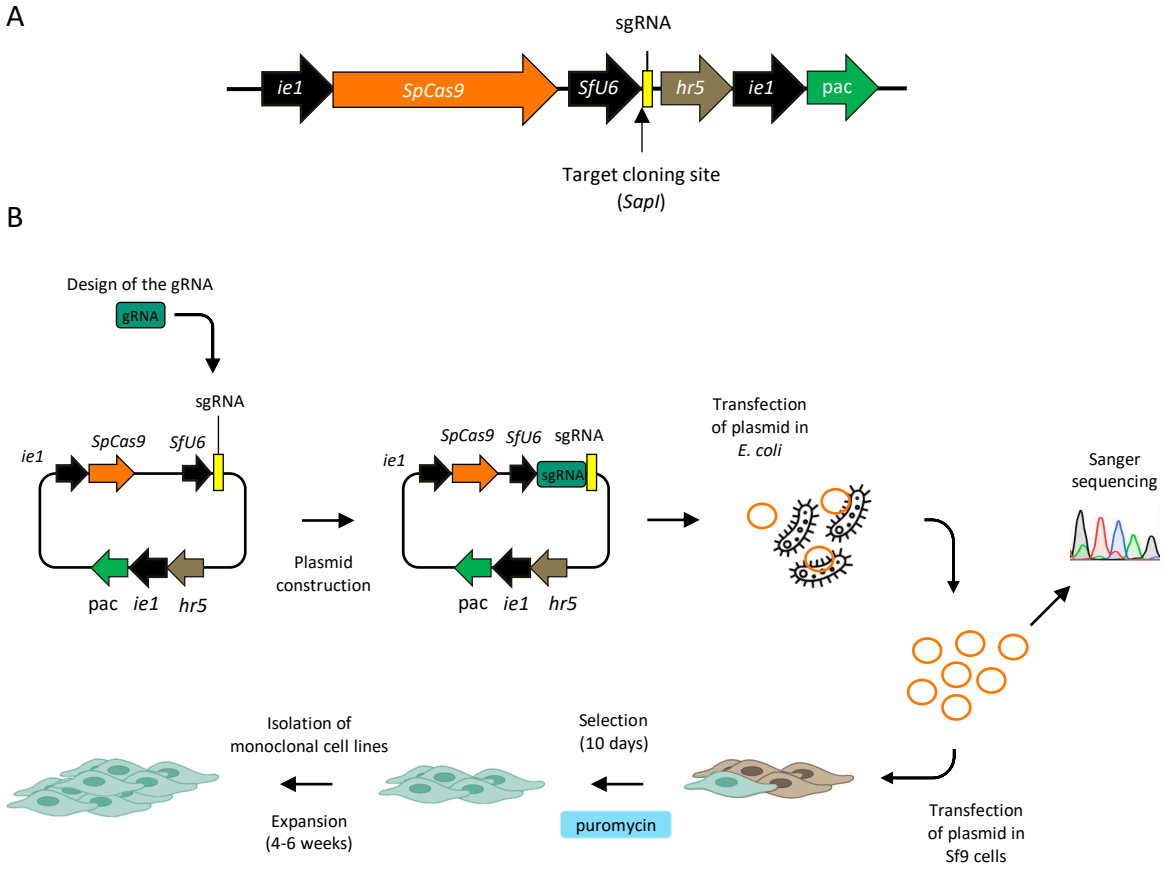

Fig. 16 Procedure for CRISPR/Cas9-induced mutations in Sf9 cells.
(**A**) Reproduction of Fig. 1A and caption from Mabashi-Asazuma and Jarvis (2017). Diagram showing the CRISPR/Cas9 vector encoding, (Left to Right) *Sp*Cas9 under the control of a baculovirus *ie1* promoter, an sgRNA expression cassette that includes an insect *Spodoptera*-specific *U6* promoter and a puromycin-resistance marker under the control of baculovirus *hr5* enhancer and *ie1* promoter elements. (**B**) The CRISPR/Cas9-mediated edition of Sf9 cells is a six-to-eight weeks procedure. The sgRNAs were inserted into the CRISPR vector using SapI cloning sites prior to be amplified and validated by Sanger sequencing from *E. coli*. Single-sgRNA plasmids were transfected to Sf9 cells for 24 hours and selected for 10 days with puromycin. After 10 days, monoclonal cell lines were isolated and expanded for four to six weeks before cryopreservation.

The PCR product of one cell-line ($Sf9^{CncC\text{-}08}$) was cloned into pGEM®-T Easy (Promega, France) according to the manufacturer's specifications. 96 representative white colonies were selected and inoculated in two 96-well agarose plates for bacterial clone sequencing (LGC Genomics, Germany) using two primers PR17 and PR18 (Appendix C, Table S1). All sequences were analyzed and aligned using Unipro UGENE (v37.0) (Okonechnikov et al., 2012).

Inference of CRISPR Edits (ICE) analysis

ICE analysis was performed as described previously (Hsiau et al., 2018). The chromatograms from Sanger sequencing results were used as queries for the ICE web program (ice.synthego.com). All analyses were performed with a default setting.

RNA extractions, cDNA synthesis and RT-qPCR

Basal expression of *CncC* and *Maf* genes in stably transformed cell lines was assessed using RNA extracted 24 h after seeding the cells onto six-well plates at 2.10^5 cells/ml. Cells were washed with 1 ml DPBS and RNA extractions were all performed for three independent biological replicates using 1 ml TRIzol Reagent (Life Technologies, Germany) following manufacturer's instruction. The procedure and conditions for RT-qPCR assays in this chapter are identical as those described in the previous chapter (Chapter 1).

Cell viability assays

MTT

MTT assays were performed for two media conditions: in serum-free Insect-XPRESS (IX) medium ± antioxidant sodium pyruvate (SP, 18 mM). The procedure and conditions for MTT bioassays conducted in this chapter are identical as those described in the previous chapter (Chapter 1).

Cell imaging microplate assays and cellomics – ArrayScan^{XTI} scanning details

Prior to experiments cells were seeded onto black 96-well flat- and clear-bottom microplates (Corning Inc., USA) at 2.10^5 cells/ml and allowed to attach for 24 h at 27°C. Cytotoxicity of I3C and MTP was assessed using molecular probes and High Content Screening (HCS) with an automated microscopy approach. Three fluorescent probes were used together: the nuclear marker Hoechst 33342 (total cells), the Propidium Iodide marker (dead cells) and the Calcein AM Viability Dye (viable cells). Cells were treated with the same range of concentrations of I3C and MTP used in the MTT assay, with DMSO as a control. Each concentration was used for three wells (technical replicates) and the experiment was reproduced for three independent biological replicates. 24 hours after treatment, the medium was removed and 100 µl of the staining medium was added to each well. The fluorescent probes stock solutions contained in DMSO were diluted in 25 mM NaCl-supplemented HANK's medium at final concentrations of 9 µM for Hoechst 33342, 0.3 µM for propidium iodide and 1 µM for calcein-AM. The plates

were incubated 15 min at 27°C and scanned with the ArrayScan^{XTI} instrument (Cellomics Inc., Pittsburgh, USA). The detection was performed with the "spot detector" bio-application (Cellomics Inc., Pittsburgh, USA). An objective of 20X was used for the image acquisitions. Total cells were detected with Hoechst in channel 1 (blue). Dead cells were detected in channel 2 (propidium iodide, red) and viable cells in channel 3 (calcein-AM, green). The data was analyzed in Statistica v13.2 (Tibco, Palo Alto, USA) using a Random Forest Classification based on ± 1000 random manual calls ("dead", "live" or "chimeric", *e.g.* "dead"+"live"). Dose-response modeling (IC_{50}) was produced for each cell line and both xenobiotics tested. For each plate, the mean of the three control wells (DMSO) was used as a reference and rescaled to 100 %. Each well value was expressed relative to this reference.

ROS measurements

The assessment of ROS production after xenobiotic exposure was performed in two conditions: in serum-free Insect-XPRESS (IX) medium ± antioxidant sodium pyruvate (SP, 18 mM). Prior to experiments cells were seeded onto black 96-well flat- and clear-bottom microplates (Corning Inc., USA) at 2.10^5 cells/ml and allowed to attach for 24 h at 27°C. Pilot assays were carried out to maximize fluorescence detection and the treatment incubation was set to 6 hours. Two fluorescent probes were used together: the nuclear marker Hoechst 33342 and the general oxidative stress indicator carboxy-H_2DCFDA. Cells were treated for 6 h with 150 µM I3C and 150 µM MTP in Grace's Insect Medium supplemented with L15 medium (GIM-L15, 7:3). In this experiment, an equal volume of DMSO served as negative control and tert-butyl hydroperoxide (t-BHP) (1 mM) and fenoxycarb (150 µM) were used as positive controls. t-BHP is a known ROS inducer while fenoxycarb is a Juvenile Hormone Agonist (JHA) insecticide. Both medium conditions (with and without SP antioxidant) and all treatments were laid out on one plate so that three identical plates served as technical replicates. ROS measurements were reproduced for three independent, biological replicates. After 6 h of treatment, the fluorescent probes stock solutions contained in DMSO were diluted in GIM-L15. 20 µl of this staining solution was added to each well (3.5 µM final Hoechst 33342 and 10 µM final H_2-DCFDA) and plates were incubated for 15 min at 27°C. Plates were washed twice with GIM-L15 before scanning cells in 250 mM (final) Trypan blue-supplemented GIM-L15 to quench the extracellular fluorescence using the ArrayScan^{XTI} instrument (Cellomics Inc., Pittsburgh, USA). An objective of 10X was used for the image acquisitions. The detection was

performed with the “spot detector” bio-application (Cellomics Inc., Pittsburgh, USA). Four images were taken for each fluorescence channel. Total cells (Hoechst, blue) were detected in channel 1. ROS were detected in channel 2 (H_2-DCFDA, green). The Cellomics ArrayScan^{XTI} output features “mean circ spot total intensity” and “mean circ total intensity” depending on the probe tested were used to analyze the scans (Appendix C, Fig. S1).

To analyze the quantitative data for ROS accumulation obtained after the image analysis, a workflow was built in Statistica v13.2 (Tibco, Palo Alto, USA). First, each independent plate was standardized in order to eliminate intra- and inter-experiment variation: data sets (independent plates) the ROS spot total intensity within cells was submitted to a median MAD standardization in order to fix the values in the same order of magnitude (robust Z-score). Then the three independent experiments were grouped.

Protein extractions and enzymatic activities

For CE and GST enzymatic assays, *ca*. 8-10.10^6 cells were pelleted and resuspended in 50 mM HEPES buffer (pH 7) containing 0.01% (v/v) Triton X-100. Cells were homogenized with two ion beads using a Tissue Lyser LT (QIAGEN, Germany) three times 30 secs at 50 Hz with intermittent cooling on ice for 2 min. The lysate was centrifuged 5 min at 10 000 x g and 4°C. The pellet was discarded and the supernatant was used for protein quantification, aliquoted and stored at -80°C. Protein quantification was done using Pierce™ 660nm Protein Assay Reagent (Pierce Biotechnology, USA) and BSA as a reference. All protein extractions and microsome preparations have been replicated three to four times.

Carboxylesterase activity

Carboxylesterase activity was measured according to Dary et al. (1990) with minor modifications. The reaction mixtures (final volume 165 µl) consisted of 55 µl enzyme source (2.5 µg protein) and 110 µl substrate solution containing 0.375 mM 1-naphtyl acetate (1-NA) or 2-naphtyl acetate (2-NA) (final concentration 0.25 mM) in 50 mM HEPES buffer (pH 7). Reaction mixtures without the enzyme source served as control. Each reaction was run in triplicate in transparent flat-bottom 96-well microplates for four biological replicates per cell-line. Plates were incubated 30 min at 30 °C and reactions were terminated by addition of 85 µl of a reagent solution (30 mg Fast Garnet, 0.75 ml 20% SDS in 10 ml final volume of ddH_2O). The solution was incubated for 5 min at room temperature and the absorbance was

determined at 568 nm for both 1- and 2-naphthol products in a spectrophotometer (SpectraMax 382, Molecular Devices, USA). Specific activity was calculated based on 1-naphtol and 2-naphtol products standard curves.

Glutathione S-transferase activity

The GST activity using CDNB and GSH as substrates was measured following the method previously described by Habig et al. (1974), with slight modifications. Reactions consisted of 100 µl enzyme source (20 µg protein) and 100 µl substrate solution (50 mM HEPES buffer pH 7, CDNB and GSH at 2 mM and 4 mM final concentration, respectively). Reactions were run in triplicates for four biological replicates per cell line in transparent flat-bottom 96-well microplates. The change in absorbance was measured continuously for 5 min at 340 nm, and 25 °C using a microplate reader (SpectraMax 382, Molecular Devices, USA).

Measuring GST activity using MCB and GSH as substrates was performed in flat-black 96-well microplates (Corning Inc., USA). The reactions consisted of 100 µl enzyme source (15 µg protein) and 100 µl substrate solution containing MCB (final concentration 0.1 mM) and GSH (final concentration 0.5 mM) in 50 mM HEPES buffer (pH 7). Measurements were taken every 2 min for 20 min at kinetic modus and 25 °C on a spectrofluorometer (Cary Eclipse, Agilent Technologies, USA) at emission and excitation wavelengths of 465 nm and 410 nm, respectively. Reactions consisting of CDNB/MCB and GSH without enzyme source served as control.

Statistical Analyses

Dose-response assays were analyzed in GraphPad Software (V9.2.0) using a nonlinear regression (Sigmoidal, four parameters logistic (4PL) regression model). For statistical analysis of ROS measurements assays, the nonparametric Kruskal–Wallis test was performed. Statistical significance was assumed at $p < 0.05$.

RESULTS

Overexpression of *CncC* and *Maf* by a stable transformation of Sf9 cells

The pBiEx-1 expression vectors containing the coding sequence of either *CncC*, *Maf*, or both transcription factors designed in the first chapter were used in this experiment. In total, 18 viable cell lines were isolated and cryopreserved. Six cell lines were transfected with pBiEx:CncC, seven were transformed using pBiEx:Maf while four were obtained with transfection of both plasmids. One cell line transfected with an "empty" pBiEx-1 expression vector was also isolated as a control cell line.

The transcriptional expression of *CncC* and *Maf* genes were monitored in each cell line by RT-qPCR and results are presented in Fig. 17. The expression level of *CncC* was significantly higher (2.73-FC, p = 0,0087) in a one cell line out of six transformed with the pBiEx:CncC vector (Fig. 17A). *Maf* transcript levels were higher in all cell lines transformed with the pBiEx:Maf vector, with expression ranging from 3- to 14.6-fold change (Fig. 17B). The co-transfection of both vectors resulted in a significant increase of expression in one cell line: pCncC:Maf-a with a 1.53-fold change (p = 0.03) for *CncC* and a 3-fold change (p = 0.0014) for Maf (Fig. 17C). One cell line from each transformant condition, respectively pCncC-b, pMaf-b and pCncC:Maf-a, were selected for subsequent experiments.

Stable overexpression of *CncC* and *Maf* genes increase Sf9 cells tolerance to xenobiotics

All cell transformants presented similar shape, size, adherence and growth rate to the Sf9 *Wt* cell line (Appendix C, Fig. S2). However, pCncC:Maf-a displayed a visible improved fitness and displayed much fewer dead cells as compared to all other lines. To establish whether the CncC:Maf pathway has a role to play in the tolerance towards I3C and MTP I carried out dose-response assays using MTT on all cell lines. The overexpression of *CncC* and *Maf* genes had only a little impact on the tolerance to xenobiotics, although a slight increase of IC_{50} was observed for pMaf-b towards I3C (1.3-fold) and MTP (1.2-fold) (Table 3). On the other hand, the concomitant overexpression of *CncC* and *Maf* in pCncC:Maf-a resulted in a strong increase of tolerance to I3C: IC_{50} of 137.2 µM as compared to 47.7 µM for pBiEx-1, and to MTP: IC_{50} of 122.9 µM as compared to 86.1 µM for the control (Fig. 18). In conclusion, only the

simultaneous overexpression of *CncC* and *Maf* had a significant impact on the tolerance of cell transformants to xenobiotics.

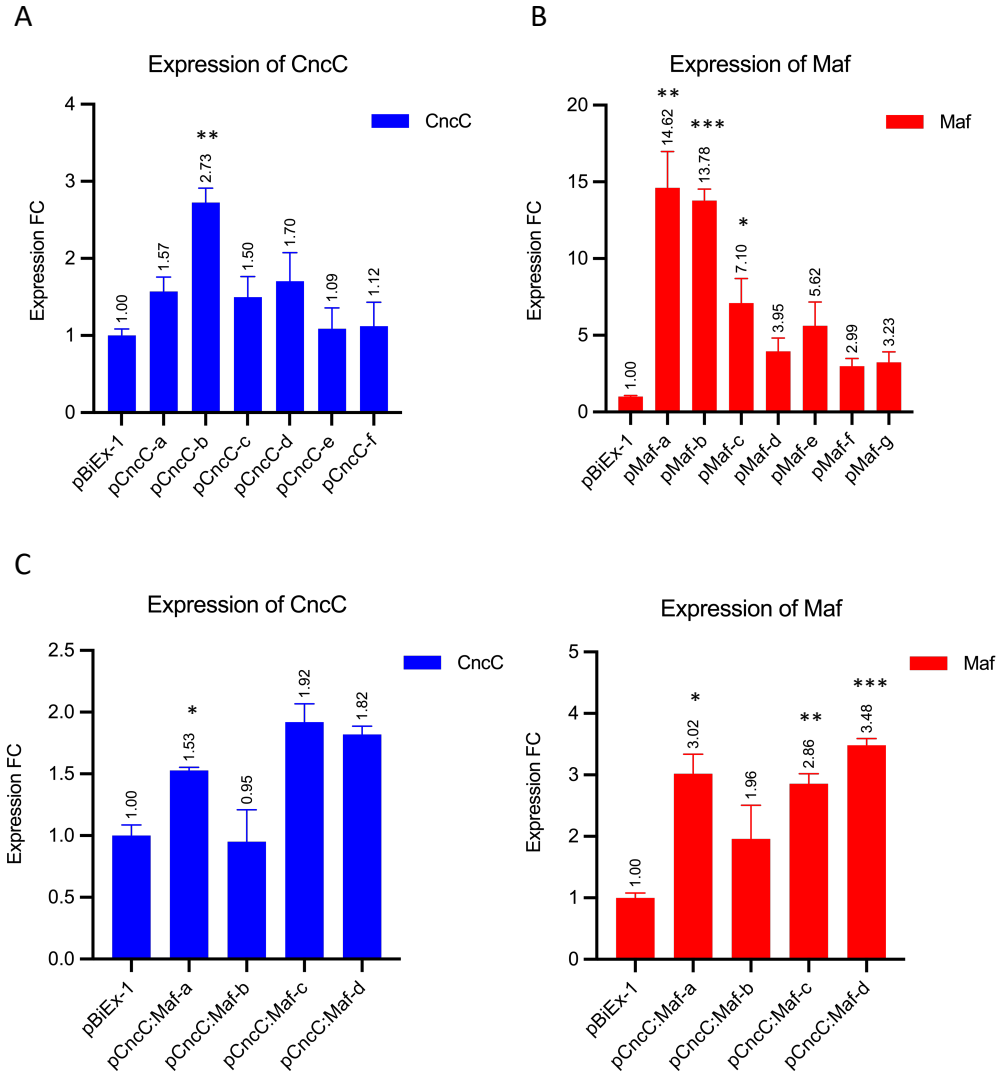

Fig. 17 Transcript levels of *CncC* and *Maf* in stably transformed Sf9 cells.
Expression of *CncC* (blue) and *Maf* (red) were monitored in cell lines transfected with either (**A**) pCncC, (**B**) pMaf or (**C**) both expression vectors. Gene expression was normalized using the expression of the ribosomal protein L4, L10 and L17 reference genes and shown as fold-change relative to the expression of cell lines transfected with an "empty" plasmid, pBiEx-1. Data are mean values ± SEM.

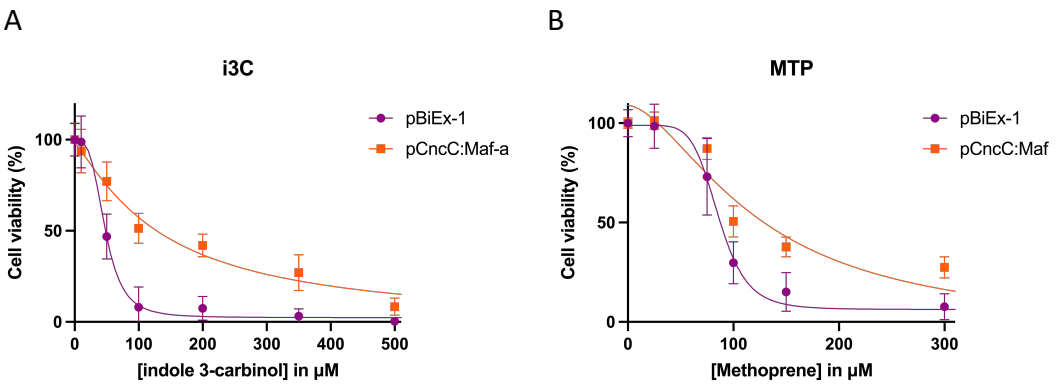

Fig. 18 Dose-response curves of I3C and MTP in MTT bioassays.
Toxicity of (**A**) I3C and (**B**) MTP towards pCncC:Maf-a (orange) and the control cell lines, pBiEx-1 (purple) obtained by MTT bioassays. Each point was expressed as a percentage of the maximum viability (DMSO treatment). Curves are nonlinear regressions (sigmoidal, 4PL).

Table 3 IC_{50} values of i3C and MTP towards stably transformed cell lines.

Cell line	Treatment	IC50	95% CI	Tolerance ratio
pBiEx-1	I3C	47.7	[41.1 ; 51.2]	-
	MTP	86.8	[82.7 ; 91]	-
pCncC-b	I3C	44.5	[ND ; 100]	0.93
	MTP	88.2	[84.1 ; 91.8]	1
pMaf-b	I3C	60.9	[55.65 ; 67.4]	1.3
	MTP	103.3	[98.8 ; 111.9]	1.2
pCncC:Maf-a	I3C	137.2	[78.55 ; 214.5]	2.9
	MTP	119	[ND ; 139.8]	1.4

MTT reduction occurs throughout cell compartments and can be significantly affected by a number of factors, including metabolic disruptions, changes in the activity of oxidoreductases and oxidative stress (Stepanenko and Dmitrenko, 2015). Thus, to avoid result misinterpretation, complementary results using non-metabolic assays is usually recommended. The viability assays were therefore reproduced using fluorescent molecular probes coupled with HCS. I used propidium iodide as a marker of dead cells and calcein-AM to dye viable cells. Automated microscopy and a machine learning-based analysis method allowed to count and sort dead from living cells and in turn to determine IC_{50} values (Table 4). Although IC_{50} values were overall much higher than those obtained with the MTT assay, the relative susceptibility to xenobiotics among cell lines was consistent between the two assays. For example, IC_{50s} of both molecules were significantly higher in pCncC:Maf-a as compared to the control while the overexpression of *CncC* and *Maf* had only little impact on cell tolerance to I3C (Fig. 19, Table 4).

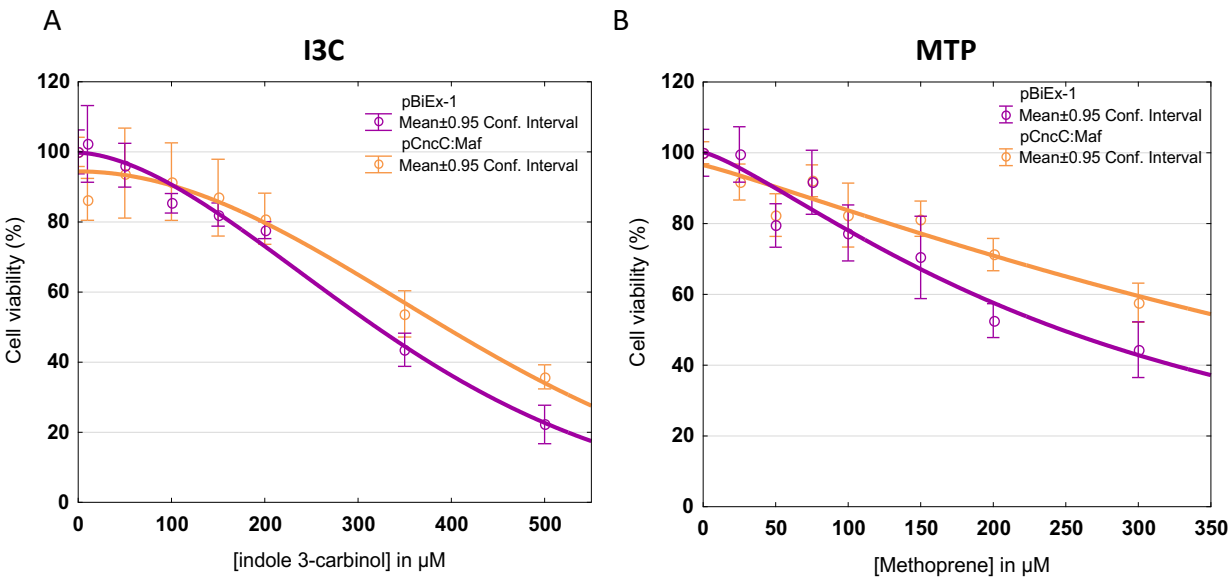

Fig. 19 Dose-response curves of I3C and MTP in HCS bioassays.
Toxicity of (**A**) I3C and (**B**) MTP towards pCncC:Maf-a (orange) and the control cell lines, pBiEx-1 (purple) obtained by HCS bioassays. For further details refer to Materials and Methods.

Table 4 IC_{50} values of i3C and MTP towards stably transformed cell lines

	i3C		MTP	
Cell line	**IC_{50}**	**ratio**	**IC_{50}**	**ratio**
pBiEx-1	320.1	-	246.8	-
pCncC-b	342.3	1.1	414	1.7
pMaf-b	328.5	1	424.3	1.7
pCncC:Maf-a	410.7	1.3	415.15	1.7

Knockout of *CncC* and *Keap1* using the CRISPR/Cas9 system

The attempt to induce CRISPR/Cas9-mediated mutations in Sf9 cells was the first in our lab. The development of the present protocol is the result of several failures which were identified and alleviated thanks to the help and counsel of international collaborators.

I initially undertook the use of the CRISPR/Cas9 system according to two strategies: the first by delivering a plasmid containing the coding sequences of a sgRNA and the Cas9 enzyme, and the second by using the Cas9d10A, a nickase introducing single-strand breaks (SSB), electroporated to Sf9 cells as a Cas9d10A:sgRNA complex. Delivery of a nickase as a protein complex has two advantages i) the use of two sgRNAs located a few base pairs apart strongly increases the site-specificity of CRISPR/Cas9-directed mutations and ii) it allows more control over quantity and duration of cell exposure to the CRISPR/Cas9 system.

For this first attempt, two sgRNAs were designed and used with both delivery methods. I developed a protocol using on one hand the pAc-sgRNA-Cas9 vector (Bassett et al., 2013)

and the FuGENE® transfection reagent, as determined for OE cell lines, and on the other hand eGFP-Cas9 enzymes for perfecting delivery of Cas9 complexes to Sf9 cells by electroporation. However, I overlooked the species-specificity of the *U6* promoter driving the expression of the sgRNAs in the pAc-sgRNA-Cas9 vector, designed for *D. melanogaster* (Huang et al., 2017). In addition, one of the two guides proved to be non-efficient which prevented the double-strand break with Cas9d10A.

I present below the development and outcome of the current procedure used in our lab.

Protocol setting using a Sf9-eGFP cell line

Four sgRNAs were designed to target the first exon of *CncC* (sg145, sg166, sg556 and sg1014) and the second exon of *Keap1* (sg97, sg119, sg121 and sg173) (Fig. 20A, B). To test the validity of the sgRNA I checked the editing efficiency of synthetic *CncC* sgRNA complexed to Cas9 enzyme on a PCR amplicon spanning the expected cutting site. Cas9 purified enzyme was mixed to each sgRNA before incubation with the PCR amplicon. After incubation, the resulting products were migrated onto an agarose gel and results are presented in Fig. 20C.

The data shows that all Cas9:sgRNA complexes cleave the DNA sequence with high efficiency as no band of the *Wt* expected size can be seen in sg556, sg1014, sg145 and sg166 respective lanes. Bands of higher molecular weight are believed to be constituted of the Cas9:sgRNA complex fused to one end of the targeted DNA double-strand. Indeed, a final step of the experiment, using protein kinase A to end the editing activity of the Cas9, was not performed. The data shows that the four sgRNAs designed to target the first exon *CncC* have high CRISPR/Cas9 efficiency and are well suited for *in vivo* editing. CRISPR/Cas9-mediated mutations in Sf9 cells had previously been achieved by Dr Jarvis' group who kindly provided us with the pIE1-Cas9-SfU6-sgRNA-Puro vector and Sf9-eGFP cells (Mabashi-Asazuma and Jarvis, 2017). The protocol for Sf9 transformation by CRISPR/Cas9 *as per* (Mabashi-Asazuma and Jarvis, 2017) was adapted in our lab using the Sf9-eGFP cell line (Fig. 20D). The pIE1-Cas9-SfU6-eGFP-Puro plasmid was transfected into Sf9-eGFP cells and two weeks post-transfection monoclonal cell lines that had lost the GFP fluorescence could be isolated (Fig. 20D) This confirmed the successful mutation of the *eGFP* gene leading to suppression of eGFP fluorescence.

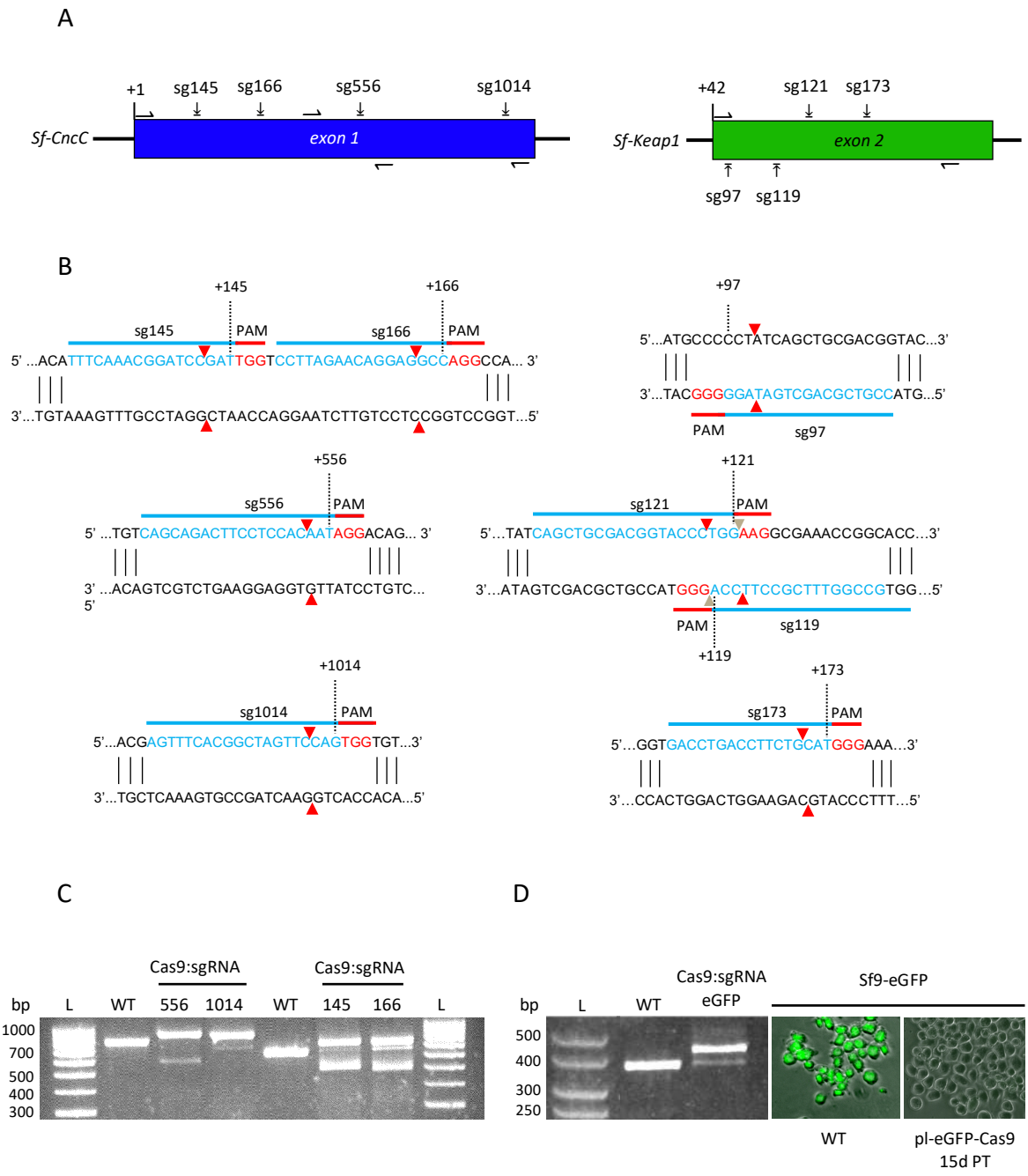

Fig. 20 CRISPR/Cas9 protocol development to silence *CncC* and *Keap1*.

(**A**) Diagram showing the target sites of four sgRNAs designed on exon 1 of *CncC* (blue) and *Keap1* (green). The location of primers used for amplification the region spanning the target sites are represented by half arrows. (**B**) Detailed sequences of the sgRNAs used in this study. The name of each guide is given based on the position of the nucleotide immediately after the PAM motif. The PAM sequence is shown in red while the guide sequence is shown in blue. Red arrows mark the expected Cas9 enzyme cutting site. (**C**) *In vitro* efficiency assay of sgRNAs targeting *CncC*. Cas9 enzyme was complexed to synthesized sgRNA (sg556, sg1014, sg145 and sg166) and the digestion product was migrated onto a 1% agarose gel. The expected *Wt* sequence size is 800 bp. L = Ladder. (**D**) The CRISPR/Cas9 protocol was developed using Sf9-eGFP cells and a sgRNA targeting the *eGFP* gene. The efficiency of the guide was tested *in vitro* (right) before proceeding to plasmid transfection in *Wt* Sf9-eGFP cells (middle). Patches of cells that had lost the eGFP fluorescence could be isolated 15 days post-transfection (PT) (right).

Table 5 Total number of CRISPR/Cas9 cell lines isolated and Sanger sequenced.

Gene	sgRNA	Nb of cell lines isolated	Nb of successful edits based on Sanger sequencing profiles	Total
CncC	sg145	4	3	17
	sg166	5	4	
	sg556	6	6	
	sg1014	5	4	
Keap1	sg97	4	2	11
	sg119	5	4	
	g121	6	0	
	sg173	6	5	

Knockout of CncC and Keap1

To knockout *CncC* and *Keap1*, Sf9 cells were independently transfected with one of the eight pIE1-Cas9-SfU6-sgRNA-Puro plasmid constructions, containing the coding sequence of the eight sgRNAs (Table 5, Fig. 16). Four to six monoclonal cell lines per sgRNA were successfully isolated with a total of 20 and 21 cell lines putatively KO for *CncC* and *Keap1*, respectively (Table 4).

Characterization of CRISPR/Cas9-induced mutations using Sanger sequencing.

As a first assessment of CRISPR/Cas9-induced mutations, a sequence of *ca.* 700 to 800 base pair (bp) spanning the Cas9 target site was amplified by PCR from genomic DNA for all the isolated cell lines and Sanger sequenced. Most sequences obtained using two to three sequencing primers were difficult to align. When a clear consensus was obtained the sequence usually matched the *Wt* sequence of *CncC* or *Keap1* demonstrating no successful edition (Table 4). Sanger profiles often showed noisy chromatograms surrounding the predicted cutting site, thus impairing basecalling and resulting in poor sequences quality (Fig. 21B). These profiles suggested an overlay of several close sequences such as allelic variants. Based on these noisy profiles, the number of putative successful CRISPR/Cas9-edited cell lines could be assessed. All four *CncC* sgRNAs produced mutated transformants with a total of 17 cell lines out of the 20 isolated. As for *Keap1*, one sgRNA out of the four designed was inefficient (sg121, Table 4) and resulted in no DNA edition. The overall number of edited cell lines for *Keap1* amounted to 11 out of the 21 isolated cell lines.

Characterization of CRISPR/Cas9-induced mutations using amplicon sequencing vs ICE computational analysis

To further characterize the mutations produced by CRISPR/Cas9 editing *i.e.*, allele sequences and frequencies, I confronted two analysis methods: a sequencing-based to a computational method (Fig. 21A). On one hand, Sanger sequences from Sf9$^{CncC\text{-}08}$ were analyzed using the ICE online tool (ice.synthego.com, Hsiau et al., 2018) (Fig. 21C). On the other hand, the PCR amplicon from the same cell line was cloned into the pGEM-T vector and 96 bacterial clones were picked for amplicon sequencing (Fig. 21D).

ICE analysis of two Sanger sequences predicted successful CRISPR/Cas9-mediated mutations for Sf9$^{CncC\text{-}08}$ with 75 % of total indel efficiency (R^2 = 0.75). Two deletions, of 14 bp and 9 bp respectively, accounted for 33 % and 31% of total allelic sequences (Fig. 21C, Appendix C, Table S4) while no *Wt* sequence was predicted to remain in Sf9$^{CncC\text{-}08}$. Reconstituting the alleles into *CncC*'s genomic sequence allowed to identify frameshifts variants (69 % of sequences) from protein deleted by a few amino-acids (12 % of sequences, resulting in -1 aa and -3 aa, Table 6).

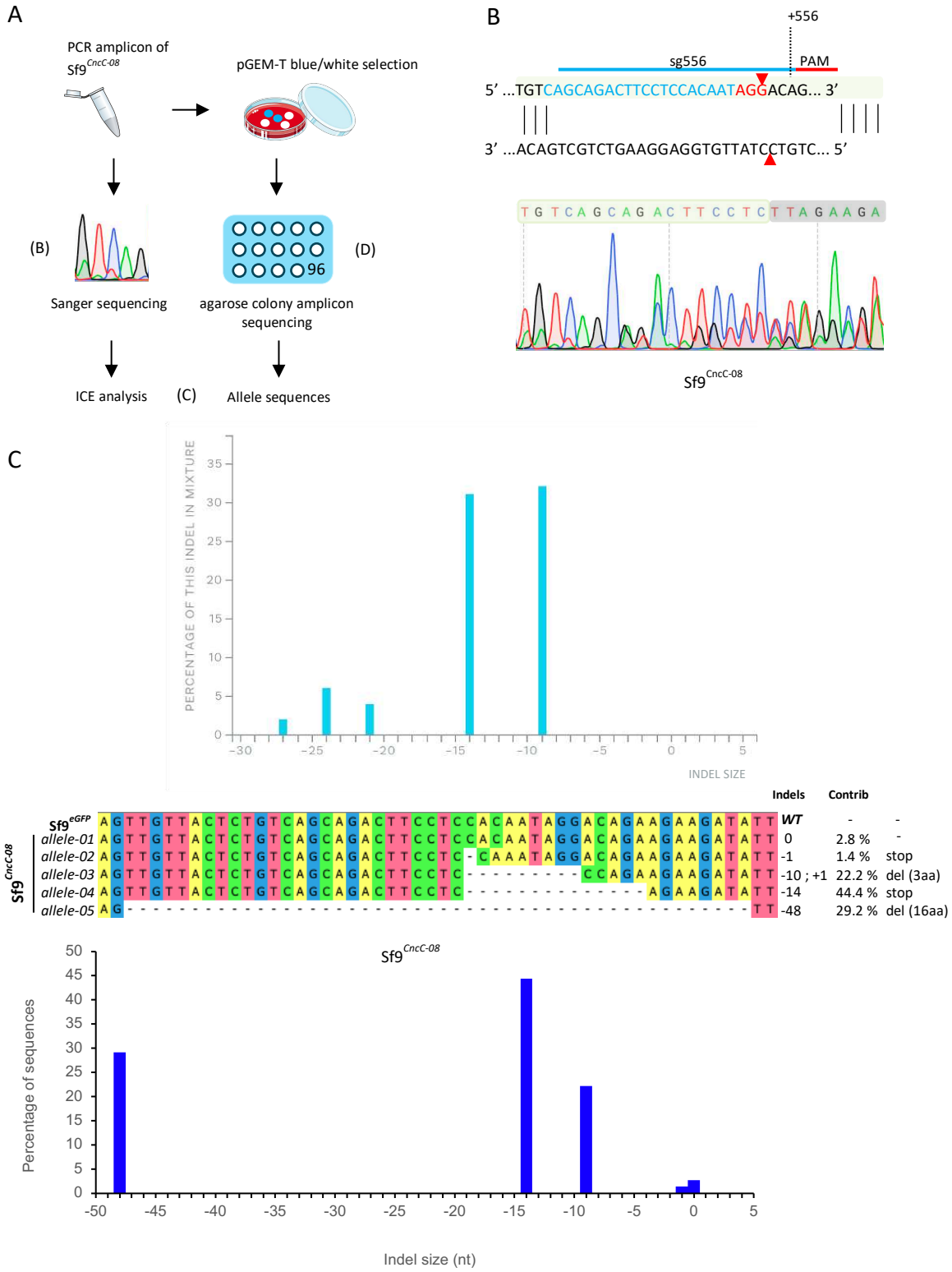

Fig. 21 Comparative analysis of CRISPR/Cas9 mutations in Sf9$^{CncC-08}$ using ICE and amplicon sequencing.
(**A**) A PCR amplicon spanning the CRISPR/Cas9 target site was amplified from Sf9$^{CncC-08}$ for Sanger and colony amplicon sequencing. (**B**) Sanger sequencing chromatogram showing noise around the expected CRISPR cutting site. The computational analysis of this Sanger profile using the ICE online tool (**C**) predicted two main indel sizes of -9 and -14 nucleotides that accounted for *ca* 30% of all allelic sequences, respectively. (**D**) The Sf9$^{CncC-08}$ PCR amplicon was cloned into the pGEM-T vector and transformed into *E. coli* for blue/white selection. 96 white colonies were picked and sequenced on a 96-well agarose plate resulting in 72 clean sequences. In total, CRISPR/Cas9 editing generated four deletions of -48, -14, -9 and -1 nucleotides respectively.

73 clean consensus sequences were obtained by amplicon sequencing using two primers (Fig. 21C, Appendix C, Fig. S4). A deletion of 14 bp was the most represented allelic sequence in Sf9$^{CncC-08}$ (44.4 %) followed by a deletion of 48 bp representing 29.2 % of alleles. A deletion of 9 bp resulting in a CncC protein deleted of 3 amino acids accounted for 22.2 % of alleles. Finally, the *Wt* CncC sequence was present in 2.8 % of all sequences (found in two bacterial clones out of 72, Appendix C, Fig. S4).

Table 6 Results of the ICE analysis of CRISPR/Cas9-mutated Sf9 cell lines.

Cell line	sgRNA	Total CRISPR eff ‡	R^2	Protein state		
				% Wt‡	% frameshift‡	% DEL‡
Sf9$^{CncC-01}$	sg145	13	0.99	86-87	12-13	ND
Sf9$^{CncC-02}$	sg145	13	0.99	86	13	ND
Sf9$^{CncC-03}$	**sg166**	**47**	**0.94**	**5**	**47**	**42**
Sf9$^{CncC-04}$	**sg166**	**81**	**0.98**	**3**	**81**	**14 (-1 aa)**
Sf9$^{CncC-05}$	sg166	36	0.96	43	36	17 (-1 aa)
Sf9$^{CncC-06}$	sg556	44	0.81	32-37	22-30	11-18
Sf9$^{CncC-07}$	**sg556**	**46**	**0.91**	**0**	**40**	**40 (-1 aa)**
Sf9$^{CncC-08}$	**sg556**	**41**	**0.76**	**0**	**69**	**12 (-1;-3)**
Sf9$^{CncC-09}$	sg556	5	0.9	84-96	3	ND
Sf9$^{CncC-10}$	sg556	14	0.97	74-76	10-14	8
Sf9$^{CncC-11}$	sg556	14	0.97	74-81	4-14	5-8
Sf9$^{CncC-12}$	sg1014	14	0.99	85-92	6-14	NA
Sf9$^{CncC-13}$	**sg1014**	**98**	**0.98**	**0**	**98**	**NA**
Sf9$^{Keap1-01}$	**sg97**	**77**	**0.94**	**4 - 12**	**69**	**12 (-1 aa, -3 aa)**
Sf9$^{Keap1-02}$	**sg97**	**46**	**0.84**	**20 - 25**	**50**	**12 (+2aa; -1aa; -7aa)**
Sf9$^{Keap1-03}$	sg119	30	0.97	65-66	23-24	ND
Sf9$^{Keap1-04}$	sg119	19	0.96	64-65	31-32	ND
Sf9$^{Keap1-05}$	**sg119**	**59**	**0.83**	**18 - 19**	**48**	**10 (-7aa)**
Sf9$^{Keap1-06}$	**sg119**	**60**	**0.78**	**7 - 10**	**56**	**13 (+2aa; -8aa)**
Sf9$^{Keap1-07}$	**sg173**	**76**	**0.9**	**0**	**33-41**	**43-46**
Sf9$^{Keap1-08}$	**sg173**	**76**	**0.9**	**0**	**41**	**43 (-7aa; -4aa)**
Sf9$^{Keap1-09}$	sg173	41	0.88	34	39	12 (-1aa)
Sf9$^{Keap1-10}$	sg173	20	0.95	44-45	17-18	19-20

‡ The best scored cell lines are highlighted in green.
Additional well-scored cell lines are in bold.

The ICE analysis was thus performed on all putative KO-cell lines using two Sanger profiles (Table 6, Appendix C, Table S4). The CRISPR/Cas9 efficiency predicted for KO-CncC cell lines ranged from 5 to 98 %. Sf9$^{CncC-03}$, Sf9$^{CncC-04}$, Sf9$^{CncC-07}$, Sf9$^{CncC-08}$ and Sf9$^{CncC-13}$ had high predicted

knockout scores of respectively 47, 81, 46, 41 and 98 %, which made them good candidate for *CncC* knockout. In addition, $Sf9^{CncC-04}$, $Sf9^{CncC-08}$ and $Sf9^{CncC-13}$ were predicted to bear very low levels of *Wt* sequences and high percentage of frameshifts-based mutations (Table 6). The $Sf9^{CncC-13}$ cell line for instance was predicted to bear 98 % of frameshift mutations and no *Wt* allele, which made it the best candidate for a *CncC* loss-of-function mutation (knockout score: 98%, $R^2 = 0.98$).

The CRISPR/Cas9 efficiency ranged from 19 to 74 %. $Sf9^{Keap1-01}$ and $Sf9^{Keap1-06}$ cell lines stood out for their CRISRP/Cas9 efficiency of 77 and 60, respectively. Out of these two, $Sf9^{Keap1-01}$ seemed to be the best cell lines for *Keap1* loss-of-function mutation.

Assessment of CncC and Keap1 transcript levels in CRISPR/Cas9 mutated cell lines

I next assessed the transcript levels of *CncC* and *Keap1* genes by RTqPCR in a number of KO cell lines (14 out of 17 *CncC*-mutated lines and 10 out of 11 *Keap1*-mutated lines) (Fig. 22A). The expression of *CncC* was lower in seven cell lines ($Sf9^{CncC-01}$, $Sf9^{CncC-04}$, $Sf9^{CncC-05,}$ $Sf9^{CncC-07}$, $Sf9^{CncC-08}$, $Sf9^{CncC-12}$ and $Sf9^{CncC-13}$) and the levels ranged from 0.39- to 0.55-fold change. At the same time, the expression of *Keap1* in these cell lines was moderately but consistently upregulated by 2.1-fold in average (n = 13) (Fig. 22A). In retrospection, I checked mRNA levels of *Keap1* in OE cell lines and found no significant change in expression after overexpressing *CncC*, *Maf* or both genes (Appendix C, Fig. S3). In *Keap1*-mutated cell lines, expression of *Keap1* was strikingly not lower (Fig. 22B). Instead, transcript levels were higher than the control, as high as 6.65-fold ($Sf9^{Keap1-02}$, $p = 0.0002$) or 5.2-fold ($Sf9^{Keap1-07}$, $p = 0.002$). Assessment of *CncC* mRNA levels revealed no significant change in expression for this gene after mutating *Keap1*.

The cell lines with the lowest expression levels were also those that had the highest CRISPR/Cas9 efficiency ($Sf9^{CncC-04}$, $Sf9^{CncC-05,}$ $Sf9^{CncC-07}$, $Sf9^{CncC-08}$ for example). Although statistically not significant ($p = 0.055$) the $Sf9^{CncC-13}$ cell line was yet under-expressed as compared to the control (expression fold change: 0.47). Consistent with the transcript levels measured for *CncC* in these cell lines, $Sf9^{CncC-02}$, $Sf9^{CncC-09}$, $Sf9^{CncC-10}$, $Sf9^{CncC-11}$ and $Sf9^{CncC-12}$ had knockout scores ranging from 5 to 14% in the ICE analysis.

Interestingly, the cell lines with the highest *Keap1* expression levels were also those with the highest knockout scores. For example, the knockout score predicted for $Sf9^{Keap1-01}$

was 74 % although the gene was expressed 4.7-times higher than the control (p = 0.01). In Sf9$^{Keap1\text{-}07}$ the CRISPR/Cas9 efficiency was 73.5 % while the gene was also expressed more than 5-fold (p = 0.002).

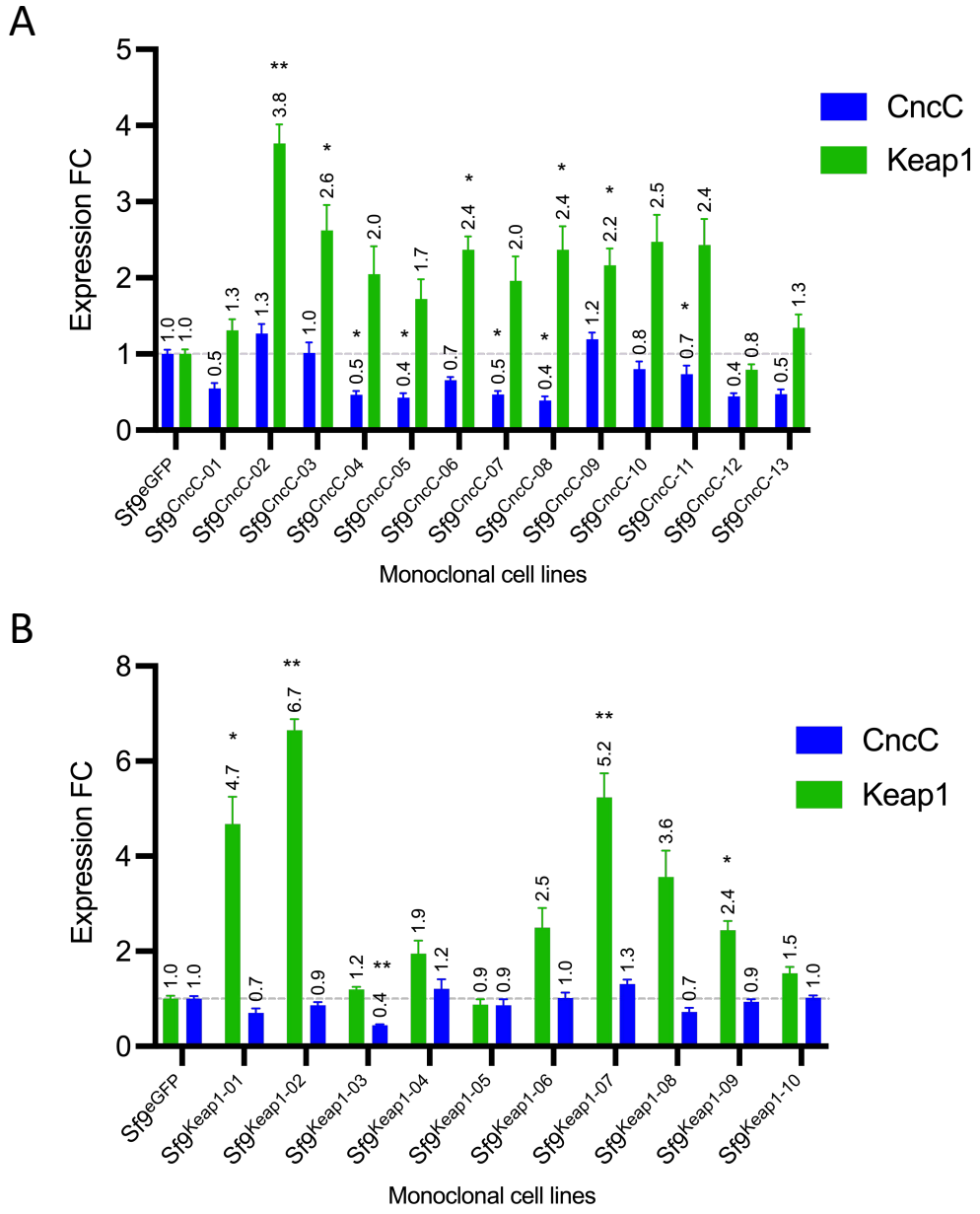

Fig. 22 Transcript levels of *CncC* and *Keap1* in CRISPCR/Cas9-edited cells.
Expression of *CncC* (blue) and *Keap1* (green) were monitored in cell lines transfected with either (**A**) CRISPR vectors containing CncC-targeting sgRNAs or (**B**) CRISPR vectors containing CncC-targeting sgRNA. Gene expression was normalized using the expression of the ribosomal protein *L4*, *L10* and *L17* reference genes and shown as fold-change relative to the expression of cell lines transfected with an "empty" plasmid, pBiEx-1. Data are mean values ± SEM.

Based on these results, Sf9$^{CncC\text{-}13}$ and Sf9$^{Keap1\text{-}01}$ were selected as reference KO-*CncC* and *Keap1*-mutated cell lines and used in following experiments to characterize the phenotypic effects of the mutations in respective genes.

Viability assays with CRISPR/Cas9 mutated Sf9 cell lines

Most cell transformants presented similar shape, size, adherence and growth rate than the Sf9 *Wt* cell line. However, a few cell lines knocked out for *CncC* including $Sf9^{CncC\text{-}13}$ presented deleterious traits and weaker resilience to cell culture handling. Indeed, $Sf9^{CncC\text{-}13}$ cells were substantially bigger than the Sf9 *Wt* and culture flasks contained high and steady levels of cell debris and vesicles. (Appendix C, Fig. S2). More importantly, the ratio of dead *vs* living cells in trypan blue exclusion assays was very often close to 1, showing weak viability for this cell lines. KO-*CncC* cell lines tested in viability assays using MTT were more susceptible to I3C ($Sf9^{CncC\text{-}05}$) and MTP ($Sf9^{CncC\text{-}04}$, $Sf9^{CncC\text{-}05}$, $Sf9^{CncC\text{-}07}$) as compared to the control (Table 7). Surprisingly, the IC_{50s} of $Sf9^{CncC\text{-}08}$ and $Sf9^{CncC\text{-}13}$ were significantly higher than the control (Fig. 23, Table 7). For example, $Sf9^{CncC\text{-}08}$ was 5.9-times more tolerant to MTP than the $Sf9^{eGFP}$ cell line. This result, quite surprising, was nonetheless reproducible.

Table 7 IC_{50} values of i3C and MTP towards CRISPR mutated cell lines.

Cell line	Treatment	IC_{50}	95% CI	Tolerance ratio
$Sf9^{eGFP}$	i3C	92.56	[80 ; 130.5]	-
	MTP	97.31	[151.8 ; 225.4]	-
$Sf9^{CncC\text{-}04}$	i3C	61.84	[55.7 ; 95.8]	0.7
	MTP	87.57	[79.5 ; 91.7]	0.9
$Sf9^{CncC\text{-}05}$	i3C	61.41	[52.4 ; 73.6]	0.7
	MTP	87.17	[81.9 ; 88.7]	0.9
$Sf9^{CncC\text{-}07}$	i3C	73.12	[58.7 ; 86]	0,8
	MTP	87.09	[83.7 ; 93.4]	0,9
$Sf9^{CncC\text{-}08}$	i3C	162.1	[153.3 ; 226.7]	1.75
	MTP	574.5	ND	5.9
$Sf9^{CncC\text{-}13}$	i3C	212.5	[206.2 ; 235.8]	2.3
	MTP	217.2	[199.6 ; 225.7]	2.2
$Sf9^{Keap1\text{-}01}$	i3C	399.3	[388.6 ; 414.1]	4.3
	MTP	492.8	[ND ; 796.1]	5.1
$Sf9^{Keap1\text{-}02}$	i3C	129.3	[109.1 ; 155.5]	1.4
	MTP	148.4	[116.3 ; 214.1]	1.5
$Sf9^{Keap1\text{-}06}$	i3C	130.2	[109.9 ; 158.8]	1.4
	MTP	154.6	[136.3 ; 178.5]	1.6
$Sf9^{Keap1\text{-}07}$	i3C	151.4	[111.6 ; 185.3]	1.6
	MTP	99.7	[81.4 ; 120.9]	1

The IC_{50} of I3C and MTP was higher for most *Keap1*-mutated cell lines (Table 7), the tolerance increasing up to 4.3-fold and 5.1-fold respectively in $Sf9^{Keap1\text{-}01}$ which was established as the best *Keap1*-mutated candidate cell line after ICE analysis (Fig. 23, Table 7).

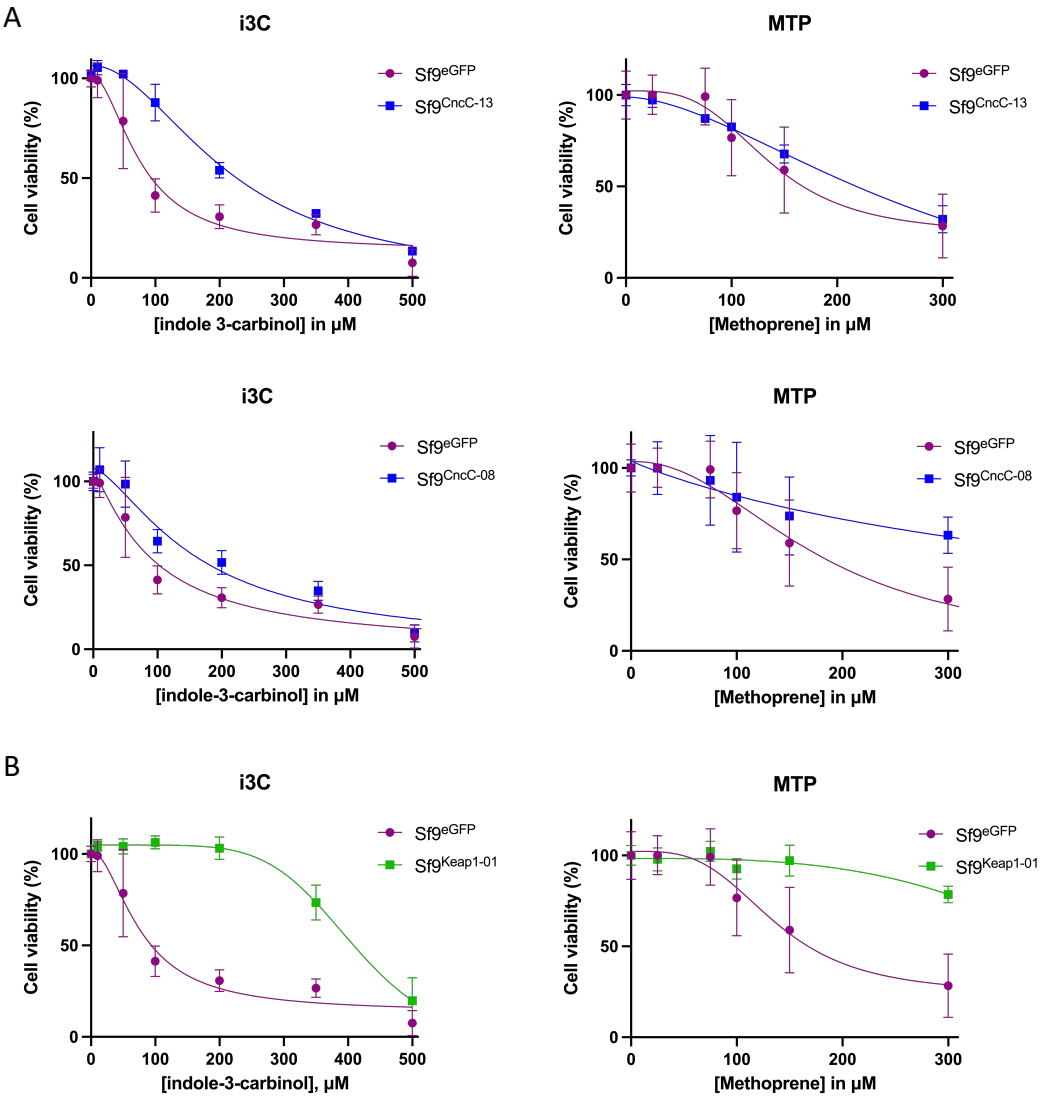

Fig. 23 Dose-response curves of I3C and MTP in MTT bioassays.
Toxicity of I3C (left) and MTP (right) towards (**A**) $Sf9^{CncC\text{-}08}$ and $Sf9^{CncC\text{-}13}$ (blue) as well as (**B**) KO-Keap1 (green) cell lines compared to the control $Sf9^{eGFP}$ (purple) obtained by MTT bioassays. Each point was expressed as a percentage of the maximum viability (DMSO treatment). Curves are nonlinear regressions (sigmoidal, 4PL).

Enzymatic activity

In the first chapter I showed that constitutive upregulation of *CncC* and *Maf* transcription factors led to upregulation of P450 and GST detoxification genes. I now showed that this was correlated to increased tolerance to I3C and MTP. To test whether transcriptional induction of detoxification genes by *CncC* and *Maf* leads to enhanced activity of detoxification enzymes, bioassays using model substrates of P450s, GSTs, and CEs were performed.

Carboxylesterase activity

The activity of CEs was tested on 1-NA and 2-NA. The activity profiles of the seven cell lines assayed were highly consistent between the two substrates used (Fig. 24). In stable OE cell lines, the highest enzymatic activity was obtained for pCncC-b and pCncC:Maf and both had activities twice as high as the control cell line. The activity of pMaf-b was only slightly lower than the control. In knockout cell lines, the suppression of *CncC* resulted in a decrease of CE activity towards the two substrates while the suppression of *Keap1* significantly increased the activity of $Sf9^{Keap1\text{-}01}$ (1.5-fold towards 1-NA and 1.3-fold towards 2-NA).

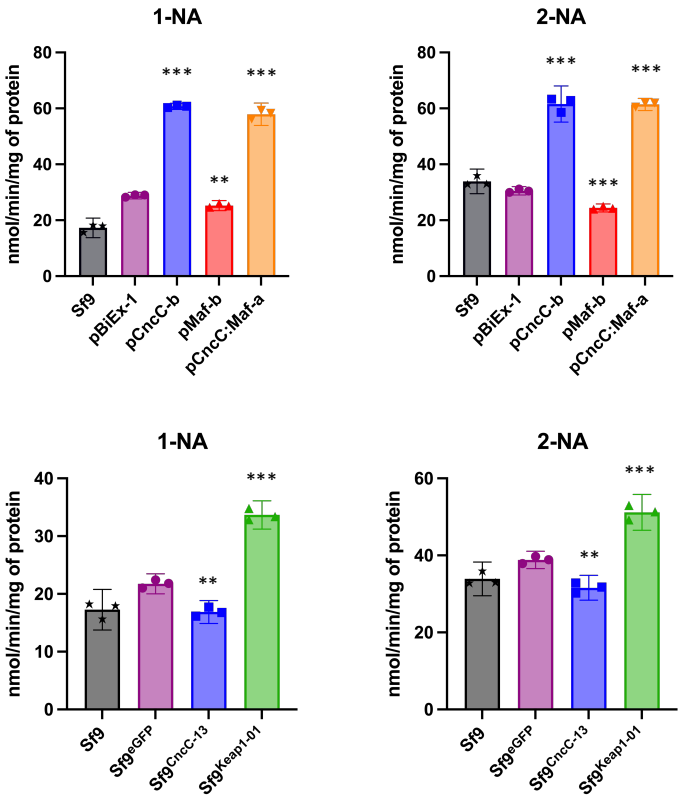

Fig. 24 Carboxylesterases enzymatic activity.
Comparison of enzyme activity obtained from Sf9 cells homogenates for CEs using two model substrates, 1-naphtyl acetate (1-NA) and 2-naphtyl acetate (2-NA). Activities were statistically analyzed by Student's t-test comparing mean values of overexpressing (top) and knocked out (bottom) cell lines to their respective control (pBiEx-1 and $Sf9^{eGFP}$).

Glutathione S-transferase activity

GST activity was recorded using two model substrates, CDNB and the fluorescent MCB (Fig. 25). The activity of pCncC-b towards CDNB and MCB was not significantly different from the control, however a decrease in metabolic activity was observed in the pMaf-b and pCncC:Maf-a cell lines, towards both substrates. The knockout of *CncC* and *Keap1* had antagonistic effects

on the activity of GST enzymes. Indeed, metabolism of CDNB and MCB was slightly lower for the KO-*CncC* cell line than for the control line, while activity towards CDNB and MCB was 5- and 2-times higher, respectively, in the *Keap1*-mutated cell line.

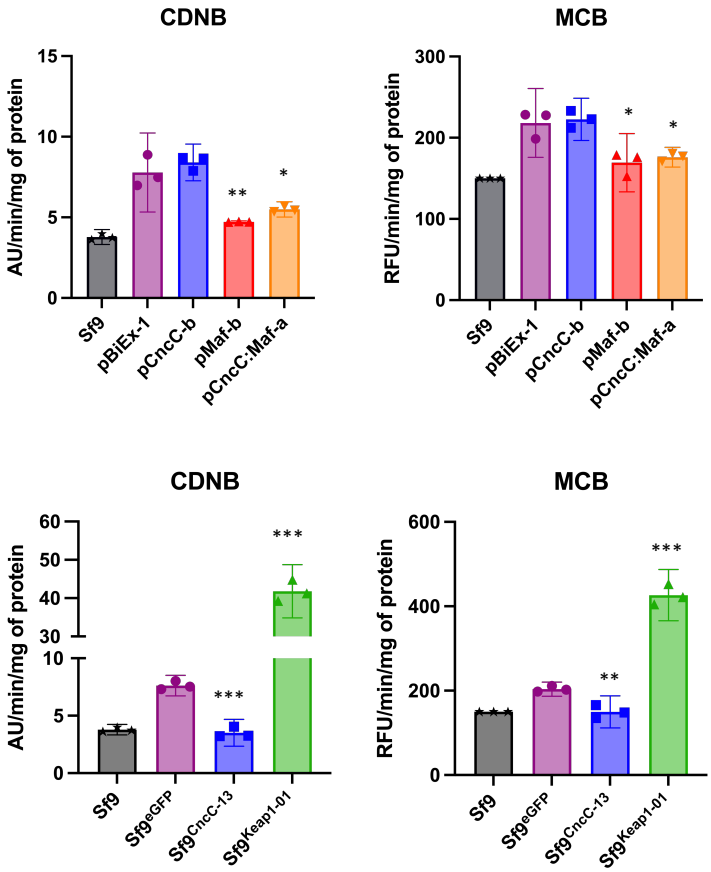

Fig. 25 Glutathione S-transferases enzymatic activity.
Comparison of enzyme activity obtained from Sf9 cells homogenates for GSTs using two model substrates, 1-chloro-2,4-dinitrobenzene (CDNB) and monochlorobimane (MCB). Activities were statistically analyzed by Student's t-test comparing mean values of overexpressing (top) and knocked out (bottom) cell lines to their respective control (pBiEx-1 and $Sf9^{eGFP}$).

The activation of the CncC:Maf pathway is modulated by ROS production

To determine whether P450 and GST gene induction were related to oxidative stress induced by I3C and MTP, ROS content was monitored 6 hours after xenobiotic exposure using carboxy-H_2DCFDA and HCS (Fig. 26). I3C and MTP triggered moderate but significant ROS production in Sf9 cells while exposure to fenoxycarb and t-BHP had no significant effect. MTP was a more potent ROS inducer than I3C and presented twice the amount of fluorescence intensity than the plant compound. This suggests that ROS caused by exposure to insecticides might enhance the expression of detoxification genes. The incubation of cells with sodium pyruvate (SP)

systematically reduced ROS levels in all treatment conditions, except for t-BHP and the strongest effect was observed with fenoxycarb, MTP and I3C treatments.

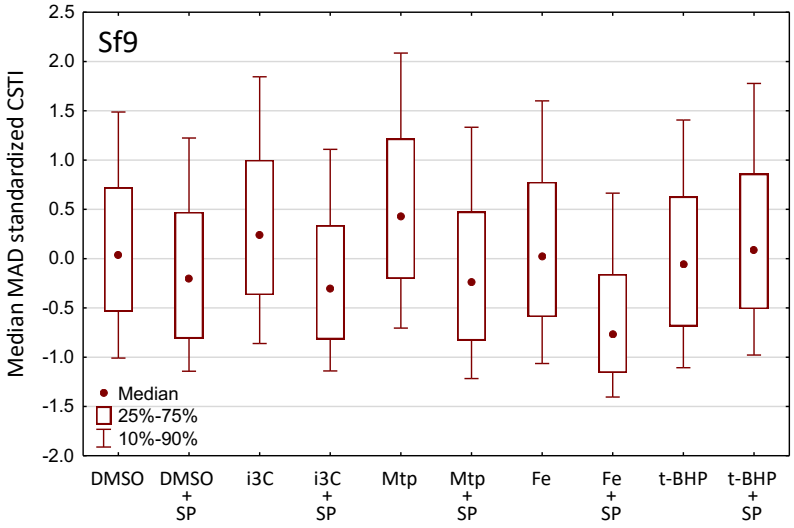

Fig. 26 ROS content in Sf9 cells under xenobiotic treatment and anti-oxidant treatment.
Sf9 cells were exposed for 6 hours to DMSO and four xenobiotics with and without sodium pyruvate (SP) as antioxidant. ROS levels were expressed as circular spots total (fluorescence) intensity (CSTI) and submitted to a median MAD standardization in order to fix the values in the same order of magnitude (robust Z-score). From left to right: DMSO, I3C, MTP, fenoxycarb (Fe) and tert-butyl hydroperoxide (t-BHP) with alternative SP. Results are presented as box plot median ± percentile 25% and 75% and nonoutlier data. For statistical analysis, the nonparametric Kruskal−Wallis test was performed. Statistical significance was assumed at $p < 0.05$.

To test if the constitutive activation of *CncC* and *Maf* modulates the basal and xenobiotics-induced oxidative stress in Sf9 cells, I measured ROS content in all transformants after I3C, MTP, fenoxycarb and t-BHP exposure. Treatments with xenobiotics had very little effect on ROS content in OE cell lines. For example, i3C- and MTP-induced similar ROS levels in pBiEx-1, pCncC-b, pMaf-b and pCncC:Maf-a (median comprised between 0 and +0.5 on average, Fig. 27B). However, ROS content was overall greatly increased in $Sf9^{CncC\text{-}13}$ as compared to control and overexpressing cell lines (Fig. 27B) and for all treatment conditions (median values > 0 for every treatment, Fig. 27A). On the contrary, ROS production was significantly reduced in $Sf9^{Keap1\text{-}01}$ regardless of the treatment used (median values < 0) and as compared to all other cell lines (Fig. 27A, B). Taken together, these results suggest that CncC:Maf are potent regulators of basal oxidative stress in Sf9 cells and might control the expression of genes involved in ROS modulation. Furthermore, the antioxidant effect of SP was confirmed with all cell lines as its supplementation to the culture medium reduced significantly ROS levels induced by xenobiotic treatments, with the strongest effect observed with I3C, MTP and fenoxycarb (Fig. 27A).

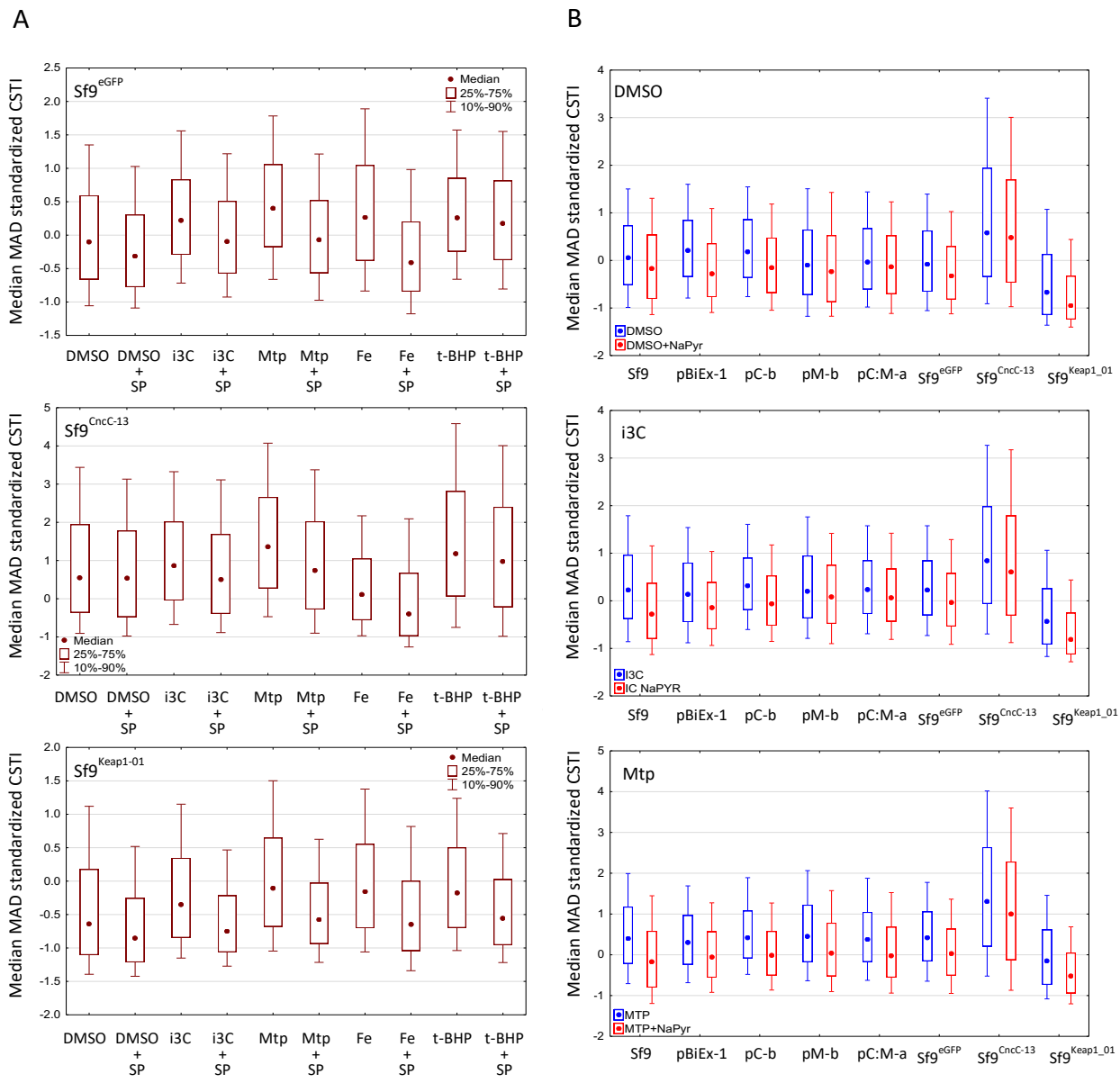

Fig. 27 ROS content in Sf9 cells under xenobiotic and antioxidant treatment.

(**A**) ROS levels in (top to bottom) $Sf9^{eGFP}$, $Sf9^{CncC-13}$ and $Sf9^{Keap1-01}$ after exposure for 6 hours to DMSO and four xenobiotics with and without sodium pyruvate (SP) as antioxidant. From left to right: DMSO, I3C, MTP, fenoxycarb (Fe) and tert-butyl hydroperoxide (t-BHP) with alternative SP. (**B**) The effect of (top to bottom) DMSO, I3C and MTP is shown for each cell line. ROS levels were expressed as circular spots total (fluorescence) intensity (CSTI) and submitted to a median MAD standardization in order to fix the values in the same order of magnitude (robust Z-score). Results are presented as box plot median ± percentile 25% and 75% and nonoutlier data. For statistical analysis, the nonparametric Kruskal–Wallis test was performed. Statistical significance was assumed at $p < 0.05$.

Effect of scavenging ROS on Sf9 transformants viability.

Antioxidants are often used to suppress xenobiotics-induced ROS bursts and hence prevent the activation of the CncC:Maf pathway and deployment of cytoprotective agents. However, the determination of ROS levels in Sf9 transformants showed that basal oxidative stress was significantly increased in *CncC*-mutated cells, while strongly lowered in $Sf9^{Keap1\text{-}01}$. In addition, the presence of stress vesicles suggested that high ROS content may be a primary determinant of $Sf9^{CncC\text{-}13}$ weaker viability. Following this rationale, the use of SP as an antioxidant should have differential effects on cell transformants. We can expect a more potent effect on $Sf9^{CncC\text{-}13}$ cells as well as control cell lines as compared to $Sf9^{Keap1\text{-}01}$ for which ROS levels are basically very low. To test this hypothesis and better understand the link between the CncC:Maf pathway and ROS signaling, I reproduced MTT viability assays using an SP to suppress ROS content and xenobiotic-mediated ROS bursts. Preincubation of cells with SP led to significant decrease of ROS content for all cell lines and after every xenobiotic treatment except for t-BHQ (Fig. 26 and Fig. 27). SP had a potent effect on xenobiotic-induced ROS bursts such as those induced by I3C and MTP while it had very little effect on the ROS content of cells treated with t-BHP and DMSO (Fig. 26 and Fig. 27A). Supplementing SP in the medium before performing MTT viability assays resulted in inconsistent gains of tolerance towards I3C and MTP among OE and KO cell lines. Indeed, while SP supplementation dramatically increased the IC_{50} of both compounds for control cell lines, the tolerance ratio was much lower for cell lines activated for the CncC:Maf pathway like pCncC:Maf-a (Table 8, Fig. 28). As expected, SP had very little to no effect on cell viability in $Sf9^{Keap1\text{-}01}$ (Table 8, Fig. 28B), for which ROS levels before and after xenobiotic treatments were among the lowest among all cell lines and treatments combined (Fig. 27A). Although SP application significantly improved $Sf9^{CncC\text{-}13}$ apparent viability (data not shown), ROS levels after xenobiotic treatments remained higher than those obtained in control cell lines with median values between 0.5 and 1 for I3C+SP and MTP+SP treatments (Fig. 27). In agreement with this, IC_{50} of I3C and MTP for this cell line increased with SP treatments, in proportions similar to those of the control (Table 8, Fig. 28).

Table 8 Effect of sodium pyruvate on cells tolerance to xenobiotics.

Cell line	Treatment	IC_{50}	95% CI	Ratio‡
pBiEx-1	i3C	343.9	[319.9 ; 371.9]	7.2
	MTP	393.1	[317.3 ; 442.5]	4.5
pCncC-b	i3C	339.4	[327.3 ; 349.8]	7.6
	MTP	510.4	[500 ; 520.7]	5.8
pMaf-b	i3C	253.3	[239.4 ; 266]	4.2
	MTP	305	[ND ; 329]	2.9
pCncC:Maf-a	i3C	233.8	[218.7 ; 244.9]	1.7
	MTP	313.2	[283.3 ; 346.3]	2.6
$Sf9^{eGFP}$	i3C	319.9	[306.3 ; 332.9]	3.45
	MTP	342.8	[305.5 ; 356.3]	1.9
$Sf9^{CncC-13}$	i3C	370.5	[352.3 ; 393.4]	1.7
	MTP	500.7	[ND ; ND]	2.3
$Sf9^{Keap1-01}$	i3C	383.7	[372.4 ; 396]	1.0
	MTP	500.3	[436.6 ; 532.1]	1.0

‡ Ratios were calculated by dividing the IC_{50s} obtained in MTT assays with and without SP (IC_{50}^{-}/IC_{50}^{SP})

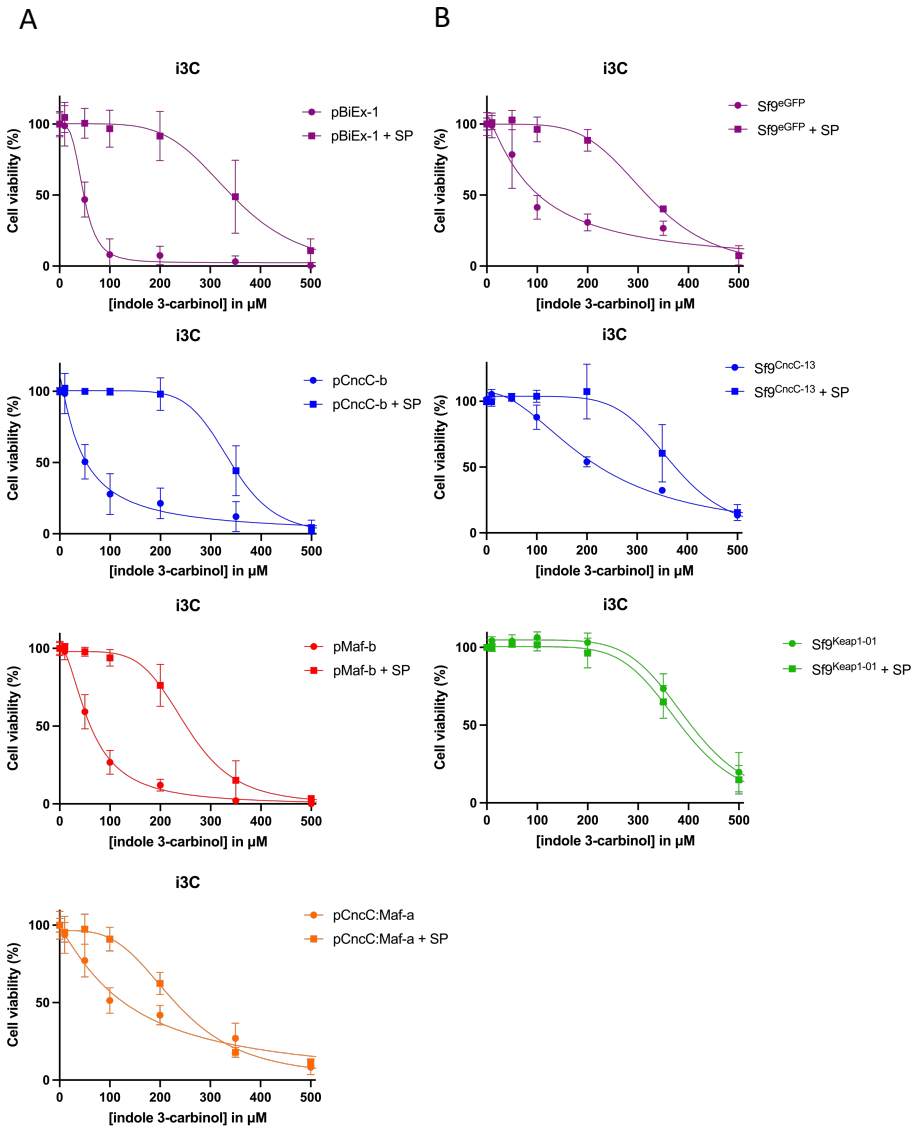

Fig. 28 Effect of sodium pyruvate on dose-response curves of I3C in Sf9.
Toxicity of I3C towards (**A**) cell lines overexpressing *CncC*, *Maf* or CncC:Maf and (**B**) cell lines knocked out for *CncC* and *Keap1* was assessed using the antioxidant sodium pyruvate (SP, squares) and compared to control MTT assays (circles). Each point was expressed as a percentage of the maximum viability (DMSO treatment). Curves are nonlinear regressions (sigmoidal, 4PL).

DISCUSSION

Although the metabolic activity of detoxification enzymes are well studied, the mechanisms leading from chemical exposure to transcriptional activation are poorly understood in insects. The focus of this chapter was to determine whether the CncC:Maf pathways plays a role in the protection and tolerance of Sf9 cells to plant secondary metabolites and insecticides. In the previous chapter we used transient expression of *CncC*, *Maf* or both genes to show that the CncC:Maf pathway is involved in the upregulation of P450 and GST genes. However, transcripts levels of *CncC* and *Maf* were dramatically high, reaching up to 1000-fold that of the control cell line. Here I established stably transformed Sf9 cell lines to recreate physiological conditions of *CncC* and *Maf* activation seen in field populations. Moreover, cell lines stably overexpressing *CncC* and *Maf* allow toxicological testing on cells that have not been in recent contact with transfection reagents that may have an effect on membrane permeability.

The expression of *CncC* and *Maf* in the stable transformants did not exceed 1.5- to 15-fold that of the control, which remains in the same range seen in resistance populations of insects for which *CncC* and *Maf* genes are overexpressed or induced by xenobiotics(Chen et al., 2018a; Hu et al., 2019b; Lu et al., 2020; Shi et al., 2021c). For example, CncC was induced by 2-fold after *S. litura* larvae were treated with 400 µM I3C and by 3-fold in larvae fed with 6 $mg.kg^{-1}$ (LD_{50}) λ-cyhalothrin supplemented diet (Lu et al., 2020). *CncC* and *Maf* were also found constitutively overexpressed in serval resistant *Spodoptera* populations. For instance, a *S. exigua* strain resistant to chlorpyrifos had levels of *CncC* and *Maf* 8- and 3-times higher than the susceptible population, respectively (Hu et al., 2019b). In *S. litura*, an indoxacarb resistant population had *CncC* transcripts levels 3.3-times higher than the susceptible population (Shi et al., 2021c).

Simultaneously, we implemented the CRISPR/Cas9 system to knockout *CncC* and *Keap1* genes. Knockout experiments resulted in a number of cell lines showing complex Sanger traces located at the CRISPR/Cas9 target sites. Therefore, refining the analysis of the different alleles produced in the various cell lines isolated was necessary to increase the likability of identifying loss-of-function mutations. The computational approach using ICE analysis proved to be a highly useful tool to sort out the 28 isolated cell lines putatively mutated for *CncC* and *Keap1*. The knockout of *CncC* resulted in significantly lower (0.44-fold in average) transcript levels in comparison to levels measured in the control cell line. This

variation in expression was likely to result in significant differential expression of detoxification genes as shown by previous studies using RNAi to knockdown *CncC* in other insect species (Chen et al., 2018a; Gaddelapati et al., 2018; Kalsi and Palli, 2017a, b; Lu et al., 2020; Shi et al., 2017).

While CRISPR/Cas9-induced mutations in *CncC* resulted in lower *CncC* expression levels, mutating *Keap1* resulted in a significant increase of *Keap1* transcripts in most $Sf9^{Keap1}$ cell lines assessed (Fig. 22). The amplification of *Keap1* transcription despite the introduction of a mutation in its coding sequence challenges the idea of having succeeded to establish a true gene knock-out, as when a mutation impedes a gene's function. As it stands, I am not able to account for the increase in *Keap1*'s expression. Nevertheless, several hypotheses exist that would need to be tested. First, *Keap1* may be a gene subject to alternative splicing. However, the RNA-seq data available on BIPAA (bipaa.genouest.org) for *S. frugiperda* does not support this hypothesis (Gouin et al., 2017). Second, the CRISPR/Cas9 mutation may have introduced an alternative translation initiation (ATI) or resulted in an exon skipping event typically preventing mRNA degradation and promoting translation of the pseudo-mRNAs (Tuladhar et al., 2019). Antibodies targeting *Keap1* would be very useful for detecting native as well as potentially ablated proteins that emerge from these events. Similarly, antibodies targeting *CncC* may be also useful to detect its stabilization and recruitment to the nucleus after *Keap1* knockout. Third, these results may suggest that *Keap1* is involved in the regulation of its own expression. A few studies have demonstrated the existence of an auto-regulation loop of the CncC:Maf pathway involving *Keap1* and *CncC* (Deng, 2014; Sykiotis and Bohmann, 2008). However, these examples in *Drosophila* report a feed-forward regulatory loop which is in contradiction with what we observe here. Finally, *Keap1* may interact with other regulatory pathways that controls its expression. Nevertheless, the apparent increase of *Keap1* mRNA correlated well with strong CRISPR/Cas9 efficiency, increased cell viability and enzymatic activity.

Cell viability assays with OE cells lines depicts the requirement of both transcription factors to observe a significant increase in xenobiotics tolerance. The overexpression of the two transcription factors in pCncC:Maf-a had a greater effect on the tolerance of Sf9 cells to I3C and MTP than when a single factor was overexpressed. These results reflect those obtained in the first chapter where the transient expression of the two transcription factors together led to higher transcript levels of *CYP4M14*, *CYP4M15*, *CYP321A9* and *GSTe1* than in

single-gene transformants. Work on the mammalian orthologs Nrf2 and Maf has shown that these transcription factors function as heterodimers and that the joint effect of their activation depends on increasing their titer in a 1:1 ratio (Itoh et al., 1997). This also agrees with previous studies in other insect species demonstrating that the presence of both CncC and Maf had an additive effect on promoter activity of xenobiotic genes (Hu et al., 2019b; Kalsi and Palli, 2015, 2017b; Shi et al., 2017).

Knocking out *CncC* resulted in a moderate decrease in cell tolerance to I3C and MTP in three out of five cell lines assayed. The decrease in IC_{50} is consistent with reduced tolerance to xenobiotics observed in several insect species from studies that repressed *CncC* using RNAi. For example, incubating *S. litura* Spli-221 cells with dsRNA targeting *CncC* resulted in higher mortality under I3C exposure as compared to cells silenced for a mock-gene (Chen et al., 2018a). Similarly, silencing *CncC* in *S. litura* larvae increased mortality by 29.17 % after λ-cyhalothrin exposure compared to the control (Lu et al., 2020). *CncC*-silencing was associated with downregulation of *CYP6AB12* and decrease in P450 enzymatic activity suggesting that *CncC* conveyed λ-cyhalothrin tolerance by regulating a P450 involved in its metabolism (Lu et al., 2020). Very surprisingly however, the two cell lines which obtained the highest knockout scores, *i.e.* $Sf9^{CncC\text{-}13}$ (98% ICE score, R^2 = 0.98) and $Sf9^{CncC\text{-}08}$ (confirmed by amplicon sequencing) were unexpectedly more tolerant to treatment with xenobiotics. These cell lines were indeed more sensitive to manipulation and showed consistent accumulation of cell debris, scattered vesicles from burst cells and a high number of large apoptotic cells (Appendix C, Fig. S2). Several hypotheses can explain the seemingly higher tolerance of $Sf9^{CncC\text{-}08}$ and $Sf9^{CncC\text{-}13}$ in viability assays. First, the number of viable cells during counts by trypan blue exclusion could have been underestimated. $Sf9^{CncC\text{-}08}$ and $Sf9^{CncC\text{-}13}$ seemed highly prone to trypan blue staining with often more than half of the cells tinted in blue, suggesting weak viability. However, trypan blue measures the ability of cells to exclude the negatively charged chromophore and is hence a marker of membrane integrity. Overestimation of dead cells can result when cell membranes are more permeable, resulting in blue-stained yet viable cells. Second, reduction of MTT to formazan crystal has been reported to be widely affected by a number of factors, including oxidative stress (Stepanenko and Dmitrenko, 2015). MTT reduction occurs throughout a cell and the activity of cytosolic and microsomal oxidoreductases as well as general oxidative stress may significantly impact the MTT assay readout (Berridge et al., 2005; Stepanenko and Dmitrenko, 2015). Although our comparative

analysis of viability assays using MTT and propidium iodide (using HCS) for the OE cell lines did not show major discrepancy between the two methods, this may need reconsideration for the KO-*CncC* cell lines. An examination of $Sf9^{CncC\text{-}13}$ viability under I3C and MTP stress using an additional method is necessary to rule out the possibility that higher ROS levels or a change in oxidoreductases activity due to *CncC* knockout do not undermine the MTT reduction and overestimate the viability of $Sf9^{CncC\text{-}13}$ under xenobiotic stress.

The mutation of *Keap1* led to an increase of IC_{50} for I3C and MTP in all cell lines, as a result of the presumably reduction or lack of *CncC* proteasomal degradation. The increase in tolerance to xenobiotics was the most considerable in $Sf9^{Keap1\text{-}01}$ (I3C tolerance ratio = 4.3 and MTP = 2.77). This is in line with the prediction made by the computational analysis where $Sf9^{Keap1\text{-}01}$ obtained one of the best ICE CRISPR efficiency score with a strong model fit (77%, R^2 = 0.94). Targeting *Keap1* as a mean of modulating the action of *CncC* is a strategy that has been successfully employed in previous studies on *Drosophila* flies (Misra et al., 2011; Misra et al., 2013; Sykiotis and Bohmann, 2008). Misra and coworkers modulated the CncC:Maf pathway using both overexpression of *Keap1* (Misra et al., 2011) or its RNAi-mediated silencing (Misra et al., 2013). Both strategies resulted in a change of expression of CncC target genes such as *cyp6a2* and *cyp6a8* (Misra et al., 2011; Misra et al., 2013) or increased the tolerance of UAS-Keap1-RNAi mutant flies to malathion treatments (Misra et al., 2011). Similarly, we show here that the mutation of *Keap1* leads to increased tolerance of cells to xenobiotics. The shift of IC_{50} observed with OE and KO cell transformant suggest that CncC:Maf regulate the expression of cytoprotective and detoxification enzymes involved in the metabolism of xenobiotics.

I therefore measured the activity of known detoxifying enzymes against model substrates in selected Keap1/CncC/Maf Sf9 transformants. The overexpression of *CncC* in pCncC-b and pCncC:Maf-a cell lines enhanced 2-fold the level of their CE activity towards 1-NA and 2-NA. Conversely, the overexpression of *Maf* seemed to have very little impact on the metabolism of these substrates. Very similar to what could be observed in cell lines overexpressing *CncC* (pCncC-b and pCncC:Maf-a), $Sf9^{Keap1\text{-}01}$ presented a drastic increase of CE activity. While *CncC* overexpression nearly doubled CE activity, *CncC* knockout led to a slight decrease of activity in $Sf9^{CncC\text{-}13}$. This difference of activity compared to the control and the increase seen in *CncC*-

OE cell lines may depict the proportion of enzymatic activity that can be attributed to basal *vs* induced CncC activity.

Furthermore, a strong increase of GST activity towards both CDNB and MCB substrates was observed in $Sf9^{Keap1\text{-}01}$ while the activity moderately decreased in $Sf9^{CncC\text{-}13}$. Despite the upregulation of *GSTe1* in transient overexpression of *CncC* and *Maf* (chapter 1) and the known control of CncC:Maf over the expression of GST genes (Chen et al., 2018a; Hu et al., 2019a; Hu et al., 2019b), GST activity towards CDNB and MCB was not enhanced in OE cell lines. CncC was reported to directly control the promoter activity of *GSTe6* in a resistant strain of *S. exigua.* In this strain resistant to chlorpyrifos, *CncC* was found overexpressed 8-fold and the GST activity of resistant larvae towards CDNB was 3-times higher than in the susceptible strain. Taken together, the data provided by Hu et al. (2019b) show a direct link between insecticide resistance and the transcriptional activity of CncC:Maf on GST enzymes. However, the level of *CncC* mRNA obtained in OE cell lines might be too low to result in significant increase of GST enzymatic activity. Whether the level of CncC:Maf overexpression in OE cell lines is not potent enough to increase GST activity and whether *Keap1* modulates GST activity through its known role as CncC repressor needs further investigation. Transcriptomic analysis of differentially expressed genes in OE and KO cell lines might enlighten these results.

Taken together, the modifications of CE and GST enzymatic activity in OE cell lines do not seem to completely explain the gain in tolerance observed in viability assays with pCncC:Maf-a. Indeed, the overexpression of the full CncC:Maf complex was needed to increase the tolerance of Sf9 cells to I3C and MTP. Here, CE activity seemed to be enhanced by *CncC* only, while activity of the GST enzymes was not significantly modified by the overexpression of CncC:Maf. The activity of detoxifying enzymes in these Sf9 transformants should be complemented with P450 activity assays. It is well established that P450s are largely involved in metabolism of plant secondary metabolites and insecticides (Feyereisen, 2012; Li et al., 2001). In addition, several studies have also reported that this family of xenobiotic enzymes is widely regulated by the CncC:Maf pathway as revealed by transcriptomic analyses (Gaddelapati et al., 2018; Kalsi and Palli, 2017a; Lu et al., 2021a; Misra et al., 2013).

Although the precise mechanisms underlying the initiation of the CncC/Keap1 transcription pathway in insects is not fully understood, it seems that they are conserved with those determined in mammals. An increasing body of evidence from several insect pest species has

recently pointed out the role of ROS in activating the Keap1/CncC/Maf pathway (Chen et al., 2018a; Hu et al., 2019a; Lu et al., 2020; Lu et al., 2019a; Lu et al., 2021a; Lu et al., 2021b; Lu et al., 2021c; Tang et al., 2020). I measured ROS content of control and transformant cell lines after xenobiotic treatments using carboxy-H_2DCFDA to better understand the link between ROS signaling and the activation of CncC:Maf in Sf9 cells. Treatments with I3C and MTP significantly increased ROS content of Sf9 cells 6 hours after treatment agreeing with several recent studies showing that plant secondary metabolites such as I3C, xanthotoxin and flavone (Chen et al., 2018a; Lu et al., 2021a; Lu et al., 2021b) but also insecticides including acetamiprid, imidacloprid and chlorpyrifos (Chen et al., 2018a; Lu et al., 2021c; Tang et al., 2020) elicit ROS bursts in various insect tissues and cells. The accumulation of H_2O_2 in these studies was shown to activate the expression of CncC:Maf target genes and provide increased tolerance towards these compounds (Chen et al., 2018a; Lu et al., 2021a; Lu et al., 2021b). Basal ROS content in all untreated OE cells was in the same range and did not differ from the control cells. On the other hand, ROS level in the cell line knocked out for *CncC*, $Sf9^{CncC\text{-}13}$ was much higher than the control, while significantly lower in $Sf9^{Keap1\text{-}01}$. The role of the CncC:Maf pathway as a regulator of oxidative stress has been pointed out before. Previous studies have shown that CncC controls the expression of antioxidant enzymes such as SOD and CAT which are also activated upon exposure to phytochemicals and insecticides (Hu et al., 2018; Pan et al., 2020). The discrepancy between ROS levels in OE and KO cell lines remains yet surprising. While the knockout of *CncC* had a major impact on ROS levels, the activation of the CncC:Maf pathway did not result in a significant decrease of the basal oxidative level. On the other hand, the suppression of *Keap1* drastically reduced in-cell ROS content. Whether the overexpression of *CncC* and *Maf* in pCncC:Maf-a is not potent enough to modulate ROS content as compared to $Sf9^{Keap1\text{-}01}$ needs to be clarified. In addition, data may also indicate that *Keap1* modulates the expression of genes, other than *CncC*, involved in keeping a low basal level of ROS production.

Sodium pyruvate (SP) is a natural oxidant scavenger known to protect cell damage caused by H_2O_2 (Giandomenico et al., 1997; Jagtap et al., 2003). The supplementation of SP significantly reduced I3C- and MTP-induced ROS generation in all cell transformants. However, SP supplementation had an heterogenous effect on tolerance gain between cell transformants. While control cell lines showed a substantial increase of tolerance towards I3C and MTP with

SP, the tolerance of pCncC:Maf-a and Sf9$^{Keap1\text{-}01}$ to both chemicals was far less affected by SP. This may indicate that the constitutive overexpression of the CncC:Maf pathway in these cell lines was sufficient to reduce basal and I3C- and MTP-induced ROS bursts and alleviate the toxic effect of xenobiotic exposure. The use of SP is another demonstration of the requirement of both *CncC* and *Maf* to activate cytoprotective genes, as shown by the little to no increase of tolerance observed with SP supplementation to pCncC-b and pMaf-b.

While the use of SP dramatically increased the tolerance of Sf9 cells to xenobiotics, combining antioxidants to viability assays with insects has commonly the opposite effect and increases the toxicity of xenobiotics. The suppression of xenobiotic-induced ROS bursts prevents the activation of the CncC:Maf pathways and the deployment of detoxifying and cytoprotective enzymes. For instance, the use of N-acetylcysteine (NAC) as a diet supplement, a known and widely used ROS scavenger, significantly increased the susceptibility of *S. litura* to λ-cyhalothrin exposure (Lu et al., 2020; Lu et al., 2021b). The discrepancy observed between these studies and our data with Sf9 cells is likely due to the mode of toxicity of I3C and MTP in the cellular model. The mechanism by which I3C and MTP induce cell death in Sf9 cells is unclear and it is possible that xenobiotic-induced ROS production and content is the main cause of Sf9 cell death after exposure to these chemicals (Snezhkina et al., 2019). In agreement with this, the use of SP substantially reduced ROS content in Sf9$^{CncC\text{-}13}$ as measured by HCS and was associated with a strong reduction of signs of oxidative stress such as vesicles, cell debris and weaker resilience to cell handling.

The further study the link between ROS production and the activation of CncC:Maf a few additional experiments should be carried out. First, the induction of detoxifying genes would further need to be assessed under SP and xenobiotic treatment. Many studies in other species have shown that the use of an antioxidant such as NAC suppresses *CncC*-meditated induction of detoxification enzymes. Lu et al. (2021b) for example recently revealed that suppressing xanthotoxin-induced ROS production in *S. litura* larvae reduced the mRNA levels of 21 detoxification genes. In an earlier study, the same group showed that suppressing flavone induced ROS in *S. litura* also resulted in the repression of 10 detoxification genes (Lu et al., 2021a). It would be of great interest to test whether the use of SP suppresses the expression of *CYP321A9* and *GSTe1* for example, as they were shown to be induced by CncC:Maf in the first chapter. Following the same idea, the activity of detoxifying enzymes in Sf9 cells after I3C and MTP treatment could be determined in the presence and absence of SP

to show whether *CncC*-dependent induction of enzymatic activity is also mediated by ROS production.

In this chapter I was able to successfully produce cell lines overexpressing one or both transcription factors of the CncC:Maf complex. In addition, I adapted a protocol using CRISPR/Cas9 to introduce loss-of-function mutations in the coding sequences of *CncC* and *Keap1*. These mutations and transformants (OE and KO) were first characterized and then assessed for their effects on cell viability, ROS content and enzymatic activity of known detoxifying enzymes. I showed that CncC:Maf has cytoprotective effects on Sf9 cells when challenged with I3C and MTP. Their upregulation is also linked to enhanced activity of detoxifying enzymes including GSTs and CEs. The data further demonstrated that the toxicity of I3C and MTP is mainly mediated by the production of ROS upon exposure of cells to these chemicals. Viability assays using SP showed that the activation of the CncC:Maf pathway allowed substantial protection of Sf9 cells against ROS-induced toxicity and cell death. These experiments helped me to identify cell transformants with satisfactory genotypes and phenotypes to further examine the role of *CncC* and *Maf* in a transcriptomic assay using RNA-seq.

CHAPTER 4

INTRODUCTION

In the previous chapter, I demonstrated that the activation of the CncC:Maf pathway by co-overexpression of *CncC* and *Maf* was sufficient to drastically increase Sf9 cells tolerance to I3C and Mtp. In agreement with this, the activity of CE and GST enzymes, two known detoxifying gene superfamilies, were coordinately increased. Similarly, knocking out *CncC* had the opposite effect on both viability and enzymatic activity although two cell lines, $Sf9^{CncC\text{-}08}$ and $Sf9^{CncC\text{-}13}$ had apparent increased viability using MTT assays. In addition, the RT-qPCR assay carried out after transient overexpression of *CncC* and *Maf* in Sf9 cells (chapter1) resulted in upregulation of five out of eight detoxification genes, including P450s and *GSTe1*. There is growing evidence suggesting that the detoxification ability of *S. frugiperda* is directly related to its success as a polyphagous pest (Amezian et al., 2021a; Hilliou et al., 2021). Given the high number of detoxification genes uncovered in the genome of this insect (Gimenez et al., 2020b; Gouin et al., 2017; Xiao et al., 2020), it becomes urgent to identify those whose regulation could be controlled by CncC. What is the scope of CncC's regulation over detoxification genes in *S. frugiperda*? Were these genes shown to be involved in insecticide and plant allelochemicals sensitivity? Indeed, CncC and Maf were reported to activate the expression of many detoxification genes in other insect species. For example, the transcriptional profiling of *D. melanogaster* revealed that 70% of the genes induced by phenobarbital were also regulated by *CncC* (Misra et al., 2011). To gain a comprehensive view of the genes under the control of *CncC* and *Maf,* I carried out a transcriptomic analysis of selected Sf9 transformants. The cell lines, *i.e.*, pCncC-b, pMaf-b pCncC:Maf-a from OE cell lines and $Sf9^{CncC\text{-}13}$ and $Sf9^{Keap1\text{-}01}$ from KO cell lines, were chosen based on the analysis of their genotype and phenotypes (transcript levels, CRISPR/Cas9 efficiency, cell viability). I thus used RNA sequencing coupled to a differential expression analysis to compare the genes commonly regulated in these cell lines, respectively overexpressing and knocked out for the *CncC*, *Maf* and *Keap1* genes.

I present in this chapter the result of this transcriptomic study and discuss the biological relevance of the genes identified.

MATERIALS & METHODS

RNA extraction, library preparation and sequencing

Total RNA was extracted from Sf9 cell lines using the RNeasy Plus Mini Kit (QIAGEN, Germany) with three biological replications (*i.e.* each cell line at independent time points). Cells from 25 cm^2 culture flasks were collected before reaching confluence (*ca*. 8-10.10^6 cells) and washed twice in 2 ml cold DPBS with intermittent centrifugation for 3 min at 700 x g. The resulting pellet was resuspended in 350 µl extraction buffer from the RNeasy Plus Mini Kit and followed by all manufacturer's instruction including a genomic DNA eliminator column step. The integrity of RNA samples was assessed by electrophoresis on a 1% agarose gel and quantity was measured by spectrophotometry using a Qubit 2 device (Life Technologies, Germany) and the Qubit™ RNA HS Assay kit (Life Technologies, Germany). Each RNA sample was sequenced by the sequencing service company Fasteris SA (Switzerland) according to the "Stranded mRNA protocol for Illumina library preparation" with the NovaSeq 6000 Illumina technology generating strand-specific paired-reads of 150 bp. Read counts and quality scores are shown in (Appendix D, Table S1).

RNA-seq transcriptomic analysis and differential expression

All RNA-seq reads were mapped to the *S. frugiperda* corn genome (v6.0) of 2020.11.19 obtained from BIPAA (bipaa.genouest.org, Gimenez et al., 2020b) using STAR 2.7.4a (Linux_x86_64). Annotations were obtained from the official gene set OGS6.1 on BIPAA. Annotations of detoxification genes (cytochrome P450s, carboxylesterases (CEs), glutathione-S-transferases (GSTs), UDP-glucuronosyltransferases (UGTs) and ABC transporters (ABCs) were done manually by specialist from the field. The alignment was performed using STAR (v2.7.4a, Dobin et al., 2013) with the following parameters '—outFilterScoreMinOverLread' and '–outFilterMatchNminOverLread' set to 0.3. Mapped read-pairs were quantified using subread-2.0.2 featureCounts (Liao et al., 2014) at the transcript level and excluding chimeric fragments. The Bioconductor (v3.13) DESeq2 package (v1.32.0, Love et al., 2014) was used in the R environment (v4.0.1) to identify differentially expressed genes. A P-adjusted value (P_{adj}) ≤0.05 indicated statistical significance and log_2-fold changes (log_2FC) of ≥ ±1 marked up- and downregulation, respectively. Distance matrices and principal component plots were

generated using the R package pcaExplorer (Marini and Binder, 2019). Heatmaps were generated using the R package gplots (v3.1.0) (https://github.com/talgalili/gplots). Gene expression patterns of detoxification genes were visualized with heatmaps generated with the relative transcript levels (log_2FC) of four differential expression analyses of upregulated transcripts (pCncC-b *vs* pBiEx-1, pMaf-b *vs* pBiEx-1, pCncC:Maf-a *vs* pBiEx-1 and $Sf9^{Keap1\text{-}01}$ *vs* $Sf9^{eGFP}$; $Log_2FC > 1$ and a Benjamini-Hochberg q value (BHq) < 0.05) and one differential expression analysis of downregulated transcripts ($Sf9^{CncC\text{-}13}$ *vs* $Sf9^{eGFP}$). Fisher's Exact Test Analysis of over-represented biological processes was performed in Genedata Selector Analyst (https://www.genedata.com/products/selector/software#c417).

RESULTS

In total, 21 RNA samples were sequenced from 7 cell lines on an Illumina NovaSeq 6000 flow cell. RNA-expression profiles of cell transformants were assessed in comparison to control cell lines (*i.e.* pBiEx-1 and $Sf9^{eGFP}$). For the 21 mRNA libraries, approximately 724 million clean reads containing 213.4 Gb of sequence data were generated after quality control. The Q30 percentage of the reads was more than 91.65 %, with an average of 95.13 % indicating a robust quality of transcriptome sequencing and data filtering. In total, 82.9 % of all reads could be assigned to the 21830 genes of the *S. frugiperda* genome annotation (OGS6.1, corn variant) with adjusted parameters. On average, 71.7 % of all transcripts were assigned an expression value. The expression level of *CncC*, *Maf* and *Keap1* was checked in each cell line and was in line with the results obtained by RT-qPCR in the previous chapter (Appendix D, Table S2). The overexpression of *CncC* and *Maf* transcription factors and the knockout of *CncC* and *Keap1* had a strong effect on gene expression profiles of the cell lines, as shown by principal component analysis (PCA) of RNA-seq data (Fig. 29). These results show that the sequencing data are of good quality and can be used in downstream analyses.

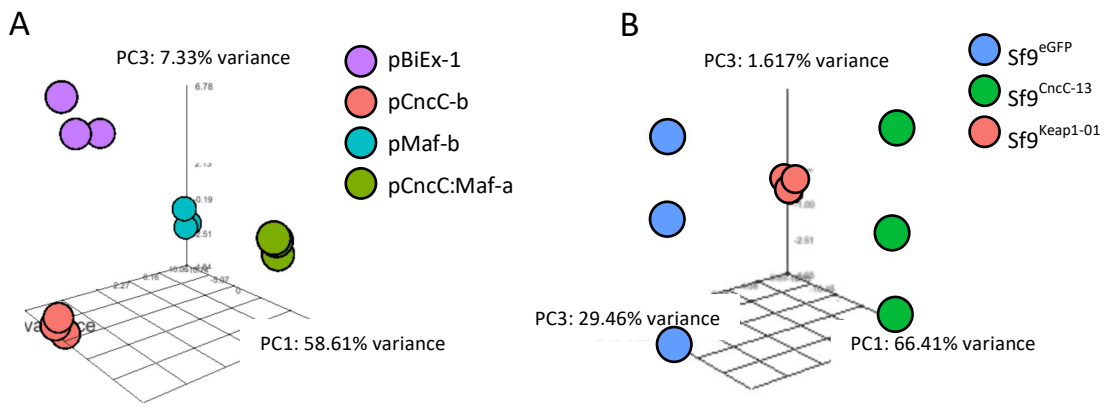

Fig. 29 PCA analysis of gene expression.
(**A**) cell lines over-expressing the transcription factors CncC and Maf and in (**B**) cell lines knocked out for *CncC* and *Keap1*.

Statistical analysis revealed that detoxification genes (n = 489 from the annotation set) were over-represented in the total number of genes up- (Fisher's Exact, p = 0.001227) and downregulated (Fisher's Exact, $p = 1.228^{-12}$) (Fig. 31A,B ; Appendix D Tables S2 and S3) among all cell lines.

To determine the biological significance of the CncC:Maf pathway, I performed an enrichment analysis of GO annotated differentially expressed genes. Significantly ($p \leq 0.05$) enriched GO terms were categorized as "biological processes", "molecular functions" and "cellular components". Upregulated transcripts in overexpressing cell lines led to 18 over-represented "biological processes" (Fig. 30A), among which the top enriched GO terms were *cyclic nucleotide metabolic process*, *small molecule catabolic process*, *G protein-coupled receptor signaling pathway* and *serine family amino acid metabolic process*. A few other biological processes related to alkaloid metabolism were significantly over-represented, including *indolalkylamine* and *indole-containing compound metabolic process* (Fig. 30A). 19 "biological processes" were over-represented in downregulated transcripts among which the major enriched GO-terms were *biological process involved in interspecies interaction between organisms*, *defense response* and *defense response to other organisms* (Fig. 30B). Other GO-terms related to defense to pathogens were enriched in this category such as *defense response to bacterium* and *antimicrobial humoral response*.

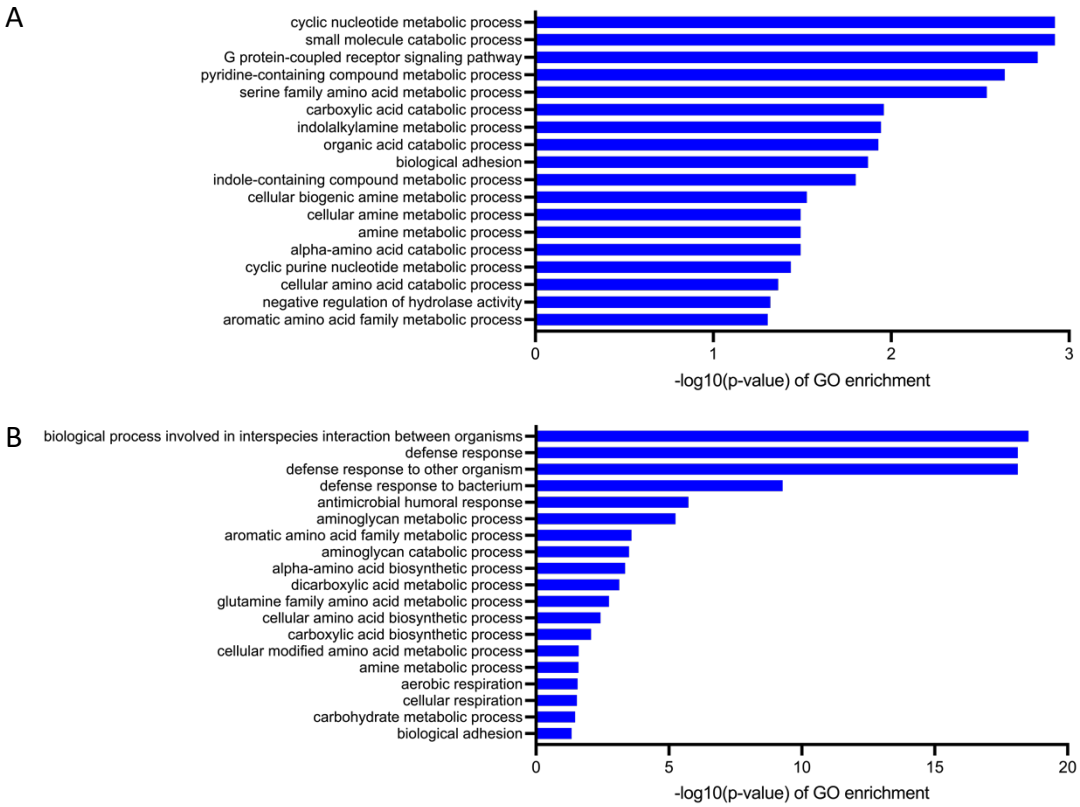

Fig. 30 GO terms enrichment from "biological processes" in the over-expressed genes.
Enrichment analysis of GO annotation output for (**A**) 617 upregulated transcripts and (**B**) 947 downregulated transcripts. Horizontal histograms represent significance of each GO term as given by the -$\log_{10}$(*p*-value).

Upregulation of *CncC* in pCncC-b led to the induction of only a few genes, 74 in total, as compared to 280 by overexpression of *Maf* in pMaf-b and 316 with the two transcription factors in pCncC:Maf-a (Fig. 32C). More specifically, there was four, 15, and 11 detoxification transcripts significantly upregulated in pCncC-b, pMaf-b and pCncC:Maf-a respectively (Fig. 32A, B, C) with some overlap: *CXE3* was highly expressed in both pCncC-b and pCncC:Maf-a while the transcripts of acetylcholinesterase and esterases were also share between pMaf-b and pCncC:Maf-a.

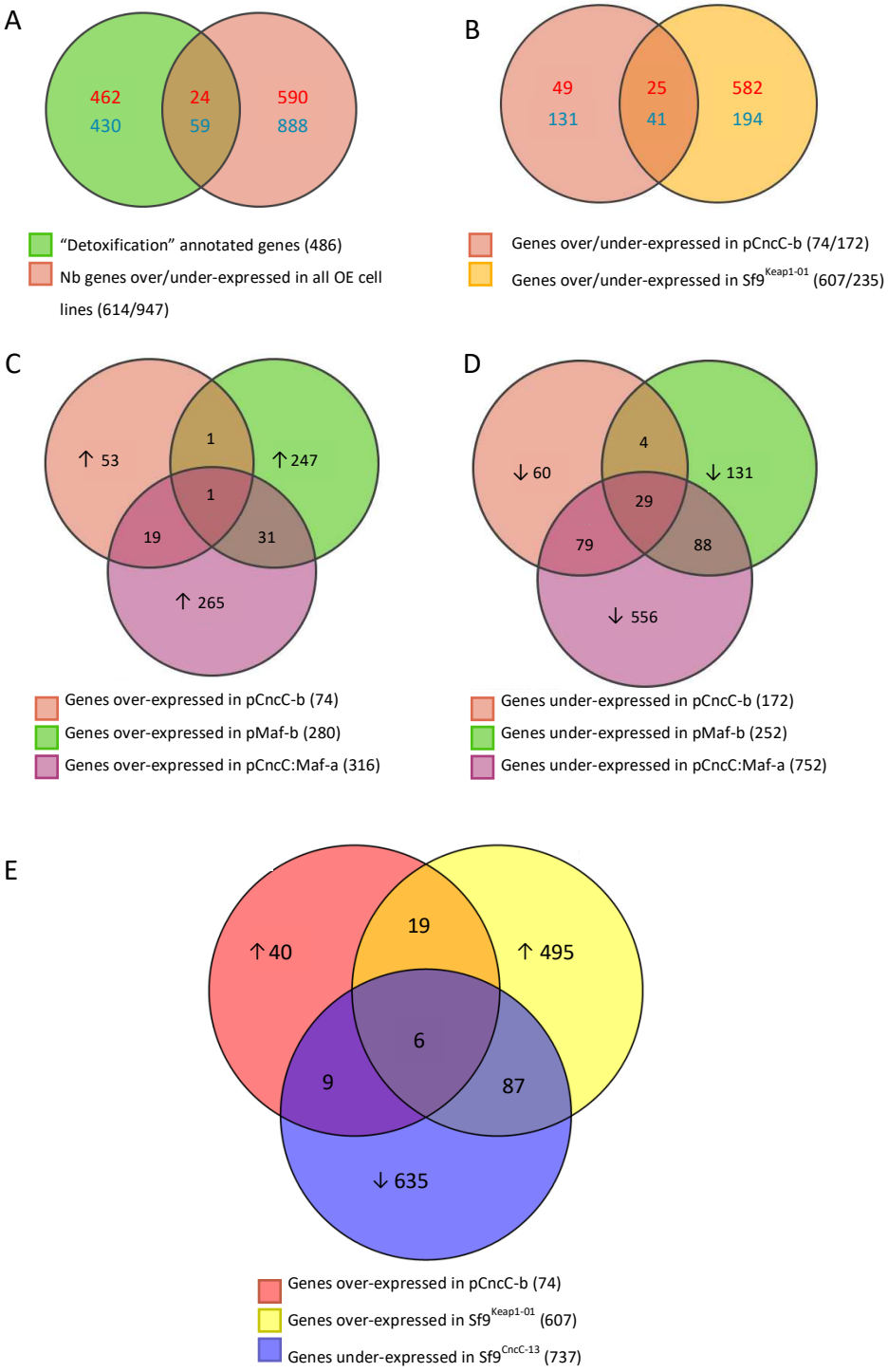

Fig. 31 Summary of genes that are differentially expressed between the cell lines.
The Venn diagrams represent the numbers of genes commonly over- (red numbers, upward arrow) and under-expressed (blue numbers, downward arrow) in (**A**) all OE cell lines vs all genes annotated as detoxification genes, (**B**) differentially expressed genes (DEG) between pCncC-b and $Sf9^{Keap1\text{-}01}$; genes overexpressed (**C**) and underexpressed (**D**) between pCncC-b, pMaf-b, pCncC:Maf-a and (**E**) genes overlapping between those overexpressed in pCncC-b and $Sf9^{Keap1\text{-}01}$ and those underexpressed in $Sf9^{CncC\text{-}13}$.

Furthermore, *CYP9A75* was the most highly expressed transcript in pCncC-b while *CYP315A1* and *CXE3* were among the most highly over-expressed genes in pCncC:Maf-a. A few detoxification genes upregulated in pCncC-b and pMaf-b were even more so expressed in pCncC:Maf, such as *CYP315A1*, *CXE64*, *CXE3* and *ABCG1* (Fig. 32C).

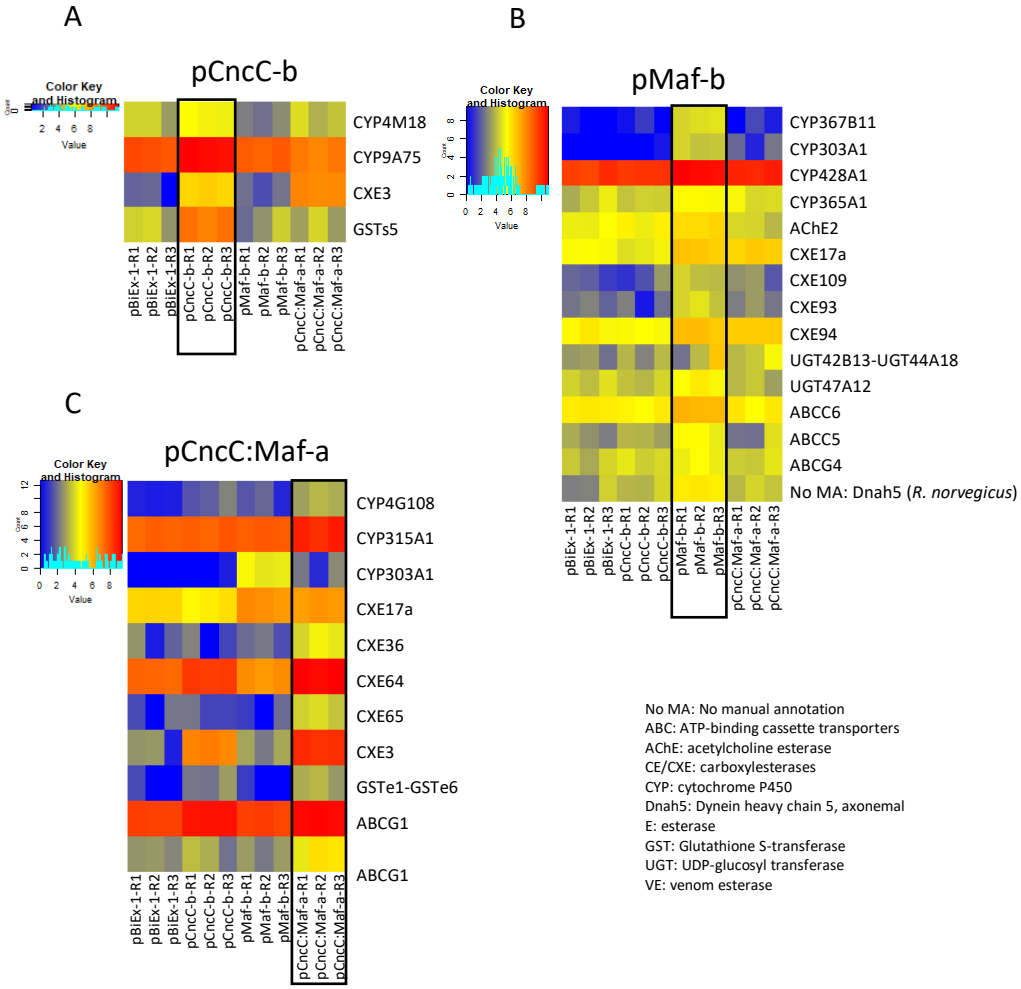

Fig. 32 Heatmaps summarizing the RNA-seq data of over-expressed detoxification genes in OE cell lines. Heatmaps represent the relative expression level of significantly over-expressed ($log_2FC \geq 1$, Benjamini-Hochberg q value (BHq) < 0.05) detoxification transcripts in (**A**) pCncC-b (**B**) pMaf-b and (**C**) pCncC:Maf-a samples as compared to pBiEx-1 and other OE cell lines (pCncC-b, pMaf-b and pCncC:Maf-a). Not all gene names follow the official nomenclatures (*e.g.*, David Nelson, University of Tennessee for CYP genes), but are based on the name of their best BLAST hits for which the species is given in brackets. There were some instances of multisequence locus, whereby several gene names are given. Red indicates relative upregulation and blue indicates downregulation.

Half of the genes upregulated in pCncC-b were also expressed in the *Keap1* knockout cell line (Fig. 31B), among which the most overexpressed were found *CYP4M18*, *CYP9A75* and *GSTs5* (Fig. 32). A total of 607 genes were upregulated in $Sf9^{Keap1\text{-}01}$ including 66 detoxification genes. More specifically, 22 CYPs, eight CEs, 13 GSTs, eight UGTs and 10 ABC transporters (Fig. 33). *CYP6AE44* (log_2FC: 8.1), *CYP9A32*, *CYP9A31* and *CYP9A27* were among the most highly

expressed P450s. One transcript out of the eight of CE genes was particularly overexpressed and matched with a multisequence locus encompassing *CXE28a-CXE28b-CXE47* (Fig. 33). Furthermore, *GSTo2*, *GSTe14*, *GSTs3-GSTs2-GSTs1* and *GSTd4* were the most over-expressed GSTs in this data set. Among the eight differentially expressed UGTs, *UGT40R1* was the most highly overexpressed. ABC transporters on the other hand were only moderately over-expressed.

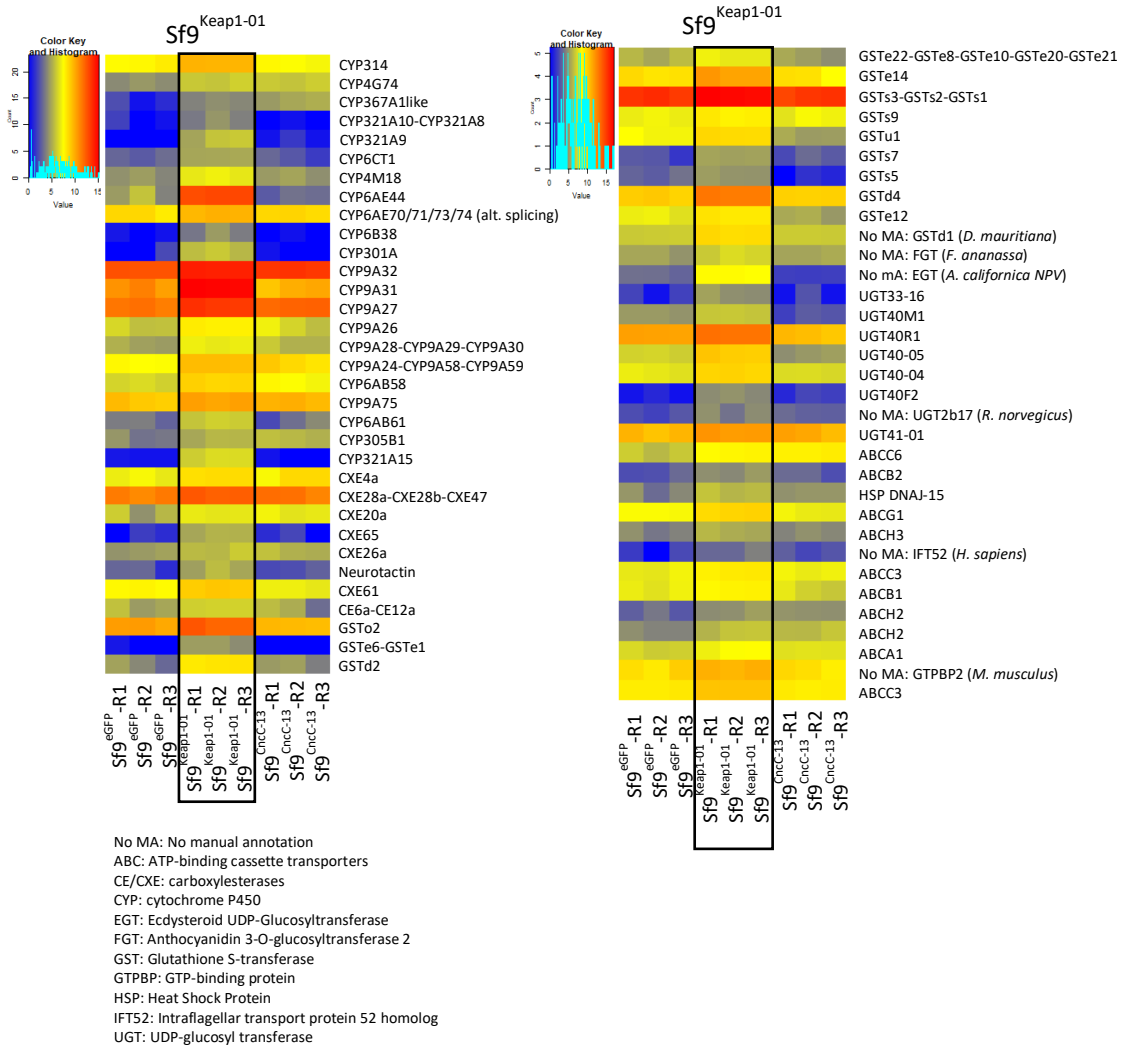

Fig. 33 Heatmaps summarizing the RNA-seq data of over-expressed detoxification genes in Sf9$^{Keap1-01}$. Heatmaps represent the relative expression level of significantly over-expressed (L2fc ≥ 1, BHq < 0.05) detoxification transcripts in Sf9$^{Keap1-01}$ samples as compared to Sf9^{eGFP} and Sf9$^{CncC-13}$. Not all gene names follow the official nomenclatures (*e.g.*, David Nelson, University of Tennessee for CYP genes), but are based on the name of their best BLAST hits for which the species is given in brackets. There were some instances of multisequence locus, whereby several gene names are given. Red indicates relative upregulation and blue indicates downregulation.

The knockout of *CncC* in Sf9$^{CncC-13}$ resulted in the downregulation of 737 genes (Fig. 31E) among which were 36 detoxification genes including 9 CYPs, 3 esterases, 4 GSTs, 5 UGTs, 4 ABC transporters and additional detoxification and transport related genes (Fig. 34). The

most downregulated detoxification genes were the *CYP324A16, CXE17a*, *GSTs5* as well as a gene similar to an ecdysteroid UDP-glucosyltransferase (EGT, *S. littoralis NPV*).

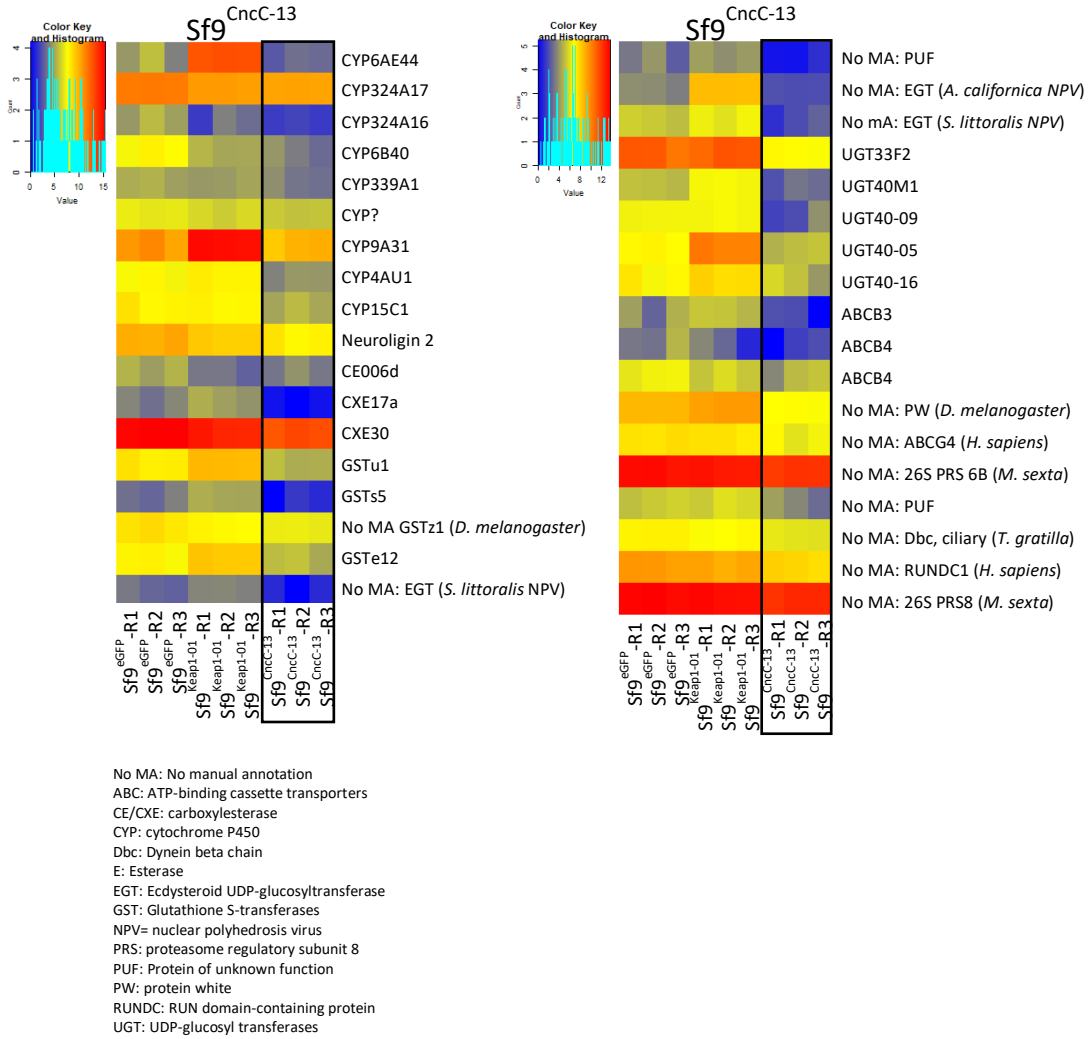

No MA: No manual annotation
ABC: ATP-binding cassette transporters
CE/CXE: carboxylesterase
CYP: cytochrome P450
Dbc: Dynein beta chain
E: Esterase
EGT: Ecdysteroid UDP-glucosyltransferase
GST: Glutathione S-transferases
NPV= nuclear polyhedrosis virus
PRS: proteasome regulatory subunit 8
PUF: Protein of unknown function
PW: protein white
RUNDC: RUN domain-containing protein
UGT: UDP-glucosyl transferases

Fig. 34 Heatmaps summarizing the RNA-seq data of under-expressed detoxification genes in Sf9$^{CncC-13}$. Heatmaps represent the relative expression level of significantly under-expressed (L2fc ≤ 1, BHq < 0.05) detoxification transcripts in Sf9$^{CncC-13}$ samples as compared to Sf9^{eGFP} and Sf9$^{Keap1-01}$. Not all gene names follow the official nomenclatures (*e.g.*, David Nelson, University of Tennessee for CYP genes), but are based on the name of their best BLAST hits for which the species is given in brackets. There were some instances of multisequence locus, whereby several gene names are given. Red indicates relative upregulation and blue indicates downregulation.

The genes commonly upregulated in pCncC-b and Sf9$^{Keap1-01}$ and those downregulated in Sf9$^{CncC-13}$ were analysed (Fig. 31E). Six genes were differentially regulated in those three data sets including the *GSTs5*, a transcript similar to "*C-Maf-inducing protein-like*" [S. litura] and two transcripts related to cell adherence (collagen alpha-1(XVIII) chain-like and nidogen-1, *S. litura*). An overlap of 93 genes was generated between the genes under-expressed in Sf9$^{CncC-13}$ and those over-expressed in Sf9$^{Keap1-01}$. Among those transcripts, eight were

annotated as detoxification genes: *CYP6AE44*, *CYP9A31*, *GSTe12*, *GSTs5*, *GSTu1*, *UGT40M1*, *UGT40-05* as well as a gene similar to an EGT (*A. californica NPV*).

A number of non-detoxification gene families were represented by transcripts overexpressed in OE cell lines and Sf9$^{Keap1\text{-}01}$ and underexpressed in Sf9$^{CncC\text{-}13}$. For instance, transcripts from the odorant-binding and chemosensory protein gene family were often over-expressed by CncC:Maf activation such as the "general odorant-binding protein 72-like" which log_2FC was 14.9 in pCncC-b, 15.5 in pCncC:Maf-a and 5.4 in Sf9$^{Keap1\text{-}01}$. Transcripts related to chemosensory protein genes such as gustatory and odorant receptors (GRs and ORs) were over-expressed in *CncC*-enhanced cell lines including *GR22-like*, *OR22b*, *OR85c-like* and *OR46a-like*.

Given the strong increase and decrease of basal ROS content that was observed in Sf9$^{CncC\text{-}13}$ and Sf9$^{Keap1\text{-}01}$ mutants respectively, I further investigated whether genes coding for ROS producing enzymes such as nitric oxide synthase (NOS), NADPH oxidases (NOX), dual oxidases (DUOX) and hydroxyacid oxidase 1 (HAO-1) as well as enzymatic ROS scavengers, *i.e.* superoxide dismutases (SOD), catalases (CAT) and peroxidases (POD) were modulated in the different data sets (Appendix D , Table S5). Two PODs and one CAT were overexpressed in the *Keap1*-mutated cell line (log_2FC = 1.33, 1.95, and 2.57, respectively) while their expression did not change in Sf9$^{CncC\text{-}13}$. Interestingly, the levels of two transcript matching ROS producing enzymes, namely *Nos1* and *HAO1* were substantially lower in the *CncC*-KO cell lines while not differentially expressed in Sf9$^{Keap1\text{-}01}$. Many other genes were differentially expressed (log_2FC > ±1) however with poor statistical significance (Appendix D, Table S5).

Several signaling pathways involved in the expression regulation of detoxification genes and insecticide sensitivity have been identified in recent years (for a review see Amezian et al., 2021b). Yet, we are still far from having a complete understanding of the detoxification signaling networks in insects. Thus, I checked if the modulation of the CncC:Maf pathway in my Sf9 transformants induced transcriptional changes in known markers of these pathways, *i.e. AhR*, *ARNT*, *HR96*, *USP, EcR, CREB proteins*, and *CPGRs*. Among the latter, the expression of two were consistently modulated across the datasets, including the Aryl hydrocarbon receptor (*AhR*) and G-protein coupled receptors (GPCRs). *AhR* was upregulated in all the OE cell lines with the strongest upregulation observed when both transcription factors were overexpressed (log_2FC = 2.02, n.s.). Conversely, *AhR* was downregulated when *CncC* was knocked out in Sf9$^{CncC\text{-}13}$ (log_2FC = -2.06, n.s.). Interestingly, the expression level of *AhR* was

also found downregulated in Sf9$^{Keap1\text{-}01}$. The expression of *ARNT*, the partner dimer of *AhR*, was only modulated in pCncC:Maf-a (log_2FC = 3.296, *p*-adj = 1.14E-22). Similarly, many GPCRs transcripts were upregulated in OE cell lines. However, one transcript matching *GPCR18* (*S. litura*, SFRUCORN610000029684-RA) was the most overexpressed GPCR in pCncC-b and pCncC:Maf-a (log_2FC = 3, n.s.) while being also overexpressed in Sf9$^{Keap1\text{-}01}$ (log_2FC = 3, n.s.). In pMaf-b this transcript was the third most overexpressed GPCR. Expression of this gene was however not changed by the KO of *CncC* in Sf9$^{CncC\text{-}13}$.

In addition, genes linked to the immunity signaling pathway such as Toll-like receptors 3 and 7, Protein Spätzle 3 and 5, the threonine/serine kinase Pelle, phenoloxidase and antimicrobial peptide transcripts were upregulated by the knockout of *CncC*. In particular, toll-like receptor 6 was among the 25 overexpressed genes overlapping between pCncC-b and Sf9$^{Keap1\text{-}01}$.

DISCUSSION

The detoxification capabilities of *S. frugiperda* are thought to play a critical role in its ability to develop resistance and to degrade and excrete plant allelochemicals (Amezian et al., 2021a; Hilliou et al., 2021). *CncC* and *Maf* transcription factors were shown to be central actors of detoxification gene expression in other insect species such as *D. melanogaster*, *L. decemlineata* and *S. litura* (Kalsi and Palli, 2017a; Lu et al., 2021a; Misra et al., 2011). However, information about how this pathway contributes to the detoxifying abilities in *S. frugiperda* is scant (Amezian et al. 2021). The primary goal of the present chapter was to identify the detoxification genes under the control of *CncC* and *Maf* in Sf9 cells to better understand the adaptive mechanisms of this insect to its host-plants and to insecticides. The major add-on of this chapter is the data it provides: a comprehensive identification of genes differentially regulated in five different transcriptomic datasets. An RNA-seq analysis was performed on five Sf9 cell lines having each a specific and unique genotype: overexpression of *CncC*, *Maf* or both genes simultaneously, as well as the mutation of *CncC* and *Keap1*. These cell lines were chosen based on experiments characterizing both the genotypes and phenotypes of all cell lines as established in the previous chapter. An analysis of genes differentially expressed identified the specific and common genes modulated by these three transcription factors.

Differential expression analysis of transcripts identified a total of 614 genes overexpressed (DE > 2-fold) in OE cell lines. The number of genes upregulated in pCncC-b led to the induction of only a few genes, 74 in total, much less than the 280 genes upregulated by *Maf* in pMaf-b. This dissimilarity may be due to the relatively low level of *CncC* overexpression in pCncC-b: RT-qPCR revealed 2.7-fold (chapter 2) while transcriptomic data predicted levels 1.5-times higher than in the control. Comparatively, *Maf* would be 13.8- and 8.2-times higher in pMaf-b as measured by RT-qPCR and RNA-seq, respectively. The mutation in *Keap1* resulted in 842 transcripts differentially regulated among which 607 were overexpressed (Fig. 30). Conversely, the knockout of *CncC* resulted in a total of 737 underexpressed genes. These numbers are in the same range as those identified in other RNA-seq analyses performed for *CncC*-silenced and *CncC*-activated insects. For example, differential expression analysis in *CncC*-knockdown *Tribolium castaneum* beetles identified 622 genes showing a decrease in their expression (Kalsi and Palli, 2017a). In *Drosophila*, the overexpression of *CncC* lead to upregulation of 712 genes (Misra et al., 2011). To determine the genes under the control of *CncC,* I compared the transcripts commonly upregulated in pCncC-b and $Sf9^{keap1\text{-}01}$ to those repressed in $Sf9^{CncC\text{-}13}$ (Fig. 30D). The analysis revealed that these three data sets shared a total of six genes, among which was *GSTs5*. The highest overlap accounted for 93 transcripts and was obtained between the genes upregulated by the mutation of *Keap1* and those downregulated by the suppression of *CncC*. In a study where 1406 transcripts were upregulated by *CncC*, 103 had also a *CncC*-binding site within 2kb of the gene region. Taken together, my data suggests that *CncC* and *Maf* may control the expression of close to 100 genes. This also implies that up to 500 genes overexpressed in $Sf9^{Keap1\text{-}01}$ and 640 underexpressed in $Sf9^{CncC\text{-}13}$ are differentially regulated by the potential activity of Keap1 and CncC with other regulatory pathways as it was shown with Nrf2/Maf in mammals with the ERK, JNK and MAPK pathways (Basak et al., 2017). Earlier studies have highlighted the role of *CncC* in modulating the expression of large sets of insecticide-responsive genes in *Diptera* and *Coleoptera* (Gaddelapati et al., 2018; Kalsi and Palli, 2017a; Misra et al., 2011; Misra et al., 2013). For example, in *Drosophila* 70% of genes regulated by phenobarbital were also regulated by CncC. It is only recently that the role of *CncC* in *Lepidoptera* species was emphasized (Hu et al., 2019a; Hu et al., 2019b; Hu et al., 2020a; Hu et al., 2018; Lu et al., 2020; Lu et al., 2021a; Lu et al., 2021b) and shown to also control many allelochemical-responsive genes (Lu et al., 2021a; Lu et al., 2021b). Since the primary goal of this study is to identify the

detoxification genes potentially involved in xenobiotic metabolism, I first follow my analysis with a focus on the genes differentially upregulated in OE cell lines and Sf9$^{Keap1\text{-}01}$ and downregulated in Sf9$^{CncC\text{-}13}$.

The genes differentially regulated were analyzed for gene ontology using the official *S. frugiperda* gene set (OGS6.1, Gimenez et al., 2020b) and manual annotation of detoxification genes (Hilliou, Chertemps and Le Goff personal communication). Among the 614 transcripts upregulated in the three OE cell lines, the number of genes meeting the "detoxification" criteria were overrepresented as revealed by a Fisher's Exact test and amounted to 24 genes (Fig. 31, Appendix D, Table S3 and S4). These genes included those coding for eight P450s, eight CEs, two GSTs, two UGTs and four ABC transporters (Fig. 31). Similarly, 25 genes among the 737 transcripts repressed in Sf9$^{CncC\text{-}13}$ belonged to P450s (nine), CEs (three), GSTs (four), UGTs (five) and ABCs (four). These numbers agree with those found in RNA-seq analyses of *CncC*-knockdown beetles such as *Leptinotarsa decemlineata* where 12 P450s, two GSTs, two esterases and five ABC transporters differentially regulated were identified (Gaddelapati et al., 2018). On the other hand, the number of detoxification genes upregulated after repression of *Keap1* was much higher and included 60 genes belonging to the five families described above (Fig. 32). Interestingly, the proportions of genes differentially regulated from each superfamily in these three subsets (OE, Sf9$^{CncC\text{-}13}$ and Sf9$^{Keap1\text{-}01}$) were very consistent. For example, P450s were always the most induced detoxification genes and accounted for 36 % of xenobiotic transcripts in each subset, while ABCs ubiquitously represented 16% of all detox genes.

P450s are one of the largest gene families present in living organisms and it is now well established that they are involved in the metabolism of xenobiotics (Feyereisen, 2012). P450s of clan 3 most importantly have been widely associated with the detoxification of plant secondary metabolites and insecticides (Dermauw et al., 2020; Feyereisen, 2012). The data presented here agrees with the known role of *CncC* as a regulator of detoxification genes. Indeed, the majority of P450s differentially regulated in the gene subsets belong to CYP3 genes, representing 50 % and 73 % of CYPs upregulated in OE cell lines and Sf9$^{Keap1\text{-}01}$ respectively, and 63 % of CYPs downregulated in Sf9$^{CncC\text{-}13}$. CYP3 genes differentially regulated here were also found to be *CncC*-target genes in other studies. For example, *CYP321A10* (or *CYP321A8* see Fig. 32) which was found upregulated in Sf9$^{Keap1\text{-}01}$ was also reported to be

potentially regulated by CncC in *S. litura* larvae (Lu et al., 2021a; Lu et al., 2021b). *CYP321A10* and *CYP321A8* are two genes organized in a cluster of tandemly duplicated genes in close synteny with *CYP321A7* and *CYP321A9*. Interestingly, *CYP321A7* was also found downregulated in *dsCncC*-silenced *S. litura* larvae (Lu et al., 2021a). Further, *CYP321A9* was overexpressed by transient expression of CncC:Maf in Sf9 cells (chapter 1) and induced by many other xenobiotics (Cheng et al., 2017b; Giraudo et al., 2015; Wang et al., 2017a). Taken together, the recent data available on *CYP321* expression and regulation strongly suggest that xenobiotic inducibility of CYPs from this subfamily/cluster in *Spodoptera* might be mediated by the CncC:Maf pathway. Lu et al. (2021a,b) reported many other P450s like *CYP6AE43, CYP6AE48* and *CYP6AE68* or *CYP6B47* and *CYP6B48* to be induced by flavone and xanthotoxin and likely under the control of CncC. These P450s belong to the notorious detoxifying enzyme subfamilies CYP6AE and CYP6B (Heckel, 2014; Krempl et al., 2016a; Li et al., 2007) which are known to be widely induced by plant secondary metabolites and insecticides in *Spodoptera* species (Amezian et al., 2021a). Here, I show that *CYP6AE44* is overexpressed by a *Keap1* mutation and underexpressed by a *CncC* KO (Fig. 32 and 33). *CYP6AE44* is induced in *S. frugiperda* larvae by harmine (Cui et al., 2020) and chlorpyrifos (Carvalho et al., 2013) suggesting that the induction of *CYP6AE44* by these compounds might be mediated by CncC. Similarly, the data shows that *CYP6B38* and *CYP6B40* are differentially regulated in $Sf9^{Keap1\text{-}01}$ and $Sf9^{CncC\text{-}13}$ respectively. *CYP6B40* for example has been reported to be induced by xanthotoxin, indole, imidacloprid and phenobarbital (Cheng et al., 2017b; Giraudo et al., 2015). Similarly, *CYP9A31* was differentially regulated in both $Sf9^{Keap1\text{-}01}$ and $Sf9^{CncC\text{-}13}$ while *CYP9A75* was upregulated in pCncC-b and $Sf9^{Keap1\text{-}01}$ (Fig. 31 and 32). *CYP9A31* is another P450 identified as potentially under the control of CncC (Fig. 32 and 33). Interestingly, *CYP9A31* was not induced by the transient overexpression of *CncC* and *Maf* in Sf9 cells (chapter 1). However, when gene induction reaches a certain threshold, it may turn into gene repression as reported by Giraudo et al. (2015). Nevertheless, *CYP9A31* as the many other CYP9As upregulated in $Sf9^{Keap1\text{-}01}$ were reported to be induced by plant secondary metabolites and insecticides in *Spodoptera* by several studies (Amezian et al., 2021a). CYP9A P450s were reported to be highly overexpressed in *S. frugiperda* populations resistant to pyrethroids (Boaventura et al., 2020b; Gimenez et al., 2020b). It would be of great interest to investigate the implication of the CncC:Maf pathway in the resistance phenotype of those populations.

CE enzymes are, like P450s, detoxification phase I enzymes and represent a large superfamily present in all kingdoms of life. The activation and repression of the CncC:Maf pathway in Sf9 cells resulted in expression change of a limited number of CE genes. The RNA-seq data predicted five CEs to be upregulated in the pCncC:Maf-a overexpressing cell line, among which were *CXE3* and *CXE17a*, *CXE65*. Two of these genes were also significantly regulated in the KO-cell lines. *CX65* for instance was strongly upregulated in $Sf9^{Keap1\text{-}01}$ while *CXE17a* was downregulated in the *CncC* knockout cell line. In their recent studies on *S. litura* Lu et al. (2021a,b) identified seven and six xanthotoxin and flavone inducible CEs, respectively. Among these, respectively four and six were shown to be potentially regulated by CncC.

GST enzymes represent a major phase II detoxification gene family. The RNA-seq data revealed that *GSTs5*, *GSTe1* and *GSTd2* were commonly differentially regulated in the three expression subsets (Fig. 31, 32 and 33). *GSTe1* is induced by a wide variety of plant allelochemicals such as allyl-isothiocyanate, asatone, isoasatone A, indole 3-carbinol, xanthotoxin (Ling et al., 2019; Zou et al., 2016) as well as insecticides like chlorpyrifos, deltamethrin and fluralaner (Chen et al., 2018a; Hu et al., 2019b; Zhang et al., 2016a). *GSTe1* catalyzes the conjugation of many xenobiotics including deltamethrin, malathion, phoxim and DDT (Huang et al., 2011; Xu et al., 2015; Zhang et al., 2016a; Zou et al., 2016). *GSTe1* was also inducible by I3C and Mtp in Sf9 cells and was the most strongly overexpressed detoxification gene in the transient expression assays conducted in the first chapter. This new data strongly supports previous studies presenting *GSTe1* as a *CncC*-target gene in *S. litura* (Chen et al., 2018a; Lu et al., 2021a), *S. exigua* (Hu et al., 2019b) and *Drosophila* (Deng and Kerppola, 2013; Sykiotis and Bohmann, 2008). Furthermore, *GSTo2* was the most strongly upregulated gene, by far, in a chlorpyrifos resistant *S. exigua* population (Hu et al., 2019a; Hu et al., 2019b). The authors found a CncC:Maf *cis*-regulatory sequence in the promoter region of three GSTs including *GSTo2*, which was essential for the promoter activity in a luciferase reporter assay (Hu et al., 2019b). The induction of *GSTo2* by xanthotoxin and flavone was shown to be mediated by CncC:Maf in two recent studies with *S. litura* (Lu et al., 2021a; Lu et al., 2021b). Here, I show that the suppression of *Keap1* in Sf9 cells results in the overexpression of *GSTo2*.

The RNA-seq analysis revealed that a few UGTs were differentially regulated by overexpression or repression of the CncC:Maf pathway. Among those, the UGT33 and UGT40 subfamily were overrepresented (Fig. 31, 32 and 33). For example, out of eight UGTs upregulated in $Sf9^{Keap1\text{-}01}$ five were UGT40s. Among these, *UGT40M1* and *UGT40-05* were also

downregulated in Sf9$^{CncC\text{-}13}$. UGT40 and UGT33 enzymes are largely associated with insecticide resistance and the metabolism of plant allelochemicals. For example, *UGT33-06* and *UGT40-07* were overexpressed in a *S. frugiperda* population resistant to λ-cyhalothrin (Carvalho et al., 2013). Previous studies have also identified UGT enzymes that are regulated by CncC in other species. In *T. castaneum* for instance, *UGT2C1-like* and *UGT1-7C-like* were repressed after insects were treated with *dsCncC* (Kalsi and Palli, 2017a). More recently, 14 UGTs were identified as CncC target genes in *S. litura*, out of which six were UGT33s and four UGT40s (Lu et al., 2021a; Lu et al., 2021b).

The role of ABC transporters in insecticide resistance has been demonstrated for many insecticide chemicals and involve mainly three ABC families: ABCBs, ABCCs and ABCGs (Denecke et al., 2021; Dermauw and Van Leeuwen, 2014; Epis et al., 2014). An increasing body of evidence shows the involvement of ABCs in the development of resistance seen in a few *Spodoptera* species, including to *Bt* toxins (for a review see Hilliou et al., 2021). In the current RNA-seq analysis, I identified a total of 12 ABC transporters that showed a significant differential expression after CncC activation or knockout in Sf9 cells, suggesting that the expression of these ABCs may be regulated by the transcription factors CncC and Maf. A few of these genes were commonly regulated among the expression subsets, as for example *ABCG1* found overexpressed in pCncC:Maf-a and Sf9$^{Keap1\text{-}01}$, and *ABCC6* in pMaf-b and Sf9$^{Keap1\text{-}01}$. Previous studies in Coleoptera have exemplified the role of the CncC:Maf pathway in regulating ABCs involved in insecticide sensitivity. For example, RNAi-mediated knockdown of *TcABCA-UB*, *TcABCA-A1/L*, and *TcABCA-9B* coupled to bioassays using pyrethroids increased *T. castaneum* susceptibility to these insecticides. In another study conducted by the same group on *L. decemlineata*, three ABC transporters, *ABCH278B*, *ABCH278C*, and *ABCG1041A* were shown to have their expression driven by the CncC/Keap1 pathway and participate in imidacloprid tolerance (Gaddelapati et al., 2018).

The RNA-seq analysis further identified genes regulated by *CncC*, *Maf* and *Keap1* that are not directly related to xenobiotic response. A few other CYP genes involved in either endogenous functions or both endogenous and exogenous functions were differentially regulated. P450s from CYP2 and mito clans in particular were highlighted in the differential expression analysis. These genes are highly conserved in insects, forming small to single-gene families and are commonly associated with physiological functions such as the biosynthesis

and metabolism of endogenous compounds (Dermauw et al., 2020; Feyereisen, 2005). However, a few were reported to be induced by plant allelochemicals and insecticides (Hu et al., 2019c; Le Goff et al., 2006; Zhang et al., 2016b). Recently, Shi et al. (2021c) investigated the ability of *H. armigera* CYP2 and mito P450s to metabolize model substrates and xenobiotics. Their work highlighted for example the ability of *CYP303A1* to metabolize 2-tridecanone (2-TD) at a rate higher than previously reported for CYP6AE P450s (Wang et al., 2018a). Similarly, *CYP305B1* showed high rate of esfenvalerate metabolism and epoxidase activity against aldrin (Shi et al., 2021c). CYP303A1, of which the substrate is so far still unknown is involved in *Drosophila* eclosion, embryonic development and regulation of cuticular hydrocarbon synthesis in *Locusta migratoria* (Wu et al., 2019; Wu et al., 2020; Zhang et al., 2018). In *H. armigera CYP303A1* and *CYP305A1* were relatively highly expressed in antenna, which given the role of 2-TD as a volatile insecticidal chemical in *Solanaceae,* the authors speculated to act as odorant degrading enzymes (ODP). The unprecedented proof of catalytic activity against exogenous compounds for CYP303A1 and CYP305B1 revealed their probable function in catabolism of both endogenous compounds and xenobiotics. Here, I show that *CYP303A1* was strongly overexpressed in pMaf-b and pCncC:Maf-a while *CYP305B1* was upregulated in $Sf9^{Keap1\text{-}01}$. Whether *CYP303A1* and *CYP305B1* are direct target genes of CncC:Maf requires further investigation. Nevertheless, given the known transcriptional activity of CncC:Maf in both development and xenobiotic response, this data could partly explain the origin of physiological ubiquity of genes such as *CYP303A1* (Shi et al., 2021c). In addition, gustatory and odorant receptors (GRs and ORs) were over-expressed in *CncC*-enhanced cell lines (data not shown) which further suggest that CncC may modulate the expression of enzymes involved in chemosensory functions.

Ecdysteroidogenic P450s, also known as the *Halloween* genes in *Drosophila*, belong to both the mito (*CYP302A1*, *CYP314A1* and *CYP315A1*) and CYP2 (*CYP306A1* and *CYP307A1*) clans (Dermauw et al., 2020; Lafont et al., 2012; Niwa and Niwa, 2014). Ecdysteroidogenic P450s were differentially regulated in this RNA-seq analysis as for example *CYP314* in $Sf9^{Keap1\text{-}01}$ and *CYP315* in pCncC:Maf-a. In addition, *CYP15C1*, a P450s associated with the biosynthesis of juvenile hormone (JH) was underexpressed in the *CncC*-KO cell lines (Daimon and Shinoda, 2013; Helvig et al., 2004; Nouzova et al., 2021). Several JH epoxide hydrolases (JHEH), JH esterases (JHE) and JH acid O-methyltransferase (JHAMT) were also found differentially regulated in the RNA-seq data. Taken together, these findings are consistent with previous

studies that identified *JHEH* and ecdysteroidogenic genes as CncC targets and reaffirms the involvement of *CncC* and *Maf* in modulation of JH and 20E pathways (Deng and Kerppola, 2013; Misra et al., 2013).

The expression of *Keap1* was checked (Appendix D, Table S2) and found moderately upregulated in pCncC-b, pCncC:Maf-a and strongly overexpressed in $Sf9^{Keap1\text{-}01}$, while being slightly downregulated in the *CncC*-KO cell line which confirmed the results determined by RT-qPCR in chapter 2. Despite the higher mRNA level of *Keap1*, the RNA-seq analysis revealed that the CRISPR/Cas9 induced mutation in *Keap1* resulted in many genes differentially expressed, 36 being annotated as detoxification genes. In addition, the genes significantly upregulated in this data set shared 93 transcripts with those downregulated by the knockout of *CncC* in $Sf9^{CncC\text{-}08}$ which partly supports antagonistic activation and suppression in these two well lines.

Given the strong increase and decrease of basal ROS content in $Sf9^{CncC\text{-}13}$ and $Sf9^{Keap1\text{-}01}$ mutants respectively, the expression of genes associated with oxidative stress such as ROS-producing enzymes (Nos, Nox, Duox, HAO-1) and ROS-scavenging enzymes (POD, CAT, SOD) was investigated. While the expression of a few genes such as *Nos2-like*, *Nox1* and *HAO1* was significantly repressed by *CncC*-KO, the expression of others like *CAT* and *POD* was upregulated in $Sf9^{Keap1\text{-}01}$. There was little consistency in the differential expression of these genes and others between the two cell lines (Appendix D, Table S5). The data poorly accounted for the strong overall ROS increase in $Sf9^{CncC\text{-}08}$ and the putative direct involvement of *CncC* and *Maf* in their regulation. For example, the expression of one SOD was shown to be regulated by CncC in a previous study with Sf9 cells, as demonstrated by overexpression and repression of this gene after ectopic overexpression and RNAi-mediated silencing of *CncC* (Pan et al., 2020). In insects, the role of NADPH oxidases (Nox, Duox) has primarily been exemplified in *Drosophila* and are associated with gut immunity (Ha et al., 2005; Patel et al., 2019; Xiao et al., 2017). A recent study in *S. litura* revealed that flavone ingestion led to an increase of *Duox*, *Nox4*, and *Nox5* mRNAs in the larval midgut while the activity of ROS-scavenging enzymes such as SOD and POD were also increased (Lu et al., 2021a). Whether these genes are modulated by the canonical CncC:Maf pathway in *S. frugiperda* remains yet to be demonstrated. Furthermore, the role played by ROS-producing enzymes such as NADPH oxidases and HAO-1 in ROS/Keap1/CncC signaling is largely unknown and would require more attention.

A downregulation of several genes involved in innate immune response such as the Toll receptor and antimicrobial peptides emerged from the differential expression analysis. This is in accordance with data from Misra et al. (2013) in *D. melanogaster* who showed downregulation of immune effectors like cecropin genes, *Mtk*, *Def*, *Drs* and *dro3*. The repression of innate immune response genes was largely reflected by enrichment analysis of GO terms, as the top "biological process" over-represented in the downregulated transcripts of OE cell lines were "defense response to other organisms", "defense response to bacterium" and "antimicrobial humoral response". This coordinate cross-regulation of the immune and oxidative/xenobiotics responses agrees with the high fitness cost associated with activation of the CncC:Maf pathway. Other transcripts matching genes involved in insect stress signaling pathways like the AhR/ARNT and GPCRs were found differentially expressed throughout the RNA-seq datasets. AhR is a xenobiotic sensor that binds to various ligands including toxic chemicals and controls numerous genes by dimerizing with ARNT and operating on xenobiotic response elements (XRE) to AhR (XRE-AhR) (Nakata et al., 2006). The XRE-AhR motif was found several instances located in close synteny with an ARE motif such as in the promoter of *Papilio polyxenes* CYP6B1 and *Papilio glaucus* CYP6B4 (Brown et al., 2005; McDonnell et al., 2004) or in *S. exigua* upstream *GSTd3, GSTe8* and *GSTo2* (Hu et al., 2019a; Hu et al., 2019b). Is the expression of some detoxifying enzymes controlled by the joint action of CncC:Maf and AhR:ARNT heterodimers? Is there a cross-regulation between these two pathways? Similarly, the GPCRs signaling pathway was the third most significant GO term enrichment found among upregulated transcripts. GCPRs initiate a myriad of signaling cascades after binding to various ligands including xenobiotics which was shown to lead to upregulation of detoxification genes in *Culex* mosquitos (Liu et al., 2021). Downstream effector molecules of GPCRs include protein kinases (PK) such as PKA which may activate xenobiotic transcription factors by phosphorylation in *Culex* mosquitoes (Li et al., 2015; Li et al., 2014; Liu and Li, 2017; Liu et al., 2021). Here too, whether the CncC:Maf pathway and GCPRs act in conjunction towards xenobiotic response is largely unknown and requires more work.

In conclusion, we gather in this chapter substantial data of transcriptional activity from CncC-deficient and enhanced Sf9 cell lines. The analysis of differentially regulated genes revealed that *CncC* controls the transcriptional activity of a large number of detoxification genes involved in oxidative and xenobiotic response. This response seems to be mainly mediated by the expression of P450 genes. Furthermore, our data shows that CncC is at the

cross road of multiple biologically fundamental pathways as its suppression or activation results in modulation of many non-xenobiotic genes. One of the major adds-on of this study is the availability of transcriptomic data from pMaf-b and Sf9$^{Keap1\text{-}01}$ representing crucial information that may shed light of the respective roles of Maf and Keap1 proteins in the Keap1/CncC/Maf pathway, and others (Deng and Kerppola, 2013, 2014; Ingham et al., 2020; Ingham et al., 2017). Further analysis of the cis-regulatory elements located in the promoter regions of the potential target genes identified in these RNA-seq data sets will contribute to refine the CncC:Maf gene network established by this work in *S. frugiperda*.

GENERAL DISCUSSION

The ability to rapidly overcome the chemical challenges encountered when expanding to new environments and new host plants is at the basis of *S. frugiperda's* tremendous success. This versatility is argued to find ground in its "DETOXome" on top of broad substrate specificity and transcriptional plasticity. In that respect, the comparison of the genomes and the biology of generalist *Spodoptera* species such as *S. frugiperda* to specialist *Spodoptera* species, such as *S. picta* feeding on a few Amaryllidaceae plant species, would be of great interest (number of genes, blooms, cluster conservation and organization, etc.). The amount of information on inducibility and inducers of detoxification genes in *Spodoptera* has greatly advanced our knowledge that metabolism of xenobiotics plays an important role in their ability to adapt to new chemicals (Amezian et al., 2021a). Over the past decade, the Cap'n'collar isoform C (CncC) transcription factor has emerged as a major regulator of detoxification genes shown to often involved in insecticide sensitivity in other insect species (Palli, 2020). However, its role in *S. frugiperda* resistance mechanisms remains to date largely unexplored.

My research focused on using Sf9 cells, the cellular model of *S. frugiperda*, to study the molecular mechanisms underlying CncC-associated regulation of detoxification genes that may be involved in metabolic resistance adaptation to plant allelochemicals. Chapter 1 aimed at determining whether the CncC:Maf pathways can mediate induction of detoxification genes after exposure to two xenobiotics, a plant allelochemical (indole 3-carbinol) and an insecticide (methoprene). Chapter 2 can be divided in two parts. First was the development of cellular tools using reverse genetic methods, *i.e.* overexpression and CRISPR/Cas9-mediated knockout of *CncC*. This allowed to further investigate in a second part the role of CncC in cell tolerance to xenobiotic exposure, activity of detoxification enzymes and modulation of ROS content. Chapter 3 focused on the identification of CncC-mediated modulation of detoxification gene expression by using a comprehensive transcriptomic approach (RNA-seq).

My work enlightened some aspects of the molecular mechanisms underlying CncC:Maf mediated xenobiotic response of Sf9 cells. I was able to show that detoxification genes, including CYPs and GSTs were induced by I3C and MTP, and that only some were further

upregulated by transient overexpression of CncC:Maf. The constitutive overexpression of *CncC* and *Maf* in stably transformed cells resulted in a significant gain of tolerance towards I3C and MTP challenges as well as increased CE activity. Similarly, the mutation of *CncC* and *Keap1* resulted in decreased and increased CE and GST activities, respectively, agreeing with the expected effector-repressor interaction known for these two proteins and their role in deployment of cytoprotective agents. In addition, the knockout transformants highlighted the possible role of CncC in modulating in-cell basal ROS production. Finally, the transcriptomic analysis allowed to identify large sets of detoxification genes commonly differentially regulated between the various transformants and thus putatively under the transcriptional control of the CncC:Maf pathway.

The mechanisms unveiled in the cellular model of *S. frugiperda* may shed light on those taking place in insects from the field. Indeed, a good proportion of the detoxification genes identified in the RNA-seq analysis belonged to the main detoxification gene families. Some of these genes were shown to be involved in plant compound metabolism resistance phenotypes, from field-collected or laboratory insects. For example, *CYP321A8* (or *CYP321A10* see Fig. 4) was found upregulated in the $Sf9^{Keap1\text{-}01}$ cell lines suggesting its expression might be controlled by CncC. Previous studies carried out in *Spodoptera* insects have shown that this CYP is potentially involved in sensitivity to xenobiotics. In *S. litura* larvae, *CYP31A8* was strongly induced by xanthotoxin and flavone treatments (Lu et al., 2021a; Lu et al., 2021b) suggesting it might be involved in the xenobiotic response deployed by the insect towards flavonoids and furanocoumarins. In *S. exigua*, CYP321A8 was strongly overexpressed in a population resistant to chlorpyrifos, an organophosphate (Hu et al., 2021). The mechanisms of *SlCYP321A8* induction and *SeCYP321A8* overexpression were uncovered and shown to be both mediated by the CncC:Maf pathway. Indeed, RNAi-mediated knockdown of *CncC* in *S. litura* resulted in significant decrease of *CYP321A8* transcript levels, as well as those of many other genes (Lu et al., 2021a). In *S. exigua,* Hu et al. (2021) demonstrated using a reporter gene assay that a mutated ARE sequence located in the promoter region of CYP321A8 was responsible for the constitutive overexpression seen in the chlorpyrifos resistant strain. More recently, Chen and Palli (2021a) established transgenic FAW larvae overexpressing the *CYP321A8* gene. The transgene was successfully expressed in different tissues including midgut and fat bodies and resulted in increased P450 enzymatic activity compared to the wild type. More importantly, transgenic larvae were 10-times more tolerant to deltamethrin as

compared to the control, which nicely shows that *CYP321A8* can confer resistance to deltamethrin in *S. frugiperda*. Furthermore, the cell-based assays carried out in chapter 1, with the addition of experiment carried out by collaborators could also illustrate the selectivity of detoxification genes induction. Indeed, while I3C and MTP could both induce the upregulation of *CYP9A30*, *CYP9A31* and *CYP9A32*, only MTP seemed to be potentially metabolized by heterologously expressed CYP9As, as shown by a fluorescent probe inhibition assays (Amezian et al. 2022, *submitted*). Taken together, these studies show that Sf9 cells could be considered as a good cellular model for studying molecular aspects of FAW xenobiotic response. In addition, Sf9 cells benefit from the easier and quicker implementation of a large molecular toolkit (CRISPR/Cas9, gene reporter assays, heterologous expression etc.). Nevertheless, the extent of the transcriptional signature of Sf9 cells from the RNA-seq experiment is specific to this cell type and may not reflect transcription profiles of FAW midgut for example. Indeed, a previous study from my group showed discrepancies between transcription profiles of Sf9 cells compared to lab-reared FAW larvae (Giraudo et al., 2015). Therefore, functional validation and proof-of-concept studies in the insect should be an absolute necessity to conclude on the biological relevance of CncC at the organismal level.

The present work brought new questions regarding the role that ROS play in the activation of the Keap1/CncC pathway. The link between ROS variations and the activation of the pathway remains largely unknown. Many studies have reported an increase of ROS content in various insect tissues and cells after treatment with plant secondary metabolites such as I3C, xanthotoxin and flavone (Chen et al., 2018b; Lu et al., 2021a; Lu et al., 2021b) or insecticides including acetamiprid, imidacloprid and chlorpyrifos (Chen et al., 2018a; Lu et al., 2021c; Tang et al., 2020). ROS measurements using carboxy-H_2DCFDA showed an increase of basal oxidative stress in the cell line KO for *CncC*, while the levels of ROS were significantly decreased in the cell line KO for *Keap1*, altogether suggesting that CncC might be involved in modulating in-cell basal ROS content. Interestingly, Tang et al. (2020) found higher H_2O_2 levels in a resistant population of *Nilaparvata lugens* as compared to the susceptible insects and that this was correlated to constitutive overexpression of *CncC*. CncC is known to control the expression of antioxidant enzymes including SOD and CAT, however, whether CncC also controls the expression of ROS producing enzymes in insects is unclear. In mammals, Nrf2 is a known modulator of the hemoxygenase-1 (HO-1) (Loboda et al., 2016). In *S. litura*, a recent study showed that transcripts levels of *Nox* and *Duox* genes were upregulated in the midgut

of flavone treated larvae (Lu et al., 2021a). To test this hypothesis, I examined the expression of ROS producing and scavenging enzymes in the RNA-seq data sets. However, the comparative analysis of mRNA levels of these genes could not account for the ROS levels observed in $Sf9^{CncC\text{-}13}$ and $Sf9^{Keap1\text{-}01}$ and does not allow to draw any conclusion but definitely raises questions about the link between ROS signaling and the Keap1/CncC pathway. Is the expression or the activity of *Nox* and *Duox* controlled by CncC? What is/are the origin(s) of the so-called "ROS bursts" that activate the Keap1/CncC pathway? More work is needed to provide answers to these questions.

A few additional experiments using the cell lines established in this project should be carried out in order to further validate some results. For example, the apparent increased tolerance of MTT toxicological tests showed that two cell lines mutated for *CncC*, respectively $Sf9^{CncC\text{-}08}$ and $Sf9^{CncC\text{-}13}$, were unexpectedly more tolerant to xenobiotic challenges than the control. ROS level measurements showed high basal oxidative stress in $Sf9^{CncC\text{-}13}$ which might partly explain the discrepancies observed in MTT-based viability assays (Stepanenko and Dmitrenko, 2015). Toxicological tests should hence be complemented with viability experiments using a different approach, such as the propidium iodide and calcein-AM based assay carried out for OE cell lines. In addition, the upregulation of the *Keap1* gene in most *Keap1*-mutated cell lines is an issue. Although the results from the characterization experiments corroborate the loss-of-function for this gene, the overexpression is surprising and needs further clarification. As discussed in chapter 3, CRISPR/Cas9-mediated mutations may result in exon skipping events and alternative translation initiation (ATI) preventing mRNA degradation before translation (Tuladhar et al., 2019). In addition, the involvement of *Keap1* in the regulation of its own expression was also proposed (Deng and Kerppola, 2014; Sykiotis and Bohmann, 2010). However, these examples in *Drosophila* reported a feed-forward regulatory loop which is in contradiction with what we observe here (the mutation of *Keap1* leads to *Keap1* upregulation). Finally, *Keap1* may also interact with other regulatory pathways that controls its expression. Therefore, sequencing the region spanning the CncC-target site would be crucial to fully describe the mutation in $Sf9^{Keap1\text{-}01}$ and shed light on the mechanism at play. More generally, these results highlight the lack of information on how the Keap1/CncC/Maf canonical pathway can be modulated by other interacting proteins in insects. A few studies in arthropods have started to exemplified Keap1-independent regulation of the CncC:Maf pathway such as through the action of the CncC repressor Fs(1)h.

Fs(1)h was identified as the sole ortholog of mammalian bromodomain containing BET proteins found in *Drosophila* and shown to physically interact with CncC (Chatterjee and Bohmann, 2018; Chatterjee et al., 2016). Nevertheless, how CncC relates to the broader scheme of signaling molecular network in insects is largely unknown and comprehensive knowledge from research in mammalian models shows that much remains to be uncovered (Basak et al., 2017). Therefore, future studies in insects could implement more holistic and unbiased approaches to identify binding sites and interacting proteins of TFs involved in xenobiotics signaling. For example, the use of yeast-2-hybrid (Y2H) and proximity labeling-based methods such as BioID (proximity-dependent biotin identification) or its more recent variant TurboID (Branon et al., 2018) have been widely used to determine protein-protein and DNA-protein interaction in bacterial, plant and animal biosystems (Zhang et al., 2021).

RNA-seq studies enable to grasp the complete transcriptional changes that occur when insects are exposed to xenobiotics (Birnbaum and Abbot, 2020; Vandenhole et al., 2020). Differential expression analyses were used previously in other species to comprehensively determine the gene regulatory network of TF, including CncC. In Diptera and Coleoptera more specifically, CncC was shown to regulate large sets of genes (Gaddelapati et al., 2018; Kalsi and Palli, 2017a; Misra et al., 2011). Here, I showed that CncC modulates the expression of hundreds of genes in Sf9 cells including many detoxification genes, several of which may be involved in insecticide and plant secondary metabolite sensitivity in *S. frugiperda*. It would be of great interest to analyze the phenotype of a double mutant for both *CncC* and *Maf* genes. This work has been initiated this year in our lab with the isolation of several cell lines mutated for either *Maf* alone or the complete CncC:Maf pathway, however, they require further characterization. A few additional bioinformatical analyses could be performed to complete the understanding of *CncC*, *Maf* and *Keap1* modulations in the cell transformants. For example, the GO annotation analysis encompasses “biological processes” but omits “molecular component” and “molecular function” enrichment terms. In addition, a KEGG pathway enrichment analysis may help to discern the metabolic pathways that are activated or repressed by the modulation of these genes. Furthermore, although the expression levels of the target genes in the RNA-seq data were somewhat consistent with those assessed by RT-qPCR (chapter 4, Table S1), assessing the mRNA levels of a few additional genes would be necessary to fully validate the transcriptomic data. One alternative approach to determine

transcription factors target-genes is to identify the transcription factors binding sites (TFBS) in promoter regions. It would therefore be interesting to analyze the promoters of the genes identified as putative CncC targets for the presence of ARE consensus sequences. The methods for identifying and characterizing TFBS have been extensively reviewed (Suryamohan and Halfon, 2015). Computational methods facilitating the discovery of potential TFBS using positional matrix screening (PMS) are among the preferred methods. A previous study conducted by Giraudo et al. (2015) used the regulatory sequence analysis tool (RSAT, rsat.sb-roscoff.fr) to screen the promoter regions of 23 P450 genes of *S. frugiperda*. A total of ten CYP promoters bared a putative ARE motif including, CYP6B39, CYP9A25, CYP9A26, CYP9A27, CYP9A28 and CYP9A25, but not CYP9A31. However, the study used a motif scan approach using *Papilio glaucus* and *Papilio canadensis* PSM and might not provide accurate estimation of TFBS locations in *S. frugiperda*. Indeed, TFs recognize and bind DNA in a consensus sequence-specific fashion that is conserved among species, throughout developmental stages and cell types. Therefore, *cis*-regulatory motifs identification requires experimental validation. In that respect, testing these sequences in promoter constructs and reporter gene assays was shown to be highly robust (Kalsi and Palli, 2017b). Species-specificity and conservation of *cis*-regulatory sequences throughout cell types are two additional features in favor of using Sf9 cells. The preferred strategy to experimentally identify TFBS involves chromatin immunoprecipitation followed by high-throughput sequencing (ChIP-seq) (Landt et al., 2012), a strategy allowing to accurately identify the binding capability of a transcription factor *in vivo*. A major downside of this method is to obtain ChIP-seq grade antibodies of transcription factors, which remains a challenge for non-model species as illustrated in this project. In the course of my work, I have tried to produce CncC-specific antibodies. One initial goal of the present project was to implement a ChIP-seq assay to determine the binding locations of CncC in Sf9 cells. In order to maintain the highest level of conformational conservation with the native protein, I wished to raise antibodies against the N-terminal isoform C-specific domain of the Cnc gene. However, the production of this protein was unfruitful in both Sf9 cells and *E. coli* due to substantial protein degradation. Eventually, antibodies were produced using short peptides and yet resulted in low specific binding. The use of antibodies could have also been decisive to validate the knockout of *CncC* and *Keap1* genes at the protein level. Therefore, I have tested two commercially available antibodies targeting Keap1, without success (data not shown). In the future however, the use of CRISPR/Cas9 in non-model species

to introduce tags to native proteins will allow to bypass this constraint (Partridge et al., 2016; Savic et al., 2015).

The selection in the field for increased insecticide detoxification and subsequent development of resistance is a major threat to sustainable yields and global food safety. Therefore, the detection of insecticide resistance and its major molecular drivers are of utmost importance for developing new and more efficient management strategies. Permanent changes in detoxification genes expression may occur due to gene copy number variation (CNV) or duplication events, changes in *cis*-acting factors and distal regulatory modules such as SNPs and TEs, changes in *trans*-acting factors such as upregulation or activation of transcription factors (Amezian et al., 2021b; Feyereisen et al., 2015; Nakata et al., 2006). In addition, mutation(s) in the amino-acid sequence of a detoxifying enzymes may result in increased metabolism or a change in substrate specificity, however these changes are much rarer (Riveron et al., 2014; Zimmer et al., 2018; Zuo et al., 2021). My work has essentially focused on the mechanisms of CncC:Maf activation leading to induction of target detoxification genes, and their identification. Further work would benefit from functional studies in *S. frugiperda* insects to explain the origin of enhanced activity of detoxification genes. The recent development of CRISPR tools for FAW (Zhu et al., 2020) as well as more robust dsRNA delivery methods for RNAi-mediated gene silencing in Lepidoptera species (Laisney et al., 2020) will allow functional studies and validation of the role of *CncC* in FAW.

In addition to the genetic validation, biochemical and pharmacokinetic studies utilizing recombinantly expressed CncC-regulated enzymes and LC or GC-MS/MS should be carried out to functionally validate xenobiotic detoxification capabilities and identify the resulting metabolites. Indeed, metabolism (of a compound) is not synonymous with detoxification. Detoxification requires proof that the product of the reaction is less toxic than its parent (as demonstrated for 4-hydroxylated metabolites of pyrethroid insecticides (Zimmer et al., 2014; Zimmer and Nauen, 2011) and flupyradifurone metabolites (Haas et al., 2021)). Indeed, such proof is rarely provided. For example, my recent review of detoxification gene expression data in *Spodoptera* highlighted that in *S. litura* close to 300 detoxification genes have been transcriptionally assessed in the context of xenobiotic response (Amezian et al., 2021a). Out of these, only 26 were investigated at the genetic level while three were validated using biochemical/functional studies. This year, two additional functional validation studies have

demonstrated the involvement of P450s in *S. exigua* (Hu et al., 2021; Zuo et al., 2021) and more similar work is expected in the years to come for *Spodoptera* species. In *S. frugiperda* the acknowledgement of the role of detoxification genes in insecticide metabolism is largely hampered by the paucity of genetic functional validation studies and heterologous expressed enzymes.

The levels of metabolic insecticide resistance are usually directly linked to the expression level of respective detoxification genes. Upregulation and activation of *trans*-acting factors are usually at the core of gene inducibility. In this respect, future work is needed to identify the overarching diagnostic potential of transcription factors to monitor field-relevant resistance against a broad range of insecticidal chemotypes. In addition, they potentially provide a nodal point for insect population control. Nrf2 for example has drawn attention for it was shown to be involved in the development of metastasis and chemoresistance through activation of detoxification enzymes (Sanchez-Ortega et al., 2021). Hence, cancer research has focused on identifying Nrf2 inhibitors to alleviate therapeutic resistance in e.g. Keap1-deficient types of tumors (Singh et al., 2016). Thus, finding CncC modulators may provide a solution for controlling emergence of metabolic resistance in the field.

References

Ahmad, A., Biersack, B., Li, Y., Kong, D., Bao, B., Schobert, R., Padhye, S.B., Sarkar, F.H., 2013. Targeted regulation of PI3K/Akt/mTOR/NF-kappaB signaling by indole compounds and their derivatives: mechanistic details and biological implications for cancer therapy. Anticancer Agents Med Chem 13, 1002-1013.

Ahn, S.J., Vogel, H., Heckel, D.G., 2012. Comparative analysis of the UDP-glycosyltransferase multigene family in insects. Insect Biochem Mol Biol 42, 133-147.

Amezian, D., Nauen, R., Le Goff, G., 2021a. Comparative analysis of the detoxification gene inventory of four major *Spodoptera* pest species in response to xenobiotics. Insect Biochem Mol Biol 138, 103646.

Amezian, D., Nauen, R., Le Goff, G., 2021b. Transcriptional regulation of xenobiotic detoxification genes in insects - An overview. Pestic Biochem Physiol 174, 104822.

Argentine, J.A., Clark, J.M., 1990. Selection for abamectin resistance in colorado potato beetle (Coleoptera: Chrysomelidae). Pesticide Science 28, 17–24.

Asmann, Y.W., Dong, M., Miller, L.J., 2004. Functional characterization and purification of the secretin receptor expressed in baculovirus-infected insect cells. Regul Pept 123, 217-223.

Bai, H., Gelman, D.B., Palli, S.R., 2010. Mode of action of methoprene in affecting female reproduction in the African malaria mosquito, *Anopheles gambiae*. Pest Manag Sci 66, 936-943.

Balabanidou, V., Kampouraki, A., MacLean, M., Blomquist, G.J., Tittiger, C., Juarez, M.P., Mijailovsky, S.J., Chalepakis, G., Anthousi, A., Lynd, A., Antoine, S., Hemingway, J., Ranson, H., Lycett, G.J., Vontas, J., 2016. Cytochrome P450 associated with insecticide resistance catalyzes cuticular hydrocarbon production in *Anopheles gambiae*. Proc Natl Acad Sci U S A 113, 9268-9273.

Basak, P., Sadhukhan, P., Sarkar, P., Sil, P.C., 2017. Perspectives of the Nrf-2 signaling pathway in cancer progression and therapy. Toxicol Rep 4, 306-318.

Bassett, A.R., Tibbit, C., Ponting, C.P., Liu, J.L., 2013. Highly efficient targeted mutagenesis of *Drosophila* with the CRISPR/Cas9 system. Cell Rep 4, 220-228.

Bateman, M.L., Day, R.K., Luke, B., Edgington, S., Kuhlmann, U., Cock, M.J., 2018. Assessment of potential biopesticide options for managing fall armyworm (Spodoptera frugiperda) in Africa. Journal of applied entomology 142, 805-819.

Baudron, F., Zaman-Allah, M.A., Chaipa, I., Chari, N., Chinwada, P., Understanding the factors influencing fall armyworm (Spodoptera frugiperda JE Smith) damage in African smallholder maize fields and quantifying its impact on yield. A case study in Eastern Zimbabwe. Crop Protection 120, 141-150.

Behle, R.W., Popham, H.J., 2012. Laboratory and field evaluations of the efficacy of a fast-killing baculovirus isolate from Spodoptera frugiperda. J Invertebr Pathol 109, 194-200.

Berenbaum, M.R., Johnson, R.M., 2015. Xenobiotic detoxification pathways in honey bees. Curr Opin Insect Sci 10, 51-58.

Berridge, M.V., Herst, P.M., Tan, A.S., 2005. Tetrazolium dyes as tools in cell biology: new insights into their cellular reduction. Biotechnology annual review 11, 127-152.

Birnbaum, S.S.L., Abbot, P., 2020. Gene Expression and Diet Breadth in Plant-Feeding Insects: Summarizing Trends. Trends Ecol Evol 35, 259-277.

Biswas, S., Reinhard, J., Oakeshott, J., Russell, R., Srinivasan, M.V., Claudianos, C., 2010. Sensory regulation of neuroligins and neurexin I in the honeybee brain. PLoS One 5, e9133.

Boaventura, D., Bolzan, A., Padovez, F.E., Okuma, D.M., Omoto, C., Nauen, R., 2020a. Detection of a ryanodine receptor target-site mutation in diamide insecticide resistant fall armyworm, *Spodoptera frugiperda*. Pest Manag Sci 76, 47-54.

Boaventura, D., Buer, B., Hamaekers, N., Maiwald, F., Nauen, R., 2020b. Toxicological and molecular profiling of insecticide resistance in a Brazilian strain of fall armyworm resistant to Bt Cry1 proteins. Pest Manag Sci.

Bock, K.W., 2016. The UDP-glycosyltransferase (UGT) superfamily expressed in humans, insects and plants: Animal-plant arms-race and co-evolution. Biochem Pharmacol 99, 11-17.

Bozzolan, F., Siaussat, D., Maria, A., Durand, N., Pottier, M.A., Chertemps, T., Maibeche-Coisne, M., 2014. Antennal uridine diphosphate (UDP)-glycosyltransferases in a pest insect: diversity and putative function in odorant and xenobiotics clearance. Insect Mol Biol 23, 539-549.

Branon, T.C., Bosch, J.A., Sanchez, A.D., Udeshi, N.D., Svinkina, T., Carr, S.A., Feldman, J.L., Perrimon, N., Ting, A.Y., 2018. Efficient proximity labeling in living cells and organisms with TurboID. Nat Biotechnol 36, 880-887.

Breeschoten, T., Ros, V.I.D., Schranz, M.E., Simon, S., 2019. An influential meal: host plant dependent transcriptional variation in the beet armyworm, *Spodoptera exigua* (Lepidoptera: Noctuidae). BMC Genomics 20, 845.

Brown, R.P., McDonnell, C.M., Berenbaum, M.R., Schuler, M.A., 2005. Regulation of an insect cytochrome P450 monooxygenase gene (CYP6B1) by aryl hydrocarbon and xanthotoxin response cascades. Gene 358, 39-52.

Brun-Barale, A., Hema, O., Martin, T., Suraporn, S., Audant, P., Sezutsu, H., Feyereisen, R., 2010. Multiple P450 genes overexpressed in deltamethrin-resistant strains of *Helicoverpa armigera*. Pest Manag Sci 66, 900-909.

Bueno, R.C., Bueno Ade, F., Moscardi, F., Parra, J.R., Hoffmann-Campo, C.B., 2011. Lepidopteran larva consumption of soybean foliage: basis for developing multiple-species economic thresholds for pest management decisions. Pest Manag Sci 67, 170-174.

Busato, G.R., Grützmacher, A.D., Garcia, M.S., Giolo, F.P., Zotti, M.J., Stefanello Júnior, G.J., 2005. Biologia comparada de populações de Spodoptera frugiperda (JE Smith)(Lepidoptera: Noctuidae) em folhas de milho e arroz. Neotropical Entomology 34, 743-750.

Carvalho, R.A., Omoto, C., Field, L.M., Williamson, M.S., Bass, C., 2013. Investigating the molecular mechanisms of organophosphate and pyrethroid resistance in the fall armyworm *Spodoptera frugiperda*. PLoS One 8, e62268.

Casida, J.E., 1980. Pyrethrum flowers and pyrethroid insecticides. Environ Health Perspect 34, 189-202.

Castillejos, V., Trujillo, J., Ortega, L.D., Santizo, J.A., Cisneros, J., Penagos, D.I., Valle, J., Williams, T., 2002. Granular phagostimulant nucleopolyhedrovirus formulations for control of Spodoptera frugiperda in maize. Biological Control 24, 300-310.

Celorio-Mancera Mde, L., Ahn, S.J., Vogel, H., Heckel, D.G., 2011. Transcriptional responses underlying the hormetic and detrimental effects of the plant secondary metabolite gossypol on the generalist herbivore *Helicoverpa armigera*. BMC Genomics 12, 575.

Chatterjee, N., Bohmann, D., 2018. BET-ting on Nrf2: How Nrf2 Signaling can Influence the Therapeutic Activities of BET Protein Inhibitors. Bioessays 40, e1800007.

Chatterjee, N., Tian, M., Spirohn, K., Boutros, M., Bohmann, D., 2016. Keap1-Independent Regulation of Nrf2 Activity by Protein Acetylation and a BET Bromodomain Protein. PLoS Genet 12, e1006072.

Chelvanayagam, G., Parker, M.W., Board, P., 2001. Fly fishing for GSTs: a unified nomenclature for mammalian and insect glutathione transferases.

Chen, S., Lu, M., Zhang, N., Zou, X., Mo, M., Zheng, S., 2018a. Nuclear factor erythroid-derived 2-related factor 2 activates glutathione S-transferase expression in the midgut of *Spodoptera litura* (Lepidoptera: Noctuidae) in response to phytochemicals and insecticides. Insect Mol Biol 27, 522-532.

Chen, S., Lu, M., Zhang, N., Zou, X., Mo, M., Zheng, S., 2018b. Nuclear factor erythroid-derived 2-related factor 2 activates glutathione S-transferase expression in the midgut of Spodoptera litura (Lepidoptera: Noctuidae) in response to phytochemicals and insecticides. Insect Mol Biol.

Chen, X., Palli, S.R., 2021a. Transgenic overexpression of P450 genes confers deltamethrin resistance in the fall armyworm, *Spodoptera frugiperda*. Journal of Pest Science, 1-9.

Chen, X., Palli, S.R., 2021b. Transgenic overexpression of P450 genes confers deltamethrin resistance in the fall armyworm, *Spodoptera frugiperda*. Journal of Pest Science.

Cheng, T., Wu, J., Wu, Y., Chilukuri, R.V., Huang, L., Yamamoto, K., Feng, L., Li, W., Chen, Z., Guo, H., Liu, J., Li, S., Wang, X., Peng, L., Liu, D., Guo, Y., Fu, B., Li, Z., Liu, C., Chen, Y., Tomar, A., Hilliou, F., Montagne, N., Jacquin-Joly, E., d'Alencon, E., Seth, R.K., Bhatnagar, R.K., Jouraku, A., Shiotsuki, T., Kadono-Okuda, K., Promboon, A., Smagghe, G., Arunkumar, K.P., Kishino, H., Goldsmith, M.R., Feng, Q., Xia, Q., Mita, K., 2017a. Genomic adaptation to polyphagy and insecticides in a major East Asian noctuid pest. Nat Ecol Evol.

Cheng, T., Wu, J., Wu, Y., Chilukuri, R.V., Huang, L., Yamamoto, K., Feng, L., Li, W., Chen, Z., Guo, H., Liu, J., Li, S., Wang, X., Peng, L., Liu, D., Guo, Y., Fu, B., Li, Z., Liu, C., Chen, Y., Tomar, A., Hilliou, F., Montagne, N., Jacquin-Joly, E., d'Alencon, E., Seth, R.K., Bhatnagar, R.K., Jouraku, A., Shiotsuki, T., Kadono-Okuda, K., Promboon, A., Smagghe, G., Arunkumar, K.P., Kishino, H., Goldsmith, M.R., Feng, Q., Xia, Q., Mita, K., 2017b. Genomic adaptation to polyphagy and insecticides in a major East Asian noctuid pest. Nat Ecol Evol 1, 1747-1756.

Chimweta, M., Nyakudya, I.W., Jimu, L., Bray Mashingaidze, A., 2020. Fall armyworm [*Spodoptera frugiperda* (JE Smith)] damage in maize: management options for flood-recession cropping smallholder farmers. International journal of pest management 66, 142-154.

Clark, A.G., Eisen, M.B., Smith, D.R., Bergman, C.M., Oliver, B., Markow, T.A., Kaufman, T.C., Kellis, M., Gelbart, W., Iyer, V.N., Pollard, D.A., Sackton, T.B., Larracuente, A.M., Singh, N.D., Abad, J.P., Abt, D.N., Adryan, B., Aguade, M., Akashi, H., Anderson, W.W., Aquadro, C.F., Ardell, D.H., Arguello, R., Artieri, C.G., Barbash, D.A., Barker, D., Barsanti, P., Batterham, P., Batzoglou, S., Begun, D., Bhutkar, A., Blanco, E., Bosak, S.A., Bradley, R.K., Brand, A.D., Brent, M.R., Brooks, A.N., Brown, R.H., Butlin, R.K., Caggese, C., Calvi, B.R., Bernardo de Carvalho, A., Caspi, A., Castrezana, S., Celniker, S.E., Chang, J.L., Chapple, C., Chatterji, S., Chinwalla, A., Civetta, A., Clifton, S.W., Comeron, J.M., Costello, J.C., Coyne, J.A., Daub, J., David, R.G., Delcher, A.L., Delehaunty, K., Do, C.B., Ebling, H., Edwards, K., Eickbush, T., Evans, J.D., Filipski, A., Findeiss, S., Freyhult, E., Fulton, L., Fulton, R., Garcia, A.C., Gardiner, A., Garfield, D.A., Garvin, B.E., Gibson, G., Gilbert, D., Gnerre, S., Godfrey, J., Good, R., Gotea, V., Gravely, B., Greenberg, A.J., Griffiths-Jones, S., Gross, S., Guigo, R., Gustafson, E.A., Haerty, W., Hahn, M.W., Halligan, D.L., Halpern, A.L., Halter, G.M., Han, M.V., Heger, A., Hillier, L., Hinrichs, A.S., Holmes, I., Hoskins, R.A., Hubisz, M.J., Hultmark, D., Huntley, M.A., Jaffe, D.B., Jagadeeshan, S., Jeck, W.R., Johnson, J., Jones, C.D., Jordan, W.C., Karpen, G.H., Kataoka, E., Keightley, P.D., Kheradpour, P., Kirkness, E.F., Koerich, L.B., Kristiansen, K., Kudrna, D., Kulathinal, R.J., Kumar, S., Kwok, R., Lander, E., Langley, C.H., Lapoint, R., Lazzaro, B.P., Lee, S.J., Levesque, L., Li, R., Lin, C.F., Lin, M.F., Lindblad-Toh, K., Llopart, A., Long, M., Low, L., Lozovsky, E., Lu, J., Luo, M., Machado, C.A., Makalowski, W., Marzo, M., Matsuda, M., Matzkin, L., McAllister, B., McBride, C.S., McKernan, B., McKernan, K., Mendez-Lago, M., Minx, P., Mollenhauer, M.U., Montooth, K., Mount, S.M., Mu, X., Myers, E., Negre, B., Newfeld, S., Nielsen, R., Noor, M.A., O'Grady, P., Pachter, L., Papaceit, M., Parisi, M.J., Parisi, M., Parts, L., Pedersen, J.S., Pesole, G., Phillippy, A.M., Ponting, C.P., Pop, M., Porcelli, D., Powell, J.R., Prohaska, S., Pruitt, K., Puig, M., Quesneville, H., Ram, K.R., Rand, D., Rasmussen, M.D., Reed, L.K., Reenan, R., Reily, A., Remington, K.A., Rieger, T.T., Ritchie, M.G., Robin, C., Rogers, Y.H., Rohde, C., Rozas, J., Rubenfield, M.J., Ruiz, A., Russo, S., Salzberg, S.L., Sanchez-Gracia, A., Saranga, D.J., Sato, H., Schaeffer, S.W., Schatz, M.C., Schlenke, T., Schwartz, R., Segarra, C., Singh, R.S., Sirot, L., Sirota, M., Sisneros, N.B., Smith, C.D., Smith, T.F., Spieth, J., Stage, D.E., Stark, A., Stephan, W., Strausberg, R.L., Strempel, S., Sturgill, D., Sutton, G., Sutton, G.G., Tao, W., Teichmann, S., Tobari, Y.N., Tomimura, Y., Tsolas, J.M., Valente, V.L., Venter, E., Venter, J.C., Vicario, S., Vieira, F.G., Vilella, A.J., Villasante, A., Walenz, B., Wang, J., Wasserman, M., Watts, T., Wilson, D., Wilson, R.K., Wing, R.A., Wolfner, M.F., Wong, A., Wong, G.K., Wu, C.I., Wu, G., Yamamoto, D., Yang, H.P., Yang, S.P., Yorke, J.A., Yoshida, K., Zdobnov, E., Zhang, P., Zhang, Y., Zimin, A.V., Baldwin, J., Abdouelleil, A., Abdulkadir, J., Abebe, A., Abera, B., Abreu, J., Acer, S.C., Aftuck, L., Alexander, A., An, P., Anderson, E., Anderson, S., Arachi, H., Azer, M., Bachantsang, P., Barry, A., Bayul, T., Berlin, A., Bessette, D., Bloom, T., Blye, J., Boguslavskiy, L., Bonnet, C., Boukhgalter, B., Bourzgui, I., Brown, A., Cahill, P., Channer, S., Cheshatsang, Y., Chuda, L., Citroen, M., Collymore, A., Cooke,

P., Costello, M., D'Aco, K., Daza, R., De Haan, G., DeGray, S., DeMaso, C., Dhargay, N., Dooley, K., Dooley, E., Doricent, M., Dorje, P., Dorjee, K., Dupes, A., Elong, R., Falk, J., Farina, A., Faro, S., Ferguson, D., Fisher, S., Foley, C.D., Franke, A., Friedrich, D., Gadbois, L., Gearin, G., Gearin, C.R., Giannoukos, G., Goode, T., Graham, J., Grandbois, E., Grewal, S., Gyaltsen, K., Hafez, N., Hagos, B., Hall, J., Henson, C., Hollinger, A., Honan, T., Huard, M.D., Hughes, L., Hurhula, B., Husby, M.E., Kamat, A., Kanga, B., Kashin, S., Khazanovich, D., Kisner, P., Lance, K., Lara, M., Lee, W., Lennon, N., Letendre, F., LeVine, R., Lipovsky, A., Liu, X., Liu, J., Liu, S., Lokyitsang, T., Lokyitsang, Y., Lubonja, R., Lui, A., MacDonald, P., Magnisalis, V., Maru, K., Matthews, C., McCusker, W., McDonough, S., Mehta, T., Meldrim, J., Meneus, L., Mihai, O., Mihalev, A., Mihova, T., Mittelman, R., Mlenga, V., Montmayeur, A., Mulrain, L., Navidi, A., Naylor, J., Negash, T., Nguyen, T., Nguyen, N., Nicol, R., Norbu, C., Norbu, N., Novod, N., O'Neill, B., Osman, S., Markiewicz, E., Oyono, O.L., Patti, C., Phunkhang, P., Pierre, F., Priest, M., Raghuraman, S., Rege, F., Reyes, R., Rise, C., Rogov, P., Ross, K., Ryan, E., Settipalli, S., Shea, T., Sherpa, N., Shi, L., Shih, D., Sparrow, T., Spaulding, J., Stalker, J., Stange-Thomann, N., Stavropoulos, S., Stone, C., Strader, C., Tesfaye, S., Thomson, T., Thoulutsang, Y., Thoulutsang, D., Topham, K., Topping, I., Tsamla, T., Vassiliev, H., Vo, A., Wangchuk, T., Wangdi, T., Weiand, M., Wilkinson, J., Wilson, A., Yadav, S., Young, G., Yu, Q., Zembek, L., Zhong, D., Zimmer, A., Zwirko, Z., Alvarez, P., Brockman, W., Butler, J., Chin, C., Grabherr, M., Kleber, M., Mauceli, E., MacCallum, I., 2007. Evolution of genes and genomes on the *Drosophila* phylogeny. Nature 450, 203-218.

Claudianos, C., Ranson, H., Johnson, R.M., Biswas, S., Schuler, M.A., Berenbaum, M.R., Feyereisen, R., Oakeshott, J.G., 2006. A deficit of detoxification enzymes: pesticide sensitivity and environmental response in the honeybee. Insect Mol Biol 15, 615-636.

Cohen, M.B., Schuler, M.A., Berenbaum, M.R., 1992. A host-inducible cytochrome P-450 from a host-specific caterpillar: molecular cloning and evolution. Proc Natl Acad Sci U S A 89, 10920-10924.

Cui, F., Lin, Z., Wang, H., Liu, S., Chang, H., Reeck, G., Qiao, C., Raymond, M., Kang, L., 2011. Two single mutations commonly cause qualitative change of nonspecific carboxylesterases in insects. Insect Biochem Mol Biol 41, 1-8.

Cui, G., Sun, R., Veeran, S., Shu, B., Yuan, H., Zhong, G., 2020. Combined transcriptomic and proteomic analysis of harmine on *Spodoptera frugiperda* Sf9 cells to reveal the potential resistance mechanism. J Proteomics 211, 103573.

Daimon, T., Shinoda, T., 2013. Function, diversity, and application of insect juvenile hormone epoxidases (CYP15). Biotechnol Appl Biochem 60, 82-91.

Dary, O., Georghiou, G.P., Parsons, E., Pasteur, N., 1990. Microplate adaptation of Gomori's assay for quantitative determination of general esterase activity in single insects. J Econ Entomol 83, 2187-2192.

Day, R., Abrahams, P., Bateman, M., Beale, T., Clottey, V., Cock, M., Colmenarez, Y., Corniani, N., Early, R., Godwin, J., 2017. Fall armyworm: impacts and implications for Africa. Outlooks on Pest Management 28, 196-201.

De Groote, H., Kimenju, S.C., Munyua, B., Palmas, S., Kassie, M., Bruce, A., 2020. Spread and impact of fall armyworm (*Spodoptera frugiperda* J.E. Smith) in maize production areas of Kenya. Agric Ecosyst Environ 292, 106804.

Denecke, S., Rankic, I., Driva, O., Kalsi, M., Luong, N.B.H., Buer, B., Nauen, R., Geibel, S., Vontas, J., 2021. Comparative and functional genomics of the ABC transporter superfamily across arthropods. BMC Genomics 22, 553.

Deng, H., 2014. Multiple roles of Nrf2-Keap1 signaling: regulation of development and xenobiotic response using distinct mechanisms. Fly (Austin) 8, 7-12.

Deng, H., Huang, Y., Feng, Q., Zheng, S., 2009. Two epsilon glutathione S-transferase cDNAs from the common cutworm, *Spodoptera litura*: characterization and developmental and induced expression by insecticides. J Insect Physiol 55, 1174-1183.

Deng, H., Kerppola, T.K., 2013. Regulation of *Drosophila* metamorphosis by xenobiotic response regulators. PLoS Genet 9, e1003263.

Deng, H., Kerppola, T.K., 2014. Visualization of the *Drosophila* dKeap1-CncC interaction on chromatin illumines cooperative, xenobiotic-specific gene activation. Development 141, 3277-3288.
Dermauw, W., Pym, A., Bass, C., Van Leeuwen, T., Feyereisen, R., 2018. Does host plant adaptation lead to pesticide resistance in generalist herbivores? Curr Opin Insect Sci 26, 25-33.
Dermauw, W., Van Leeuwen, T., 2014. The ABC gene family in arthropods: Comparative genomics and role in insecticide transport and resistance. Insect Biochem Mol Biol 45C, 89-110.
Dermauw, W., Van Leeuwen, T., Feyereisen, R., 2020. Diversity and evolution of the P450 family in arthropods. Insect Biochem Mol Biol 127, 103490.
Dermauw, W., Wybouw, N., Rombauts, S., Menten, B., Vontas, J., Grbic, M., Clark, R.M., Feyereisen, R., Van Leeuwen, T., 2013. A link between host plant adaptation and pesticide resistance in the polyphagous spider mite *Tetranychus urticae*. Proc Natl Acad Sci U S A 110, E113-122.
Despres, L., David, J.P., Gallet, C., 2007. The evolutionary ecology of insect resistance to plant chemicals. Trends Ecol Evol 22, 298-307.
Dobin, A., Davis, C.A., Schlesinger, F., Drenkow, J., Zaleski, C., Jha, S., Batut, P., Chaisson, M., Gingeras, T.R., 2013. STAR: ultrafast universal RNA-seq aligner. Bioinformatics 29, 15-21.
Durand, N., Carot-Sans, G., Chertemps, T., Bozzolan, F., Party, V., Renou, M., Debernard, S., Rosell, G., Maibeche-Coisne, M., 2010. Characterization of an antennal carboxylesterase from the pest moth *Spodoptera littoralis* degrading a host plant odorant. PLoS One 5, e15026.
Durand, N., Chertemps, T., Maibeche-Coisne, M., 2012. Antennal carboxylesterases in a moth, structural and functional diversity. Commun Integr Biol 5, 284-286.
Ebbinghaus-Kintscher, U., Lummen, P., Raming, K., Masaki, T., Yasokawa, N., 2007. Phthalic acid diamides activate ryanodine-sensitive Ca2+ release channels in insects. Cell Calcium 39, 21–33.
Elliott, M., Janes, N.F., Potter, C., 1978. The Future of Pyrethroids in Insect Control. Annual review of entomology 2, 443–469.
Enayati, A.A., Ranson, H., Hemingway, J., 2005. Insect glutathione transferases and insecticide resistance. Insect Mol Biol 14, 3-8.
Epis, S., Porretta, D., Mastrantonio, V., Comandatore, F., Sassera, D., Rossi, P., Cafarchia, C., Otranto, D., Favia, G., Genchi, C., Bandi, C., Urbanelli, S., 2014. ABC transporters are involved in defense against permethrin insecticide in the malaria vector Anopheles stephensi. Parasit Vectors 7, 349.
FAO, 2021. Prevention, preparedness and response guidelines for Spodoptera frugiperda., in: Secretariat, I. (Ed.), Rome, Italy.
Fatoretto, J.C., Michel, A.P., Silva Filho, M.C., Silva, N., 2017. Adaptive potential of fall armyworm (Lepidoptera: Noctuidae) limits Bt trait durability in Brazil. Journal of Integrated Pest Management 8, 17.
Fautrel, A., Chesne, C., Guillouzo, A., de Sousa, G., Placidi, M., Rahmani, R., Braut, F., Pichon, J., Hoellinger, H., Vintezou, P., Diarte, I., Melcion, C., Cordier, A., Lorenzon, G., Benicourt, M., Vannier, B., Fournex, R., Peloux, A.F., Bichet, N., Gouy, D., Cano, J.P., Lounes, R., 1991. A multicentre study of acute in vitro cytotoxicity in rat liver cells. Toxicol In Vitro 5, 543-547.
Ferkovich, S.M., Oliver, J.E., Dillard, C., 1982. Pheromone hydrolysis by cuticular and interior esterases of the antennae, legs, and wings of the cabbage looper moth, *Trichoplusia ni* (Hubner). J Chem Ecol 8, 859-866.
Ferry, N., Edwards, M.G., Gatehouse, J.A., Gatehouse, A.M., 2004. Plant-insect interactions: molecular approaches to insect resistance. Curr Opin Biotechnol 15, 155-161.
Feyereisen, R., 1995. Molecular biology of insecticide resistance. Toxicol Lett 82-83, 83-90.
Feyereisen, R., 2005. Evolution of insect P450. Biochem Soc Trans 34, 1252-1255.
Feyereisen, R., 2011. Arthropod CYPomes illustrate the tempo and mode in P450 evolution. Biochim Biophys Acta 1814, 19-28.
Feyereisen, R., 2012. Insect CYP Genes and P450 enzymes, in: Gilbert, L.I. (Ed.), Insect Molecular Biology and Biochemistry. Elsevier, London, pp. 236-316.

Feyereisen, R., 2020. Origin and evolution of the CYP4G subfamily in insects, cytochrome P450 enzymes involved in cuticular hydrocarbon synthesis. Mol Phylogenet Evol 143, 106695.
Feyereisen, R., Dermauw, W., Van Leeuwen, T., 2015. Genotype to phenotype, the molecular and physiological dimensions of resistance in arthropods. Pestic Biochem Physiol 121, 61-77.
Fournier, D., Mutero, A., Pralavorio, M., Bride, J.M., 1993. Drosophila acetylcholinesterase: mechanisms of resistance to organophosphates. Chem Biol Interact 87, 233-238.
Fuentes, F., Paredes-Gonzalez, X., Kong, A.N., 2015. Dietary Glucosinolates Sulforaphane, Phenethyl Isothiocyanate, Indole-3-Carbinol/3,3'-Diindolylmethane: Anti-Oxidative Stress/Inflammation, Nrf2, Epigenetics/Epigenomics and In Vivo Cancer Chemopreventive Efficacy. Curr Pharmacol Rep 1, 179-196.
Gaddelapati, S.C., Kalsi, M., Roy, A., Palli, S.R., 2018. Cap 'n' collar C regulates genes responsible for imidacloprid resistance in the Colorado potato beetle, *Leptinotarsa decemlineata*. Insect Biochem Mol Biol 99, 54-62.
Giandomenico, A.R., Cerniglia, G.E., Biaglow, J.E., Stevens, C.W., Koch, C.J., 1997. The importance of sodium pyruvate in assessing damage produced by hydrogen peroxide. Free Radic Biol Med 23, 426-434.
Gimenez, S., Abdelgaffar, H., Goff, G.L., Hilliou, F., Blanco, C.A., Hanniger, S., Bretaudeau, A., Legeai, F., Negre, N., Jurat-Fuentes, J.L., d'Alencon, E., Nam, K., 2020a. Adaptation by copy number variation increases insecticide resistance in the fall armyworm. Commun Biol 3, 664.
Gimenez, S., Abdelgaffar, H., Le Goff, G., Hilliou, F., Blanco, C.A., Hanniger, S., Bretaudeau, A., Legeai, F., Negre, N., Jurat-Fuentes, J.L., d'Alencon, E., Nam, K., 2020b. Adaptation by copy number variation increases insecticide resistance in the fall armyworm. Commun Biol 3, 664.
Giraudo, M., Audant, P., Feyereisen, R., Le Goff, G., 2013. Nuclear receptors HR96 and ultraspiracle from the fall armyworm (*Spodoptera frugiperda*), developmental expression and induction by xenobiotics. J Insect Physiol 59, 560-568.
Giraudo, M., Califano, J., Hilliou, F., Tran, T., Taquet, N., Feyereisen, R., Le Goff, G., 2011. Effects of hormone agonists on Sf9 cells, proliferation and cell cycle arrest. PLoS One 6, e25708.
Giraudo, M., Hilliou, F., Fricaux, T., Audant, P., Feyereisen, R., Le Goff, G., 2015. Cytochrome P450s from the fall armyworm (*Spodoptera frugiperda*): responses to plant allelochemicals and pesticides. Insect Mol Biol 24, 115-128.
Glauser, G., Marti, G., Villard, N., Doyen, G.A., Wolfender, J.L., Turlings, T.C., Erb, M., 2011. Induction and detoxification of maize 1,4-benzoxazin-3-ones by insect herbivores. Plant J 68, 901-911.
Goergen, G., Kumar, P.L., Sankung, S.B., Togola, A., Tamo, M., 2016. First Report of Outbreaks of the Fall Armyworm *Spodoptera frugiperda* (J E Smith) (Lepidoptera, Noctuidae), a New Alien Invasive Pest in West and Central Africa. PLoS One 11, e0165632.
Gordon, H., 1961. Nutritional factors in insect resistance to chemicals. Annual review of entomology 6, 27-54.
Gouin, A., Bretaudeau, A., Nam, K., Gimenez, S., Aury, J.M., Duvic, B., Hilliou, F., Durand, N., Montagne, N., Darboux, I., Kuwar, S., Chertemps, T., Siaussat, D., Bretschneider, A., Mone, Y., Ahn, S.J., Hanniger, S., Grenet, A.G., Neunemann, D., Maumus, F., Luyten, I., Labadie, K., Xu, W., Koutroumpa, F., Escoubas, J.M., Llopis, A., Maibeche-Coisne, M., Salasc, F., Tomar, A., Anderson, A.R., Khan, S.A., Dumas, P., Orsucci, M., Guy, J., Belser, C., Alberti, A., Noel, B., Couloux, A., Mercier, J., Nidelet, S., Dubois, E., Liu, N.Y., Boulogne, I., Mirabeau, O., Le Goff, G., Gordon, K., Oakeshott, J., Consoli, F.L., Volkoff, A.N., Fescemyer, H.W., Marden, J.H., Luthe, D.S., Herrero, S., Heckel, D.G., Wincker, P., Kergoat, G.J., Amselem, J., Quesneville, H., Groot, A.T., Jacquin-Joly, E., Negre, N., Lemaitre, C., Legeai, F., d'Alencon, E., Fournier, P., 2017. Two genomes of highly polyphagous lepidopteran pests (*Spodoptera frugiperda*, Noctuidae) with different host-plant ranges. Sci Rep 7, 11816.
Grbić, M., Van Leeuwen, T., Clark, R.M., Rombauts, S., Rouze, P., Grbic, V., Osborne, E.J., Dermauw, W., Ngoc, P.C., Ortego, F., Hernandez-Crespo, P., Diaz, I., Martinez, M., Navajas, M., Sucena, E., Magalhaes, S., Nagy, L., Pace, R.M., Djuranovic, S., Smagghe, G., Iga, M., Christiaens, O., Veenstra, J.A., Ewer, J., Villalobos, R.M., Hutter, J.L., Hudson, S.D., Velez, M., Yi, S.V., Zeng, J.,

Pires-daSilva, A., Roch, F., Cazaux, M., Navarro, M., Zhurov, V., Acevedo, G., Bjelica, A., Fawcett, J.A., Bonnet, E., Martens, C., Baele, G., Wissler, L., Sanchez-Rodriguez, A., Tirry, L., Blais, C., Demeestere, K., Henz, S.R., Gregory, T.R., Mathieu, J., Verdon, L., Farinelli, L., Schmutz, J., Lindquist, E., Feyereisen, R., Van de Peer, Y., 2011. The genome of *Tetranychus urticae* reveals herbivorous pest adaptations. Nature 479, 487-492.

Groot, A.T., Marr, M., Heckel, D.G., Schöfl, G., 2010. The roles and interactions of reproductive isolation mechanisms in fall armyworm (Lepidoptera: Noctuidae) host strains. Ecological Entomology 35, 105-118.

Gunning, R.V., Moores, G.D., 2001. Insensitive acetylcholinesterase as sites for resistance to organophosphates and carbamates in insects: insensitive acetylcholinesterase confers resistance in Lepidoptera, Biochemical Sites of Insecticide Action and Resistance. Springer, pp. 221-238.

Guo, Y., Zhang, X., Wu, H., Yu, R., Zhang, J., Zhu, K.Y., Guo, Y., Ma, E., 2015. Identification and functional analysis of a cytochrome P450 gene CYP9AQ2 involved in deltamethrin detoxification from *Locusta migratoria*. Pestic Biochem Physiol 122, 1-7.

Guo, Z., Qin, J., Zhou, X., Zhang, Y., 2018. Insect Transcription Factors: A Landscape of Their Structures and Biological Functions in Drosophila and beyond. Int J Mol Sci 19.

Gutierrez-Moreno, R., Mota-Sanchez, D., Blanco, C.A., Whalon, M.E., Teran-Santofimio, H., Rodriguez-Maciel, J.C., DiFonzo, C., 2019. Field-Evolved Resistance of the Fall Armyworm (Lepidoptera: Noctuidae) to Synthetic Insecticides in Puerto Rico and Mexico. J Econ Entomol 112, 792-802.

Ha, E.M., Oh, C.T., Bae, Y.S., Lee, W.J., 2005. A direct role for dual oxidase in Drosophila gut immunity. Science 310, 847-850.

Haas, J., Zaworra, M., Glaubitz, J., Hertlein, G., Kohler, M., Lagojda, A., Lueke, B., Maus, C., Almanza, M.T., Davies, T.G.E., Bass, C., Nauen, R., 2021. A toxicogenomics approach reveals characteristics supporting the honey bee (*Apis mellifera* L.) safety profile of the butenolide insecticide flupyradifurone. Ecotoxicol Environ Saf 217, 112247.

Habig, W.H., Pabst, M.J., Jakoby, W.B., 1974. Glutathione S-transferases. The first enzymatic step in mercapturic acid formation. J Biol Chem 249, 7130-7139.

Hafeez, M., Liu, S., Jan, S., Shi, L., Fernandez-Grandon, G.M., Gulzar, A., Ali, B., Rehman, M., Wang, M., 2019a. Knock-Down of Gossypol-Inducing Cytochrome P450 Genes Reduced Deltamethrin Sensitivity in *Spodoptera exigua* (Hubner). Int J Mol Sci 20.

Hafeez, M., Liu, S., Yousaf, H.K., Jan, S., Wang, R.L., Fernandez-Grandon, G.M., Li, X., Gulzar, A., Ali, B., Rehman, M., Ali, S., Fahad, M., Lu, Y., Wang, M., 2019b. RNA interference-mediated knockdown of a cytochrome P450 gene enhanced the toxicity of alpha-cypermethrin in xanthotoxin-fed larvae of *Spodoptera exigua* (Hubner). Pestic Biochem Physiol 162, 6-14.

Hafeez, M., Qasim, M., Ali, S., Yousaf, H.K., Waqas, M., Ali, E., Ahmad, M.A., Jan, S., Bashir, M.A., Noman, A., Wang, M., Gharmh, H.A., Khan, K.A., 2020. Expression and functional analysis of P450 gene induced tolerance/resistance to lambda-cyhalothrin in quercetin fed larvae of beet armyworm *Spodoptera exigua* (Hubner). Saudi J Biol Sci 27, 77-87.

Hajra, S., Patra, A.R., Basu, A., Bhattacharya, S., 2018. Prevention of doxorubicin (DOX)-induced genotoxicity and cardiotoxicity: Effect of plant derived small molecule indole-3-carbinol (I3C) on oxidative stress and inflammation. Biomed Pharmacother 101, 228-243.

Hankinson, O., 1995. The aryl hydrocarbon receptor complex. Annu Rev Pharmacol Toxicol 35, 307-340.

Harari, O.A., Santos-Garcia, D., Musseri, M., Moshitzky, P., Patel, M., Visendi, P., Seal, S., Sertchook, R., Malka, O., Morin, S., 2020. Molecular Evolution of the Glutathione S-Transferase Family in the *Bemisia tabaci* Species Complex. Genome Biol Evol 12, 3857-3872.

Hardke, J.T., Jackson, R.E., Leonard, B.R., Temple, J.H., 2015. Fall Armyworm (Lepidoptera: Noctuidae) Development, Survivorship, and Damage on Cotton Plants Expressing Insecticidal Plant-Incorporated Protectants. J Econ Entomol 108, 1086-1093.

He, C., Liang, J., Liu, S., Wang, S., Wu, Q., Xie, W., Zhang, Y., 2019a. Changes in the expression of four ABC transporter genes in response to imidacloprid in *Bemisia tabaci* Q (Hemiptera: Aleyrodidae). Pestic Biochem Physiol 153, 136-143.

He, P., Li, Z.Q., Liu, C.C., Liu, S.J., Dong, S.L., 2014. Two esterases from the genus *Spodoptera* degrade sex pheromones and plant volatiles. Genome 57, 201-208.

He, P., Mang, D.Z., Wang, H., Wang, M.M., Ma, Y.F., Wang, J., Chen, G.L., Zhang, F., He, M., 2020. Molecular characterization and functional analysis of a novel candidate of cuticle carboxylesterase in *Spodoptera exigua* degradating sex pheromones and plant volatile esters. Pestic Biochem Physiol 163, 227-234.

He, Q., Yan, Z., Si, F., Zhou, Y., Fu, W., Chen, B., 2019b. ATP-Binding Cassette (ABC) Transporter Genes Involved in Pyrethroid Resistance in the Malaria Vector *Anopheles sinensis*: Genome-Wide Identification, Characteristics, Phylogenetics, and Expression Profile. Int J Mol Sci 20.

Heckel, D., 2012. Learning the ABCs of Bt: ABC transporters and insect resistance to *Bacillus thuringiensis* provide clues to a crucial step in toxin mode of action. Pesticide Biochemistry and Physiology 104.

Heckel, D.G., 2014. Insect detoxification and sequestration strategies. Annual Plant Reviews, 77-114.

Heidel-Fischer, H.M., Vogel, H., 2015. Molecular mechanisms of insect adaptation to plant secondary compounds. Curr Opin Insect Sci 8, 8-14.

Helvig, C., Koener, J.F., Unnithan, G.C., Feyereisen, R., 2004. CYP15A1, the cytochrome P450 that catalyzes epoxidation of methyl farnesoate to juvenile hormone III in cockroach corpora allata. Proc Natl Acad Sci U S A 101, 4024-4029.

Higgins, L.G., Hayes, J.D., 2011. Mechanisms of induction of cytosolic and microsomal glutathione transferase (GST) genes by xenobiotics and pro-inflammatory agents. Drug Metab Rev 43, 92-137.

Hilliou, F., Chertemps, T., Maibeche, M., Le Goff, G., 2021. Resistance in the Genus Spodoptera: Key Insect Detoxification Genes. Insects 12.

Hirotsu, Y., Katsuoka, F., Funayama, R., Nagashima, T., Nishida, Y., Nakayama, K., Engel, J.D., Yamamoto, M., 2012. Nrf2-MafG heterodimers contribute globally to antioxidant and metabolic networks. Nucleic Acids Res 40, 10228-10239.

Hopkins, T.L., Kramer, K.J., 1992. Insect cuticle sclerotization. Annual review of entomology 37, 273-302.

Hou, W.T., Staehelin, C., Elzaki, M.E.A., Hafeez, M., Luo, Y.S., Wang, R.L., 2021. Functional analysis of CYP6AE68, a cytochrome P450 gene associated with indoxacarb resistance in *Spodoptera litura* (Lepidoptera: Noctuidae). Pestic Biochem Physiol 178, 104946.

Hsiau, T., Maures, T., Waite, K., Yang, J., Kelso, R., Holden, K., Stoner, R., 2018. Inference of CRISPR edits from Sanger trace data. BioRxiv 251082.

Hu, B., Hu, S., Huang, H., Wei, Q., Ren, M., Huang, S., Tian, X., Su, J., 2019a. Insecticides induce the co-expression of glutathione S-transferases through ROS/CncC pathway in *Spodoptera exigua*. Pestic Biochem Physiol 155, 58-71.

Hu, B., Huang, H., Hu, S., Ren, M., Wei, Q., Tian, X., Esmail Abdalla Elzaki, M., Bass, C., Su, J., Reddy Palli, S., 2021. Changes in both trans- and cis-regulatory elements mediate insecticide resistance in a lepidopteron pest, *Spodoptera exigua*. PLoS Genet 17, e1009403.

Hu, B., Huang, H., Wei, Q., Ren, M., Mburu, D.K., Tian, X., Su, J., 2019b. Transcription factors CncC/Maf and AhR/ARNT coordinately regulate the expression of multiple GSTs conferring resistance to chlorpyrifos and cypermethrin in *Spodoptera exigua*. Pest Manag Sci 75, 2009-2019.

Hu, B., Miaomiao, R., Jianfeng, F., Sufang, H., Xia, W., Elzaki, M.E.A., Chris, B., Palli, S.R., Jianya, S., 2020a. Xenobiotic transcription factors CncC and maf regulate expression of CYP321A16 and CYP332A1 that mediate chlorpyrifos resistance in *Spodoptera exigua*. J Hazard Mater 398, 122971.

Hu, B., Ren, M., Fan, J., Huang, S., Wang, X., Elzaki, M.E.A., Bass, C., Palli, S.R., Su, C., 2020b. Xenobiotic transcription factors CncC and maf regulate expression of CYP321A16 and CYP332A1 that mediate chlorpyrifos resistance in *Spodoptera exigua*. J Hazard Mater 398, 122971.

Hu, B., Zhang, S.H., Ren, M.M., Tian, X.R., Wei, Q., Mburu, D.K., Su, J.Y., 2019c. The expression of *Spodoptera exigua* P450 and UGT genes: tissue specificity and response to insecticides. Insect Sci 26, 199-216.

Hu, J., Chen, J., Wang, H., Mao, T., Li, J., Cheng, X., Hu, J., Xue, B., Li, B., 2018. Cloning and Functional Analysis of CncC and Keap1 Genes in Silkworm. J Agric Food Chem 66, 2630-2636.

Huang, Y., Wang, Y., Zeng, B., Liu, Z., Xu, X., Meng, Q., Huang, Y., Yang, G., Vasseur, L., Gurr, G.M., You, M., 2017. Functional characterization of Pol III U6 promoters for gene knockdown and knockout in Plutella xylostella. Insect Biochem Mol Biol 89, 71-78.

Huang, Y., Xu, Z., Lin, X., Feng, Q., Zheng, S., 2011. Structure and expression of glutathione S-transferase genes from the midgut of the Common cutworm, *Spodoptera litura* (Noctuidae) and their response to xenobiotic compounds and bacteria. J Insect Physiol 57, 1033-1044.

Hung, C.F., Harrison, T.L., Berenbaum, M.R., Schuler, M.A., 1995. CYP6B3: a second furanocoumarin-inducible cytochrome P450 expressed in *Papilio polyxenes*. Insect Mol Biol 4, 149-160.

Hung, C.F., Holzmacher, R., Connolly, E., Berenbaum, M.R., Schuler, M.A., 1996. Conserved promoter elements in the CYP6B gene family suggest common ancestry for cytochrome P450 monooxygenases mediating furanocoumarin detoxification. Proc Natl Acad Sci U S A 93, 12200-12205.

Ingham, V.A., Anthousi, A., Douris, V., Harding, N.J., Lycett, G., Morris, M., Vontas, J., Ranson, H., 2020. A sensory appendage protein protects malaria vectors from pyrethroids. Nature 577, 376-380.

Ingham, V.A., Pignatelli, P., Moore, J.D., Wagstaff, S., Ranson, H., 2017. The transcription factor Maf-S regulates metabolic resistance to insecticides in the malaria vector *Anopheles gambiae*. BMC Genomics 18, 669.

Israni, B., Wouters, F.C., Luck, K., Seibel, E., Ahn, S.J., Paetz, C., Reinert, M., Vogel, H., Erb, M., Heckel, D.G., Gershenzon, J., Vassao, D.G., 2020. The Fall Armyworm *Spodoptera frugiperda* Utilizes Specific UDP-Glycosyltransferases to Inactivate Maize Defensive Benzoxazinoids. Front Physiol 11, 604754.

Itoh, K., Chiba, T., Takahashi, S., Ishii, T., Igarashi, K., Katoh, Y., Oyake, T., Hayashi, N., Satoh, K., Hatayama, I., Yamamoto, M., Nabeshima, Y., 1997. An Nrf2/small Maf heterodimer mediates the induction of phase II detoxifying enzyme genes through antioxidant response elements. Biochem Biophys Res Commun 236, 313-322.

Jagtap, J.C., Chandele, A., Chopde, B.A., Shastry, P., 2003. Sodium pyruvate protects against H(2)O(2) mediated apoptosis in human neuroblastoma cell line-SK-N-MC. J Chem Neuroanat 26, 109-118.

Jakka, S.R., Knight, V.R., Jurat-Fuentes, J.L., 2014. Fitness costs associated with field-evolved resistance to Bt maize in Spodoptera frugiperda (Lepidoptera: Noctuidae). J Econ Entomol 107, 342-351.

Jarvis, D.L., 2009. Baculovirus-insect cell expression systems. Methods Enzymol 463, 191-222.

Jarvis, D.L., Weinkauf, C., Guarino, L.A., 1996. Immediate-early baculovirus vectors for foreign gene expression in transformed or infected insect cells. Protein Expr Purif 8, 191-203.

Jia, Z.Q., Liu, D., Peng, Y.C., Han, Z.J., Zhao, C.Q., Tang, T., 2020. Identification of transcriptome and fluralaner responsive genes in the common cutworm *Spodoptera litura* Fabricius, based on RNA-seq. BMC Genomics 21, 120.

Jin, M., Liao, C., Chakrabarty, S., Zheng, W., Wu, K., Xiao, Y., 2019. Transcriptional response of ATP-binding cassette (ABC) transporters to insecticides in the cotton bollworm, *Helicoverpa armigera*. Pestic Biochem Physiol 154, 46-59.

Jing, W.A.N., Huang, C., Li, C.Y., Zhou, H.X., Ren, Y.L., Li, Z.Y., Xing, L.-S., Zhang, B., Qiao, X., Liu, B., Liu, C.-H., Xi, Y., Liu, W.-X., Wang, W.-K., Qian, W.-Q., McKirdy, S., Wan, F.H., 2021. Biology, invasion and management of the agricultural invader: Fall armyworm, *Spodoptera frugiperda* (Lepidoptera: Noctuidae). Journal of Integrative Agriculture 20, 646-663.

Jurat-Fuentes, J.L., Heckel, D.G., Ferré, J., 2021. Mechanisms of Resistance to Insecticidal Proteins from *Bacillus thuringiencis*. Annu Rev Entomol 66, 121-140.

Kalleshwaraswamy, C., Asokan, R., Swamy, H.M., Maruthi, M., Pavithra, H., Hegbe, K., Navi, S., Prabhu, S., Goergen, G.E., 2018. First report of the fall armyworm, Spodoptera frugiperda (JE Smith)(Lepidoptera: Noctuidae), an alien invasive pest on maize in India.

Kalsi, M., Palli, S.R., 2015. Transcription factors, CncC and Maf, regulate expression of CYP6BQ genes responsible for deltamethrin resistance in *Tribolium castaneum*. Insect Biochem Mol Biol 65, 47-56.

Kalsi, M., Palli, S.R., 2017a. Cap n collar transcription factor regulates multiple genes coding for proteins involved in insecticide detoxification in the red flour beetle, *Tribolium castaneum*. Insect Biochem Mol Biol 90, 43-52.

Kalsi, M., Palli, S.R., 2017b. Transcription factor cap n collar C regulates multiple cytochrome P450 genes conferring adaptation to potato plant allelochemicals and resistance to imidacloprid in *Leptinotarsa decemlineata* (Say). Insect Biochem Mol Biol 83, 1-12.

Kefi, M., Balabanidou, V., Douris, V., Lycett, G., Feyereisen, R., Vontas, J., 2019. Two functionally distinct CYP4G genes of *Anopheles gambiae* contribute to cuticular hydrocarbon biosynthesis. Insect Biochem Mol Biol 110, 52-59.

Kensler, T.W., Wakabayashi, N., Biswal, S., 2007. Cell survival responses to environmental stresses via the Keap1-Nrf2-ARE pathway. Annu Rev Pharmacol Toxicol 47, 89-116.

Kost, S., Heckel, D.G., Yoshido, A., Marec, F., Groot, A.T., 2016. A Z-linked sterility locus causes sexual abstinence in hybrid females and facilitates speciation in *Spodoptera frugiperda*. Evolution 70, 1418-1427.

Kost, T.A., Condreay, J.P., Jarvis, D.L., 2005. Baculovirus as versatile vectors for protein expression in insect and mammalian cells. Nat Biotechnol 23, 567-575.

Krempl, C., Heidel-Fischer, H.M., Jimenez-Aleman, G.H., Reichelt, M., Menezes, R.C., Boland, W., Vogel, H., Heckel, D.G., Joussen, N., 2016a. Gossypol toxicity and detoxification in *Helicoverpa armigera* and *Heliothis virescens*. Insect Biochem Mol Biol 78, 69-77.

Krempl, C., Sporer, T., Reichelt, M., Ahn, S.J., Heidel-Fischer, H., Vogel, H., Heckel, D.G., Joussen, N., 2016b. Potential detoxification of gossypol by UDP-glycosyltransferases in the two Heliothine moth species *Helicoverpa armigera* and *Heliothis virescens*. Insect Biochem Mol Biol 71, 49-57.

Lafont, R., Dauphin-Villemant, C., Warren, J.T., Rees, H., 2012. Ecdysteroid chemistry and biochemistry, Insect Endocrinology. Academic Press, pp. 106-176.

Lahm, G.P., Selby, T.P., Freudenberger, J.H., Stevenson, T.M., Myers, B.J., Seburyamo, G., Smith, B.K., Flexner, L., Clark, C.E., Cordova, D., 2005. Insecticidal anthranilic diamides: a new class of potent ryanodine receptor activators. Bioorg Med Chem Lett 15, 4898-4906.

Laisney, J., Gurusamy, D., Baddar, Z.E., Palli, S.R., Unrine, J.M., 2020. RNAi in *Spodoptera frugiperda* Sf9 Cells via Nanomaterial Mediated Delivery of dsRNA: A Comparison of Poly-l-arginine Polyplexes and Poly-l-arginine-Functionalized Au Nanoparticles. ACS Appl Mater Interfaces 12, 25645-25657.

Landt, S.G., Marinov, G.K., Kundaje, A., Kheradpour, P., Pauli, F., Batzoglou, S., Bernstein, B.E., Bickel, P., Brown, J.B., Cayting, P., Chen, Y., DeSalvo, G., Epstein, C., Fisher-Aylor, K.I., Euskirchen, G., Gerstein, M., Gertz, J., Hartemink, A.J., Hoffman, M.M., Iyer, V.R., Jung, Y.L., Karmakar, S., Kellis, M., Kharchenko, P.V., Li, Q., Liu, T., Liu, X.S., Ma, L., Milosavljevic, A., Myers, R.M., Park, P.J., Pazin, M.J., Perry, M.D., Raha, D., Reddy, T.E., Rozowsky, J., Shoresh, N., Sidow, A., Slattery, M., Stamatoyannopoulos, J.A., Tolstorukov, M.Y., White, K.P., Xi, S., Farnham, P.J., Lieb, J.D., Wold, B.J., Snyder, M., 2012. ChIP-seq guidelines and practices of the ENCODE and modENCODE consortia. Genome Res 22, 1813-1831.

Le Goff, G., Hilliou, F., 2017. Resistance evolution in *Drosophila*: the case of CYP6G1. Pest Manag Sci 73, 493-499.

Le Goff, G., Hilliou, F., Siegfried, B.D., Boundy, S., Wajnberg, E., Sofer, L., Audant, P., ffrench-Constant, R.H., Feyereisen, R., 2006. Xenobiotic response in *Drosophila melanogaster*: sex dependence of P450 and GST gene induction. Insect Biochem Mol Biol 36, 674-682.

Li, Q., Sun, Z., Shi, Q., Wang, R., Xu, C., Wang, H., Song, Y., Zeng, R., 2019. RNA-Seq Analyses of Midgut and Fat Body Tissues Reveal the Molecular Mechanism Underlying *Spodoptera litura* Resistance to Tomatine. Front Physiol 10, 8.

Li, T., Cao, C., Yang, T., Zhang, L., He, L., Xi, Z., Bian, G., Liu, N., 2015. A G-protein-coupled receptor regulation pathway in cytochrome P450-mediated permethrin-resistance in mosquitoes, *Culex quinquefasciatus*. Sci Rep 5, 17772.

Li, T., Liu, L., Zhang, L., Liu, N., 2014. Role of G-protein-coupled receptor-related genes in insecticide resistance of the mosquito, *Culex quinquefasciatus*. Sci Rep 4, 6474.

Li, T., Liu, N., 2019. Role of the G-Protein-Coupled Receptor Signaling Pathway in Insecticide Resistance. Int J Mol Sci 20.

Li, W., Berenbaum, M.R., Schuler, M.A., 2001. Molecular analysis of multiple CYP6B genes from polyphagous *Papilio* species. Insect Biochem Mol Biol 31, 999-1011.

Li, W., Petersen, R.A., Schuler, M.A., Berenbaum, M.R., 2002. CYP6B cytochrome p450 monooxygenases from *Papilio canadensis* and *Papilio glaucus*: potential contributions of sequence divergence to host plant associations. Insect Mol Biol 11, 543-551.

Li, X., Schuler, M.A., Berenbaum, M.R., 2007. Molecular mechanisms of metabolic resistance to synthetic and natural xenobiotics. Annu Rev Entomol 52, 231-253.

Li, X., Zangerl, A.R., Schuler, M.A., Berenbaum, M.R., 2000. Cross-resistance to alpha-cypermethrin after xanthotoxin ingestion in *Helicoverpa zea* (Lepidoptera: Noctuidae). J Econ Entomol 93, 18-25.

Li, X.J., Wu, M.F., Ma, J., Gao, B.Y., Wu, Q.L., Chen, A.D., Liu, J., Jiang, Y.Y., Zhai, B.P., Early, R., Chapman, J.W., Hu, G., 2020a. Prediction of migratory routes of the invasive fall armyworm in eastern China using a trajectory analytical approach. Pest Manag Sci 76, 454-463.

Li, Z., Cai, T., Qin, Y., Zhang, Y., Jin, R., Mao, K., Liao, X., Wan, H., Li, J., 2020b. Transcriptional Response of ATP-Binding Cassette (ABC) Transporters to Insecticide in the Brown Planthopper, *Nilaparvata lugens* (Stal). Insects 11.

Liao, Y., Smyth, G.K., Shi, W., 2014. featureCounts: an efficient general purpose program for assigning sequence reads to genomic features. Bioinformatics 30, 923-930.

Ling, R., Yang, R., Li, P., Zhang, X., Shen, T., Li, X., Yang, Q., Sun, L., Yan, J., 2019. Asatone and Isoasatone A Against *Spodoptera litura* Fab. by Acting on Cytochrome P450 Monoxygenases and Glutathione Transferases. Molecules 24.

Liu, D., Jia, Z.Q., Peng, Y.C., Sheng, C.W., Tang, T., Xu, L., Han, Z.J., Zhao, C.Q., 2018a. Toxicity and sublethal effects of fluralaner on *Spodoptera litura* Fabricius (Lepidoptera: Noctuidae). Pestic Biochem Physiol 152, 8-16.

Liu, N., Li, M., Gong, Y., Liu, F., Li, T., 2015. Cytochrome P450s--Their expression, regulation, and role in insecticide resistance. Pestic Biochem Physiol 120, 77-81.

Liu, N., Li, T., 2017. Regulation of P450-mediated permethrin resistance in *Culex quinquefasciatus* by the GPCR/Gαs/AC/cAMP/PKA signaling cascade. Biochemistry and Biophysics Reports 12, 12 - 19.

Liu, N., Wang, Y., Li, T., Feng, X., 2021. G-Protein Coupled Receptors (GPCRs): Signaling Pathways, Characterization, and Functions in Insect Physiology and Toxicology. International Journal of Molecular Sciences 22, 5260.

Liu, S.W., Elzaki, M.E.A., Staehelin, C., Ma, Z.H., Qin, Z., Wang, R.L., 2018b. Exposure to herbicides reduces larval sensitivity to insecticides in *Spodoptera litura* (Lepidoptera: Noctuidae). Insect Sci.

Liu, S.W., Elzaki, M.E.A., Staehelin, C., Ma, Z.H., Qin, Z., Wang, R.L., 2019. Exposure to herbicides reduces larval sensitivity to insecticides in *Spodoptera litura* (Lepidoptera: Noctuidae). Insect Sci 26, 711-720.

Liu, Y., Ge, M., Zhang, T., Chen, L., Xing, Y., Liu, L., Li, F., Cheng, L., 2020. Exploring the correlation between deltamethrin stress and Keap1-Nrf2-ARE pathway from *Drosophila melanogaster* RNASeq data. Genomics 112, 1300-1308.

Liu, Z., Williamson, M.S., Lansdell, S.J., Han, Z., Denholm, I., Millar, N.S., 2006. A nicotinic acetylcholine receptor mutation (Y151S) causes reduced agonist potency to a range of neonicotinoid insecticides. J Neurochem 99, 1273-1281.

Loboda, A., Damulewicz, M., Pyza, E., Jozkowicz, A., Dulak, J., 2016. Role of Nrf2/HO-1 system in development, oxidative stress response and diseases: an evolutionarily conserved mechanism. Cell Mol Life Sci 73, 3221-3247.

Love, M.I., Huber, W., Anders, S., 2014. Moderated estimation of fold change and dispersion for RNA-seq data with DESeq2. Genome Biol 15, 550.

Lu, K., Cheng, Y., Li, W., Li, Y., Zeng, R., Song, Y., 2020. Activation of CncC pathway by ROS burst regulates cytochrome P450 CYP6AB12 responsible for λ-cyhalothrin tolerance in *Spodoptera litura*. J Hazard Mater 387, 121698.

Lu, K., Cheng, Y., Li, W., Ni, H., Chen, X., Li, Y., Tang, B., Chen, D., Zeng, R., Song, Y., 2019a. Copper-induced H_20_2 accumulation confers larval tolerance to xanthotoxin by modulating CYP6B50 expression in *Spodoptera litura*. Pestic Biochem Physiol 159, 118-126.

Lu, K., Cheng, Y., Li, Y., Li, W., Zeng, R., Song, Y., 2021a. Phytochemical Flavone Confers Broad-Spectrum Tolerance to Insecticides in *Spodoptera litura* by Activating ROS/CncC-Mediated Xenobiotic Detoxification Pathways. J Agric Food Chem 69, 7429-7445.

Lu, K., Li, W., Cheng, Y., Ni, H., Chen, X., Li, Y., Tang, B., Sun, X., Liu, T., Qin, N., Chen, D., Zeng, R., Song, Y., 2019b. Copper exposure enhances *Spodoptera litura* larval tolerance to β-cypermethrin. Pestic Biochem Physiol 160, 127-135.

Lu, K., Li, Y., Cheng, Y., Li, W., Zeng, B., Gu, C., Zeng, R., Song, Y., 2021b. Activation of the ROS/CncC and 20-Hydroxyecdysone Signaling Pathways Is Associated with Xanthotoxin-Induced Tolerance to lambda-Cyhalothrin in *Spodoptera litura*. J Agric Food Chem 69, 13425-13435.

Lu, Z., Ye, W., Feng, P., Dai, M., Bian, D., Ren, Y., Zhu, Q., Mao, T., Su, W., Li, F., Sun, H., Wei, J., Li, B., 2021c. Low concentration acetamiprid-induced oxidative stress hinders the growth and development of silkworm posterior silk glands. Pestic Biochem Physiol 174, 104824.

Luginbill, P., 1928. The fall army worm. US Department of Agriculture.

Ma, J., Wang, Y.-P., Wu, M.-F., Gao, B.-Y., Liu, J., Lee, G.-S., Otuka, A., Hu, G., 2019. High risk of the Fall Armyworm invading into Japan and the Korean Peninsula via overseas migration. bioRxiv, 662387.

Ma, R., Cohen, M.B., Berenbaum, M.R., Schuler, M.A., 1994. Black swallowtail (*Papilio polyxenes*) alleles encode cytochrome P450s that selectively metabolize linear furanocoumarins. Arch Biochem Biophys 310, 332-340.

Maag, D., Dalvit, C., Thevenet, D., Kohler, A., Wouters, F.C., Vassao, D.G., Gershenzon, J., Wolfender, J.L., Turlings, T.C., Erb, M., Glauser, G., 2014. 3-beta-D-Glucopyranosyl-6-methoxy-2-benzoxazolinone (MBOA-N-Glc) is an insect detoxification product of maize 1,4-benzoxazin-3-ones. Phytochemistry 102, 97-105.

Mabashi-Asazuma, H., Jarvis, D.L., 2017. CRISPR-Cas9 vectors for genome editing and host engineering in the baculovirus-insect cell system. Proc Natl Acad Sci U S A 114, 9068-9073.

Mackenzie, P.I., Owens, I.S., Burchell, B., Bock, K.W., Bairoch, A., Bélanger, A., Fournel-Gigleux, S., Green, M., Hum, D.W., Iyanagi, T., Lancet, D., Louisot, P., Magdalou, J., Chowdhury, J.R., Ritter, J.K., Schachter, H., Tephly, T.R., Tipton, K.F., Nebert, D.W., 1997. The UDP glycosyltransferase gene superfamily: recommended nomenclature update based on evolutionary divergence. Pharmacogenetics 7, 255-269.

Manjon, C., Troczka, B.J., Zaworra, M., Beadle, K., Randall, E., Hertlein, G., Singh, K.S., Zimmer, C.T., Homem, R.A., Lueke, B., Reid, R., Kor, L., Kohler, M., Benting, J., Williamson, M.S., Davies, T.G.E., Field, L.M., Bass, C., Nauen, R., 2018. Unravelling the Molecular Determinants of Bee Sensitivity to Neonicotinoid Insecticides. Curr Biol 28, 1137-1143 e1135.

Mansuy, D., 1998. The great diversity of reactions catalyzed by cytochromes P450. Comp Biochem Physiol C Pharmacol Toxicol Endocrinol 121, 5-14.

Mao, T., Cheng, X., Fang, Y., Li, M., Lu, Z., Qu, J., Chen, J., Wang, H., Li, F., Li, B., 2020. Induction of ER stress, antioxidant and detoxification response by sublethal doses of chlorantraniliprole in the silk gland of silkworm, *Bombyx mori*. Pestic Biochem Physiol 170, 104685.

Mao, T., Li, F., Fang, Y., Wang, H., Chen, J., Li, M., Lu, Z., Qu, J., Li, J., Hu, J., Cheng, X., Ni, M., Li, B., 2019. Effects of chlorantraniliprole exposure on detoxification enzyme activities and detoxification-related gene expression in the fat body of the silkworm, *Bombyx mori*. Ecotoxicol Environ Saf 176, 58-63.

Marenco, R.J., Foster, R.E., Sanchez, C.A., 1992. Sweet corn response to fall armyworm (Lepidoptera: Noctuidae) damage during vegetative growth. Journal of Economic Entomology 85, 1285-1292.

Marini, F., Binder, H., 2019. pcaExplorer: an R/Bioconductor package for interacting with RNA-seq principal components. BMC Bioinformatics 20, 331.

Masaki, T., Yasokawa, N., Tohnishi, M., Nishimatsu, T., Tsubata, K., Inoue, K., Motoba, K., Hirooka, T., 2006. Flubendiamide, a novel Ca2+ channel modulator, reveals evidence for functional cooperation between Ca2+ pumps and Ca2+ release. Mol Pharmacol 69, 1733-1739.

McDonnell, C.M., Brown, R.P., Berenbaum, M.R., Schuler, M.A., 2004. Conserved regulatory elements in the promoters of two allelochemical-inducible cytochrome P450 genes differentially regulate transcription. Insect Biochem Mol Biol 34, 1129-1139.

McKenzie, J.A., Batterham, P., 1994. The genetic, molecular and phenotypic consequences of selection for insecticide resistance. Trends in Ecology & Evolution 9, 166-169.

Meng, X., Yang, X., Wu, Z., Shen, Q., Miao, L., Zheng, Y., Qian, K., Wang, J., 2020. Identification and transcriptional response of ATP-binding cassette transporters to chlorantraniliprole in the rice striped stem borer, *Chilo suppressalis*. Pest Manag Sci.

Merlin, C., Lucas, P., Rochat, D., Francois, M.C., Maibeche-Coisne, M., Jacquin-Joly, E., 2007. An antennal circadian clock and circadian rhythms in peripheral pheromone reception in the moth *Spodoptera littoralis*. J Biol Rhythms 22, 502-514.

Misra, J.R., Horner, M.A., Lam, G., Thummel, C.S., 2011. Transcriptional regulation of xenobiotic detoxification in *Drosophila*. Genes Dev 25, 1796-1806.

Misra, J.R., Lam, G., Thummel, C.S., 2013. Constitutive activation of the Nrf2/Keap1 pathway in insecticide-resistant strains of *Drosophila*. Insect Biochem Mol Biol 43, 1116-1124.

Molina-Ochoa, J., Carpenter, J.E., Heinrichs, E.A., Foster, J.E., 2003. Parasitoids and parasites of Spodoptera frugiperda (Lepidoptera: Noctuidae) in the Americas and Caribbean Basin: an inventory. Florida Entomologist 86, 254-289.

Montezano, D.G., Specht, A., Sosa-Gómez, D.R., Roque-Specht, V.F., Sousa-Silva, J.C., Paula-Moraes, S.V., Peterson, J.A., Hunt, T.E., 2018. Host Plants of *Spodoptera frugiperda* (Lepidoptera: Noctuidae) in the Americas. African Entomology 26, 286-300.

Mota-Sanchez, D., Wise, J.C., 2020. The Arthropod Pesticide Resistance Database, in: University, M.S. (Ed.), pp. On-line at: http://www.pesticideresistance.org.

Muller, R., de Vos, M., Sun, J.Y., Sonderby, I.E., Halkier, B.A., Wittstock, U., Jander, G., 2010. Differential effects of indole and aliphatic glucosinolates on lepidopteran herbivores. J Chem Ecol 36, 905-913.

Nagoshi, R.N., Brambila, J., Meagher, R.L., 2011. Use of DNA barcodes to identify invasive armyworm *Spodoptera species* in Florida. J Insect Sci 11, 154.

Nagoshi, R.N., Fleischer, S., Meagher, R.L., 2017a. Demonstration and Quantification of Restricted Mating Between Fall Armyworm Host Strains in Field Collections by SNP Comparisons. J Econ Entomol 110, 2568-2575.

Nagoshi, R.N., Goergen, G., Plessis, H.D., van den Berg, J., Meagher, R., Jr., 2019. Genetic comparisons of fall armyworm populations from 11 countries spanning sub-Saharan Africa provide insights into strain composition and migratory behaviors. Sci Rep 9, 8311.

Nagoshi, R.N., Koffi, D., Agboka, K., Tounou, K.A., Banerjee, R., Jurat-Fuentes, J.L., Meagher, R.L., 2017b. Comparative molecular analyses of invasive fall armyworm in Togo reveal strong

similarities to populations from the eastern United States and the Greater Antilles. PLoS One 12, e0181982.
Nagoshi, R.N., Silvie, P., Meagher, R.L., Lopez, J., Machado, V., 2007. Identification and comparison of fall armyworm (Lepidoptera: Noctuidae) host strains in Brazil, Texas, and Florida. Annals of the Entomological Society of America 100, 394-402.
Nakata, K., Tanaka, Y., Nakano, T., Adachi, T., Tanaka, H., Kaminuma, T., Ishikawa, T., 2006. Nuclear receptor-mediated transcriptional regulation in Phase I, II, and III xenobiotic metabolizing systems. Drug Metab Pharmacokinet 21, 437-457.
Nalim, D., 1991. Biology, quantitative nutrition and quality control of populations of Spodoptera frugiperda (JE Smith, 1797)(Lepidoptera: Noctuidae) in two artificial diets.
Nascimento, A.R., Fresia, P., Consoli, F.L., Omoto, C., 2015. Comparative transcriptome analysis of lufenuron-resistant and susceptible strains of *Spodoptera frugiperda* (Lepidoptera: Noctuidae). BMC Genomics 16, 985.
Nauen, R., Bretschneider, T., 2002. New modes of action of insecticides. Pesticide Outlook 13, 241–245.
Nauen, R., Zimmer, C.T., Vontas, J., 2021. Heterologous expression of insect P450 enzymes that metabolize xenobiotics. Curr Opin Insect Sci 43, 78-84.
Negre, V., Hotelier, T., Volkoff, A.N., Gimenez, S., Cousserans, F., Mita, K., Sabau, X., Rocher, J., Lopez-Ferber, M., d'Alencon, E., Audant, P., Sabourault, C., Bidegainberry, V., Hilliou, F., Fournier, P., 2006. SPODOBASE: an EST database for the lepidopteran crop pest *Spodoptera*. BMC Bioinformatics 7, 322.
Nelson, D.R., 1998. Metazoan cytochrome P450 evolution. Comp Biochem Physiol C Pharmacol Toxicol Endocrinol 121, 15-22.
Nguyen, T., Nioi, P., Pickett, C.B., 2009. The Nrf2-antioxidant response element signaling pathway and its activation by oxidative stress. J Biol Chem 284, 13291-13295.
Niwa, R., Niwa, Y.S., 2014. Enzymes for ecdysteroid biosynthesis: their biological functions in insects and beyond. Biosci Biotechnol Biochem 78, 1283-1292.
Nouzova, M., Edwards, M.J., Michalkova, V., Ramirez, C.E., Ruiz, M., Areiza, M., DeGennaro, M., Fernandez-Lima, F., Feyereisen, R., Jindra, M., Noriega, F.G., 2021. Epoxidation of juvenile hormone was a key innovation improving insect reproductive fitness. Proc Natl Acad Sci U S A 118.
Oakeshott, J., Claudianos, C., Campbell, P.M., Newcomb, R., Russell, R.J., 2005. Biochemical genetics and genomics of insect esterases, in: Gilbert, L.I., Iatrou, K., Gill, S.S. (Eds.), Comprehensive Molecular Insect Science - Pharmacology. Elsevier, Amsterdam, pp. 309-381.
Okonechnikov, K., Golosova, O., Fursov, M., team, U., 2012. Unipro UGENE: a unified bioinformatics toolkit. Bioinformatics 28, 1166-1167.
Orsucci, M., Moné, Y., Audiot, P., Gimenez, S., Nhim, S., Naït-Saïdi, R., Frayssinet, M., Dumont, G., Pommier, A., Boudon, J.P., 2020. Transcriptional plasticity evolution in two strains of Spodoptera frugiperda (Lepidoptera: Noctuidae) feeding on alternative host-plants.
Overton, K., Maino, J.L., Day, R., Umina, P.A., Bett, B., Carnovale, D., Ekesi, S., Meagher, R., Reynolds, O.L., 2021. Global crop impacts, yield losses and action thresholds for fall armyworm (*Spodoptera frugiperda*): A review. Crop Protection.
Palli, S.R., 2020. CncC/Maf-mediated xenobiotic response pathway in insects. Arch Insect Biochem Physiol 104, e21674.
Pan, Y., Zeng, X., Wen, S., Liu, X., Shang, Q., 2020. Characterization of the Cap 'n' Collar Isoform C gene in *Spodoptera frugiperda* and its Association with Superoxide Dismutase. Insects 11.
Pardini, R.S., 1995. Toxicity of oxygen from naturally occurring redox-active pro-oxidants. Arch Insect Biochem Physiol 29, 101-118.
Partridge, E.C., Watkins, T.A., Mendenhall, E.M., 2016. Every transcription factor deserves its map: Scaling up epitope tagging of proteins to bypass antibody problems. Bioessays 38, 801-811.

Pascussi, J.M., Gerbal-Chaloin, S., Duret, C., Daujat-Chavanieu, M., Vilarem, M.J., Maurel, P., 2008. The tangle of nuclear receptors that controls xenobiotic metabolism and transport: crosstalk and consequences. Annu Rev Pharmacol Toxicol 48, 1-32.

Pashley, D.P., 1986. Host-associated genetic differentiation in fall armyworm (Lepidoptera: Noctuidae): a sibling species complex? Annals of the Entomological Society of America 76, 898-904.

Patel, P.H., Pénalva, C., Kardorff, M., Roca, M., Pavlović, B., Thiel, A., Teleman, A.A., Edgar, B.A., 2019. Damage sensing by a Nox-Ask1-MKK3-p38 signaling pathway mediates regeneration in the adult *Drosophila* midgut. Nat Commun 10, 4365.

Pavlidi, N., Vontas, J., Van Leeuwen, T., 2018. The role of glutathione S-transferases (GSTs) in insecticide resistance in crop pests and disease vectors. Curr Opin Insect Sci 27, 97-102.

Pearce, S.L., Clarke, D.F., East, P.D., Elfekih, S., Gordon, K.H.J., Jermiin, L.S., McGaughran, A., Oakeshott, J.G., Papanicolaou, A., Perera, O.P., Rane, R.V., Richards, S., Tay, W.T., Walsh, T.K., Anderson, A., Anderson, C.J., Asgari, S., Board, P.G., Bretschneider, A., Campbell, P.M., Chertemps, T., Christeller, J.T., Coppin, C.W., Downes, S.J., Duan, G., Farnsworth, C.A., Good, R.T., Han, L.B., Han, Y.C., Hatje, K., Horne, I., Huang, Y.P., Hughes, D.S.T., Jacquin-Joly, E., James, W., Jhangiani, S., Kollmar, M., Kuwar, S.S., Li, S., Liu, N.Y., Maibeche, M.T., Miller, J.R., Montagne, N., Perry, T., Qu, J., Song, S.V., Sutton, G.G., Vogel, H., Walenz, B.P., Xu, W., Zhang, H.J., Zou, Z., Batterham, P., Edwards, O.R., Feyereisen, R., Gibbs, R.A., Heckel, D.G., McGrath, A., Robin, C., Scherer, S.E., Worley, K.C., Wu, Y.D., 2017. Genomic innovations, transcriptional plasticity and gene loss underlying the evolution and divergence of two highly polyphagous and invasive *Helicoverpa* pest species. BMC Biol 15, 63.

Peng, T., Pan, Y., Gao, X., Xi, J., Zhang, L., Yang, C., Bi, R., Yang, S., Xin, X., Shang, Q., 2016. Cytochrome P450 CYP6DA2 regulated by cap 'n'collar isoform C (CncC) is associated with gossypol tolerance in *Aphis gossypii* Glover. Insect Mol Biol 25, 450-459.

Pereira, R.B., Pinto, N.F.S., Fernandes, M.J.G., Vieira, T.F., Rodrigues, A.R.O., Pereira, D.M., Sousa, S.F., Castanheira, E.M.S., Fortes, A.G., Goncalves, M.S.T., 2021. Amino Alcohols from Eugenol as Potential Semisynthetic Insecticides: Chemical, Biological, and Computational Insights. Molecules 26.

Petersen, R.A., Zangerl, A.R., Berenbaum, M.R., Schuler, M.A., 2001. Expression of CYP6B1 and CYP6B3 cytochrome P450 monooxygenases and furanocoumarin metabolism in different tissues of *Papilio polyxenes* (Lepidoptera: Papilionidae). Insect Biochem Mol Biol 31, 679-690.

Petryk, A., Warren, J.T., Marqués, G., Jarcho, M.P., Gilbert, L.I., Kahler, J., Parvy, J.P., Li, Y., Dauphin-Villemant, C., O'Connor, M.B., 2003. Shade is the *Drosophila* P450 enzyme that mediates the hydroxylation of ecdysone to the steroid insect molting hormone 20-hydroxyecdysone. Proc Natl Acad Sci U S A 100, 13773-13778.

Pitoniak, A., Bohmann, D., 2015. Mechanisms and functions of Nrf2 signaling in Drosophila. Free Radic Biol Med 88, 302-313.

Pitre, H.N., Hogg, D.B., 1983. Development of the fall armyworm on cotton, soybean and corn [Spodoptera frugiperda]. Journal of the Georgia Entomological Society.

Pogue, M.G., 2002. A world revision of the genus Spodoptera Guenée:(Lepidoptera: Noctuidae). American Entomological Society.

Prasanna, B.M., Huesing, J.E., Eddy, R., Peshke, V.M., 2018. Fall Armyworm in Africa: a guide for integrated pest management. CIMMYT, USAID, Oakside editorial services, Mexico, p. 110.

Qiu, Y., Tittiger, C., Wicker-Thomas, C., Le Goff, G., Young, S., Wajnberg, E., Fricaux, T., Taquet, N., Blomquist, G.J., Feyereisen, R., 2012. An insect-specific P450 oxidative decarbonylase for cuticular hydrocarbon biosynthesis. Proc Natl Acad Sci U S A 109, 14858-14863.

Rancurel, C., van Tran, T., Elie, C., Hilliou, F., 2019. SATQPCR: Website for statistical analysis of real-time quantitative PCR data. Mol Cell Probes 46, 101418.

Rane, R.V., Ghodke, A.B., Hoffmann, A.A., Edwards, O.R., Walsh, T.K., Oakeshott, J.G., 2019. Detoxifying enzyme complements and host use phenotypes in 160 insect species. Curr Opin Insect Sci 31, 131-138.

Rane, R.V., Walsh, T.K., Pearce, S.L., Jermiin, L.S., Gordon, K.H., Richards, S., Oakeshott, J.G., 2016. Are feeding preferences and insecticide resistance associated with the size of detoxifying enzyme families in insect herbivores? Curr Opin Insect Sci 13, 70-76.

Ranson, H., Claudianos, C., Ortelli, F., Abgrall, C., Hemingway, J., Sharakhova, M.V., Unger, M.F., Collins, F.H., Feyereisen, R., 2002. Evolution of supergene families associated with insecticide resistance. Science 298, 179-181.

Ranson, H., Rossiter, L., Ortelli, F., Jensen, B., Wang, X., Roth, C.W., Collins, F.H., Hemingway, J., 2001. Identification of a novel class of insect glutathione S-transferases involved in resistance to DDT in the malaria vector Anopheles gambiae. Biochem J 359, 295-304.

Reed, J.R., Vanderwel, D., Choi, S., Pomonis, J.G., Reitz, R.C., Blomquist, G.J., 1994. Unusual mechanism of hydrocarbon formation in the housefly: cytochrome P450 converts aldehyde to the sex pheromone component (Z)-9-tricosene and CO2. Proc Natl Acad Sci U S A 91, 10000-10004.

Rewitz, K.F., Rybczynski, R., Warren, J.T., Gilbert, L.I., 2006. The Halloween genes code for cytochrome P450 enzymes mediating synthesis of the insect moulting hormone. Biochem Soc Trans 34, 1256-1260.

Richardson, E.B., Troczka, B.J., Gutbrod, O., Davies, T.G.E., Nauen, R., 2020. Diamide resistance: 10 years of lessons from lepidopteran pests. Journal of Pest Science 93, 911-928.

Riveron, J.M., Yunta, C., Ibrahim, S.S., Djouaka, R., Irving, H., Menze, B.D., Ismail, H.M., Hemingway, J., Ranson, H., Albert, A., Wondji, C.S., 2014. A single mutation in the GSTe2 gene allows tracking of metabolically based insecticide resistance in a major malaria vector. Genome Biol 15, R27.

Roelofs, D., Zwaenepoel, A., Sistermans, T., Nap, J., Kampfraath, A.A., Van de Peer, Y., Ellers, J., Kraaijeveld, K., 2020. Multi-faceted analysis provides little evidence for recurrent whole-genome duplications during hexapod evolution. BMC Biol 18, 57.

Rose, R.L., Goh, D., Thompson, D.M., Verma, K.D., Heckel, D.G., Gahan, L.J., Roe, R.M., Hodgson, E., 1997. Cytochrome P450 (CYP)9A1 in Heliothis virescens: the first member of a new CYP family. Insect Biochem Mol Biol 27, 605-615.

Rosner, J., Merzendorfer, H., 2020. Transcriptional plasticity of different ABC transporter genes from *Tribolium castaneum* contributes to diflubenzuron resistance. Insect Biochem Mol Biol 116, 103282.

Rostant, W.G., Wedell, N., Hosken, D.J., 2012. Transposable elements and insecticide resistance. Adv Genet 78, 169-201.

Roy, A., Walker, W.B., 3rd, Vogel, H., Chattington, S., Larsson, M.C., Anderson, P., Heckel, D.G., Schlyter, F., 2016a. Diet dependent metabolic responses in three generalist insect herbivores *Spodoptera* spp. Insect Biochem Mol Biol 71, 91-105.

Roy, A., Walker, W.B., 3rd, Vogel, H., Kushwaha, S.K., Chattington, S., Larsson, M.C., Anderson, P., Heckel, D.G., Schlyter, F., 2016b. Data set for diet specific differential gene expression analysis in three *Spodoptera* moths. Data Brief 8, 448-455.

Rupasinghe, S.G., Wen, Z., Chiu, T.L., Schuler, M.A., 2007. *Helicoverpa zea* CYP6B8 and CYP321A1: different molecular solutions to the problem of metabolizing plant toxins and insecticides. Protein Eng Des Sel 20, 615-624.

Russell, R.J., Claudianos, C., Campbell, P.M., Horne, I., Sutherland, T.D., Oakeshott, J.G., 2004. Two major classes of target site insensitivity mutations confer resistance to organophosphate and carbamate insecticides. Pesticide Biochemistry and Physiology 79, 84-93.

Ruttanaphan, T., de Sousa, G., Pengsook, A., Pluempanupat, W., Huditz, H.I., Bullangpoti, V., Le Goff, G., 2020. A Novel Insecticidal Molecule Extracted from Alpinia galanga with Potential to Control the Pest Insect *Spodoptera frugiperda*. Insects 11.

Rwomushana, I., Bateman, M., Beale, T., Beseh, P., Cameron, K., Chiluba, M., Clottey, V., Davis, T., Day, R., Early, R., 2018. Fall armyworm: impacts and implications for Africa Evidence Note Update, October 2018, Report to DFID. Wallingford, UK: CAB International.

Sakka, M.K., Riga, M., Ioannidis, P., Baliota, G.V., Tselika, M., Jagadeesan, R., Nayak, M.K., Vontas, J., Athanassiou, C.G., 2021. Transcriptomic analysis of s-methoprene resistance in the lesser grain

borer, *Rhyzopertha dominica*, and evaluation of piperonyl butoxide as a resistance breaker. BMC Genomics 22, 65.
Sanchez-Ortega, M., Carrera, A.C., Garrido, A., 2021. Role of NRF2 in Lung Cancer. Cells 10.
Sasabe, M., Wen, Z., Berenbaum, M.R., Schuler, M.A., 2004. Molecular analysis of CYP321A1, a novel cytochrome P450 involved in metabolism of plant allelochemicals (furanocoumarins) and insecticides (cypermethrin) in *Helicoverpa zea*. Gene 338, 163-175.
Sattelle, D.B., Cordova, D., Cheek, T.R., 2008. Insect ryanodine receptors: molecular targets for novel pest control chemicals. Invert Neurosci 8, 107-119.
Savic, D., Partridge, E.C., Newberry, K.M., Smith, S.B., Meadows, S.K., Roberts, B.S., Mackiewicz, M., Mendenhall, E.M., Myers, R.M., 2015. CETCh-seq: CRISPR epitope tagging ChIP-seq of DNA-binding proteins. Genome Res 25, 1581-1589.
Schneider, E.H., Seifert, R., 2010. Sf9 cells: a versatile model system to investigate the pharmacological properties of G protein-coupled receptors. Pharmacol Ther 128, 387-418.
Schramm, K., Vassao, D.G., Reichelt, M., Gershenzon, J., Wittstock, U., 2012. Metabolism of glucosinolate-derived isothiocyanates to glutathione conjugates in generalist lepidopteran herbivores. Insect Biochem Mol Biol 42, 174-182.
Sezutsu, H., Le Goff, G., Feyereisen, R., 2013. Origins of P450 diversity. Philos Trans R Soc Lond B Biol Sci 368, 20120428.
Sharanabasappa, S., Kalleshwaraswamy, C.M., Poorani, J., Maruthi, M.S., Pavithra, H.B., Diraviam, J., 2019. Natural enemies of Spodoptera frugiperda (JE Smith)(Lepidoptera: Noctuidae), a recent invasive pest on maize in South India. The Florida Entomologist 103, 619-623.
Shi, L., Shi, Y., Liu, M.F., Zhang, Y., Liao, X.L., 2020. Transcription factor CncC potentially regulates the expression of multiple detoxification genes that mediate indoxacarb resistance in *Spodoptera litura*. Insect Sci.
Shi, L., Shi, Y., Liu, M.F., Zhang, Y., Liao, X.L., 2021a. Transcription factor CncC potentially regulates the expression of multiple detoxification genes that mediate indoxacarb resistance in Spodoptera litura. Insect Sci 28, 1426-1438.
Shi, L., Shi, Y., Zhang, Y., Liao, X., 2019. A systemic study of indoxacarb resistance in *Spodoptera litura* revealed complex expression profiles and regulatory mechanism. Sci Rep 9, 14997.
Shi, L., Wang, M., Zhang, Y., Shen, G., Di, H., Wang, Y., He, L., 2017. The expression of P450 genes mediating fenpropathrin resistance is regulated by CncC and Maf in *Tetranychus cinnabarinus* (Boisduval). Comp Biochem Physiol C Toxicol Pharmacol 198, 28-36.
Shi, Y., Jiang, Q., Yang, Y., Feyereisen, R., Wu, Y., 2021b. Pyrethroid metabolism by eleven Helicoverpa armigera P450s from the CYP6B and CYP9A subfamilies. Insect Biochem Mol Biol, 103597.
Shi, Y., Qu, Q., Wang, C., He, Y., Yang, Y., Wu, Y., 2021c. Involvement of CYP2 and mitochondrial clan P450s of *Helicoverpa armigera* in xenobiotic metabolism. Insect Biochem Mol Biol 140, 103696.
Shi, Y., Wang, H., Liu, Z., Wu, S., Yang, Y., Feyereisen, R., Heckel, D.G., Wu, Y., 2018. Phylogenetic and functional characterization of ten P450 genes from the CYP6AE subfamily of *Helicoverpa armigera* involved in xenobiotic metabolism. Insect Biochem Mol Biol 93, 79-91.
Shylesha, A., Jalali, S., Gupta, A., Varshney, R., Venkatesan, T., Shetty, P., Ojha, R., Ganiger, P.C., Navik, O., Subaharan, K., 2018. Studies on new invasive pest Spodoptera frugiperda (JE Smith)(Lepidoptera: Noctuidae) and its natural enemies. Journal of Biological Control 32, 145-151.
Siebert, M.W., Tindall, K.V., Leonard, B.R., Van Duyn, J.W., Babcock, J.M., 2008. Evaluation of Corn Hybrids Expressing CrylF (Herculex® I Insect Protection) Against Fall Armyworm (Lepidoptera: Noctuidae) in the Southern United States. Journal of Entomological Science 43, 41-51.
Silva, D.M.D., Bueno, A.D.F., Andrade, K., Stecca, C.D.S., Neves, P.M.O.J., Oliveira, M.C.N.D., 2017. Biology and nutrition of *Spodoptera frugiperda* (Lepidoptera: Noctuidae) fed on different food sources. Scientia Agricola 74, 18-31.

Silva-Brandão, K.L., Horikoshi, R.J., Bernardi, D., Omoto, C., Figueira, A., Brandão, M.M., 2017. Transcript expression plasticity as a response to alternative larval host plants in the speciation process of corn and rice strains of *Spodoptera frugiperda*. BMC genomics 18, 792.

Simon, O., Palma, L., Williams, T., Lopez-Ferber, M., Caballero, P., 2012. Analysis of a naturally-occurring deletion mutant of Spodoptera frugiperda multiple nucleopolyhedrovirus reveals sf58 as a new per os infectivity factor of lepidopteran-infecting baculoviruses. J Invertebr Pathol 109, 117-126.

Singh, A., Venkannagari, S., Oh, K.H., Zhang, Y.Q., Rohde, J.M., Liu, L., Nimmagadda, S., Sudini, K., Brimacombe, K.R., Gajghate, S., Ma, J., Wang, A., Xu, X., Shahane, S.A., Xia, M., Woo, J., Mensah, G.A., Wang, Z., Ferrer, M., Gabrielson, E., Li, Z., Rastinejad, F., Shen, M., Boxer, M.B., Biswal, S., 2016. Small Molecule Inhibitor of NRF2 Selectively Intervenes Therapeutic Resistance in KEAP1-Deficient NSCLC Tumors. ACS Chem Biol 11, 3214-3225.

Singh, G., Sachdev, B., Sharma, N., Seth, R., Bhatnagar, R.K., 2010. Interaction of Bacillus thuringiensis vegetative insecticidal protein with ribosomal S2 protein triggers larvicidal activity in Spodoptera frugiperda. Appl Environ Microbiol 76, 7202-7209.

Small, G.J., Hemingway, J., 2000. Molecular characterization of the amplified carboxylesterase gene associated with organophosphorus insecticide resistance in the brown planthopper, *Nilaparvata lugens*. Insect molecular biology 9, 647-653.

Snezhkina, A.V., Kudryavtseva, A.V., Kardymon, O.L., Savvateeva, M.V., Melnikova, N.V., Krasnov, G.S., Dmitriev, A.A., 2019. ROS Generation and Antioxidant Defense Systems in Normal and Malignant Cells. Oxid Med Cell Longev 2019, 6175804.

Soderlund, D.M., 2012. Molecular mechanisms of pyrethroid insecticide neurotoxicity: recent advances. Arch Toxicol 86, 165-181.

Somers, J., Luong, H.N.B., Batterham, P., Perry, T., 2018. Deletion of the nicotinic acetylcholine receptor subunit gene Dalpha1 confers insecticide resistance, but at what cost? Fly (Austin) 12, 46-54.

Sparks, T.C., Crossthwaite, A.J., Nauen, R., Banba, S., Cordova, D., Earley, F., Ebbinghaus-Kintscher, U., Fujioka, S., Hirao, A., Karmon, D., Kennedy, R., Nakao, T., Popham, H.J.R., Salgado, V., Watson, G.B., Wedel, B.J., Wessels, F.J., 2020. Insecticides, biologics and nematicides: Updates to IRAC's mode of action classification - a tool for resistance management. Pestic Biochem Physiol 167, 104587.

Stepanenko, A.A., Dmitrenko, V.V., 2015. Pitfalls of the MTT assay: Direct and off-target effects of inhibitors can result in over/underestimation of cell viability. Gene 574, 193-203.

Stokstad, E., 2017. New crop pest takes Africa at lightning speed. Science 356, 473-474.

Summers, M.D., Smith, G.E., 1987. A manual of methods for baculovirus vectors and insect cell culture procedures. Texas Agric Experiment Station Bull, 1–56.

Sun, X.X., Hu, C.X., Jia, H.R., Wu, Q.L., Shen, X.J., Zhao, S.Y., Jiang, Y.Y., Wu, K.M., 2019a. Case study on the first immigration of fall armyworm Spodoptera frugiperda invading into China. Journal of Integrative Agriculture 18, 2-10.

Sun, Z., Shi, Q., Li, Q., Wang, R., Xu, C., Wang, H., Ran, C., Song, Y., Zeng, R., 2019b. Identification of a cytochrome P450 CYP6AB60 gene associated with tolerance to multi-plant allelochemicals from a polyphagous caterpillar tobacco cutworm (*Spodoptera litura*). Pestic Biochem Physiol 154, 60-66.

Suryamohan, K., Halfon, M.S., 2015. Identifying transcriptional cis-regulatory modules in animal genomes. Wiley Interdiscip Rev Dev Biol 4, 59-84.

Suzuki, T., Yamamoto, M., 2015. Molecular basis of the Keap1-Nrf2 system. Free Radic Biol Med 88, 93-100.

Sykiotis, G.P., Bohmann, D., 2008. Keap1/Nrf2 signaling regulates oxidative stress tolerance and lifespan in *Drosophila*. Dev Cell 14, 76-85.

Sykiotis, G.P., Bohmann, D., 2010. Stress-activated cap'n'collar transcription factors in aging and human disease. Sci Signal 3, re3.

Tang, B., Cheng, Y., Li, Y., Li, W., Ma, Y., Zhou, Q., Lu, K., 2020. Adipokinetic hormone regulates cytochrome P450-mediated imidacloprid resistance in the brown planthopper, *Nilaparvata lugens*. Chemosphere 259, 127490.

Tang, G.H., Xiong, Y., Liu, Y., Song, Z.H., Yang, Y., Shen, G.M., Wang, J.J., Jiang, H.B., 2019. The Transcription Factor MafB Regulates the Susceptibility of *Bactrocera dorsalis* to Abamectin via GSTz2. Front Physiol 10, 1068.

Tao, X.Y., Xue, X.Y., Huang, Y.P., Chen, X.Y., Mao, Y.B., 2012. Gossypol-enhanced P450 gene pool contributes to cotton bollworm tolerance to a pyrethroid insecticide. Mol Ecol 21, 4371-4385.

Teese, M.G., Campbell, P.M., Scott, C., Gordon, K.H., Southon, A., Hovan, D., Robin, C., Russell, R.J., Oakeshott, J.G., 2010. Gene identification and proteomic analysis of the esterases of the cotton bollworm, Helicoverpa armigera. Insect Biochem Mol Biol 40, 1-16.

Tellez-Rodriguez, P., Raymond, B., Moran-Bertot, I., Rodriguez-Cabrera, L., Wright, D.J., Borroto, C.G., Ayra-Pardo, C., 2014. Strong oviposition preference for Bt over non-Bt maize in *Spodoptera frugiperda* and its implications for the evolution of resistance. BMC Biol 12, 48.

Terriere, L., Yu, S., 1973. Insect juvenile hormones: induction of detoxifying enzymes in the house fly and detoxication by house fly enzymes. Pestic Biochem Physiol 3, 96-107.

Troczka, B., Zimmer, C.T., Elias, J., Schorn, C., Bass, C., Davies, T.G., Field, L.M., Williamson, M.S., Slater, R., Nauen, R., 2012. Resistance to diamide insecticides in diamondback moth, *Plutella xylostella* (Lepidoptera: Plutellidae) is associated with a mutation in the membrane-spanning domain of the ryanodine receptor. Insect Biochem Mol Biol 42, 873-880.

Troczka, B.J., Homem, R.A., Reid, R., Beadle, K., Kohler, M., Zaworra, M., Field, L.M., Williamson, M.S., Nauen, R., Bass, C., Davies, T.G.E., 2019. Identification and functional characterisation of a novel N-cyanoamidine neonicotinoid metabolising cytochrome P450, CYP9Q6, from the buff-tailed bumblebee Bombus terrestris. Insect Biochem Mol Biol 111, 103171.

Trusov, N.V., Guseva, G.V., Aksenov, I.V., Avren'eva, L.I., Kravchenko, L.V., Tutelyan, V.A., 2010. Effects of combined treatment with resveratrol and indole-3-carbinol. Bull Exp Biol Med 149, 213-218.

Tuladhar, R., Yeu, Y., Tyler Piazza, J., Tan, Z., Rene Clemenceau, J., Wu, X., Barrett, Q., Herbert, J., Mathews, D.H., Kim, J., Hyun Hwang, T., Lum, L., 2019. CRISPR-Cas9-based mutagenesis frequently provokes on-target mRNA misregulation. Nat Commun 10, 4056.

Van de Vossenberg, B.T., Van der Straten, M.J., 2014. Development and validation of real-time PCR tests for the identification of four *Spodoptera* species: *Spodoptera eridania, Spodoptera frugiperda, Spodoptera littoralis, and Spodoptera litura* (Lepidoptera: Noctuidae). J Econ Entomol 107, 1643-1654.

Vandenhole, M., Dermauw, W., Van Leeuwen, T., 2020. Short term transcriptional responses of P450s to phytochemicals in insects and mites. Curr Opin Insect Sci 43, 117-127.

Vassao, D.G., Wielsch, N., Gomes, A., Gebauer-Jung, S., Hupfer, Y., Svatos, A., Gershenzon, J., 2018. Plant Defensive beta-Glucosidases Resist Digestion and Sustain Activity in the Gut of a Lepidopteran Herbivore. Front Plant Sci 9, 1389.

Vaughn, J.L., Goodwin, R.H., Tompkins, G.J., McCauley, P., 1977. The establishment of two cell lines from the insect *Spodoptera frugiperda* (Lepidoptera Noctuidae). In Vitro 13, 213-217.

Vlogiannitis, S., Mavridis, K., Dermauw, W., Snoeck, S., Katsavou, E., Morou, E., Harizanis, P., Swevers, L., Hemingway, J., Feyereisen, R., Van Leeuwen, T., Vontas, J., 2021. Reduced proinsecticide activation by cytochrome P450 confers coumaphos resistance in the major bee parasite *Varroa destructor*. Proc Natl Acad Sci U S A 118.

Vogel, H., Musser, R.O., de la Paz Celorio-Mancera, M., 2014. Transcriptome Responses in Herbivorous Insects Towards Host Plant and Toxin Feeding. Annual Plant Reviews 47, 197-233.

Vogt, R.G., 2005. Molecular basis of pheromone detection in insects. Comprehensive insect physiology, biochemistry, pharmacology and molecular biology 3, 753-804.

Vogt, R.G., Riddiford, L.M., 1986. Scale esterase: A pheromone-degrading enzyme from scales of silk moth *Antheraea polyphemus*. J Chem Ecol 12, 1977.

Vogt, R.G., Riddiford, L.M., Prestwich, G.D., 1985. Kinetic properties of a sex pheromone-degrading enzyme: the sensillar esterase of *Antheraea polyphemus*. Proc Natl Acad Sci U S A 82, 8827-8831.

Vorrink, S.U., Domann, F.E., 2014. Regulatory crosstalk and interference between the xenobiotic and hypoxia sensing pathways at the AhR-ARNT-HIF1α signaling node. Chemico-Biological Interactions 218, 82 - 88.

Walker, W.B., 3rd, Roy, A., Anderson, P., Schlyter, F., Hansson, B.S., Larsson, M.C., 2019. Transcriptome Analysis of Gene Families Involved in Chemosensory Function in *Spodoptera littoralis* (Lepidoptera: Noctuidae). BMC Genomics 20, 428.

Wan, H., Liu, Y., Li, M., Zhu, S., Li, X., Pittendrigh, B.R., Qiu, X., 2014. Nrf2/Maf-binding-site-containing functional Cyp6a2 allele is associated with DDT resistance in *Drosophila melanogaster*. Pest Manag Sci 70, 1048-1058.

Wang, B., Shahzad, M.F., Zhang, Z., Sun, H., Han, P., Li, F., Han, Z., 2014. Genome-wide analysis reveals the expansion of Cytochrome P450 genes associated with xenobiotic metabolism in rice striped stem borer, *Chilo suppressalis*. Biochem Biophys Res Commun 443, 756-760.

Wang, H., Lu, Z., Li, M., Fang, Y., Qu, J., Mao, T., Chen, J., Li, F., Sun, H., Li, B., 2020. Responses of detoxification enzymes in the midgut of *Bombyx mori* after exposure to low-dose of acetamiprid. Chemosphere 251, 126438.

Wang, H., Shi, Y., Wang, L., Liu, S., Wu, S., Yang, Y., Feyereisen, R., Wu, Y., 2018a. CYP6AE gene cluster knockout in *Helicoverpa armigera* reveals role in detoxification of phytochemicals and insecticides. Nat Commun 9, 4820.

Wang, L., Tang, N., Gao, X., Chang, Z., Zhang, L., Zhou, G., Guo, D., Zeng, Z., Li, W., Akinyemi, I.A., Yang, H., Wu, Q., 2017a. Genome sequence of a rice pest, the white-backed planthopper (Sogatella furcifera). Gigascience 6, 1-9.

Wang, Q., Hasan, G., Pikielny, C.W., 1999. Preferential expression of biotransformation enzymes in the olfactory organs of *Drosophila melanogaster,* the antennae. Journal of Biological Chemistry 274, 10309-10315.

Wang, R.L., He, Y.N., Staehelin, C., Liu, S.W., Su, Y.J., Zhang, J.E., 2017b. Identification of Two Cytochrome Monooxygenase P450 Genes, CYP321A7 and CYP321A9, from the Tobacco Cutworm Moth (*Spodoptera Litura*) and Their Expression in Response to Plant Allelochemicals. Int J Mol Sci 18.

Wang, R.L., Li, J., Staehelin, C., Xin, X.W., Su, Y.J., Zeng, R.S., 2015a. Expression analysis of two P450 monooxygenase genes of the tobacco cutworm moth (*Spodoptera litura*) at different developmental stages and in response to plant allelochemicals. J Chem Ecol 41, 111-119.

Wang, R.L., Liu, S.W., Baerson, S.R., Qin, Z., Ma, Z.H., Su, Y.J., Zhang, J.E., 2018b. Identification and Functional Analysis of a Novel Cytochrome P450 Gene CYP9A105 Associated with Pyrethroid Detoxification in *Spodoptera exigua* Hubner. Int J Mol Sci 19.

Wang, R.L., Staehelin, C., Xia, Q.Q., Su, Y.J., Zeng, R.S., 2015b. Identification and Characterization of CYP9A40 from the Tobacco Cutworm Moth (*Spodoptera litura*), a Cytochrome P450 Gene Induced by Plant Allelochemicals and Insecticides. Int J Mol Sci 16, 22606-22620.

Wang, R.L., Xia, Q.Q., Baerson, S.R., Ren, Y., Wang, J., Su, Y.J., Zheng, S.C., Zeng, R.S., 2015c. A novel cytochrome P450 CYP6AB14 gene in *Spodoptera litura* (Lepidoptera: Noctuidae) and its potential role in plant allelochemical detoxification. J Insect Physiol 75, 54-62.

Wang, R.L., Zhu-Salzman, K., Baerson, S.R., Xin, X.W., Li, J., Su, Y.J., Zeng, R.S., 2017c. Identification of a novel cytochrome P450 CYP321B1 gene from tobacco cutworm (*Spodoptera litura*) and RNA interference to evaluate its role in commonly used insecticides. Insect Sci 24, 235-247.

Wang, S., Li, B., Zhang, D., 2019. NlCYP4G76 and NlCYP4G115 Modulate Susceptibility to Desiccation and Insecticide Penetration Through Affecting Cuticular Hydrocarbon Biosynthesis in *Nilaparvata lugens* (Hemiptera: Delphacidae). Front Physiol 10, 913.

Wang, X., Chen, Y., Gong, C., Yao, X., Jiang, C., Yang, Q., 2018c. Molecular identification of four novel cytochrome P450 genes related to the development of resistance of *Spodoptera exigua* (Lepidoptera: Noctuidae) to chlorantraniliprole. Pest management science 74, 1938-1952.

Wang, X.G., Gao, X.W., Liang, P., Shi, X.Y., Song, D.L., 2016. Induction of Cytochrome P450 Activity by the Interaction of Chlorantraniliprole and Sinigrin in the *Spodoptera exigua* (Lepidoptera: Noctuidae). Environ Entomol 45, 500-507.

Warren, J.T., Petryk, A., Marques, G., Jarcho, M., Parvy, J.P., Dauphin-Villemant, C., O'Connor, M.B., Gilbert, L.I., 2002. Molecular and biochemical characterization of two P450 enzymes in the ecdysteroidogenic pathway of *Drosophila melanogaster*. Proc Natl Acad Sci U S A 99, 11043-11048.

Westbrook, J.K., Nagoshi, R.N., Meagher, R.L., Fleischer, S.J., Jairam, S., 2016. Modeling seasonal migration of fall armyworm moths. Int J Biometeorol 60, 255-267.

Wild, S., 2017. African countries mobilize to battle invasive caterpillar. Nature 543, 13-14.

Wilding, C.S., 2018. Regulating resistance: CncC:Maf, antioxidant response elements and the overexpression of detoxification genes in insecticide resistance. Curr Opin Insect Sci 27, 89-96.

Withers, A.J., de Boer, J., Chipabika, G., Zhang, L., Smith, J.A., Jones, C.M., Wilson, K., 2021. Microsatellites reveal that genetic mixing commonly occurs between invasive fall armyworm populations in Africa. Scientific reports 11, 1-11.

Wouters, F.C., Reichelt, M., Glauser, G., Bauer, E., Erb, M., Gershenzon, J., Vassao, D.G., 2014. Reglucosylation of the benzoxazinoid DIMBOA with inversion of stereochemical configuration is a detoxification strategy in lepidopteran herbivores. Angew Chem Int Ed Engl 53, 11320-11324.

Wu, L., Jia, Q., Zhang, X., Liu, S., Park, Y., Feyereisen, R., Zhu, K.Y., Ma, E., Zhang, J., Li, S., 2019. CYP303A1 has a conserved function in adult eclosion in Locusta migratoria and *Drosophila melanogaster*. Insect Biochem Mol Biol 113, 103210.

Wu, L., Yu, Z., Jia, Q., Zhang, X., Ma, E., Li, S., Zhu, K.Y., Feyereisen, R., Zhang, J., 2020. Knockdown of LmCYP303A1 alters cuticular hydrocarbon profiles and increases the susceptibility to desiccation and insecticides in *Locusta migratoria*. Pestic Biochem Physiol 168, 104637.

Xiao, H., Ye, X., Xu, H., Mei, Y., Yang, Y., Chen, X., Yang, Y., Liu, T., Yu, Y., Yang, W., Lu, Z., Li, F., 2020. The genetic adaptations of fall armyworm *Spodoptera frugiperda* facilitated its rapid global dispersal and invasion. Mol Ecol Resour 20, 1050-1068.

Xiao, X., Yang, L., Pang, X., Zhang, R., Zhu, Y., Wang, P., Gao, G., Cheng, G., 2017. A Mesh-Duox pathway regulates homeostasis in the insect gut. Nat Microbiol 2, 17020.

Xu, P., Han, N., Kang, T., Zhan, S., Lee, K.S., Jin, B.R., Li, J., Wan, H., 2016. SeGSTo, a novel glutathione S-transferase from the beet armyworm (*Spodoptera exigua*), involved in detoxification and oxidative stress. Cell Stress Chaperones 21, 805-816.

Xu, Z.B., Zou, X.P., Zhang, N., Feng, Q.L., Zheng, S.C., 2015. Detoxification of insecticides, allechemicals and heavy metals by glutathione S-transferase SlGSTE1 in the gut of *Spodoptera litura*. Insect Sci 22, 503-511.

Yang, Y., Yue, L., Chen, S., Wu, Y., 2008a. Functional expression of *Helicoverpa armigera* CYP9A12 and CYP9A14 in *Saccharomyces cerevisiae*. Pesticide Biochemistry and Physiology 92, 101-105.

Yang, Y., Yue, L., Chen, S., Wu, Y., 2008b. Functional expression of Helicoverpa armigera CYP9A12 and CYP9A14 in *Saccharomyces cerevisiae*. Pesticide Biochemistry and Physiology 92, 101 - 105.

Yi, Y., Dou, G., Yu, Z., He, H., Wang, C., Li, L., Zhou, J., Liu, D., Shi, J., Li, G., Pang, L., Yang, N., Huang, Q., Qi, H., 2018. Z-Ligustilide Exerted Hormetic Effect on Growth and Detoxification Enzymes of *Spodoptera litura* Larvae. Evid Based Complement Alternat Med 2018, 7104513.

Yu, S.J., 1982. Induction of microsomal oxidases by host plants in the fall armyworm, Spodoptera frugiperda (J. E. Smith). Pestic Biochem Physiol 17, 59-67.

Yu, S.J., 1983. Induction of detoxifying enzymes by allelochemicals and host plants in the fall armyworm. Pestic Biochem Physiol 19, 330-336.

Yu, S.J., 1986. Consequences of induction of foreign compound-metabolizing enzymes in insects, in: Brattsten, L.B., Ahmad, S. (Ed.), Molecular aspects of insect-plant interactions. Plenum, New York, pp. 211-255.

Yu, S.J., 1987. Microsomal oxidation of allelochemicals in generalist (*Spodoptera frugiperda*) and semispecialist (*Anticarsia gemmatalis*) insect. J Chem Ecol 13, 423-436.

Yu, S.J., Hsu, E.L., 1985. Induction of hydrolases by allelochemicals and host plants in fall armyworm (Lepidoptera : Noctuidae) larvae. Environ Entomol 14, 512-515.
Zhang, B., Zhang, Y., Liu, J.L., 2021. Highly effective proximate labeling in *Drosophila*. G3 (Bethesda) 11.
Zhang, C., Luo, X., Ni, X., Zhang, Y., Li, X., 2010. Functional characterization of cis-acting elements mediating flavone-inducible expression of CYP321A1. Insect Biochem Mol Biol 40, 898-908.
Zhang, F., Zhang, J., Yang, Y., Wu, Y., 2020. A chromosome-level genome assembly for the beet armyworm (*Spodoptera exigua*) using PacBio and Hi-C sequencing. bioRxiv, 2019.2012.2026.889121.
Zhang, N., Liu, J., Chen, S.N., Huang, L.H., Feng, Q.L., Zheng, S.C., 2016a. Expression profiles of glutathione S-transferase superfamily in *Spodoptera litura* tolerated to sublethal doses of chlorpyrifos. Insect Sci 23, 675-687.
Zhang, X., Kang, X., Wu, H., Silver, K., Zhang, J., Ma, E., Zhu, K.Y., 2018. Transcriptome-wide survey, gene expression profiling and exogenous chemical-induced transcriptional responses of cytochrome P450 superfamily genes in migratory locust (Locusta migratoria). Insect Biochem Mol Biol 100, 66-77.
Zhang, Y.-N., Li, J.-B., He, P., Sun, L., Li, Z.-Q., Fang, L.-P., Ye, Z.-F., Deng, D.-G., Zhu, X.-Y., 2016b. Molecular identification and expression patterns of carboxylesterase genes based on transcriptome analysis of the common cutworm, *Spodoptera litura* (Lepidoptera: Noctuidae). Journal of Asia-Pacific Entomology 19, 989-994.
Zhao, C., Feng, X., Tang, T., Qiu, L., 2015. Isolation and Expression Analysis of CYP9A11 and Cytochrome P450 Reductase Gene in the Beet Armyworm (Lepidoptera: Noctuidae). J Insect Sci 15.
Zhou, J., Shu, Y., Zhang, G., Zhou, Q., 2012a. Lead exposure improves the tolerance of *Spodoptera litura* (Lepidoptera: Noctuidae) to cypermethrin. Chemosphere 88, 507-513.
Zhou, J., Zhang, G., Zhou, Q., 2012b. Molecular characterization of cytochrome P450 CYP6B47 cDNAs and 5'-flanking sequence from *Spodoptera litura* (Lepidoptera: Noctuidae): its response to lead stress. J Insect Physiol 58, 726-736.
Zhou, X., Sheng, C., Li, M., Wan, H., Liu, D., Qiu, X., 2010. Expression responses of nine cytochrome P450 genes to xenobiotics in the cotton bollworm *Helicoverpa armigera*. Pesticide Biochemistry and Physiology 97, 209-213.
Zhu, F., Moural, T.W., Nelson, D.R., Palli, S.R., 2016a. A specialist herbivore pest adaptation to xenobiotics through up-regulation of multiple Cytochrome P450s. Sci Rep 6, 20421.
Zhu, G.H., Chereddy, S., Howell, J.L., Palli, S.R., 2020. Genome editing in the fall armyworm, *Spodoptera frugiperda*: Multiple sgRNA/Cas9 method for identification of knockouts in one generation. Insect Biochem Mol Biol 122, 103373.
Zhu, W., Yu, R., Wu, H., Zhang, X., Liu, Y., Zhu, K.Y., Zhang, J., Ma, E., 2016b. Identification and characterization of two CYP9A genes associated with pyrethroid detoxification in *Locusta migratoria*. Pestic Biochem Physiol 132, 65-71.
Zimmer, C.T., Bass, C., Williamson, M.S., Kaussmann, M., Wolfel, K., Gutbrod, O., Nauen, R., 2014. Molecular and functional characterization of CYP6BQ23, a cytochrome P450 conferring resistance to pyrethroids in European populations of pollen beetle, *Meligethes aeneus*. Insect Biochem Mol Biol 45, 18-29.
Zimmer, C.T., Garrood, W.T., Singh, K.S., Randall, E., Lueke, B., Gutbrod, O., Matthiesen, S., Kohler, M., Nauen, R., Davies, T.G.E., Bass, C., 2018. Neofunctionalization of Duplicated P450 Genes Drives the Evolution of Insecticide Resistance in the Brown Planthopper. Curr Biol 28, 268-274 e265.
Zimmer, C.T., Nauen, R., 2011. Pyrethroid resistance and thiacloprid baseline susceptibility of European populations of *Meligethes aeneus* (Coleoptera: Nitidulidae) collected in winter oilseed rape. Pest Manag Sci 67, 599-608.
Zou, X., Xu, Z., Zou, H., Liu, J., Chen, S., Feng, Q., Zheng, S., 2016. Glutathione S-transferase SlGSTE1 in *Spodoptera litura* may be associated with feeding adaptation of host plants. Insect Biochem Mol Biol 70, 32-43.
Zou, X.P., Lin, Y.G., Cen, Y.J., Ma, K., Qiu, B.B., Feng, Q.L., Zheng, S.C., 2020. Analyses of miRNAs and transcriptomes in the midgut of *Spodoptera litura* feeding on *Brassica juncea*. Insect Science.

Zuo, Y., Shi, Y., Zhang, F., Guan, F., Zhang, J., Feyereisen, R., Fabrick, J.A., Yang, Y., Wu, Y., 2021. Genome mapping coupled with CRISPR gene editing reveals a P450 gene confers avermectin resistance in the beet armyworm. PLoS Genet 17, e1009680.

Zuo, Y.Y., Huang, J.L., Wang, J., Feng, Y., Han, T.T., Wu, Y.D., Yang, Y.H., 2017. Knockout of a P-glycoprotein gene increases susceptibility to abamectin and emamectin benzoate in *Spodoptera exigua*. Insect Mol Biol.

Appendix A (Chapter 1 – Part II)

Insect Biochemistry and Molecular Biology 138 (2021) 103646

Contents lists available at ScienceDirect

Insect Biochemistry and Molecular Biology

journal homepage: www.elsevier.com/locate/ibmb

Comparative analysis of the detoxification gene inventory of four major *Spodoptera* pest species in response to xenobiotics

Dries Amezian [a], Ralf Nauen [b,**], Gaëlle Le Goff [a,*]

[a] Université Côte d'Azur, INRAE, CNRS, ISA, F-06903, Sophia Antipolis, France
[b] Bayer AG, Crop Science Division, R&D, Alfred Nobel-Strasse 50, 40789, Monheim, Germany

ARTICLE INFO

Keywords:
Spodoptera
Cytochrome P450
Glutathione S-transferases
Carboxylesterases
UDP-Glycosyl transferases
ABC transporters

ABSTRACT

The genus *Spodoptera* (Lepidoptera: Noctuidae) comprises some of the most polyphagous and destructive agricultural pests worldwide. The success of many species of this genus is due to their striking abilities to adapt to a broad range of host plants. Superfamilies of detoxification genes play a crucial role in the adaption to overcome plant defense mechanisms mediated by numerous secondary metabolites and toxins. Over the past decade, a substantial amount of expression data in *Spodoptera* larvae was produced for those genes in response to xenobiotics such as plant secondary metabolites, but also insecticide exposure. However, this information is scattered throughout the literature and in most cases does not allow to clearly identify candidate genes involved in host-plant adaptation and insecticide resistance. In the present review, we analyzed and compiled information on close to 600 pairs of inducers (xenobiotics) and induced genes from four main *Spodoptera* species: *S. exigua*, *S. frugiperda*, *S. littoralis* and *S. litura*. The cytochrome P450 monooxygenases (P450s; encoded by *CYP* genes) were the most upregulated detoxification genes across the literature for all four species. Most of the data was provided from studies on *S. litura*, followed by *S. exigua*, *S. frugiperda* and *S. littoralis*. We examined whether these detoxification genes were reported for larval survival under xenobiotic challenge in forward and reverse genetic studies. We further analyzed whether biochemical assays were carried out showing the ability of corresponding enzymes and transporters to breakdown and excrete xenobiotics, respectively. This revealed a clear disparity between species and the lack of genetic and biochemical information in *S. frugiperda*. Finally, we discussed the biological importance of detoxification genes for this genus and propose a workflow to study the involvement of these enzymes in an ecological and agricultural context.

1. Introduction

An immense number of complex trophic interactions were known between plants and arthropods, two groups encompassing about half of all macroscopic organisms (Strong, 1988). During the course of their co-evolution, plants and herbivorous arthropods have engaged in an arms race for survival (Ehrlich and Raven, 1964). On the one hand, plants have evolved a myriad of specialized repellent and toxic metabolites directed towards phytophagous arthropods to defend themselves from herbivory (Li et al., 2020a). On the other hand, insects have found ways to bypass these chemicals to exploit plants as a food source (Vogel et al., 2014). The ability to metabolize, sequester and detoxify plant toxins is known as one of the central evolutionary solution that arthropods have developed to feed on plants (Despres et al., 2007; Heidel-Fischer and Vogel, 2015). The detoxification pathway in insects allows the processing of toxicants present in their diet, including insecticides (Despres et al., 2007; Heckel, 2014). It is conventionally split into three phases that convert lipophilic substrates into hydrophilic products more easily excretable from the insect's body (Berenbaum and Johnson, 2015; Despres et al., 2007). In phase I (functionalization) cytochrome P450 monooxygenases (P450s) and carboxylesterases (CEs) render non-polar molecules "functional", *i.e.* with an active center by appending reactive groups suitable for subsequent conjugation. These intermediary metabolites may then fuel into phase II (conjugation) where glutathione S-transferases (GSTs) and (UDP)-glycosyl transferases (UGTs) catalyze the conjugation of target molecules, including phase I products, and facilitate their excretion. At last, phase III (transport) involves ATP-binding cassette (ABC) transporters that mediate efflux of

* Corresponding author.
** Corresponding author.
E-mail addresses: ralf.nauen@bayer.com (R. Nauen), gaelle.le-goff@inrae.fr (G. Le Goff).

https://doi.org/10.1016/j.ibmb.2021.103646
Received 27 April 2021; Received in revised form 9 August 2021; Accepted 25 August 2021
Available online 29 August 2021
0965-1748/© 2021 Elsevier Ltd. All rights reserved.

Supplementary information

Materials and methods

Figures. The data gathered in Supplementary material (Annex 1) was transcribed into a table exploitable in R (version 4.0.0). This table consisted in 15 columns (see names below) and 1231 lines each containing a single gene expression information (for example when a given gene was expressed three times in the same study such as in three different tissues, this would give three lines in the table). The table was loaded in R and figures were drawn by calling the level of information needed.

Detail of column names and features:
SPECIES
XENOBIOTIC: name of the xenobiotic inducer
XENOBITIC_KIND: insecticide, PSM, heavy metals or model inducers
XENOBIOTIC_FAMILY: class of pesticide, chemical family of PSM
DETOX_GENE_TYPE: P450, CE, GST, UGT, ABC
GENE_NAME
CYP_CLAN: Mito, CYP2, CYP3, CYP4
GENE_FAM: family level of detoxification genes in accordance with their respective nomenclature
CYP_SUBFAM: the subfamily level of P450s
EXPRESSION: up, down
TISSUE: MG, MT, FB
EXPR_TECH: semi-quantitative, microarray, RT-qPCR, RNA-seq
FUNCTIONAL_STUDY: true, false
METAB_STUDY: true, false
REF

Supplementary figures

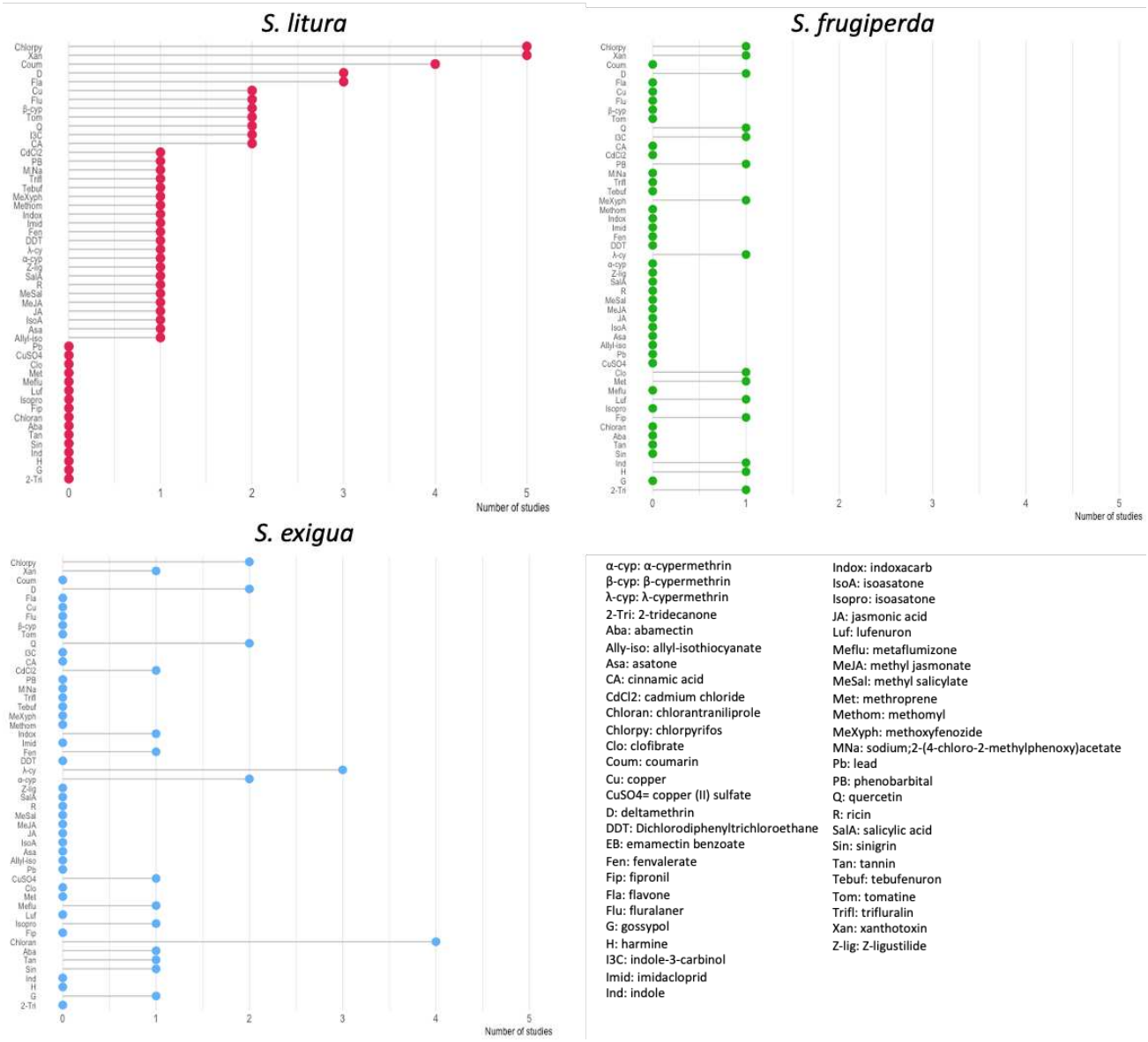

Figure S1: Xenobiotics occurrences in three *Spodoptera* species. The lollipop plots show the number of studies where a given xenobiotic was investigated for each species. Source: Amezian et al. 2021.

A - Number of genes upregulated in deltamethrin treatments for all species
(No genes were found down-regulated by deltamethrin)

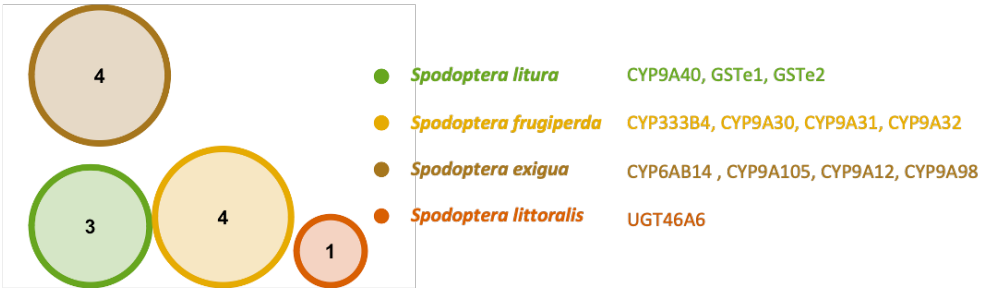

B - Number of genes upregulated in **λ-cyhalothrin** treatments for all species

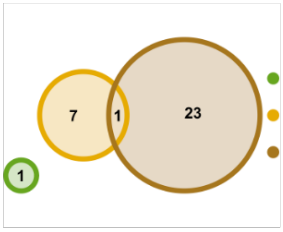

No genes DOWN-regulated in common between species

C - Number of genes upregulated in **xanthotoxin** treatments for all species

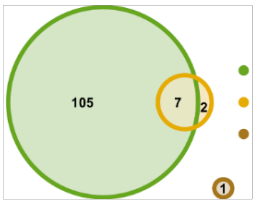

No genes were down regulated by xanthotoxin

D - Number of genes upregulated in **chlorpyrifos** treatments for all species

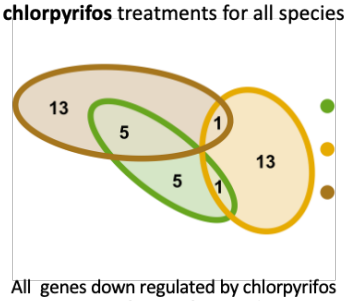

All genes down regulated by chlorpyrifos came from *S. frugiperda*

Figure S2: Number of genes upregulated by four xenobiotics The Venn diagrams show the number of genes upregulated by A) deltamethrin B) λ-cyhalothrin C) xanthotoxin and D) chlorpyrifos in each species. To date, deltamethrin is the only molecule investigated in four *Spodoptera* species. *Note:* CYP9A59 was also found upregulated in a *S. frugiperda* deltamethrin-resistant population (Boaventura et al. 2020). Source: Amezian et al. 2021.

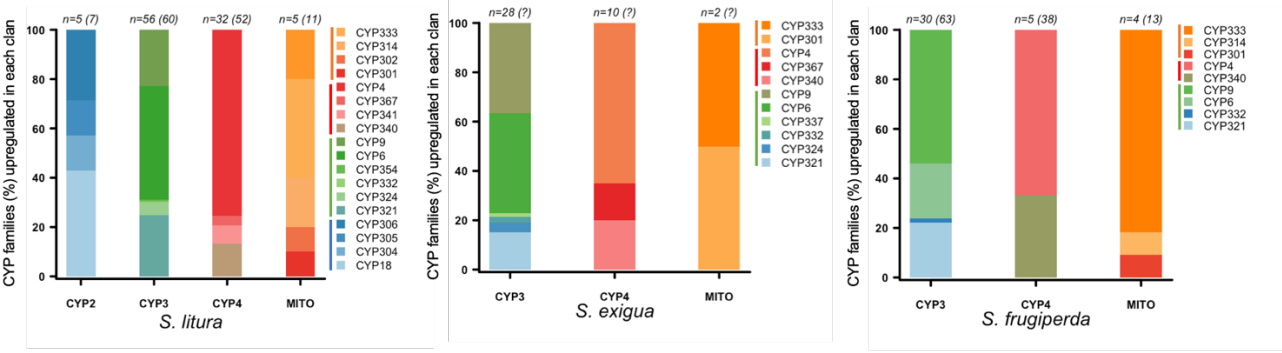

Proportion of UP regulated CYP subfamilies per CLAN in each species

Sub-families not found differentially expressed are:
- Mito: 428, 49, 315(Halloween), 339
- Clan2: 15, 303, 307(H)
- Clan3: 337, 338, 365, 3097
- Clan4: 366, 421

No data

Sub-families not found differentially expressed are:
- Mito: 49, 302(Halloween), 314(H), 315(H), 339, 428
- Clan2: (all absent) 15, 18, 303, 304, 305, 306(H), 307(H)
- Clan3: 324, 337; 338, 354, 365, 3097
- Clan4: 341, 366, 367, 421

Figure S3: Appendix to Figure 2B. The figure lists for each species the CYP sub-families that were not found upregulated in the literature. Source: Amezian et al. 2021.

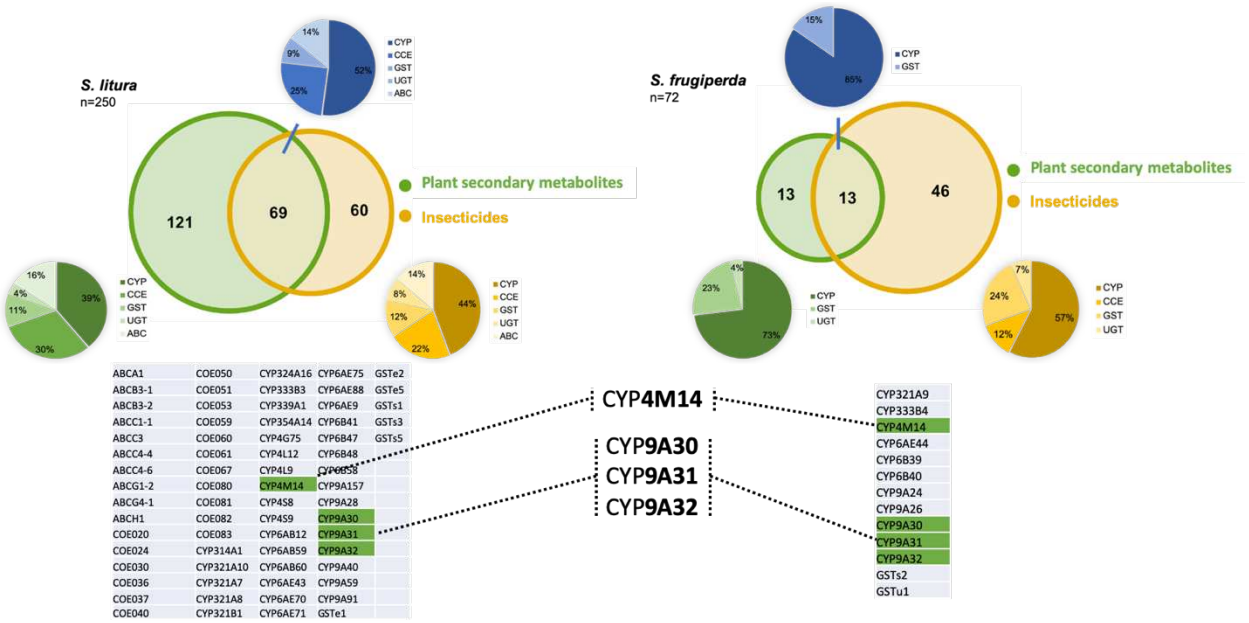

Figure S4: Appendix to Figure 1. The figure details the name of the 69 (left table in *S. litura*) and the 13 (right table in *S frugiperda*) overlapping genes between PSM and insecticide induction. Outlined in the middle are the four genes found in common in these two lists. Source: Amezian et al. 2021.

Supplementary tables

Table S1: Genomes of *Spodoptera* species compared to other Lepidoptera species.

Species	*Bombyx mori*	*Spodoptera litura*	*S. frugiperda*						*Spodoptera exigua*	*Helicoverpa armigera*	*Helicoverpa zea*	*Heliothis virescens*	*Trichoplusia ni*	*Busseola fusca*
Reference	International B. mori Genome Consortium	Cheng et al. 2017	Gouin et al. 2017		Liu et al. (Biorxiv 2019)		Zhang et al. (Biorxiv 2019)	Gimenez et al. 2019	Xiao et al. 2020	Zhang et al. 2020 (Biorxiv)	Pearce et al. 2017	Pearce et al. 2017	Fritz et al. 2017	Chen et al. 2019	Hardwick et al. 2019
Strain/population designation*	(Dazao and p50T)	Ishihara strain	Laboratory Corn strain (Guadeloupe)	Laboratory Rice strain (Florida)	Male Yunnan province (China)	Female Yunnan province (China)	Maize field population from Lusaka (Zambia)	Corn strain	Dongyang (Zhejiang, China) population	WH-S (Wuhan, China)	GR laboratory colony (Canberra, Australia)	Laboratory colony (Canberra, Australia)	Laboratory colony (NC, USA)	Cornell-1	Laboratory colony (WP, Kenya)
Accession	ASM15162v1	MTZO00000000	PRJEB13110	PRJEB13834	CNP0000513		-	PRJNA494340, PRJNA577869	WMCG00000000	WNNL00000000	PRJNA378437	PRJNA378438	NWSH00000000	PPHH00000000	VKGM00000000 PRJNA553865
Technology	-	Illumina	Illumina	Illumina	stLFR (MGI) and Hi-C	stLFR (MGI) and Hi-C	Illumina, PacBio and Hi-C	Illumina, PacBio and Hi-C	PacBio, Hi-C	Illumina, PacBio and Hi-C	454 and Illumina	454 and Illumina	Illumina and PacBio	Illumina	Illumina
Genome Assembly															
Assembly size (Mb)	431.7	438.3	437.8	371	542	531	393.25	384.46	486.3	446.80	337	341	403	333	492.9
Genome cov.	8.48	112	165	140.6	ND	ND	460	-	-	77	ND	ND	ND	337	ND
Nb of scaffolds	43,622	3 597	41 577	29 127	226	231	311	125	93	301	997	2 975	8 826	1 916	
N50 scfld size (kb)	3717.00	915.4	52.8	28.5	507	528	13 317	13 151	16 347	14 360	1 000.4	201	102.2	4 648	3.3
N90 scfld size (kb)	43.1	208.3	3.5	6.4	6.43	5.11	7 635	8 473	-	ND	175.3	52.3	21.8	1 119	
Nb of contigs	88,842	13 636	ND	ND	1 220	1 299	777	-	618	667	24 228	34 676	ND	7885	
N50 contigs size (kb)	15.5	68.4	16.9	24.3	92	83	5 607	-	1 130	3 470	18.3	12.6	ND	140.0	2 721
Quality assessment:															
BUSCO % (complete)															
genome	91.6 (73)	99.0 (98.4)	(89.8)	(94.8)	95 (85.2)	94.5 (86.7)	(98.2)	(96.6)	(93.1)	(97.9)	98.5 (97.1)	93.2 (80)	88.44 (83)	98.8 (98.4)	
protein	93.6 (87)	99.0 (97.9)	?	?			?	?	?	?	98.4 (96.0)	90.7 (82)	?	97.8 (97.3)	
Detox genes															
CYP	**79**	**138**	**117**	**136**	*200*		ND	ND	169	ND	114	108	ND	ND	ND
CCE	**78**	**110**	**93**		*84*		ND	ND	98	ND	71	67	ND	ND	ND
GST	**23**	**47**	**46**		*60*		ND	ND	59	ND	42	40	ND	ND	ND
UGT	**44**	**ND**	**47**		*31*		ND	ND	ND	ND	46	42	ND	ND	ND
ABC	**51**	**54**	**18 (partial: 8 ABCB, 10 ABCC)**		*66*		ND	ND	79	ND	54	54	ND	ND	ND

Supplementary material - Summary of selected detox genes recently (2010-2020) associated with insecticide resistance or plant secondary metabolites detoxification and significantly upregulated in qRT-PCR studies. Constitutively overexpressed detox genes in resistant phenotypes are marked by a *. Underlined genes have been evaluated by genetic-functional methods (CRISPR/Cas9, RNAi, ectopic expression). Detox genes in bold have been functionally expressed and validated as insecticide metabolizing enzymes. Italic genes were obtained from RNAseq data and were not validated by QRT-PCR. Expression profiles were assessed in either one of the insect tissues (then not specified) or in several ones : fat body (FB), midgut (MG) or Malpighian tubules (MT). When two genes had identical names, or were predicted, the gene ID was added (e.g. CYP6B38-SWUSl0090940). References followed by "sq" have used semi-quantitative methods to estimate mRNA transcript levels, those followed by "ma" have used microarrays methods (e.g. #42↑ma)

Pest species	Xenobiotics	P450s	CCEs	GSTs	UGTs	ABCs
S. litura	**PSM**					
	allyl-isothiocyanate			**GSTe1** (#35↑)		
	asatone	CYP6AB14 (#14↓)		GSTe1 (#14↑) GSTo1 (#14↑)		
	cinnamic acid	CYP9A40 (#3↑) CYP321A9 (#6↑)				
	coumarin	CYP6B58 (#4↑) CYP6AB14 (#5↑) CYP321A7 (#6↑) CYP321A9 (#6↑) CYP6AB60 (#10↑)				
	flavone	CYP6B48 (#4↑, #56↑), CYP6B58 (#4↑), CYP6AB14 (#5↑), CYP321A7 (#6↑, #56↑), CYP321A8(#56↑), CYP321A9 (#6↑), CYP321A10 (#56↑), CYP321B1 (#56↑), CYP6AE48 (#56↑), CYP6AE43 (#56↑), CYP314A1 (#56↑), CYP9A39 (#56↑), CYP321A12 (#56↑), CYP333A6 (#56↑)	CXE4 (#56↑), CXE7 (#56↑), CXE14-2 (#56↑), CXE14-1 (#56↑), CarE (#56↑), CXE8 (#56↑)	GST1 (#56↑), GSTo2 (#56↑), GSTd2 (#56↑), GSTs6 (#56↑), GSTz2 (#56↑), GST1-1 (#56↑), GSTs1 (#56↑)	UGT40F4 (#56↑), UGT40R3 (#56↑), UGT40U1 (#56↑), UGT40M2 (#56↑), UGT33T3 (#56↑), UGT33V3 (#56↑), UGT33J2 (#56↑), UGT33B15 (#56↑), UGT33B13 (#56↑), UGT33B14 (#56↑), UGT41B1 (#56↑), UGT42B2 (#56↑), UGT42C2 (#56↑), UGT46A4 (#56↑)	
	indole-3-carbinol			**GSTe1** (**#35**↑, #45↑)		
	isoasatone A	CYP321B1 (#14↓) CYP321A7 (#14↓) CYP6B47 (#14↓) CYP6AB14 (#14↓) CYP9A39 (#14↓)		GSTe1 (#14↓) GSTo1 (#14↑)		
	jasmonic acid	CYP321A7 (#6↑) CYP321A9 (#6↑)				
	methyl jasmonate	CYP321A7 (#6↑) CYP321A9 (#6↑)				
	methyl salicylate	CYP321A7 (#6↑) CYP321A9 (#6↑)				
	quercetin	CYP9A40 (#2↑) CYP6B58 (#4↑)				

S. litura	ricin	*CYP9A31 (#32↓), CYP321A7 (#32↓), CYP6B41 (#32↓), CYP6AE71 (#32, ↑MG, ↓MT), CYP9A32 (#32↓), CYP9A91 (#32↓), CYP9A91 (#32↓), CYP9A30 (#32↓), CYP9A29 (#32, ↑MG, ↓MT), CYP9A28 (#32↓), CYP9A27 (#32↓), CYP9A26 (#32↑), CYP9A25 (#32↓), CYP9A58 (#32, ↑MG, ↓MT), CYP9A59 (#32↓), CYP9A60 (#32↓), CYP321A9 (#32, ↑FB, ↓MG, MT), CYP321A8 (#32, ↑MG, ↓MT), CYP321B1 (#32↑), CYP321B4 (#32↓), CYP6B48 (#32↑), CYP6B40 (#32↓), CYP6AE138 (#32↓), CYP6AE9 (#32↓), CYP6AE70 (#32↓), CYP6AE74 (#32, ↑MG, ↓MT), CYP340AX8 (#32↑), CYP340AA1 (#32↑), CYP4M14 (#32↓), CYP4M15 (#32↓), CYP4M17(#32, ↑MT, ↓MG), CYP4M18 (#32↓), CYP4L12 (#32, ↑MG, ↓FB), CYP4L9 (#32, ↑FB, MG, ↓MT), CYP4L13 (#32↑), CYP341B19 (#32↑), CYP341B18 (#32↑), CYP333B4 (#32↓), CYP6B58 (#32↓), CYP337B5 (#32↓), CYP333B3 (#32↓), CYP306A1 (#32, ↑FB, ↓MG), CYP6AB61 (#32↓), CYP6AE43 (#32↓), CYP324A16 (#32↑), CYP6AB58 (#32, ↑MT, ↓MG), CYP324A18 (#32↓), CYP18A1 (#32, ↑FB, MT, ↓MG), CYP332A1 (#32↓), CYP9G3 (#32↑), CYP324A16 (#32↓), CYP18B1 (#32, ↑FB, ↓MG), CYP428A1 (#32↓), CYP6AW1 (#32↓), CYP9A157 (#32↓), CYP9A158 (#32↓), CYP6AN4 (#32↓), CYP4G75 (#32, ↑MG, MT, ↓FB), CYP4CG18 (#32↓), CYP4G106 (#32↓), CYP301B1 (#32↑), CYP302A1 (#32↑), CYP305B1 (#32↑), CYP6AB59 (#32↑), CYP354A14 (#32, ↑MG, ↓MT), CYP6AE88 (#32, ↑MG, ↓MT), CYP4S8 (#32↑), CYP6AB12 (#32, ↑MG, ↓MT), CYP4S9 (#32↑), CYP6AB60 (#32↑)*	*COE057 (#32↓), COE058 (#32↓), COE001 (#32, ↑MT, ↓MG), COE003 (#32↑), COE023 (#32↓), COE043 (#32↓), COE085 (#32↓), COE109 (#32↓), COE090 (#32↓), COE004 (#32↑), COE105 (#32↑), COE108 (#32↑), COE086 (#32↑), COE079 (#32↑), COE107 (#32↑), COE075 (#32, ↑MG, ↓MT), COE072 (#32↑), COE092 (#32↑), COE040 (#32↑), COE024 (#32, ↑MG, ↓FB), COE088 (#32↑), COE037 (#32, ↑MG, ↓FB,MT), COE026 (#32↑), COE028 (#32↑), COE076 (#32↓), COE005 (#32↓), COE039 (#32↓), COE021 (#32↓), COE038 (#32↓), COE014 (#32↓), COE041 (#32↓), COE097 (#32↓), COE102 (#32↓), COE062 (#32↓), COE047 (#32↓), COE087 (#32↓), COE025 (#32↓), COE016 (#32↓), COE030 (#32↓), COE060 (#32↓), COE061 (#32↓), COE095 (#32↓), COE007 (#32↓), COE008 (#32↓), COE048 (#32↓), COE049 (#32↓), COE051 (#32↓), COE017 (#32↓), COE018 (#32↓), COE019 (#32↓), COE020 (#32↓), COE064 (#32↓), COE100 (#32, ↑FB, ↓MG,MT), COE055 (#32↓), COE059 (#32↓), COE067 (#32↓), COE081 (#32↓), COE082 (#32↓), COE083 (#32↓), COE050 (#32 ↑MG,MT, ↓FB), COE053 (#32↓), COE036 (#32↓), COE080 (#32↓), COE022 (#32↓), COE042 (#32↓), COE094 (#32↓), COE063 (#32↓), COE098 (#32↓), COE074 (#32↓)*	*GSTe17 (#32↑), GSTe19 (#32↓), GSTe22 (#32↑), GSTe20 (#32↓), GSTe6 (#32↓), GSTe5 (#32↓)*		*ABCA1 (#32↑), ABCA2 (#32↑), ABCG8 (#32↑), ABCG5 (#32↑), ABCC1-1 (#32↑), ABCG-ok (#32, ↑MG, ↓MT), ABCA3-2 (#32↑), ABCG-bw (#32, ↑MG, ↓MT), ABCG-st (#32, ↑MG, ↓MT), ABCB3-1 (#32, ↑MG, ↓MT), ABCE1 (#32↑), ABCC4-4 (#32↑), ABCB3-2 (#32, ↑MG, ↓MT), ABCG4-1 (#32↑), ABCC3 (#32↑), ABCA3-1 (#32↓), ABCB8 (#32↓), ABCG1-1 (#32↓), ABCC10 (#32↓), ABCD2 (#32↓), ABCB1-1 (#32, ↑MT, ↓MG), ABCF2 (#32↓), ABCC4-5 (#32, ↑MT, ↓MG), ABCG4-3 (#32↓), ABCG4-2 (#32↓), ABCA3-3 (#32↓), ABCG1-2 (#32↓), ABCH3 (#32↓), ABCB10 (#32↓), ABCC1-2 (#32↓), ABCG1-4 (#32, ↑FB, ↓MG), ABCD3 (#32, ↑FB, ↓MG), ABCC2 (#32↓), ABCC9 (#32↓), ABCC4-6 (#32↓), ABCA3-4 (#32↓), ABCH1 (#32↑)*
	salicylic acid	CYP321A7 (#6↑)				
	tomatine	CYP6AB60 (#10↑), CYP324A6 (#22↑), CYP340AB1 (#22↑), CYP4G75 (#22↑), CYP4L10 (#22↑), CYP4S9v1 (#22↑), CYP6B6 (#22↑), CYP339A1 (#22↑)	CCE016a (#22↑), CCE025a (#22↑), CCE006a (#22↑)	GSTe11 (#22↑), GSTe13 (#22↑), GSTe2 (#22↑), GSTs1 (#22↑), GSTs2 (#22↑), GSTs3 (#22↑), GSTs5 (#22↑), GSTz2 (#22↑)	UGT33B13 (#22↑), UGT33F4 (#22↑), UGT33J2 (#22↑), UGT33T2 (#22↑), *UGT40Q1* (#22↑), UGT40U1 (#22↑), UGT42C1 (#22↑)	ABCA2 (#22↑), ABCB6 (#22↑), ABCC4 (#22↑), ABCF4 (#22↑), ABCG1 (#22↑), ABCG4 (#22↑)

S. litura	xanthotoxin	CYP6B58 (#4↑, *#32*↑, #59↑) CYP6AB14 (#5↑) CYP321A7 (#6↑, *#32*↑, #59↑) CYP321A9 (#6↑, *#32*↑) CYP6AB60 (#10↑, *#32*↑) CYP6B50 (#13↑), *CYP9A31 (#32*↑*), CYP6B41 (#32*↑*), CYP6AE71 (#32*↑*), CYP9A32 (#32, *↑*MG, ↓FB,MT), CYP9A91 (#32, *↑*MG, ↓MT), CYP9A91 (#32*↑*), CYP9A30 (#32*↑*), CYP9A29 (#32*↓*), CYP9A28 (#32*↑*), CYP9A27 (#32*↑*), CYP9A26 (#32, *↑*FB, ↓MG), CYP9A25 (#32, *↑*MG, ↓FB, MT), CYP9A59 (#32*↑*), CYP9A60 (#32, *↑*MG, ↓MT), CYP321A8 (#32*↑*, #59↑), CYP321A10 (#32*↑*, #59↑), CYP321B1 (#32*↑*), CYP321B8 (#32*↑*), CYP321B9 (#32, *↑*FB, ↓MT), CYP321B4 (#32*↓*), CYP321B4 (#32*↓*), CYP6B47 (#32*↑*, #59↑), CYP6B48 (#32*↑*, #59↑, #4↑), CYP6B40 (#32, *↑*FB, ↓MT), CYP6AE138 (#32*↑*), CYP6AE9 (#32, *↑*FB, MG, ↓MT), CYP6AE70 (#32, *↑*MG, ↓MT, #59↑), CYP6AE74 (#32*↑*MG, ↓MT), CYP340AX8 (#32*↓*), CYP340K14 (#32*↓*), CYP4M15 (#32*↓*), CYP4M18 (#32*↑*), CYP4L12 (#32*↑*), CYP4L9 (#32*↑*), CYP4L13 (#32*↑*), CYP341B17 (#32*↓*), CYP337B5 (#32↓), CYP333B3 (#32*↑*), CYP306A1 (#32*↑*), CYP6AB61 (#32*↑*), CYP314A1 (#32*↑*MG, ↓FB), CYP6AE43 (#32*↑*, #59*↑*), CYP321A15 (#32*↑*), CYP324A16 (#32*↑*), CYP6AB58 (#32*↑*), CYP324A18 (#32*↑*), CYP18A1 (#32*↓*), CYP332A1 (#32*↓*), CYP324A16 (#32, *↑*FB, ↓MG, MT), CYP18B1 (#32*↓*), CYP428A1 (#32*↓*), CYP6AW1 (#32*↓*), CYP9A157 (#32, *↑*MT, ↓FB, MG), CYP6AE75 (#32*↑*), CYP6AN4 (#32*↓*), CYP4G75 (#32*↓*), CYP4CG18 (#32*↓*), CYP4G106 (#32, *↑*MG, ↓FB), CYP4G74 (#32*↓*), CYP4G109 (#32*↓*), CYP6AB59 (#32*↑*), CYP6AE88 (#32*↓*), CYP4S8 (#32*↓*), CYP6AB12 (#32*↓*), CYP4S9 (#32*↓*), CYP6AE48 (#59↑), CYP6AE68 (#59↑), CYP6B46	*COE023 (#32*↓*), COE043 (#32*↓*), COE085 (#32*↓*), COE109 (#32*↓*), COE090 (#32*↓*), COE079 (#32*↓*), COE075 (#32*↓*), COE072 (#32*↓*), COE092 (#32*↓*), COE024 (#32, *↑*MG, ↓FB), COE088 (#32*↑*), COE037 (#32*↑*), COE026 (#32*↑*), COE028 (#32*↑*), COE035 (#32*↓*), COE076 (#32*↓*), COE021 (#32*↓*), COE038 (#32*↓*), COE041 (#32*↑*), COE097 (#32*↑*), COE102 (#32*↑*), COE047 (#32*↑*), COE087 (#32*↑*), COE025 (#32, *↑*MG, ↓MT), COE030 (#32*↑*), COE060 (#32*↑*), COE061 (#32*↑*), COE095 (#32*↑*), COE008 (#32*↑*), COE048 (#32*↑*), COE049 (#32*↑*), COE051 (#32*↑*), COE052 (#32*↑*), COE054 (#32*↑*), COE017 (#32, *↑*MG, ↓MT), COE018 (#32*↑*), COE019 (#32*↑*), COE020 (#32*↑*), COE064 (#32*↑*), COE100 (#32, *↑*MG, ↓MT), COE055 (#32, *↑*MG, ↓MT), COE059 (#32*↑*), COE067 (#32*↑*), COE056 (#32*↑*), COE065 (#32*↑*), COE066 (#32*↑*), COE081 (#32*↑*), COE082 (#32*↑*), COE083 (#32*↑*), COE050 (#32, *↑*MG,FB ↓MT), COE053 (#32, *↑*MG, ↓MT), COE036 (#32*↑*), COE080 (#32*↑*), COE022 (#32*↑*), COE042 (#32*↑*), COE094 (#32*↑*), COE098 (#32*↓*), COE074 (#32*↓*), CarE(#59↑), CXE4(#59↑), CXE7(#59↑), CXE8(#59↑), CXE14-1(#59↑), CXE14-2(#59↑)	*GSTe17 (#32*↑*), GSTe18 (#32*↑*), GSTe19 (#32*↑*), GSTe22 (#32*↑*), GSTe23 (#32, *↑*FB, ↓MG), GSTe16 (#32*↑*), GSTe20 (#32*↑*), GSTe21 (#32*↑*), GSTe6 (#32*↑*), GSTe5 (#32*↑*), GSTe7 (#32*↑*),* GSTe1 (#44↑sq), GSTe13(#59↑), GSTs1 (#44↑sq), GSTo1 (#44↑sq, #59↑), GSTs5(#59↑), GSTs6(#59↑), GSTd2(#59↑), GSTd4(#59↑), GSTz2(#59↑), GST1(#59↑), GST1-1(#59↑), GST1-2(#59↑)	UGT40F4 (#59↑), UGT42C2 (#59↑), UGT33B14 (#59↑), UGT33B15 (#59↑), UGT33T3 (#59↑), UGT33J2 (#59↑), UGT33V3 (#59↑)	
	Z-ligustilide			GSTs1 (#8↑sq)		
	Insecticides					
	α-cypermethrin	CYP6B47 (#1*↑)				
	β-cypermethrin	CYP321B1 (#7↑) CYP6AB12 (#12↑)				
	chlorpyrifos	CYP321B1 (#7↑)		**GSTe1** (#44↑sq, **#41**↑protein, #34*↑, #45↑), GSTe3 (#44↑sq, #34*↑), GSTe10 (#34*↑), GSTe15 (#34*↑), GSTo2 (#34*↑), GSTs1 (#44↑sq), GSTs3 (#44↑sq), GSTs5 (#34*↑), MGST2 (#34*↑), MGST3 (#34*↑)		

S. litura	DDT			GSTe2 (#43↑sq), GSTe3 (#43↑sq)		
	deltamethrin	CYP9A40 (#3↑)		GSTe1 (#45↑), GSTe2 (#43↑)		
	fenvalerate	CYP6B47 (#1*↑)				
	fluralaner	CYP4M14 (#9↑) CYP6B47 (#9↑) CYP6B48 (#9↑) CYP6B58 (#9↑), CYP333B3(gene11879) (#18↑), CYP9A157(gene1218) (#18↑), CYP321A8(gene9333) (#18↑), CYP367A17(gene13430) (#18↑), CYP6AE97(gene13788) (#18↓), CYP340L27(gene10843) (#18↓), CYP18B1(gene5961) (#18↓), *CYP304A1-9509 (#18↑), CYP428A1(gene2558) (#18↑), CYP341B16(gene3595) (#18↑), CYP4S9(gene9175) (#18↑), CYP4S8(gene9174) (#18↑), CYP4L12(gene11881) (#18↑), CYP341B17(gene3598) (#18↑), CYP340AX1(gene10859) (#18↑), CYP6AB12(gene4502) (#18↑), CYP9A157(gene17041) (#18↑), CYP9G17(gene12726) (#18↑), CYP9G17(gene15894) (#18↑)*	*COE099(gene8407) (#18↑), COE030(gene5053) (#18↑), COE020(gene15885) (#18↑)*	GSTe1 (#9↑) GSTe3 (#9↓) GSTe4 (#9↑) GSTe5 (#9↑), GST2-like-7753 (#18↑)		

S. litura	imidacloprid	CYP9A31 (#32↑), CYP321A7 (#32, ↑FB,MG, ↓MT), CYP6B41 (#32↑), CYP6AE71 (#32, ↑MG, ↓MT), *CYP9A32 (#32, ↑MT, ↓FB), CYP9A91 (#32, ↑FB, ↓MT), CYP9A91 (#32↓), CYP9A30 (#32↑), CYP9A29 (#32↓), CYP9A28 (#32, ↑MT, ↓MG), CYP9A26 (#32↓), CYP9A59 (#32, ↑MT, ↓MG), CYP321A9 (#32↓), CYP321A8 (#32↓), CYP321A10 (#32↑), CYP321B1 (#32↑), CYP321B4 (#32↓), CYP321B4 (#32↑), CYP6B47 (#32↓), CYP6B48 (#32, ↑MG, ↓MT), CYP6B40 (#32↓), CYP6AE138 (#32↓), CYP6AE9 (#32, ↑MG, ↓MT), CYP6AE70 (#32, ↑MG, ↓MT), CYP6AE74 (#32↓), CYP340AD3 (#32↓), CYP340AX8 (#32↓), CYP340A (#32↑), CYP4M15 (#32↓), CYP4M17(#32↓), CYP4M18 (#32↓), CYP4L12 (#32↑), CYP4L9 (#32↑), CYP4L13 (#32↓), CYP333B4 (#32↓), CYP6B58 (#32↓), CYP333B3 (#32↑), CYP306A1 (#32↓), CYP6AB61 (#32↓), CYP314A1 (#32↑), CYP6AE43 (#32, ↑FB, ↓MT), CYP321A15 (#32↓), CYP324A16 (#32↓), CYP4AV2 (#32↓), CYP18A1 (#32↓), CYP332A1 (#32↓), CYP324A16 (#32, ↑MT, ↓MG), CYP428A1 (#32, ↑FB, ↓MG), CYP9A157(#32↑), CYP6AE75 (#32↑), CYP9A158 (#32↑), CYP6AN4 (#32↓), CYP4G75 (#32, ↑MG, MT, ↓FB), CYP4G74 (#32↑), CYP4G109 (#32↑), CYP6AB59 (#32↑), CYP354A14 (#32↓), CYP6AE88 (#32, ↑MT, ↓MG), CYP4S8 (#32↑), CYP6AB12 (#32↑), CYP4S9 (#32↓), CYP6AB60 (#32↑)*	COE057 (#32↑), COE058 (#32↑), *COE023 (#32↓), COE043 (#32↓), COE090 (#32↑), COE107 (#32↓), COE072 (#32↓), COE092 (#32↓), COE040 (#32↑), COE024 (#32↑), COE088 (#32↓), COE037 (#32, ↑MT, ↓MG), COE026 (#32↓), COE035 (#32↓), COE021 (#32↓), COE038 (#32↓), COE014 (#32↓), COE041 (#32↓), COE097 (#32↓), COE102 (#32↓), COE030 (#32↑), COE060 (#32↑), COE061 (#32↑), COE007 (#32↓), COE008 (#32↓), COE051 (#32, ↑MG, ↓MT), COE052 (#32↓), COE017 (#32↓), COE059 (#32↑), COE067 (#32↑), COE081 (#32↑), COE082 (#32↑), COE083 (#32, ↑MT, ↓MG), COE050 (#32, ↑MG,MT, ↓FB), COE053 (#32↑), COE036 (#32↑), COE080 (#32↑), COE042 (#32↓), COE063 (#32↑), COE098 (#32, ↑MT, ↓FB,MG), COE074 (#32↑)*	GSTe20 (#32↓) GSTe07 (#32↓), *GSTe17 (#32↓), GSTe18 (#32↓), GSTe19 (#32↓), GSTe23 (#32↓), GSTe16 (#32↓), GSTe5 (#32, ↑FB, ↓MG,MT), GSTe7 (#32↓)*		*ABCA1 (#32↑), ABCC1-1 (#32↑), ABCG-bw (#32↓), ABCG-st (#32↓), ABCB3-1 (#32, ↑MT, ↓MG), ABCE1 (#32↓), ABCC4-4 (#32↑), ABCB3-2 (#32, ↑MT, ↓MG), ABCG4-1 (#32, ↑MT, ↓MG,FB), ABCC3 (#32, ↑MT, ↓MG,FB), ABCC4-2 (#32↓), ABCG-w (#32↓), ABCA3-1 (#32↑), ABCC10 (#32↓), ABCD2 (#32, ↑MT, ↓MG), ABCB1-1 (#32↓), ABCC4-5 (#32↓), ABCG4-3 (#32↓), ABCG4-2 (#32↓), ABCA3-3 (#32↓), ABCG1-2 (#32↓), ABCH3 (#32↓), ABCB10 (#32↓), ABCC1-2 (#32↓), ABCG1-4 (#32↓), ABCD3 (#32↓), ABCB6 (#32↓), ABCB7 (#32↓), ABCC4-6 (#32↓), ABCG1-5 (#32↑), ABCH2 (#32↑), ABCA3-4 (#32↑), ABCH1 (#32↑)*
	indoxacarb	*CYP341B (#27*↑), CYP6B38 (#27*↑), CYP305B1 (#27*↓), CYP428A1 (#27*↑), CYP341B15 (#27*↑), CYP341B22 (#27*↑), CYP4S8 (#27*↑), CYP332A1 (#27*↑), CYP6B38 (#27*↑), CYP321A10 (#27*↑), CYP339A1 (#27*↑), CYP421B1 (#27*↑), CYP340A (#27*↑), CYP340A (#27*↑), CYP340K14 (#27*↑), CYP333B3 (#27*↑), CYP367A12 (#27*↑), CYP6AE43 (#27*↑), CYP367B11 (#27*↑), CYP324A16 (#27*↑), CYP338A1 (#27*↓), CYP18B1 (#27*↓), CYP301B1 (#27*↓), CYP301A1 (#27*↓)*	*COE090 (#27*↑), COE073 (#27*↑), COE076 (#27*↓), COE062 (#27*↓), COE093 (#27*↑), COE050 (#27*↑), COE009 (#27*↑), COE111 (#27*↑), COE074 (#27*↑), COE067 (#27*↓), COE091 (#27*↓)*	*GST20 (#27*↑), GST38 (#27*↑), GST42 (#27*↓)*	*UGT11 (#27*↓), UGT01 (#27*↑), UGT02 (#27*↑), UGT03 (#27*↑), UGT04 (#27*↑), UGT05 (#27*↑), UGT06 (#27*↑), UGT07 (#27*↑), UGT08 (#27*↑), UGT09 (#27*↑), UGT10 (#27*↑),*	*ABCG1-2 (#27*↑), ABCB7 (#27*↑), ABCG5 (#27*↓), ABCH1 (#27*↑), ABCB3-1 (#27*↑), ABCC4-2 (#27*↑), ABCC4-1 (#27*↑), ABCB3-2 (#27*↑), ABCC4-6 (#27*↑), ABCC3 (#27*↑), ABCG1-3 (#27*↓), ABCG8 (#27*↓)*
	lambda-cyhalothrin	CYP6AB12 (#20↑)				
	methomyl	CYP321B1 (#7↑)				
	methoxyfenozide	CYP9A40 (#3↑)				
	tebufenozide (RH5992)			GSTe2 (#43↑)		
	Herbicides					
	trifluralin	CYP6B48 (#11↑) CYP321B1 (#11↑) CYP9A40 (#11↓)	CarE-EU783914 (#11↑)	GSTe2 (#11↑) GSTe3 (#11↑)		
	MCPA-Na	CYP6B48 (#11↑) CYP321B1 (#11↑) CYP9A40 (#11↓)		GSTe2 (#11↑) GSTe3 (#11↑)		
	Heavy metals					
	Pb (lead)	CYP9A39 (#2↑) CYP6B47 (#2↑)				

S. litura	Cu (copper)	CYP6AB12 (#12↑) CYP6B50 (#13↑)				
	CdCl2			GSTe1 (#41↑protein)		
S. exigua	**Plant secondary metabolites**					
	gossypol	CYP6AB14 (#25↑), CYP9A12 (#25↑), CYP9A98 (#25↑)				
	quercetin	CYP9A11 (#15↓), CYP6AE10 (#16↑)				
	sinigrin	CYP9A9 (#33↑), CYP6B(#33↑) CYP4G37(#33↑)				
	tannin	CYP9A11 (#15↓)				
	xanthotoxin	CYP9A10 (#23↑)				
	Insecticides					
	abamectin	CYP306A1 (#31↓), CYP305B1 (#31↓), CYP18A1 (#31↓), CYP354A14 (#31↓), CYP321B1 (#31↓), CYP321A8 (#31↓), CYP6B31 (#31↓), CYP6AN4 (#31↓), CYP367B1 (#31↓), CYP340AB1 (#31↓), CYP4M15 (#31↓), CYP4L7 (#31↓), CYP4L9 (#31↓), CYP4G75 (#31↓), CYP339A1 (#31↓), CYP333B40 (#31↓), CYP333B4 (#31↓), CYP333A12 (#31↓), CYP337B5 (#31↑), CYP324A6 (#31↑), CYP324A1 (#31↑), CYP9A9 (#31↑), CYP9A10 (#31↑), CYP9A27 (#31↑), CYP9A98 (#31↑), CYP6AE70 (#31↑), CYP6AE74 (#31↑), CYP6AE47 (#31↑), CYP6AB14 (#31↑), CYP6AB31 (#31↑), CYP6AB61 (#31↑), CYP367A1 (#31↑), CYP340K4 (#31↑), CYP4S9 (#31↑), CYP301B1 (#31↑)			UGT50A5 (#31↓), UGT44A5 (#31↓), UGT42C2 (#31↓), UGT40U2 (#31↓), UGT40D3 (#31↓), UGT39B4 (#31↓), UGT33V4 (#31↓), UGT33V3 (#31↓), UGT33V2 (#31↓), UGT33V1 (#31↓), UGT33F7 (#31↓), UGT33F6 (#31↓), UGT33F5 (#31↓), UGT33B16 (#31↓), UGT33B14(#31↓), UGT40D5 (#31↑), UGT33T3 (#31↑),	ABCB1 (#41)

S. exigua	chlorantraniliprole	CYP9A9 (#33↑), CYP6B(#33↑) CYP4G37(#33↑), CYP341A11 (#31↓), CYP332A1 (#31↑), CYP321A8 (#31↑), CYP321A9 (#31↑), CYP321A16 (#31↑), CYP9A9 (#31↑), CYP9A10 (#31↑), CYP6AE47 (#31↑), CYP6AE97 (#31↑), CYP6AE10 (#31↑), CYP6AB31 (#31↑), CYP4S9 (#31↑), CYP4S8 (#31↑), CYP4M18 (#31↑), CYP9A21v4 (#28↑), Unigene0038246-SlittCYP333B3 (#28↑), Unigene0043936-SlittCYP340AB1 (#28↑), CYP9A21v3 (#28↑), Unigene0031793-SlittCYP4L12 (#28↑), CYP9A21v1 (#28↑), CYP9A21v2 (#28↑), Unigene0039876-MbCYP4L4 (#28↑), Unigene0032146-SlittCYP6AE48 (#28↓), Unigene0027891-SfCYP4G74 (#28↓), *Unigene0031082-SeCYP6B (#28↑), Unigene0027547-SlittCYP4G75 (#28↓), Unigene0018587-HaCYP9AJ3 (#28↓), Unigene0009782-HaCYP321B1 (#28↓), Unigene0025013-HaCYP4G9 (#28↓), Unigene0025012-PxCYP4G15 (#28↓), Unigene0034186-BmCYP6B1-like (#28↓), Unigene0009280-BmCYP339A1 (#28↓)*	*Unigene0045545-BmCOEae17 (#28↑)*	GSTe6 (#24↑), GSTe14 (#24↑), GSTe9 (#24↑), GSTe1 (#24↑), GSTd1 (#24↑), GSTs6 (#24↑), GSTe7 (#24↑), GSTe8 (#24↑), GSTe11 (#24↑), GSTe12 (#24↑), GSTu2 (#24↑), GSTd2 (#24↑), GSTd3 (#24↑), GSTo1 (#24↑), GSTo2 (#24↑), GSTs5(#24↑), GSTs3 (#24↑), *Unigene0032958-SlGSTe8 (#28↑), Unigene0050101-SlGSTs5 (#28↓), Unigene0017928-CcGSTo-like2 (#28↓), Unigene0010711-probPxGST (#28↓), Unigene0002456-MultisppGST (#28↓), Unigene0013043-BiGST-DHAR1-mitochondrial-like (#28↓), Unigene0013042-BiGST-DHAR1-mitochondrial-like (#28↓), Unigene0005214-SlGSTe11 (#28↓), Unigene0015736-SlmicrosomalGST1-5 (#28↓)*	UGT40U2 (#31↓), UGT42B5 (#31↑), UGT40D5 (#31↑), UGT33V4 (#31↑), UGT33T3 (#31↑), UGT33J3 (#31↑), *Unigene0036987-SlittUGT33F4 (#28↑), Unigene0036988-SlittUGT33F4 (#28↑)*	
	chlorpyrifos	CYP4L7 (#57*↑), CYP6AB12 (#57*↑), CYP6AB61 (#57*↑), CYP6AE10 (#57*↑), CYP6AE68 (#57*↑), CYP6AE70 (#57*↑), CYP6AE74 (#57*↑), CYP6B31 (#57*↑), CYP6B68 (#57*↑), CYP9A11 (#57*↑), CYP9A27 (#57*↑), CTP9A97 (#57*↑), CYP9A98 (#57*↑), **CYP321A8** (#57*↑), CYP321A9 (#57*↑), CYP321A16 (#57*↑), CYP321B1 (#57*↑), CYP332A1 (#57*↑), CYP340K4 (#57*↑), CYP341A11 (#57*↑), CYP341B27 (#57*↑)		**GSTe6** (#24↑, **#21***↑), GSTe8 (#24↑), GSTe14 (#24↑), GSTe9 (#24↑, #21*↑), GSTe1 (#24↑, #21*↑), GSTd1 (#24↑), GSTd2 (#24↑), GSTs6 (#24↑), GSTe7 (#24↑), GSTe10 (#24↑), GSTe11 (#24↑), GSTe12 (#24↑), GSTu2 (#24↑), **GSTd3** (#24↑, **#21***↑), GSTo1 (#24↑), **GSTo2** (#24↑, **#21***↑), GSTo3 (#24↑), GSTs3 (#24↑), GSTs1 (#21*↑)		
	α-cypermethrin	CYP9A105 (#29↑), CYP9A10 (#23↑),CYP4L7 (#57*↑), CYP6AB12 (#57*↑), CYP6AB61 (#57*↑), CYP6AE10 (#57*↑), CYP6AE68 (#57*↑), CYP6AE70 (#57*↑), CYP6AE74 (#57*↑), CYP6B31 (#57*↑), CYP6B68 (#57*↑), CYP9A11 (#57*↑), CYP9A27 (#57*↑), CTP9A97 (#57*↑), CYP9A98 (#57*↑), **CYP321A8** (#57*↑), CYP321A9 (#57*↑), CYP321A16 (#57*↑), CYP321B1 (#57*↑), CYP332A1 (#57*↑), CYP340K4 (#57*↑), CYP341A11 (#57*↑), CYP341B27 (#57*↑)				

S. exigua	deltamethrin	CYP9A105 (#29↑), CYP6AB14 (#25↑), CYP9A12 (#25↑), CYP9A98 (#25↑), CYP4L7 (#57*↑), CYP6AB12 (#57*↑), CYP6AB61 (#57*↑), CYP6AE10 (#57*↑), CYP6AE68 (#57*↑), CYP6AE70 (#57*↑), CYP6AE74 (#57*↑), CYP6B31 (#57*↑), CYP6B68 (#57*↑), CYP9A11 (#57*↑), CYP9A27 (#57*↑), CTP9A97 (#57*↑), CYP9A98 (#57*↑), **CYP321A8** (#57*↑), CYP321A9 (#57*↑), CYP321A16 (#57*↑), CYP321B1 (#57*↑), CYP332A1 (#57*↑), CYP340K4 (#57*↑), CYP341A11 (#57*↑), CYP341B27 (#57*↑)				
	fenvalerate	CYP9A105 (#29↑)				
	indoxacarb	CYP367B1 (#31↓), CYP341A11 (#31↓), CYP333B40 (#31↓), CYP333A12 (#31↓), CYP332A1 (#31↑), CYP321A8 (#31↑), CYP321A9 (#31↑), CYP321A16 (#31↑), CYP9A9 (#31↑), CYP9A10 (#31↑), CYP9A98 (#31↑), CYP6AE70 (#31↑), CYP6AE74 (#31↑), CYP6AE47 (#31↑), CYP6AE97 (#31↑), CYP6AE10 (#31↑), CYP6AB31 (#31↑), CYP4S9 (#31↑)			UGT40F4 (#31↓), UGT39B4 (#31↓), UGT46A7 (#31↑), UGT42B5 (#31↑), UGT40D5 (#31↑), UGT33T3 (#31↑), UGT33J3 (#31↑)	
	isoprocarb			GSTo (#36↑)		
	lambda-cyhalothrin	CYP321A8 (#31↑), CYP321A9 (#31↑), CYP321A16 (#31↑), CYP9A9 (#31↑), CYP9A10 (#31↑), CYP9A98 (#31↑), CYP6AE74 (#31↑), CYP6AE47 (#31↑), CYP6AE10 (#31↑, #16↑), CYP6AB31 (#31↑), CYP340K4 (#31↑), CYP4S8 (#31↑), CYP4M18 (#31↑),		GSTe6 (#24↑), GSTe8 (#24↑), GSTe14 (#24↑), GSTe9 (#24↑), GSTe1 (#24↑), GSTd1 (#24↑), GSTs6 (#24↑), GSTe2 (#24↓), GSTe3 (#24↓), GSTe4 (#24↓)	UGT50A5 (#31↓), UGT42B5 (#31↑), UGT40D5 (#31↑), UGT33T3 (#31↑), UGT33J3 (#31↑)	
	metaflumizone	CYP354A14 (#31↓), CYP339A1 (#31↓), CYP333A12 (#31↓), CYP324A6 (#31↑), CYP321A8 (#31↑), CYP321A9 (#31↑), CYP321A16 (#31↑), CYP9A9 (#31↑), CYP9A10 (#31↑), CYP6AE68 (#31↑), CYP6AE70 (#31↑), CYP6AE47 (#31↑), CYP6AE10 (#31↑), CYP6AB31 (#31↑), CYP367B1 (#31↑), CYP367A1 (#31↑), CYP340K4 (#31↑), CYP4S9 (#31↑), CYP4S8 (#31↑)			UGT40U2 (#31↓), UGT39B4 (#31↓), UGT48D1 (#31↑), UGT42B5 (#31↑), UGT40R4 (#31↑), UGT40D5 (#31↑), UGT33T3 (#31↑), UGT33J3 (#31↑)	
	Emamectin benzoat	**CYP9A186** (#64*↑FB), CYP9A27 (#64*↓MG), CYP9A11 (#64*↓MG,FB)				
	Heavy metals					
	CdCl2			GSTo (#36↑)		
	CuSO4			GSTo (#36↑)		

S. frugiperda	**Plant secondary metabolites**					
	2-Tridecanone	CYP4L13 (#40↑), CYP6B39 (#40↑), CYP4M14 (#40↑), CYP9A24 (#40↑), CYP9A26 (#40↑), CYP9A30 (#40↑), CYP9A31 (#40↑), CYP9A32 (#40↑), CYP321A9 (#40↑), CYP9A28 (#40↓)				
	Harmine	CYP301A1 (#17↑), CYP333B3 (#17↓), CYP4C1-like (#17↑), CYP314A (#17↑), CYP306A1 (#17↓), CYP9A58 (#17↓), CYP9E2-like (#17↓), CYP6B6-like (#17↓), CYP4G15-like (#17↓), *CYP4L4 (#17↓), CYP4G75 (#17??), CYP6AE44 (#17↑), CYP9A27 (#17??), CYP9A59 (#17??), CYP9A60 (#17↓), CYP49A1 (#17↓)*	CXE22 (#17??), CXE28 (#17??), ppCarE071775 (#17↓), CarE6 (#17↓), CXE20 (#17↓), *CarE-012648 (#17↓)*	GSTe4 (#17↓), GSTe14 (#17↓), GSTe12 (#17↓), GST1-like (#17↓), GSTd4 (#17↑), GSTd3 (#17↑), GSTu1 (#17↑), GSTz1 (#17??), GSTs1 (#17↑), GSTs2 (#17↑), GSTs3 (#17↑),	UGT33V2 (#17??), UGT33B13 (#17↓), UGT41D2 (#17??), UGT40D3 (#17??), UGT40D5 (#17↑), UGT40F3 (#17??), UGT40F5 (#17??), UGT40Q2 (#17↓)	
	indole	CYP332A1 (#40↑), CYP321A7 (#40↑), CYP321A8 (#40↑), CYP321A9 (#40↑), CYP6B40 (#40↑), CYP6B39 (#40↑), CYP9A31 (#40↑), CYP333B4 (#40↑)				
	indole-3-carbinol	CYP321A7 (#40↑), CYP321A8 (#40↑), CYP321A9 (#40↑), CYP6B39 (#40↑), CYP333B4 (#40↑)				
	quercetin	CYP333B4 (#40↑), CYP6B39 (#40↓), CYP9A28 (#40↓)				
	xanthotoxin	CYP333B4 (#40↑), CYP4M18 (#40↓), CYP4M14 (#40↓), CYP321A7 (#40↑), CYP321A8 (#40↑), CYP321A9 (#40↑), CYP6B40 (#40↑), CYP6B39 (#40↑), CYP9A32 (#40↑), CYP9A28 (#40↓), CYP9A31 (#40↑), CYP9A27 (#40↑)				
	Insecticides					
	chlorpyrifos	CYP6AE44 (#42*↑ma), CYP340L1 fragment 3 (#42*↑ma), CYP6B fragment 2A (#42*↑ma), CYP321A10 (#42*↑ma), CYP6AB61 (#42*↑ma), CYP340L9P (#42*↑ma), CYP9A58 (#42*↑ma), *CYP333B3 (#62*↑), CYP367A6 (#62*↑), CYP340AA1 (#62*↑), CYP6AB14 (#62*↑), CYP49A1 (#62*↑), CYP6A2 (#62*↑)*	CXE13 (#42*↑ma), CXE016c (#42*↓ma), CXE18 (42*↓ma)	mGST1-1 (#42*↑ma), GSTs2 (#42*↑ma), GSTd1 (#42*↑ma), GSTs18 (#42*↑ma), GSTs5 (#42*↑ma), GSTU1 (#42*↑ma), GSTe5 (#42*↑ma), GSTe9 (#42*↓ma), GSTs4 (#42*↓ma), GSTs6 (#42*↓ma), GSTe15 (#42*↓ma), GSTe2 (#42*↓ma), *GSTe14 (#62*↑)*	*UGT39B4 (#62*↑), UGT50A5 (#62*↑)*	
	deltamethrin	CYP9A30 (#40↑), CYP9A31 (#40↑), CYP9A32 (#40↑), CYP333B4 (#40↑), **CYP321A8** (#58↑)				
	fipronil	CYP333B4 (#40↑)				

S. frugiperda	lambda-cyhalothrin	CYP6AB61 (#42*↑ma), CYP6B59 (#42*↓ma), CYP6B fragment 2A (#42*↓ma), CYP340Lunknown-fragment1 (#42*↓ma), *CYP321B1 (#62*↑), CYP6AE44 (#62*↑), CY321A8 (#62*↑), CYP321A10 (#62*↑), CYP321A7 (#62*↑)*, CYP9E2 (#54↑), CYP6B6 (#54↑), CYP4C1 (#54↑), CYP12A2 (#54↑), CYP6B7 (#54↑), CYP6B2 (#54↑), CYP4G1 (#54↑), CYP12C1 (#54↑), CYP6B4 (#54↑), CYP4G15 (#54↑)	CXE001c (#42*↑ma), CXE016c (#42*↓ma)	GSTd1 (#42*↑ma), GSTs5 (#42*↑ma), GSTe18 (#42*↑ma), GSTt1 (#42*↑ma), GSTs2 (#42*↓ma, *#62*↑*), GSTs6 (#42*↓ma), GSTs3 (#42*↓ma), GSTe9 (#42*↓ma, *#62*↑*), *GSTe2 (#62*↑)*	UGT33-06-v1 (#42*↑ma), UGT40-07 (#42*↑ma)	
	lufenuron	CYP9A9-L_464_T_3/3 (#39*↑), CYP321A1-L_406_T_12/23 (#39*↑), CYP321A1-L_669_T_9/12 (#39*↑), CYP9A9-L_1141_T_1/4 (#39*↑), CYP9A-L_1141_T_4/4 (#39*↑), *CYP-L_1649_T_1/1 (#39*↑), CYP333B11-L_1356_T_2/3 (#39*↑), CYP9A-L_289_T_5/5 (#39*↑), CYP-L_3036_T_2/7 (#39*↓), CYP9-L_4375_T_4/5 (#39*↑), CYP9A9-L_464_T_2/3 (#39*↑), CYP9A1v2-L_797_T_3/6 (#39*↓), CYP306A1-L_4231_T_3/7 (#39*↓), CYP_FAMILY4-L_1203_T_1/6, (#39*↑), CYP-L_5684_T_3/3 (#39*↑), CYP6k1-like-L_1066_T_7/7 (#39*↑), CYP4L4-L_748_T_12/14 (#39*↓), CYP6A1-L_1066_T_4/7 (#39*↓), CYP4M6-L_1814_T_3/5 (#39*↓), CYP-L_3036_T_4/7 (#39*↓), CYP-L_3036_T_3/7 (#39*↓), CYP9A-L_380_T_2/9 (#39*↑), CYP9A9-L_126_T_1/1 (#39*↑), CYP9A-L_2833_T_10/12 (#39*↑), CYP4L4-L_748_T_8/14 (#39*↓)*	*cce016b-L_2045_T_5/7 (#39*↑), cce016a-L_4453_T_2/2 (#39*↑), cce016b-L_2281_T_5/8 (#39*↑), CE-L_2894_T_8/9 (#39*↑), CE-L_597_T_8/10 (#39*↑)*	*GST-L_1819_T_1/4 (#39*↑), GST-L_1819_T_2/4 (#39*↑), GST-L_4086_T_5/5 (#39*↑), GSTzeta2-L_1877_T_1/2 (#39*↑)*	*UGT41d2-L_571_T_4/11 (#39*↑), UGT40r3-L_492_T_3/8 (#39*↓), UGT33f4-L_1390_T_6/9 (#39*↑)*	
	methoprene	CYP9A28 (#40↓), CYP4M14 (#40↑), CYP9A26 (#40↑), CYP9A30 (#40↑), CYP9A31 (#40↑), CYP9A32 (#40↑), CYP321A9 (#40↑), CYP333B4 (#40↑)				
	methoxyphenozide	CYP9A59 (#40↑), CYP9A25 (#40↑), CYP9A58 (#40↑), CYP9A24 (#40↑)				
	Model Inducers					
	phenobarbital	CYP6B40 (#40↑), CYP6B39 (#40↑), CYP9A31 (#40↑)				
	clofibrate	CYP9A24 (#40↑), CYP9A30 (#40↑), CYP9A31 (#40↑), CYP9A32 (#40↑), CYP333B4 (#40↑)				
S. littoralis	**Insecticides**					
	deltamethrin				UGT46A6 (#46↑)	

Pesticide Biochemistry and Physiology 174 (2021) 104822

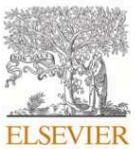

Contents lists available at ScienceDirect

Pesticide Biochemistry and Physiology

journal homepage: www.elsevier.com/locate/pest

Review

Transcriptional regulation of xenobiotic detoxification genes in insects - An overview

Dries Amezian [a], Ralf Nauen [b,*], Gaëlle Le Goff [a,*]

[a] Université Côte d'Azur, INRAE, CNRS, ISA, F-06903 Sophia Antipolis, France
[b] Bayer AG, Crop Science Division, R&D, Alfred Nobel-Strasse 50, 40789 Monheim, Germany

ARTICLE INFO

Keywords:
Signaling pathways
Transcription factors
Xenobiotic responses
Cytochrome P450
ABC transporters
Glutathione S-transferases

ABSTRACT

Arthropods have well adapted to the vast array of chemicals they encounter in their environment. Whether these xenobiotics are plant allelochemicals or anthropogenic insecticides one of the strategies they have developed to defend themselves is the induction of detoxification enzymes. Although upregulation of detoxification enzymes and efflux transporters in response to specific inducers has been well described, in insects, yet, little is known on the transcriptional regulation of these genes. Over the past twenty years, an increasing number of studies with insects have used advanced genetic tools such as RNAi, CRISPR/Cas9 and reporter gene assays to dissect the genomic grounds of their xenobiotic response and hence contributed substantially in improving our knowledge on the players involved. Xenobiotics are partly recognized by various "xenobiotic sensors" such as membrane-bound or nuclear receptors. This initiates a molecular reaction cascade ultimately leading to the translocation of a transcription factor to the nucleus that recognizes and binds to short sequences located upstream their target genes to activate transcription. To date, a number of signaling pathways were shown to mediate the upregulation of detoxification enzymes in arthropods and to play a role in either metabolic resistance to insecticides or host-plant adaptation. These include nuclear receptors AhR/ARNT and HR96, GPCRs, CncC and MAPK/CREB. Recent work reveals that upregulation and activation of some components of these pathways as well as polymorphism in the binding motifs of transcription factors are linked to insects' adaptive processes. The aim of this mini-review is to summarize and describe recent work that shed some light on the main regulatory routes of detoxification gene expression in insects.

1. Introduction

Arthropods are challenged by a wide variety of xenobiotics including both natural compounds such as plant allelochemicals and synthetic chemicals of anthropogenic origin such as insecticides to control pests (Despres et al., 2007; Li et al., 2007). To overcome detrimental effects of these xenobiotics insects possess a large collection of enzymes that detoxify these toxins and thus allowing them to survive exposure in different environments (Fig. 1) (Van Leeuwen and Dermauw, 2016). However, possessing an arsenal of detoxification tools is of little use if an adverse effect mediated by a chemical cannot be detected and addressed by appropriately deploying the enzymes that will circumvent the adverse effects of xenobiotics. The genes coding for enzymes and transporters involved in detoxification are coordinately induced upon exposures to the chemicals or sometimes even constitutively overexpressed in populations under continuous insecticide pressure, which implies the existence of pathways of gene regulation finely tuned to ensure an adequate response. The potency and duration of gene induction depends on xenobiotic concentration and time of exposure. Xenobiotics as inducing agents and/or substrates tend to trigger particularly the upregulation of large sets of genes remotely involved in their detoxification. Transcriptional regulation is commonly driven by *cis*-regulatory elements (*cis*-acting), short sequences located within the promoter region, onto which specific transcription factors bind (*trans*-acting) and further recruit the transcriptional machinery (Guo et al., 2018). In mammals, induction of detoxification and oxidative stress response genes is mediated by three main transcription factor superfamilies: the nuclear receptor superfamily such as pregnane X receptor (PXR), the constitutive androstane receptor (CAR) (or also FXR, VDR, LXR, and HNF4); the basic helix–loop–helix (bHLH)-PAS domain transcription factors superfamily including aryl hydrocarbon receptor (AhR)/AHR nuclear translocator (ARNT) and the NF-E2-related factor

* Corresponding author.
E-mail addresses: ralf.nauen@bayer.com (R. Nauen), gaelle.le-goff@inrae.fr (G. Le Goff).

https://doi.org/10.1016/j.pestbp.2021.104822
Received 16 December 2020; Received in revised form 8 February 2021; Accepted 2 March 2021
Available online 8 March 2021
0048-3575/© 2021 Elsevier Inc. All rights reserved.

Appendix B (Chapter 2)

Supplementary tables

Table S1: Primers used for amplification and cloning

Primers for amplification of CncC and Maf genes			
Gene name	*Length*	*Primer ID*	*Primer sequence*
CncC	3324	PR1 PR2 PR3 PR4	F: 5'-CTGATCTCATAAAAGTGCTC-3' R: 5'-CTGTGTAGGCGGAATCACTG-3' F: 5'-ACTGAGATCTCTATGATTTCGTTGAAGAAATTG-3' R: 5'-GCTGCGGCATTTTCGGTACGAGT-3'
Maf	417	PR5 PR6	F: 5'-ATGCAGATCTCTATGCCTCATGATTTAAAGGA-3' R: 5'-ATATGCGGCCGCCTAAGGCTGTATTTCTAGTT-3'
Primers for cloning validation			
Plasmid vector		*Primer ID*	*Primer sequence*
pBiEx-1		PR7 PR8	F: 5'-GAACGCCAGCACATGGAC-3' R: 5'-GATCCTCGGGGTCTTCCG-3'

Table S2: Primers used for RT-qPCR

Primers for RT-qPCR				
Gene name	*Amplicon size*	*Efficiency (%)*	*Primer ID*	*Primer sequence*
Ribosomal protein 4 (RPL4)	149	119	PR19	F: 5'-CAACAAGAGGGGTTCACGAT-3' R: 5'-GCACGATCAGTTCGGGTATC-3'
Ribosomal protein 10 (RPL10)[a]	ND	108,8	PR20	F: 5'-GTCGTGCCAAGTTCAAGTTC-3' R: 5'-GTCCTCACGCAGCTTCTC-3'
Ribosomal protein 10 (RPL17)[a]	ND	102,8	PR21	F: 5'-GTGACGGAAGCTATCAAGAC-3' R: 5'-ACTTGTTGCCGAGGACAC-3'
CncC	140	102,1	PR22	F: 5'-AAGGGCATCATACGGGTGAC-3' R: 5'-TCCAAGCACTTTGGTTGCTG-3'
Maf	131	114	PR23	F: 5'-CCGTAGAACGCTGAAGAACC-3' R: 5'-TGTTGTTCTCGTCCTGCATC-3'
Keap1 (exon n°7)	83	110	PR24	F: 5'-GCGATGTCAGTACCTAACGC-3' R: 5'-CTCGGCAAGCTGGAACTTTT-3'

[a] *As per* Boaventura et al., 2020 (IBMB, 116, 103280)

Appendix C (Chapter 3)

Supplementary tables

Table S1: Primers for CRISPR/Cas9 edition validation by Sanger and amplicon sequencing

Gene region covered	*Primer ID*	*Primer sequence*
CncC exon 1: 341 to 1102 bp region	PR11	F: 5'-AACGTAGCGACTGACGCAGTC-3'
	PR12	R: 5'-GCGTCAACTCGTCACCCGTATG-3'
CncC exon 1: 1 to 626 bp region	PR13	F: 5'-ATGATTTCGTTGAAGAAATTGTACGGAGAC-3'
	PR14	R: 5'-GGTTGTACTAATAGCTCGTTGACGTC-3'
Keap1 exon 2: 687 to -6 bp region	PR15	F: 5'-GTCACACGATGCCACATGAACAC-3'
	PR16	R: 5'-GGTAACATGTTGGACAACATGCCC-3'
pGEM-T amplicon sequencing on CncC exon 1 (350 to 1093 bp region)	PR17	F: 5'-TAGCGACTGACGCAGTC-3'
	PR18	R: 5'-CGTCACCCGTATGATGC-3'

Table S2: Primers for cloning validation

Plasmid vector	*Primer ID*	*Primer sequence*
pBiEx-1	PR7	F: 5'-GAACGCCAGCACATGGAC-3'
	PR8	R: 5'-GATCCTCGGGGTCTTCCG-3'
piE1-Cas9-SfU6-sgRNA-puro	PR9	F: 5'-Tccgacagaatttgtagatggcgc-3'
	PR10	R: 5'-ccagttcggttatgagccgtgtg-3'

Table S3: Sequences of sgRNA for CRISPR/Cas9-induced mutation of CncC and Keap1.

PAM position and strand	*Forward*	*Reverse*
SgRNA_cncc_145 (+)	5'-accgTTTCAAACGGATCCGAT-3'	5'-aacATCGGATCCGTTTGAAAc-3'
SgRNA_cncc_166fw	5'-accgCCTTAGAACAGGAGGCC-3'	5'-aacGGCCTCCTGTTCTAAGGc-3'
SgRNA_cncc_556fw	5'-accgCAGACTTCCTCCACAAT-3'	5'-aacATTGTGGAGGAAGTCTGC-3'
SgRNA_cncc_1014fw	5'-accgTTCACGGCTAGTTCCAG-3'	5'-aacCTGGAACTAGCCGTGAAc-3'
SgRNA_Keap1_97rev	5'-accgCCGTCGCAGCTGATAGG-3'	5'-aacCCTATCAGCTGCGACGGc-3'
SgRNA_Keap1_119rev	5'-accgGCCGGTTTCGCCTTCCA-3'	5'-aacTGGAAGGCGAAACCGGCc-3'
SgRNA_Keap1_121fw	5'-accgTGCGACGGTACCCTGGA-3'	5'-aacTCCAGGGTACCGTCGCAc-3'
SgRNA_Keap1_173fw	5'-accgGACCTGACCTTCTGCAT-3'	5'-aacATGCAGAAGGTCAGGTCc-3'
SgRNA_eGFP	5'-accgGGCGAGGAGCTGTTCAC-3'	5'-aacGTGAACAGCTCCTCGCCc-3'

Supplementary figures

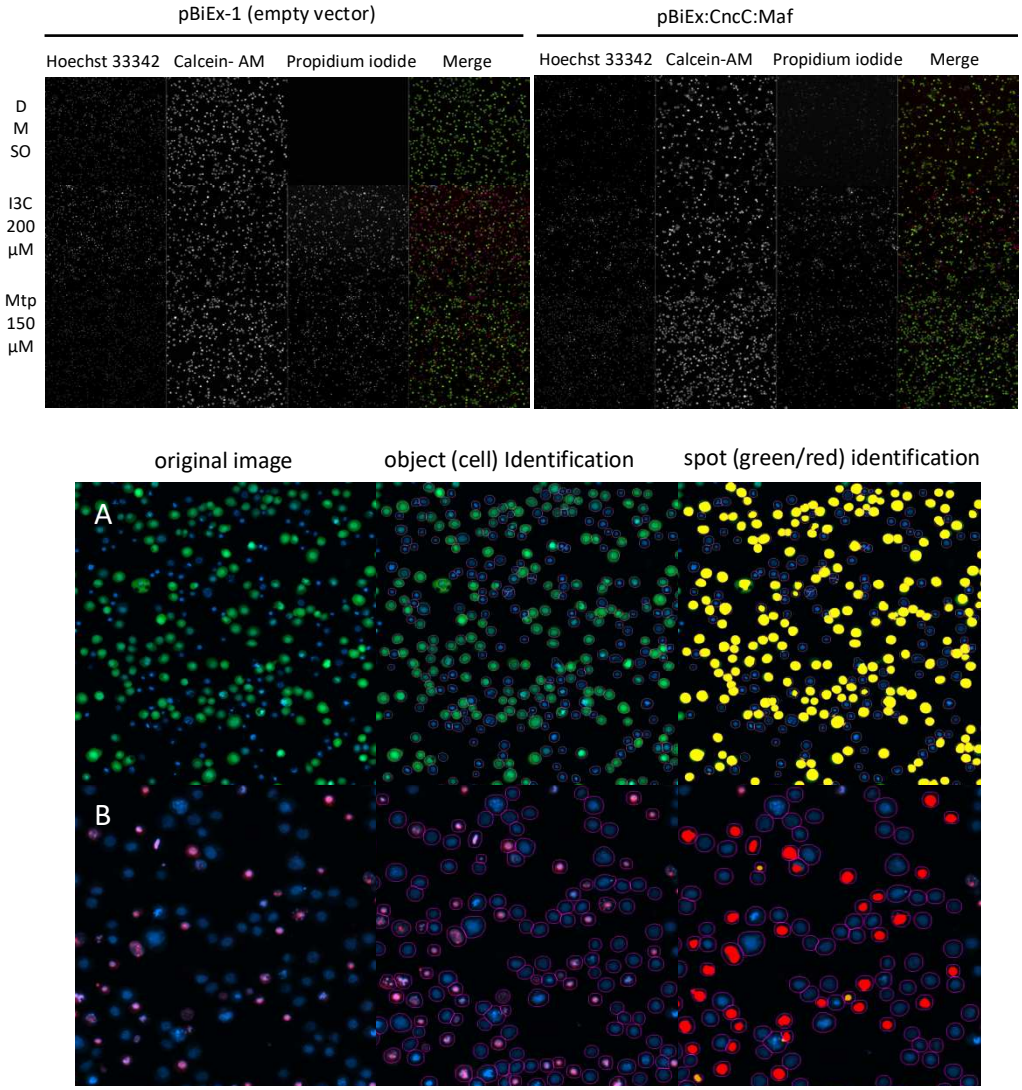

Fig. S1 Representative composite image from Sf9 cells.
Automated fluorescence microscopy was carried out using the Cellomics-ArrayScanXTI instrument. Images were collected thanks to a 20X PlanFluor objective with a 2x2 binning on the Camera (Photometrics). Individual cell segmentation was performed using the "compartmental analysis" algorithm. Nuclear stain (Hoechst 33342) is in blue, purple outlines indicate cell region segmentation, green coloration correspond to calcein-AM staining of living cells marked with the yellow spots (**A**). Dead cells have nuclei stained in red (propidium iodide) marked with the read spots (**B**).

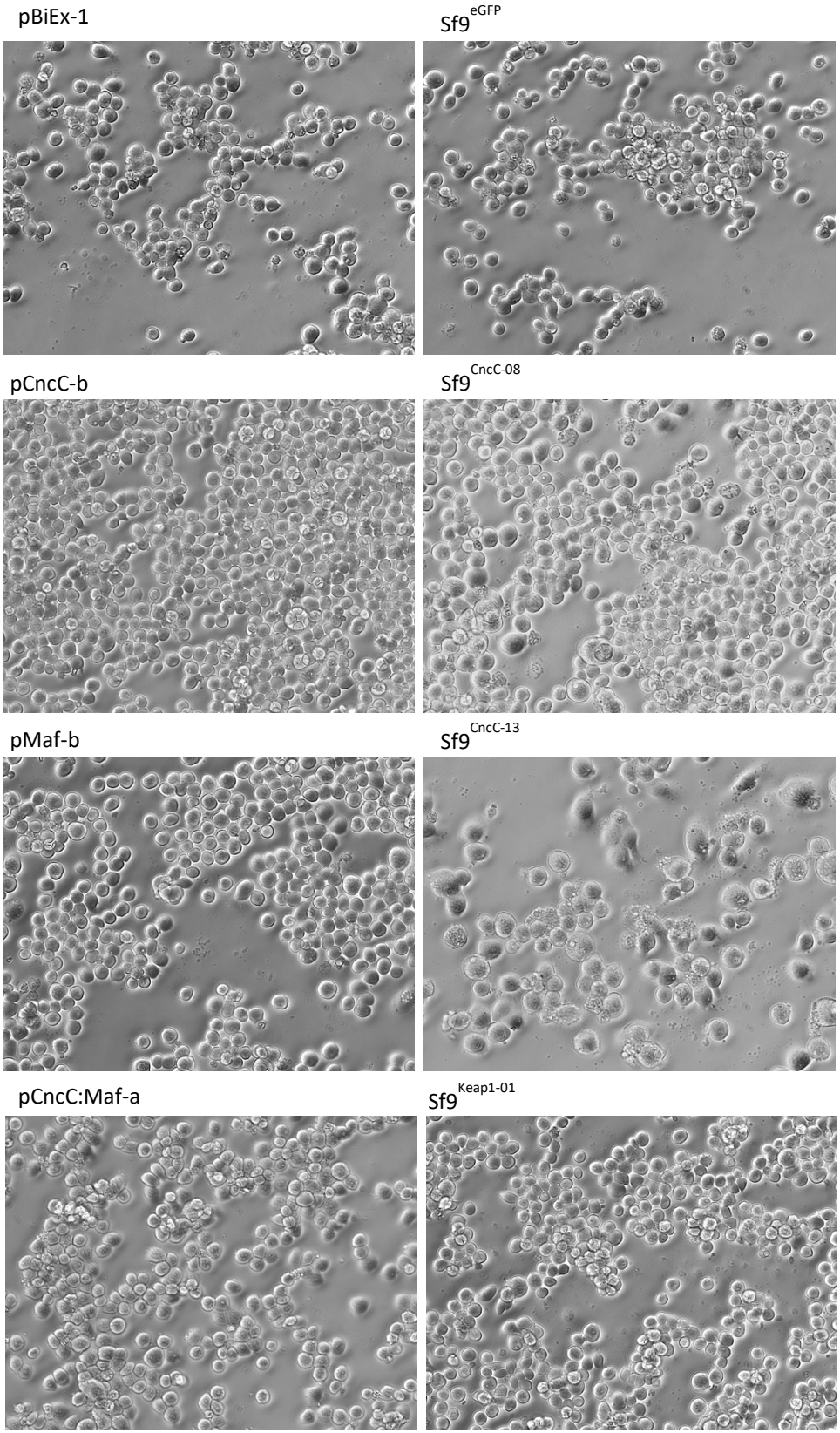

Fig. S2 Pictures of *CncC* and *Maf* cell transformants in Insect Xpress medium
All pictures were taken with a Nikon Eclypse TE2000-U at x 10. Cells were cultured in serum-free and SP-free Insect Xpress medium.

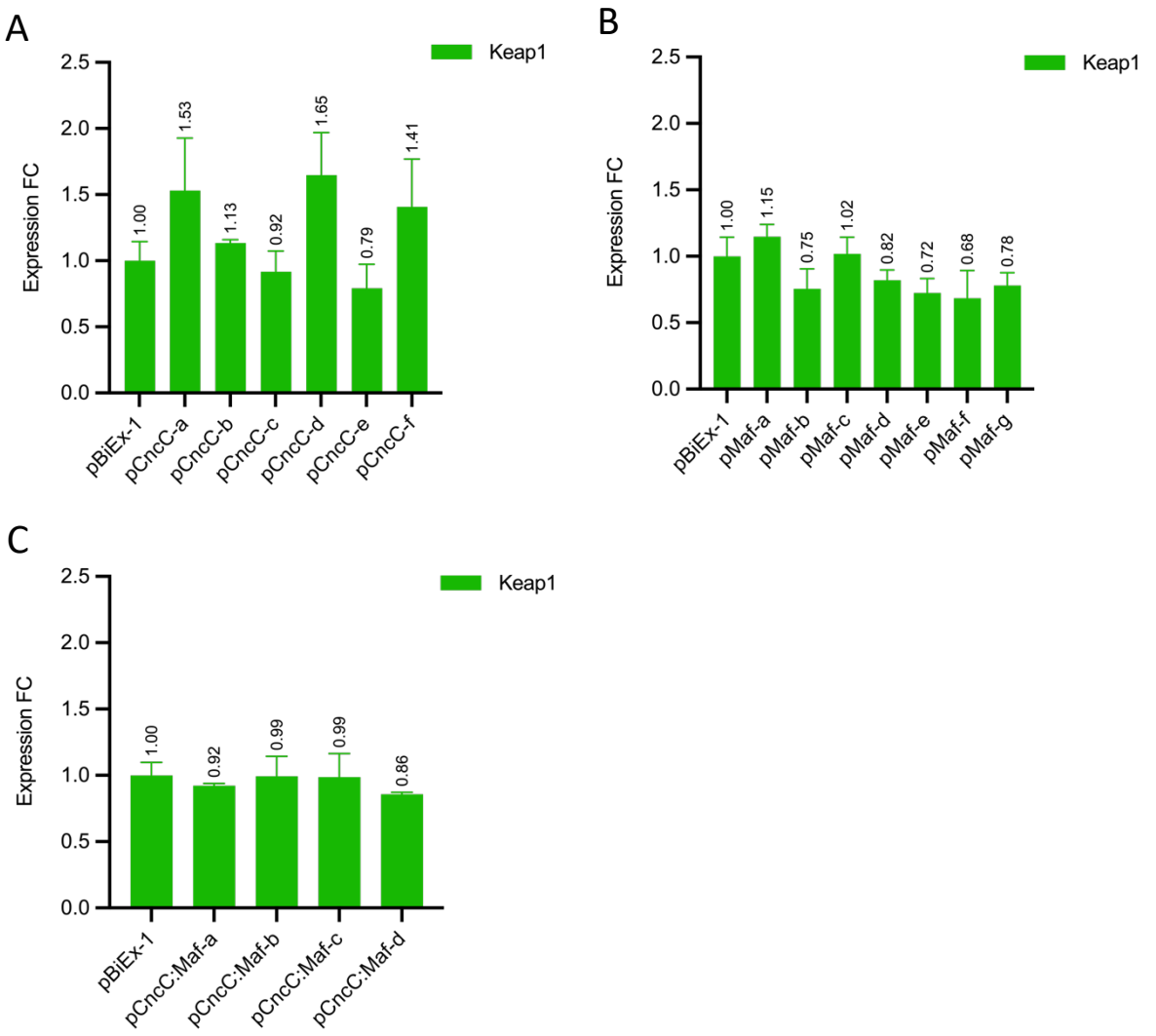

Fig. S3 Transcript levels of *Keap1* in OE cell transformants.
Expression of *Keap1* (green) was monitored in cell lines transfected with either (**A**) a vector containing *CncC* (pBiEx:CncC) (**B**) a vector containing *Maf* (pBiEx:Maf) and (**C**) two vectors containing respectively *CncC* and *Maf*. Gene expression was normalized using the expression of the ribosomal protein *L4*, *L10* and *L17* reference genes and shown as fold-change relative to the expression of cell lines transfected with an "empty" plasmid, pBiEx-1. Data are mean values ± SEM.

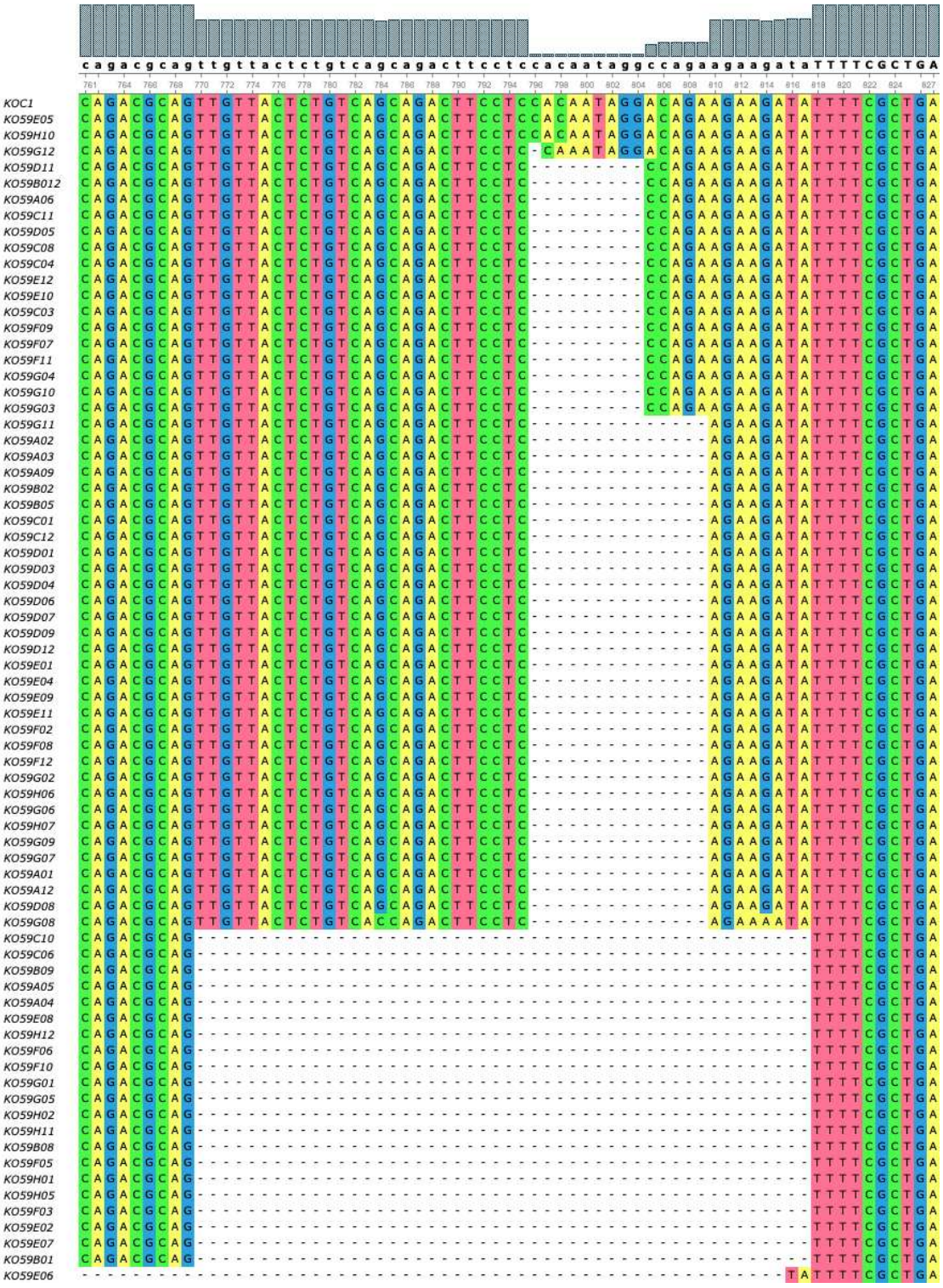

Fig. S4 Aligned clean sequences from the agarose plate colony sequencing of Sf9$^{CncC\text{-}08}$.
72 clean sequences were obtained from the sequencing of 96 bacterial colonies chosen in a blue/white pGEM-T selection assay.

Appendix D (Chapter 4)

Supplementary tables

Table S1 Sequencing results

Lane	Expected Read nb[1] (PF[2])	Library ID	Yield (Mb)	%PF	Cluster (PF)	Q30[3]	Mean qual. (PF)
1-2	27'083'333	AUJG-25	8'515	100	28'385'489	92.34	35.52
1-2	27'083'333	AUJG-26	9'288	100	30'960'540	92.64	35.58
1-2	27'083'333	AUJG-27	8'564	100	28'547'516	93.56	35.79
1-2	27'083'333	AUJG-28	10'277	100	34'257'035	94.79	36.07
1-2	27'083'333	AUJG-29	9'030	100	30'099'486	92.53	35.57
1-2	27'083'333	AUJG-30	8'853	100	29'508'779	93.53	35.79
1-2	27'083'333	AUJG-31	9'695	100	32'317'535	94.20	35.94
1-2	27'083'333	AUJG-32	7'771	100	25'902'781	92.24	35.49
1-2	27'083'333	AUJG-33	7'391	100	24'638'632	94.26	35.97
1-2	27'083'333	AUJG-34	8'376	100	27'919'602	93.97	35.88
1-2	27'083'333	AUJG-35	6'990	100	23'301'635	92.91	35.65
1-2	27'083'333	AUJG-36	8'024	100	26'746'681	93.49	35.77
1-2	27'083'333	AUJG-37	8'433	100	28'107'261	93.98	35.89
1-2	27'083'333	AUJG-38	9'547	100	31'821'945	94.43	35.98
1-2	27'083'333	AUJG-39	7'458	100	24'861'930	92.63	35.57
1-2	27'083'333	AUJG-43	9'562	100	31'872'183	93.19	35.72
1-2	27'083'333	AUJG-44	8'217	100	27'390'050	92.95	35.65
1-2	27'083'333	AUJG-45	11'035	100	36'782'332	92.61	35.58
1-2	27'083'333	AUJG-46	9'227	100	30'757'717	93.37	35.73
1-2	27'083'333	AUJG-47	10'275	100	34'251'636	94.29	35.96
1-2	27'083'333	AUJG-48	9'466	100	31'554'269	93.53	35.78

[1] Total number for all lanes combined
[2] PF stands for 'passed filter' i.e. clusters that fulfill the default Illumina quality criteria
[3] % of bases (PF) with a quality score greater or equal to 30

Table S2 Expression levels of transcription factors *CncC* and *Maf* and cytosolic repressor Keap1

		log_2FC	*p*-value	P_{adj}
CncC	Transcript ID	SFRUCORN610000011675		
	pCncC-b	0.6197	4,6E-07	1,7E-05
	pMaf-b	-0,34	8,2E-03	3,2E-02
	pCncC:Maf-a	0,49	9,5E-05	5,7E-04
	Sf9CncC-13	-1,76	4,7E-12	1,2E-10
	Sf9Keap1-01	-0,70	4,3E-03	2,3E-02
Maf	Transcript ID	SFRUCORN610000014579-RA		
	pCncC-b	0,25	3E-03	3E-02
	pMaf-b	3,04	6E-302	7E-298
	pCncC:Maf-a	2,39	3E-186	1E-182
	Sf9CncC-13	0,57	3E-07	4E-06
	Sf9Keap1-01	0,47	2E-05	3E-04
Keap1	Transcript ID	SFRUCORN610000026326-RA		
	pCncC-b	0,34	1E-01	4E-01
	pMaf-b	-0,67	3E-03	1E-02
	pCncC:Maf-a	0,34	1E-01	3E-01
	Sf9CncC-13	-0,19	7E-02	2E-01
	Sf9Keap1-01	2,13	6E-93	2E-89

Table S2: contingency table of genes upregulated in all cell lines vs detoxification genes.

	up-reg		
detox	**yes**	**no**	**total**
yes	27	462	489
no	590	20740	21330
total	617	21202	21819

Fisher‘s exact p-value = 0.001227

Table S3: contingency table of genes downregulated in all cell lines vs detoxification genes.

	down-reg.		
detox	**yes**	**no**	**total**
yes	59	430	489
no	888	20442	21330
total	947	20872	21819

Fisher‘s Exact p-value = 1.228e-12

Table S4: Differential expression analysis of selected oxidative stress-related genes in CRISPR/Cas9-edited cell lines

		log_2FC☼	
Transcript ID	**Description**❀	**Sf9$^{CncC-13}$**	**Sf9$^{Keap1-01}$**
SFRUCORN610000008037-RA	POD-like	0,387	**1,33***
SFRUCORN610000018587-RA	POD-like	**-2,55**	**-3,94**
SFRUCORN610000018579-RA	POD-like	**-2,22**	**-2,2**
SFRUCORN610000027489-RA	POD-like	0,9	0,329
SFRUCORN610000031709-RA	Chorion POD	-0,497	-0,963
SFRUCORN610000033464-RA	Chorion POD	-0,72	**1,95***
SFRUCORN610000028673-RA	Chorion POD	-0,038	-0,355
SFRUCORN610000018590-RA	Chorion POD	-0,576	-0,219
SFRUCORN610000012649-RA	Chorion POD	-0,377	-0,514
SFRUCORN610000033248-RA	Chorion POD	-0,44	0,141
SFRUCORN610000030419-RA	CAT-related PD	-0,6266	**1,57**
SFRUCORN610000033249-RA	skpo POD	0,876	**2,342**
SFRUCORN610000030422-RA	CAT-like	**2,27**	**1,085**
SFRUCORN610000022876-RA	CAT-like	**1,5**	0,734
SFRUCORN610000030418-RA	CAT-like	-0,06	0,9777
SFRUCORN610000031331-RA	CAT-like	-0,39	**2,567***
SFRUCORN610000012501-RA	SOD [Cu-Zn]-like	-0,59	0,1386
SFRUCORN610000002962-RA	SOD [Cu-Zn]-like	**1,317**	**1,8**
SFRUCORN610000000460-RA	SOD [Cu-Zn]-like	-0,184	0,22
SFRUCORN610000023404-RA	SOD Mn	-0,3359	0,1001
SFRUCORN610000002957-RA	SOD3-like	0,0138	**1,125**
SFRUCORN610000003079-RA	Nos-like	-0,895	0,0695
SFRUCORN610000031835-RA	Nos2-like	**-7,335***	**-5,29***
SFRUCORN610000033793-RA	Nos-like	**-3,243**	**-3,27**
SFRUCORN610000031839-RA	Nos-like	**2,589**	0,58
SFRUCORN610000003087-RA	Nos-like	-0,11	0,75
SFRUCORN610000003068-RA	Nox1	**-1,970***	-0,657
SFRUCORN610000024388-RA	Nox5	0.77	-0,012
SFRUCORN610000028488-RA	Nox5	**-1,42**	0,124
SFRUCORN610000028610-RA	DUOXA1	**-2**	0,168
SFRUCORN610000028607-RA	DUOX isoform X1	-0,2	0,682
SFRUCORN610000006477-RA	HAO1	**-2,13***	0,643

❀ POD: peroxidase, CAT: catalase, SOD: superoxide dismutase, Nos: nitric oxide synthase, Nox: NADPH oxidase, DUOX: dual oxidase, HAO1: hydroxyacid oxidase

☼ transcripts meeting $|log_2FC > 1|$ are boldened; * means $P_{adj} < 0.05$

Appendix E - Result article

Soon to submit to Chemosphere

Using Sf9 cells to decipher the role of detoxification enzymes in xenobiotic adaptation in the pest *Spodoptera frugiperda*

Dries Amezian [a‡], Sonja Mehlhorn [b‡], Calypso Vacher-Chicane [a], Ralf Nauen [b*] and Gaëlle Le Goff [a*]

[a] Université Côte d'Azur, INRAE, CNRS, ISA, F-06903, Sophia Antipolis, France.

[b] Bayer AG, Crop Science Division, R&D, Alfred Nobel-Strasse 50, 40789 Monheim, Germany.

‡ Authors have contributed equally to the work

*** Corresponding authors:**

Ralf Nauen (ralf.nauen@bayer.com)

Gaëlle Le Goff (gaelle.le-goff@inrae.fr)

Abstract

Spodoptera frugiperda is a major pest that feeds on numerous crops including maize and rice. It has developed sophisticated mechanisms to detoxify the toxic compounds present in its diet as well as to insecticides. The aim of the study was to understand the detoxification response of the insect when exposed to plant secondary metabolites and insecticides. To do this, we used the *S. frugiperda* cell model, Sf9 cells, and exposed the cells to a compound representing each of these classes of molecules, indole 3-carbinol and methoprene. The IC_{50} of these molecules was determined and IC_{10}, IC_{20} and IC_{30} doses were used to monitor the induction profiles of detoxification genes. CYP9As are the most inducible genes, the results also show the induction of the transcription factor Cap'n'collar isoform C (CncC). Transient overexpression of this transcription factor and its partner muscle aponeurosis fibromatosis (*Maf*) induces overexpression of *CYP4M14*, *CYP4M15*, *CYP321A9* and *GSTE1* while CYP9As are not induced. We then wanted to determine the involvement of CYP9A in the metabolism of methoprene and I3C. Fluorescence-based biochemical assays revealed an interaction of methoprene with functionally expressed CYP9A30, CYP9A31 and CYP9A32 whereas no interaction was detected for indole 3-carbinol, suggesting the ability of CYP9As to metabolize methoprene. Our results showed that Sf9 cells could be a useful model to decipher the role of detoxification enzymes in the adaptation of *S. frugiperda* to its chemical environment.

Keywords: CncC, CYP9A, Indole-3-carbinol, Maf, methoprene.

1. Introduction

The fall armyworm (FAW), *Spodoptera frugiperda*, (Lepidoptera: Noctuidae), is a polyphagous pest feeding on numerous plants of agronomic interest such as maize, rice and sorghum. Although it was originally present on the American continent, it has since invaded the world, Africa in 2016, Asia from 2018 and Australia in 2020. Its invasion of Europe is highly likely and it was detected on the Canary Islands (Spain) in July 2020. The Food and Agriculture Organisation of the United Nations (FAO)

proclaimed it in 2021 as "one of the most destructive pests jeopardizing food security across vast regions of the globe". Controlling this insect pest largely relies on the application of insecticides resulting in the development of resistance to many classes of synthetic insecticides. In fact, it is ranked in the top 15 most resistant arthropods on the planet (Sparks et al., 2020).

FAW has developed sophisticated mechanisms to eliminate toxic compounds present in its host-plants and insecticides. The detoxification enzymes, cytochromes P450, esterases and glutathione S-transferases are part of this armament. Yu's pioneering work in the 1980s showed, for example, that microsomal fractions, which carry P450 activity, extracted from *S. frugiperda* larvae could metabolize allelochemicals of various chemical structures such as alkaloids, indoles, furanocoumarin, glucosinolates, compounds found in the insect's diet (Yu, 1987). Detoxification enzymes are often expressed at a basal level and induced when the insect is exposed to toxic compounds. In *S. frugiperda*, P450, GST and esterase activities have all been shown to be inducible by allelochemicals (Yu, 1986). For example, indole 3-carbinol (I3C), which is a degradation product of glucosinolates, induces P450, GST and esterase activities by 5-, 4- and 1.6-fold respectively (Yu, 1983; Yu and Hsu, 1985). These detoxification enzymes also play a key role in the development of insecticide resistance. Several studies have shown that depending on the plant that the insect consumes its tolerance to insecticides will be modified. *S. frugiperda* larvae fed on maize leaves are less sensitive to certain pyrethroids such as permethrin and cypermethrin than larvae fed on soybean (Yu, 1982). Similarly, tolerance to cypermethrin was shown to increase in other Lepidoptera (*Helicoverpa armigera* and *S. litura*) when insects were exposed to xanthotoxin, a furanocoumarin (Li et al., 2000; Lu et al., 2021b). Insecticides, like allelochemicals, are inducers of

detoxification enzymes expression. There is a specificity of response, *i.e.* an insecticide will not necessarily induce the same genes as a secondary plant metabolite. Giraudo et al showed that P450 expression profiles in *S. frugiperda* larvae were specific to the compound tested, e.g. I3C induced *CYP321A7*, *CYP321A8* and *CYP321A9* whereas the insecticide methoxyfenozide induced *CYP9A25*, *CYP9A58* and *CYP9A59* (Giraudo et al., 2015). However, a global analysis of expression pattern of detoxification genes in response to xenobiotics in four species of the *Spodoptera* genus showed that compounds of different nature could induce some genes in common (Amezian et al., 2021a). Some of these enzymes will have the ability to metabolize both plant allelochemicals and insecticides. This is the case, for example, of CYP321A1 of the cotton bollworm, *H. armigera*, which was shown to metabolize furanocoumarins and the insecticide cypermethrin (Sasabe et al., 2004).

The signaling pathways that allow the insect, following exposure to a xenobiotic, to induce the expression of the machinery necessary for the elimination of this toxicant are still poorly understood. Of the five main pathways identified so far (Amezian et al., 2021b), the transcription factor Cap'n'collar isoform C (CncC) and its partner of heterodimerization muscle aponeurosis fibromatosis (Maf) have been identified as « master regulators » of detoxification in several insects. Identified for the first time in *Drosophila*, CncC has been shown to control more than half of the genes regulated by phenobarbital, a babiturate well known to induce many detoxification genes (Misra et al., 2011). Furthermore, in this study, the authors showed that *CncC* activation leads to resistance to the insecticide malathion because it induces over-expression of enzymes that degrade the insecticide. Since then, several studies have demonstrated the constitutive overexpression of *CncC* in resistant insect populations, first in laboratory-selected DDT-resistant strains of *Drosophila* (91R and DDTR) (Misra et al.,

2013) and more recently, for example, in lepidopterans including *S. exigua* resistant to chlorpyrifos and cypermethrin (Hu et al., 2019b) and *S. litura* resistant to indoxacarb (Shi et al., 2021a). The CncC pathway seems to play a primordial role in adaptation to insecticides but have so far been little explored in the ability of insects to adapt to plant allelochemicals (Lu et al., 2021a; Lu et al., 2021b).

Sf9 cells are derived from the ovary of the *S. frugiperda* pupa. They have been used as a model system for heterologous expression of proteins for several decades. However, they also have been employed to evaluate the potential of certain molecules to act as insecticides (Pereira et al., 2021; Ruttanaphan et al., 2020). Indeed, Sf9 cells have been shown to be a useful model of the response to xenobiotics as well as to investigate potential resistance mechanisms (Cui et al., 2020; Giraudo et al., 2011; Giraudo et al., 2015).

Here, we used Sf9 cells as a model to try to understand how *S. frugiperda* adapts to plant secondary metabolites and insecticides. We did this using a typical molecule of each of these xenobiotics, indole 3-carbinol and methoprene. The questions we tried to answer are:

(i) Does exposure of cells to these compounds induce a detoxification response?

(ii) Is this response mediated by the transcription factors CncC and Maf?

(ii) Are I3C and methoprene able to interact with the most inducible P450s in this study, namely CYP9As?

Materials & Methods

1.1. Chemicals

Indole 3-carbinol and methoprene were purchased from Sigma–Aldrich Chimie (Saint-Quentin Fallavier, France).

1.2. Cell culture

Sf9 cells were maintained as adherent cultures at 27°C in Insect-XPRESS™ protein-free insect cell medium (Lonza, France) and passaged every third day. Cell density was determined by Malassez haemocytometer (Marienfeld, Germany) counts and cell viability was evaluated by Trypan blue (1 mg/ml, v/v) staining.

1.3. Cell viability assay and induction treatments

Viable cells were determined by measuring the conversion of the tetrazolium salt MTT to formazan induced by mitochondrial succinate dehydrogenase, as previously described (Fautrel et al., 1991). Prior to experiments, cells were seeded onto 96-well plates (Techno Plastic Products AG, Switzerland) at 2.10^5 cells/ml and incubated for 24 h at 27°C. Cells were then treated for 24 h with increasing concentrations of indole 3-carbinol (10, 50, 100, 200, 350, 500 µM) and methoprene (25, 75, 100, 150, 300 µM) or DMSO as a control. After 24 h, the medium was removed and cells were loaded with MTT (5 mg/ml final concentration in Insect-Xpress medium) and incubated at 27 °C for 2 h. Formazan crystals from cell homogenates were solubilized in 100 µl DMSO and used to measure absorbance at 570 nm using a microplate reader (SpectraMax 382, Molecular Devices, USA). All MTT assays were done for three independent, biological replicates. For induction of gene expression studies, cells were seeded onto six-well plates at 2.10^5 cells/ml and incubated 24 h at 27°C for adhesion. Plated Sf9 cells were then treated for 24 h with sublethal doses of indole 3-carbinol (40, 58 and 74 µM) and methoprene (50, 65 and 74 µM) or the equal volume of DMSO, which

served as control. Induction doses were chosen at the IC_{10}, IC_{20}, IC_{30} which represents the inhibition concentration to 10, 20 and 30 % of the cells, respectively, as established by cytotoxicity assays.

1.4. Transient Transfection

1.4.1. Plasmid constructions

RNA extracted from *S. frugiperda* larvae midguts was used to synthesize cDNA which served as template for *CncC* and *Maf* amplification. Two primer pairs were designed to amplify *CncC*, and one pair to amplify *Maf*, using the genomic sequences retrieved from the genome (v3.0) on BIPAA (bipaa.genouest.org, (Gouin et al., 2017)) and customized to introduce restriction enzymes sites (Table S1). *CncC* was amplified with two successive runs using overlapping primers and a high fidelity PrimeSTAR® polymerase (Takara Bio Europe, France) on a MJ Research Tetrad PTC-225 Thermal Cycler (GMI, USA). PCR products were purified using the GenElute™ PCR Clean-Up kit (Sigma-Aldrich, France) and the purity was assessed using NanoDrop™. The BglII/NotI digested PCR amplicons of *CncC* and *Maf* were subcloned into the BglII/NotI linearized pBiEx™ Expression Vector (Novagen, Germany) at 20:1 and 3:1 (w/w) ratios using a T4 DNA Ligase (Roche, Germany). The pBiEx-Maf and pBiEx-CncC products were subsequently transformed into Subcloning Efficiency™ DH5α™ Competent Cells (Life Technologies, Germany) according to the supplier's instruction. Successfully transformed bacterial colonies were screened by direct PCR using GoTaq® DNA Polymerase (Promega, France) (Table S1). Finally, plasmids were isolated using the GenElute™ Plasmid Miniprep Kit (Sigma-Aldrich, France). All recombinant constructs were confirmed by Sanger sequencing (GENEWIZ, Germany).

1.4.2. Transient expression of CncC and Maf in Sf9 cells

Transient expression of target genes was performed by transfection of the expression vector pBiEx™ using FUGENE® transfection reagent (Life Technologies, Germany) according to the manufacturer's instructions. Briefly, Sf9 cells were seeded onto six-well plates at 1.10^6 cells/ml and incubated at 27°C for 24h prior to transfection. In each well, adherent cells were transfected with 2 µg expression vector DNA. The plasmid DNA and 3 µl FUGENE® transfection reagent were incubated 15 min in 100 µl of Insect-XPRESS medium at room temperature prior to be diluted to a final volume of 1 ml of Insect-XPRESS medium supplemented with 10% fetal bovine serum (FBS) from Invitrogen (Villebon-sur-Yvette, France). Cells were transfected with either a single expression plasmid construct, *i.e.* pBiEx:CncC or pBiEx:Maf, or transfected with both expression vectors in equal proportions. An empty vector was used to transfect control cell lines. Each transformation condition was replicated three times, *i.e.* in three different wells. Cells were incubated for 24, 48 and 72 hours at 27°C after what cells were collected for RNA extraction.

1.5. RNA extraction, cDNA synthesis and real-time quantitative PCR (RT-qPCR)

RNA was extracted either from cells treated by IC_{10}, IC_{20} and IC_{30} of Indole 3-carbinol and methoprene or from cells transiently expressing CncC and Maf at 24, 48 and 72 hours post-transfection. Cells from each well were washed with 1 ml DPBS and total RNA was extracted using 1 ml TRIzol Reagent (Life Technologies, Germany) according to the manufacturer's protocol.

Total RNA (500 ng) was reverse transcribed using the iScript cDNA Synthesis kit (Bio-Rad, France) following the manufacturer's guidelines. Quantitative real-time (qRT)-PCR reactions were carried out on an AriaMx Real-Time PCR system (Agilent

technologies, USA) using qPCR Mastermix plus for SYBR Green I no ROX (Eurogentec, Belgium). The PCR conditions were as follows: 10 min at 95 °C, 40 cycles of 5 s at 95 °C and 30 s at 60 °C and followed by a melting curve step, except for CncC for which conditions were slightly different: 40 cycles of 5 s at 95 °C and 30 s at 60 °C and 20 s at 72°C. Each reaction was performed in duplicate and the mean of three independent, biological replicates was calculated. All results were normalized using the mRNA level of three reference genes (ribosomal protein L4, ribosomal protein L10, ribosomal protein L17) and relative expression values were calculated using SATqPCR (Rancurel et al., 2019). Primers were designed using Primer3 (v0.4.0), sequences and efficiencies are listed in Table S2.

1.6. Statistical analysis

Dose-response assays were analyzed in GraphPad Software (V9.2.0) using a nonlinear regression (four-parameters logistic (4PL) regression model).

2. Results

2.1. Cytotoxity of indole 3-carbinol and methoprene on Sf9 cells

The cytotoxicity of indole 3-carbinol and methoprene was determined on Sf9 cells. Indole 3-carbinol is a plant secondary metabolite from the glucosinolate family, compounds present in Brassicaceae, whereas methoprene is a juvenile hormone (JA) mimic insecticide. These xenobiotics were chosen based on previous reports of induction of detoxification genes in Sf9 cells (Giraudo et al., 2013; Giraudo et al., 2015). Exposure for 24 hours to increasing concentrations of xenobiotic was used to calculate half maximal inhibitory concentration (IC_{50}) which represents the dose of xenobiotics inhibiting cell viability by 50%. IC_{50} values of indole 3-carbinol and methoprene were

112.7 µM and 89.4 µM respectively (Fig.1). Resulting IC_{10}, IC_{20} and IC_{30} interpolated values were 39.7, 57.8 and 73.8 µM for indole 3-carbinol and 50.7, 65.3 and 74 µM for methoprene.

2.2. Induction of detoxification genes expression by indole 3-carbinol and methoprene

The adaptive capacity of the cells to respond to these two xenobiotics was assessed by measuring the expression of selected detoxification genes by quantitative PCR. In order to determine if this response is dose-dependent, Sf9 were treated with IC_{10}, IC_{20} and IC_{30} of indole 3-carbinol and methoprene. Figure 2 shows that the expression of seven P450s (*CYP4M14*, *CYP4M15*, *CYP9A24*, *CYP9A30*, *CYP9A31*, *CYP9A32* and *CYP321A9*) and one GST (*GSTE1*) are induced at the IC_{30} of indole 3-carbinol and methoprene. This induction was dose-dependent. Some genes such as *CYP9A31* are very strongly induced (expression fold-change 101.48 at methoprene IC_{30}, $p = 0.0014$) while for others this induction is weak or even non-existent as for examples *CYP4M15* and *CYP321A9* at indole 3-carbinol IC_{10}. The levels of gene induction between the indole 3-carbinol and methoprene treatments are different but of the same order of magnitude except for *CYP9A31* where the levels of induction for methoprene are between 3 and 5 times higher than for indole 3-carbinol depending on IC considered.

2.3. Induction of CncC and Maf, transcription factors involved in the regulation of detoxification gene expression

Since the work of (Misra et al., 2011) on *Drosophila,* CncC and Maf have been demonstrated to be major regulators of the expression of detoxification genes in a

number of other insect species (see for review (Amezian et al., 2021b). To test whether these two transcription factors were also inducible in Sf9 cells by sublethal doses of indole 3-carbinol and methoprene, RT-qPCR experiments were performed. Results presented in figure 2 show that the induction of *CncC* by indole 3-carbinol and methoprene was dose-dependent, while the expression levels of *Maf* varied in a dose-independent manner. Indole 3-carbinol had the least potent effect on the expression of *CncC* with a 3-fold increase at IC_{30} as compared to methoprene (6.82-fold, n.s., p = 0.069).

2.4. Effect of transient overexpression of CncC and Maf on detoxification gene expression

To assess whether there is a causal link between the transcriptional upregulation of *CncC* and *Maf* and the activation of detoxification genes, the transcription factors were transiently overexpressed in Sf9 cells. Three types of cell lines were obtained, one line that overexpressed *CncC* alone, one that overexpressed *Maf* alone and finally one that overexpressed both transcription factors. The expression levels of *CncC* and *Maf* were monitored at 24, 48 and 72 hours after transfection in each transformed line (Fig. 3A, 3B, 3C). *CncC* and *Maf* were strongly upregulated in transformants as compared to the control cells. The highest expression fold-change was obtained at 48 hours post-transfection: 1012- and 1053-fold change respectively in *CncC* and *Maf* single-gene transformants and 1142- / 643-fold change in the double-gene transformants (Fig. 3B).

The expression of detoxification genes was assessed 48 hours post-transfection. The overexpression of *CncC* and *Maf* genes led to significant upregulation of most detoxification genes monitored such as *CYP4M15*, *CYP9A24*, *CYP321A9* and *GSTE1*

while the expression of *CYP9A30*, *CYP9A31* and *CYP9A32* were not affected. The co-transfection of *CncC* and *Maf* had a stronger impact on the induction of detoxification genes, for example the expression of *CYP4M15* was 2.5-fold higher in pCncC:Maf than in pCncC and pMaf.

2.5. Activities of recombinant CYP9A30, CYP9A31 and CYP9A32 on P450 model substrates

CYP9A31 was the most induced gene following xenobiotic exposure. It is part of a cluster that contains 12 CYP9As, with *CYP9A32* and *CYP9A30* on either side of its position in the genome (Hilliou et al., 2021). We chose to heterologously express these 3 P450s and to investigate their capacity to metabolize diverse coumarin fluorescent probe substrates. Of the 7 molecules tested, 7-benzyloxy-4-trifuluoromethyl coumarin (BFC) and 7-benzyloxymethoxy-4-trifluoromethyl coumarin (BOMFC) were the best substrates, with CYP9A31 being the most active P450, followed by CYP9A32 and CYP9A30 (Fig. 4). The worst substrate was 7-methoxy-4-trifluoromethyl coumarin (MFC) and only low activity was detected for substrates containing an ethoxy or pentoxy group.

2.6. I3C and methoprene interactions with CYP9As employing a fluorescent probe assays

We then wanted to test whether these P450s could be involved in the metabolism of the two xenobiotics in our study, I3C and methoprene. To do this, the interaction between the xenobiotics and each of the recombinantly expressed CYP9As was measured employing a fluorescent probe (BOMFC) assay.

BOMFC metabolism by CYP9A30 and CYP9A32 was significantly inhibited with increasing concentration of methoprene (Fig. 5A-C) whereas inhibition with CYP9A31 is much lower and only observed at the highest concentration of 50µM methoprene (Fig. 5B). No inhibition was detected with I3C, suggesting that those CYP9As are not able to metabolize I3C (Fig. 5).

3. Discussion

Insects have to deal with a wide range of xenobiotics present in their environment, either in their diet or insecticides used for pest control. The inducibility of detoxifying enzymes upon exposure to xenobiotics allow them to provide a timely and coordinated response to external stimuli that would otherwise be costly to implement permanently. In this study, we demonstrated that I3C and methroprene are able to induce in a dose-dependent manner several detoxification genes as well as the transcription factor *CncC* in Sf9 cells. These induction profiles were obtained after exposure to sublethal concentrations of I3C and methoprene in order to obtain specific adaptative responses of detoxification genes in *S. frugiperda* and avoid nonspecific general stress responses with higher doses. Transient overexpression of the transcription factors *CncC* and *Maf* induced the over-expression of *CYP4M14*, *CYP4M15*, *CYP9A24*, *CYP321A9* and *GSTE1* while no effect was observed on *CYP9A30*, *CYP9A31* and *CYP9A32* expression, suggesting that another signaling pathway is involved in controlling their expression. The functional expression of three FAW P450s: CYP9A30, CYP9A31 and CYP9A32 demonstrated the ability of these detoxification enzymes to metabolize diverse fluorescent coumarin substrates. The ability of CYP9A30 and CYP9A32 to interact with methoprene was demonstrated by a fluorescence-based assay and

suggest their involvement in the degradation of this insecticide while they were not involved in I3C metabolism.

CYP9As were strongly induced by both xenobiotics (up to 100-fold for *CYP9A31* by methoprene), which may suggest that they play a role in the metabolism of these compounds. CYP9As were reported inducible in the genus *Spodoptera* (*S. exigua*, *S. frugiperda* and *S. litura*) by plant secondary metabolites of various structures like terpenoids and glucosinolates, and insecticides (reviewed in (Amezian et al., 2021a). In *S. frugiperda*, their role in insecticide resistance is suggested by the fact that they are overexpressed in several field populations resistant to insecticides and in particular to pyrethroids (Boaventura et al., 2020b; Gimenez et al., 2020a). The involvement of CYP9A in resistance dates back to the work of (Rose et al., 1997) and the cloning of the first CYP9 (*CYP9A1*) in a thiodicard-resistant strain of *Heliothis virescens*. These various studies associate resistance with the overexpression of CYP9A, however there is little evidence demonstrating the ability of these enzymes to metabolize an insecticide, let alone a plant secondary metabolite. In *S. exigua,* one CYP9A, CYP9A186 was shown to play a major role in resistance to abamectin and emamectin benzoate. Heterologous expression of this P450 in insect cells shows that it is able to metabolize these insecticides into hydroxy- and O-desmethyl-metabolites (Zuo et al., 2021). In a close lepidopteran, *H. armigera*, several CYP9As (CYP9A3, CYP9A14, CYP9A15, CYP9A16, CYP9A12/17, CYP9A23) were heterologously expressed in either yeast or insect cells and could also metabolize the pyrethroid esfenvalerate into hydroxy-metabolites (Shi et al., 2021b; Yang et al., 2008a). These results show that there is functional redundancy between the six members of *H. armigera* CYP9A, each of which can metabolize pyrethroids. Whether this redundancy can be found for *S. frugiperda* CYP9As remains to be elucidated. Is this functional redundancy linked to

the cluster organization of CYP9A, six genes in *H. armigera* and twelve in *S. frugiperda*? Our results show that three of the twelve CYP9A cluster members, namely CYP9A30, CYP9A31 and CYP9A32 have the ability to interact with methoprene, albeit with variations. Indeed, the inhibition of BOMFC metabolism with increasing concentrations of methoprene is lower for CYP9A31 than for the other two CYP9As. These results suggest, as for the *H. armigera* CYP9As, a certain redundancy in the capacity of these enzymes to metabolize insecticides. However, further experiments are needed to determine whether this redundancy extends to all members of the cluster and not just three. It would also be interesting to determine whether CYP9As of *S. frugiperda* are capable of metabolizing pyrethroids.

Likewise, *CYP321A9* was induced by both I3C and methoprene suggesting it may be involved in the tolerance of Sf9 cells to these compounds. This P450 is also part of a gene cluster of which the synteny (*CYP321A9-CYP321A7-CYP321A8-CYP321A10*) is conserved within the noctuid lineage (Cheng et al., 2017). Although *CYP321A9* is the only member of the CYP321A subfamily to be expressed in Sf9 cells (Giraudo et al., 2015), genes of this cluster were reported on several occasions to be induced and to metabolize xenobiotics (Cheng et al., 2017a; Giraudo et al., 2015; Hu et al., 2019c; Jia et al., 2020; Wang et al., 2017b). For example, a recent study in *S. frugiperda* larvae showed that transgenic overexpression of *CYP321A8* increased tolerance of insects to deltamethrin by 10.3-fold based on LC_{50} value (Chen and Palli, 2021b). In *S. exigua,* CYP321A16 is able to metabolize the insecticide chlorpyrifos and CYP321A8 chlorpyrifos, cypermethrin and deltamethrin (Hu et al., 2021; Hu et al., 2020b).

The data currently available show that both CYP9A and CYP321A have the ability to metabolize certain insecticides, but their action on secondary plant metabolites remains to be tested. In our case, we did not show any interaction between the three

recombinantly expressed CYP9As and indole 3-carbinol, suggesting that this compound is not a substrate of these enzymes. Insecticides that CYP9A or CYP321A are able to metabolize include pyrethroids, avermectins and an organophosphate, yet to our knowledge no other studies than the present indicate activity on the juvenile hormone analogue methoprene. However, microsomal oxidases prepared from several strains of housefly have been shown to metabolize methoprene (Terriere and Yu, 1973). In addition, it has been suggested that P450s could be involved in methoprene resistance in the lesser grain borer, *Rhyzopertha dominica* (Sakka et al., 2021). The use of piperonil butoxide, a P450 inhibitor, increased the susceptibility of the resistant strain.

In addition to the P450s, our study showed that one GST, *GSTE1*, was inducible. The fact that the expression of this enzyme was induced by I3C was not surprising and can be compared with the results obtained in a related species like *S. litura*, where the authors showed that *GSTE1* is induced when the insect is fed on *Brassica juncea* leaves, a plant containing glucosinolates, of which one of the degradation products is I3C (Zou et al., 2016). In their further study, Zou et al. have shown that I3C alone induces GSTE1 and that it metabolizes I3C and allyl isothiocyanate. The involvement of GSTs in the metabolism of glucosinolates present in the food of *Spodoptera* species had also been highlighted by the identification of glutathione conjugates of aliphatic and aromatic isothiocyanates in their frass (Schramm et al., 2012).

In our study, the induction of *CYP4M14*, *CYP4M15*, *CYP321A9* and *GSTE1* by xenobiotics correlated well with their upregulation after transient overexpression of *CncC* and *Maf*. For all these genes the expression was also higher when *CncC* and *Maf* were co-expressed, which supports the assumption that these two transcription factors act as heterodimers. These results corroborate those obtained in previous

studies using ectopic expression of *CncC* and *Maf* in *T. castaneum* (Kalsi and Palli, 2017a) and *S. exigua* (Hu et al., 2019b; Hu et al., 2020b). *GSTE1* was unsurprisingly upregulated by CncC and Maf. Indeed it seems well established that this GST is a target gene of the CncC:Maf pathway in several species [*D. melanogaster:* (Deng and Kerppola, 2013); *S. exigua*: (Hu et al., 2019a; Hu et al., 2019b); *S. litura*: (Chen et al., 2018b); *Tribolium castaneum*: (Kalsi and Palli, 2017a)].

On the other hand, *CYP9A30*, *CYP9A31* and *CYP9A32* were not overexpressed in any of the *CncC* and *Maf* over-expressing cell lines. This clearly demonstrates that methoprene and I3C induction of these genes does not rely on the activation of the CncC/Maf pathway and is likely controlled by other actors and supports the idea of concomitant activation of several xenobiotic-responsive pathways upon xenobiotic exposure. While several of these pathways have been identified in recent years (for review see (Amezian et al., 2021b), we are still far from having a complete understanding of detoxification signaling in insects. One of the pathways potentially involved in the regulation of SfCYP9As could be the G-protein-coupled receptor (GPCR) pathway. Indeed, the work of Li and Liu on the mosquito *Culex quinquefasciatus* highlighted the role of this GPCR pathway and of the intracellular effectors G-protein alpha subunit (Gs), adenylate cyclase (AC) and protein kinase A in the development of insecticide resistance by regulating the expression of certain P450s. Most importantly, this work showed that heterologous expression of these mosquito effectors in Sf9 cells results in the over-expression of *SfCYP9A32* (Li and Liu, 2019). Thus these results suggest that the GPCR pathway regulates *CYP9A32* expression and that there is conservation between the consensus sequences of different species, here mosquito and FAW. However, further experiments are needed to determine the role of the S*. frugiperda* GPCRs in the regulation of CYP9A, as Li and

Liu further showed that the expression of *CYP9A30* and *CYP9A31* was not affected by the over-expression of GPCR effectors. Another possibility for the regulation of CYP9As is the aryl hydrocarbon receptor (AhR)/AHR nuclear translocator (ARNT) pathway. This pathway was initially shown to control the expression of *CYP6B1* and *CYP6B4* in *Papilio polyxenes* and *Papilio glaucus* and play a role in adaptation to furanocoumarins (Brown et al., 2005; Hung et al., 1996). In *S. frugiperda*, (Giraudo et al., 2015) have identified the possible presence of regulatory elements in the CYP9A promoters, including a xenobiotic response element (XRE) from the aryl hydrocarbon receptor (AhR) which suggests the possible involvement of this nuclear receptor in the regulation of *CYP9A30*, and the XRE-Xan for xanthotoxin motifs in three of them *(CYP9A31, CYP9A30* and *CYP9A24*). Even though functional validation has yet to be provided, it is therefore possible that different transcription factors or nuclear receptors are involved in the expression regulation of genes within the CYP9A cluster.

4. Conclusion

Our results show that Sf9 cells can be a good model to study the genetic adaptation mechanisms of *S. frugiperda* to its chemical environment. Different molecules of chemical origin can induce the same detoxification genes but induction does not mean direct involvement in the metabolism of the substance. Indeed, as our results show, CYP9As are able to interact with methoprene but not with I3C. Multiple signaling pathways lead to an adaptive response and CYP9As do not appear to be regulated by the CncC/Maf pathway.

Author contributions

Acknowledgements

DA is supported by a PhD scholarship funded by Bayer and Association Nationale de la Recherche et de la Technologie (CIFRE n° 2018-1283).

Appendix A. Supplementary data

References

Amezian D, Nauen R & Le Goff G (2021a) Comparative analysis of the detoxification gene inventory of four major Spodoptera pest species in response to xenobiotics. Insect Biochem Mol Biol 138: 103646. doi:10.1016/j.ibmb.2021.103646.

Amezian D, Nauen R & Le Goff G (2021b) Transcriptional regulation of xenobiotic detoxification genes in insects - An overview. Pestic Biochem Physiol 174: 104822. doi:10.1016/j.pestbp.2021.104822.

Boaventura D, Buer B, Hamaekers N, Maiwald F & Nauen R (2020) Toxicological and molecular profiling of insecticide resistance in a Brazilian strain of fall armyworm resistant to Bt Cry1 proteins. Pest Manag Sci. doi:10.1002/ps.6061.

Brown RP, McDonnell CM, Berenbaum MR & Schuler MA (2005) Regulation of an insect cytochrome P450 monooxygenase gene (CYP6B1) by aryl hydrocarbon and xanthotoxin response cascades. Gene 358: 39-52. doi:S0378-1119(05)00270-2 [pii]10.1016/j.gene.2005.05.026.

Chen S, Lu M, Zhang N, Zou X, Mo M & Zheng S (2018) Nuclear factor erythroid-derived 2-related factor 2 activates glutathione S-transferase expression in the midgut of Spodoptera litura (Lepidoptera: Noctuidae) in response to phytochemicals and insecticides. Insect Mol Biol. doi:10.1111/imb.12391.

Chen X & Palli SR (2021) Transgenic overexpression of P450 genes confers deltamethrin resistance in the fall armyworm, Spodoptera frugiperda. Journal of Pest Science. doi:https://doi.org/10.1007/s10340-021-01452-6.

Cheng T, Wu J, Wu Y, Chilukuri RV, Huang L, Yamamoto K, Feng L, Li W, Chen Z, Guo H, Liu J, Li S, Wang X, Peng L, Liu D, Guo Y, Fu B, Li Z, Liu C, Chen Y, Tomar A, Hilliou F, Montagne N, Jacquin-Joly E, d'Alencon E, Seth RK, Bhatnagar RK, Jouraku A, Shiotsuki T, Kadono-Okuda K, Promboon A, Smagghe G, Arunkumar KP, Kishino H, Goldsmith MR, Feng Q, Xia Q & Mita K (2017) Genomic adaptation to polyphagy and insecticides in a major East Asian noctuid pest. Nat Ecol Evol. doi:10.1038/s41559-017-0314-4.

Cui G, Sun R, Veeran S, Shu B, Yuan H & Zhong G (2020) Combined transcriptomic and proteomic analysis of harmine on Spodoptera frugiperda Sf9 cells to reveal the potential resistance mechanism. J Proteomics 211: 103573. doi:10.1016/j.jprot.2019.103573.

Deng H & Kerppola TK (2013) Regulation of Drosophila metamorphosis by xenobiotic response regulators. PLoS Genet 9: e1003263. doi:10.1371/journal.pgen.1003263
PGENETICS-D-12-01411 [pii].

Fautrel A, Chesne C, Guillouzo A, de Sousa G, Placidi M, Rahmani R, Braut F, Pichon J, Hoellinger H, Vintezou P, Diarte I, Melcion C, Cordier A, Lorenzon G, Benicourt M, Vannier B, Fournex R, Peloux AF, Bichet N, Gouy D, Cano JP & Lounes R (1991) A multicentre study of acute in vitro cytotoxicity in rat liver cells. Toxicol In Vitro 5: 543-547. doi:10.1016/0887-2333(91)90090-z.

Gimenez S, Abdelgaffar H, Goff GL, Hilliou F, Blanco CA, Hanniger S, Bretaudeau A, Legeai F, Negre N, Jurat-Fuentes JL, d'Alencon E & Nam K (2020) Adaptation by copy number variation increases insecticide resistance in the fall armyworm. Commun Biol 3: 664. doi:10.1038/s42003-020-01382-6.

Giraudo M, Audant P, Feyereisen R & Le Goff G (2013) Nuclear receptors HR96 and ultraspiracle from the fall armyworm (*Spodoptera frugiperda*), developmental expression and induction by xenobiotics. J Insect Physiol 59: 560-568. doi:S0022-1910(13)00062-0 [pii]
10.1016/j.jinsphys.2013.03.003.

Giraudo M, Califano J, Hilliou F, Tran T, Taquet N, Feyereisen R & Le Goff G (2011) Effects of hormone agonists on Sf9 cells, proliferation and cell cycle arrest. PLoS One 6: e25708. doi:10.1371/journal.pone.0025708
PONE-D-11-15194 [pii].

Giraudo M, Hilliou F, Fricaux T, Audant P, Feyereisen R & Le Goff G (2015) Cytochrome P450s from the fall armyworm (*Spodoptera frugiperda*): responses to plant allelochemicals and pesticides. Insect Mol Biol 24: 115-128. doi:10.1111/imb.12140.

Gouin A, Bretaudeau A, Nam K, Gimenez S, Aury JM, Duvic B, Hilliou F, Durand N, Montagne N, Darboux I, Kuwar S, Chertemps T, Siaussat D, Bretschneider A, Mone Y, Ahn SJ, Hanniger S, Grenet AG, Neunemann D, Maumus F, Luyten I, Labadie K, Xu W, Koutroumpa F, Escoubas JM, Llopis A, Maibeche-Coisne M, Salasc F, Tomar A, Anderson AR, Khan SA, Dumas P, Orsucci M, Guy J, Belser C, Alberti A, Noel B, Couloux A, Mercier J, Nidelet S, Dubois E, Liu NY, Boulogne I, Mirabeau O, Le Goff G, Gordon K, Oakeshott J, Consoli FL, Volkoff AN, Fescemyer HW, Marden JH, Luthe DS, Herrero S, Heckel DG, Wincker P, Kergoat GJ, Amselem J, Quesneville H, Groot AT, Jacquin-Joly E, Negre N, Lemaitre C, Legeai F, d'Alencon E & Fournier P (2017) Two genomes of highly polyphagous lepidopteran pests (Spodoptera frugiperda, Noctuidae) with different host-plant ranges. Sci Rep 7: 11816. doi:10.1038/s41598-017-10461-4.

Hilliou F, Chertemps T, Maibeche M & Le Goff G (2021) Resistance in the Genus Spodoptera: Key Insect Detoxification Genes. Insects 12. doi:10.3390/insects12060544.

Hu B, Hu S, Huang H, Wei Q, Ren M, Huang S, Tian X & Su J (2019a) Insecticides induce the co-expression of glutathione S-transferases through ROS/CncC pathway in Spodoptera exigua. Pestic Biochem Physiol 155: 58-71. doi:10.1016/j.pestbp.2019.01.008.

Hu B, Huang H, Hu S, Ren M, Wei Q, Tian X, Esmail Abdalla Elzaki M, Bass C, Su J & Reddy Palli S (2021) Changes in both trans- and cis-regulatory elements mediate insecticide resistance in a lepidopteron pest, Spodoptera exigua. PLoS Genet 17: e1009403. doi:10.1371/journal.pgen.1009403.

Hu B, Huang H, Wei Q, Ren M, Mburu DK, Tian X & Su J (2019b) Transcription factors CncC/Maf and AhR/ARNT coordinately regulate the expression of multiple GSTs conferring resistance to chlorpyrifos and cypermethrin in Spodoptera exigua. Pest Manag Sci 75: 2009-2019. doi:10.1002/ps.5316.

Hu B, Ren M, Fan J, Huang S, Wang X, Elzaki MEA, Bass C, Palli SR & Su C (2020) Xenobiotic transcription factors CncC and maf regulate expression of CYP321A16 and CYP332A1 that mediate chlorpyrifos resistance in Spodoptera exigua. J Hazard Mater 398: 122971. doi:10.1016/j.jhazmat.2020.122971.

Hu B, Zhang SH, Ren MM, Tian XR, Wei Q, Mburu DK & Su JY (2019c) The expression of Spodoptera exigua P450 and UGT genes: tissue specificity and response to insecticides. Insect Sci 26: 199-216. doi:10.1111/1744-7917.12538.

Hung CF, Holzmacher R, Connolly E, Berenbaum MR & Schuler MA (1996) Conserved promoter elements in the CYP6B gene family suggest common ancestry for cytochrome P450 monooxygenases mediating furanocoumarin detoxification. Proc Natl Acad Sci U S A 93: 12200-12205.

Jia ZQ, Liu D, Peng YC, Han ZJ, Zhao CQ & Tang T (2020) Identification of transcriptome and fluralaner responsive genes in the common cutworm Spodoptera litura Fabricius, based on RNA-seq. BMC Genomics 21: 120. doi:10.1186/s12864-020-6533-0.

Kalsi M & Palli SR (2017) Cap n collar transcription factor regulates multiple genes coding for proteins involved in insecticide detoxification in the red flour beetle, Tribolium castaneum. Insect Biochem Mol Biol 90: 43-52. doi:10.1016/j.ibmb.2017.09.009.

Li T & Liu N (2019) Role of the G-Protein-Coupled Receptor Signaling Pathway in Insecticide Resistance. Int J Mol Sci 20. doi:10.3390/ijms20174300.

Li X, Zangerl AR, Schuler MA & Berenbaum MR (2000) Cross-resistance to alpha-cypermethrin after xanthotoxin ingestion in Helicoverpa zea (Lepidoptera: Noctuidae). J Econ Entomol 93: 18-25.

Lu K, Cheng Y, Li Y, Li W, Zeng R & Song Y (2021a) Phytochemical Flavone Confers Broad-Spectrum Tolerance to Insecticides in Spodoptera litura by Activating ROS/CncC-Mediated Xenobiotic Detoxification Pathways. J Agric Food Chem 69: 7429-7445. doi:10.1021/acs.jafc.1c02695.

Lu K, Li Y, Cheng Y, Li W, Zeng B, Gu C, Zeng R & Song Y (2021b) Activation of the ROS/CncC and 20-Hydroxyecdysone Signaling Pathways Is Associated with Xanthotoxin-Induced Tolerance to lambda-Cyhalothrin in Spodoptera litura. J Agric Food Chem 69: 13425-13435. doi:10.1021/acs.jafc.1c04519.

Misra JR, Horner MA, Lam G & Thummel CS (2011) Transcriptional regulation of xenobiotic detoxification in *Drosophila*. Genes Dev 25: 1796-1806. doi:25/17/1796 [pii]
10.1101/gad.17280911.

Misra JR, Lam G & Thummel CS (2013) Constitutive activation of the Nrf2/Keap1 pathway in insecticide-resistant strains of *Drosophila*. Insect Biochem Mol Biol 43: 1116-1124. doi:S0965-1748(13)00172-0 [pii]
10.1016/j.ibmb.2013.09.005.

Pereira RB, Pinto NFS, Fernandes MJG, Vieira TF, Rodrigues ARO, Pereira DM, Sousa SF, Castanheira EMS, Fortes AG & Goncalves MST (2021) Amino Alcohols from Eugenol as Potential Semisynthetic Insecticides: Chemical, Biological, and Computational Insights. Molecules 26. doi:10.3390/molecules26216616.

Rose RL, Goh D, Thompson DM, Verma KD, Heckel DG, Gahan LJ, Roe RM & Hodgson E (1997) Cytochrome P450 (CYP)9A1 in Heliothis virescens: the first member of a new CYP family. Insect Biochem Mol Biol 27: 605-615. doi:10.1016/s0965-1748(97)00036-2.

Ruttanaphan T, de Sousa G, Pengsook A, Pluempanupat W, Huditz HI, Bullangpoti V & Le Goff G (2020) A Novel Insecticidal Molecule Extracted from Alpinia galanga with Potential to Control the Pest Insect Spodoptera frugiperda. Insects 11. doi:10.3390/insects11100686.

Sakka MK, Riga M, Ioannidis P, Baliota GV, Tselika M, Jagadeesan R, Nayak MK, Vontas J & Athanassiou CG (2021) Transcriptomic analysis of s-methoprene resistance in the lesser grain borer, Rhyzopertha dominica, and evaluation of piperonyl butoxide as a resistance breaker. BMC Genomics 22: 65. doi:10.1186/s12864-020-07354-8.

Sasabe M, Wen Z, Berenbaum MR & Schuler MA (2004) Molecular analysis of CYP321A1, a novel cytochrome P450 involved in metabolism of plant allelochemicals (furanocoumarins) and insecticides (cypermethrin) in Helicoverpa zea. Gene 338: 163-175. doi:10.1016/j.gene.2004.04.028
S0378111904002112 [pii].

Schramm K, Vassao DG, Reichelt M, Gershenzon J & Wittstock U (2012) Metabolism of glucosinolate-derived isothiocyanates to glutathione conjugates in generalist lepidopteran herbivores. Insect Biochem Mol Biol 42: 174-182. doi:10.1016/j.ibmb.2011.12.002.

Shi L, Shi Y, Liu MF, Zhang Y & Liao XL (2021a) Transcription factor CncC potentially regulates the expression of multiple detoxification genes that mediate indoxacarb resistance in Spodoptera litura. Insect Sci 28: 1426-1438. doi:10.1111/1744-7917.12860.

Shi Y, Jiang Q, Yang Y, Feyereisen R & Wu Y (2021b) Pyrethroid metabolism by eleven Helicoverpa armigera P450s from the CYP6B and CYP9A subfamilies. Insect Biochem Mol Biol: 103597. doi:10.1016/j.ibmb.2021.103597.

Sparks TC, Crossthwaite AJ, Nauen R, Banba S, Cordova D, Earley F, Ebbinghaus-Kintscher U, Fujioka S, Hirao A, Karmon D, Kennedy R, Nakao T, Popham HJR, Salgado V, Watson GB, Wedel BJ & Wessels FJ (2020) Insecticides, biologics and nematicides: Updates to IRAC's mode of action classification - a tool for resistance management. Pestic Biochem Physiol 167: 104587. doi:10.1016/j.pestbp.2020.104587.

Terriere L & Yu S (1973) Insect juvenile hormones: induction of detoxifying enzymes in the house fly and detoxication by house fly enzymes. Pestic Biochem Physiol 3: 96-107.

Wang RL, He YN, Staehelin C, Liu SW, Su YJ & Zhang JE (2017) Identification of Two Cytochrome Monooxygenase P450 Genes, CYP321A7 and CYP321A9, from the Tobacco Cutworm Moth (Spodoptera Litura) and Their Expression in Response to Plant Allelochemicals. Int J Mol Sci 18. doi:10.3390/ijms18112278.

Yang Y, Yue L, Chen S & Wu Y (2008) Functional expression of *Helicoverpa armigera* CYP9A12 and CYP9A14 in *Saccharomyces cerevisiae*. Pesticide Biochemistry and Physiology 92: 101-105.

Yu SJ (1982) Induction of microsomal oxidases by host plants in the fall armyworm, Spodoptera frugiperda (J. E. Smith). Pestic Biochem Physiol 17: 59-67.

Yu SJ (1983) Induction of detoxifying enzymes by allelochemicals and host plants in the fall armyworm. Pestic Biochem Physiol 19: 330-336.

Yu SJ (1986) Consequences of induction of foreign compound-metabolizing enzymes in insects: Molecular aspects of insect-plant interactions (ed. by LB Brattsten, Ahmad, S.) Plenum, New York, pp. 211-255.

Yu SJ (1987) Microsomal oxidation of allelochemicals in generalist (Spodoptera frugiperda) and semispecialist (Anticarsia gemmatalis) insect. J Chem Ecol 13: 423-436. doi:10.1007/BF01880090.

Yu SJ & Hsu EL (1985) Induction of hydrolases by allelochemicals and host plants in fall armyworm (Lepidoptera : Noctuidae) larvae. Environ Entomol 14: 512-515.

Zou X, Xu Z, Zou H, Liu J, Chen S, Feng Q & Zheng S (2016) Glutathione S-transferase SlGSTE1 in Spodoptera litura may be associated with feeding adaptation of host plants. Insect Biochem Mol Biol 70: 32-43. doi:10.1016/j.ibmb.2015.10.005.

Zuo Y, Shi Y, Zhang F, Guan F, Zhang J, Feyereisen R, Fabrick JA, Yang Y & Wu Y (2021) Genome mapping coupled with CRISPR gene editing reveals a P450 gene confers avermectin resistance in the beet armyworm. PLoS Genet 17: e1009680. doi:10.1371/journal.pgen.1009680.

Figures

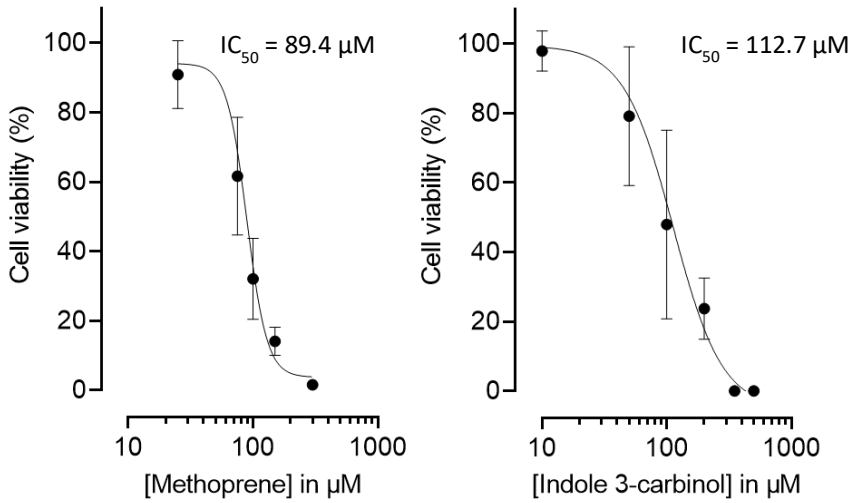

Figure 1. Dose-response curves of methoprene and indole 3-carbinol in MTT bioassays.
Toxicity of Methoprene (left) and Indole 3-carbinol (right) towards Sf9 cells obtained by MTT bioassays. Each point was expressed as a percentage of the maximum viability (DMSO treatment). Curves were obtained by nonlinear regressions (sigmoidal, 4PL).

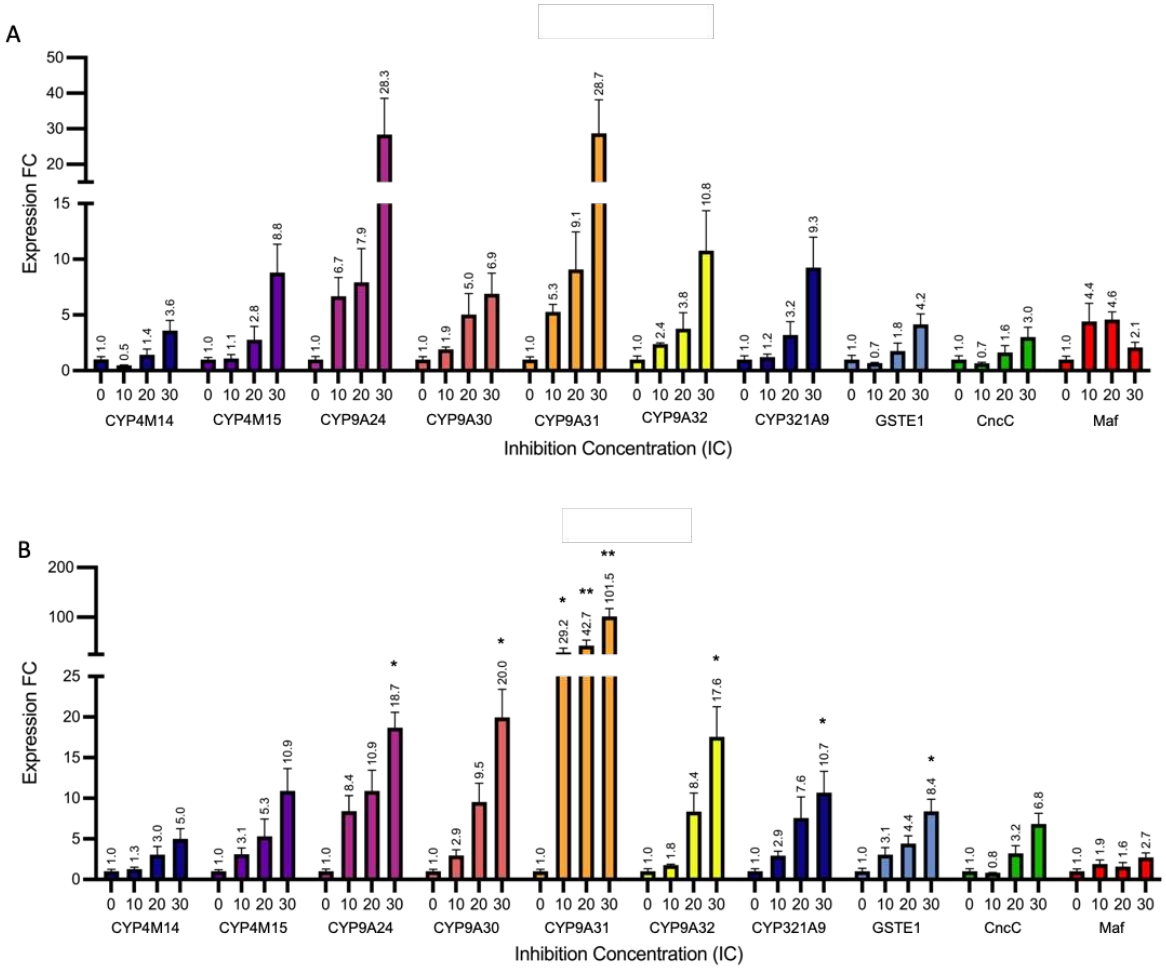

Figure 2. Induction of detoxification genes, *CncC* and *Maf* in Sf9 cells.
Expression levels of eight detoxification genes as well as *CncC* and *Maf* were monitored in Sf9 cells exposed to IC_{10}, IC_{20} and IC_{30} I3C (A) and methoprene (B). DMSO was used as control treatment (IC_0). Gene expression was normalized using the expression of the ribosomal protein L4, L10 and L17 reference genes and shown as fold-change relative to the expression of cell lines treated with DMSO. Data are mean values ± SEM.

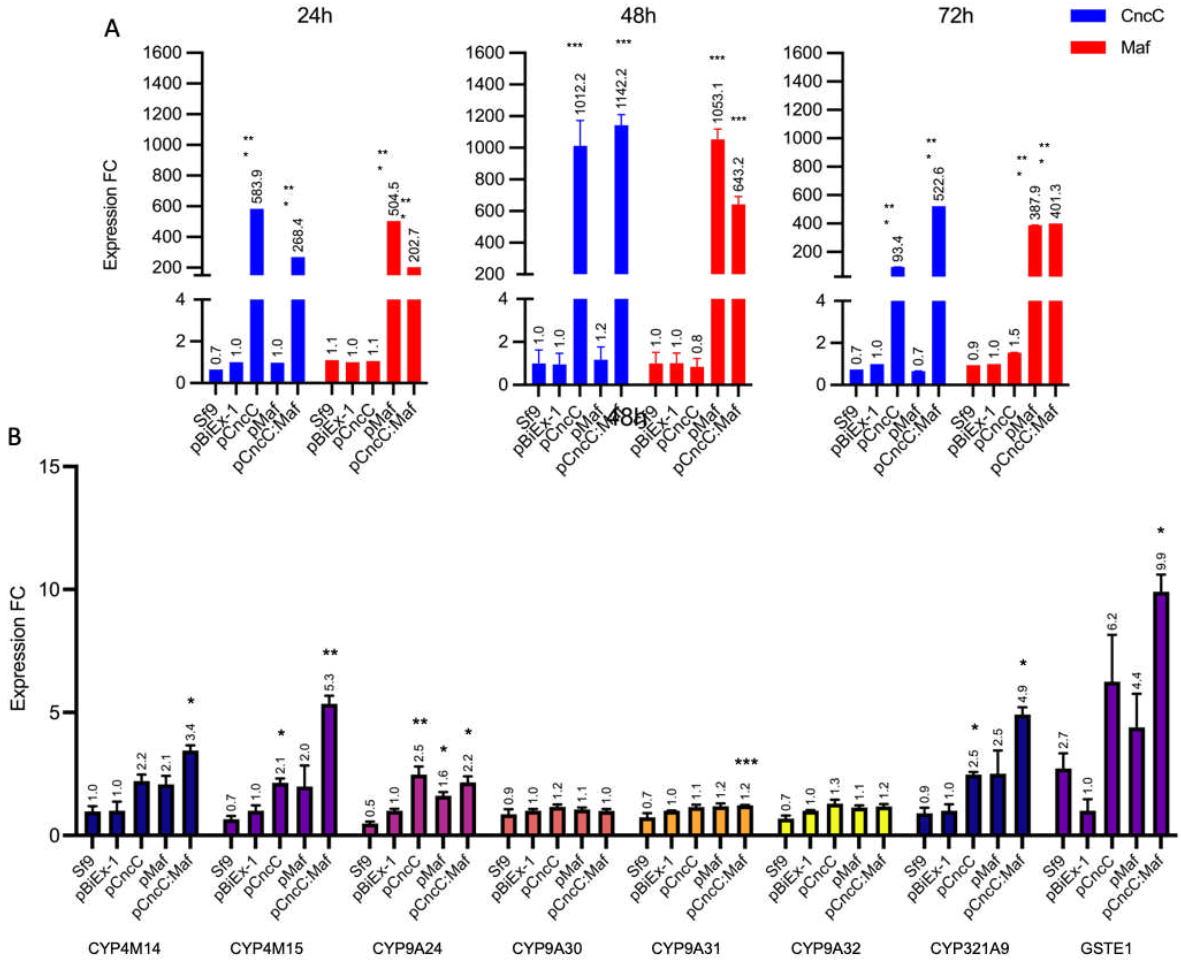

Figure 3. A) Transcript levels of *CncC* and *Maf* in transiently transformed Sf9 cells at 24, 48 and 72h post-transfection and B) Transcript levels of detoxification genes in transiently transformed Sf9 cells 48h post-transfection.

Expression of detoxification genes was monitored in cell lines transfected with either *CncC* (pCncC), *Maf* (pMaf) or both transcription factors (pCncC:Maf). Gene expression was normalized using the expression of the ribosomal protein L4, L10 and L17 reference genes and shown as fold-change relative to the expression of cell lines transfected with an "empty" plasmid, pBiEx-1. Data are mean values ± SEM.

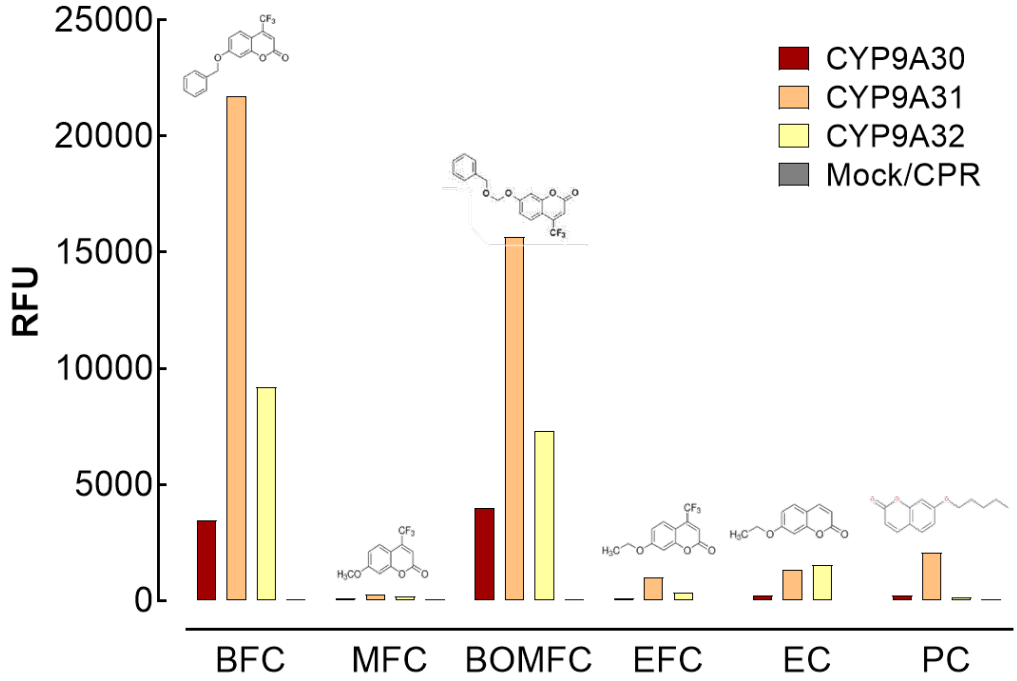

Figure 4. Metabolism of coumarin fluorescent probe substrates by recombinantly expressed CYP9A30, CYP9A31 and CYP9A32 of *Spodoptera frugiperda.* Data are mean values ± SD (n=4). Abbreviations: BFC, 7-benzyloxy-4-trifluoromethyl coumarin; MFC, 7-methoxy-4-trifluoromethyl coumarin; EFC, 7-ethoxy-4-trifluoromethyl coumarin; BOMFC, 7-benzyloxymethoxy-4-trifluoromethyl coumarin; PC, 7-n-pentoxy coumarin; EC, 7-ethoxy coumarin.

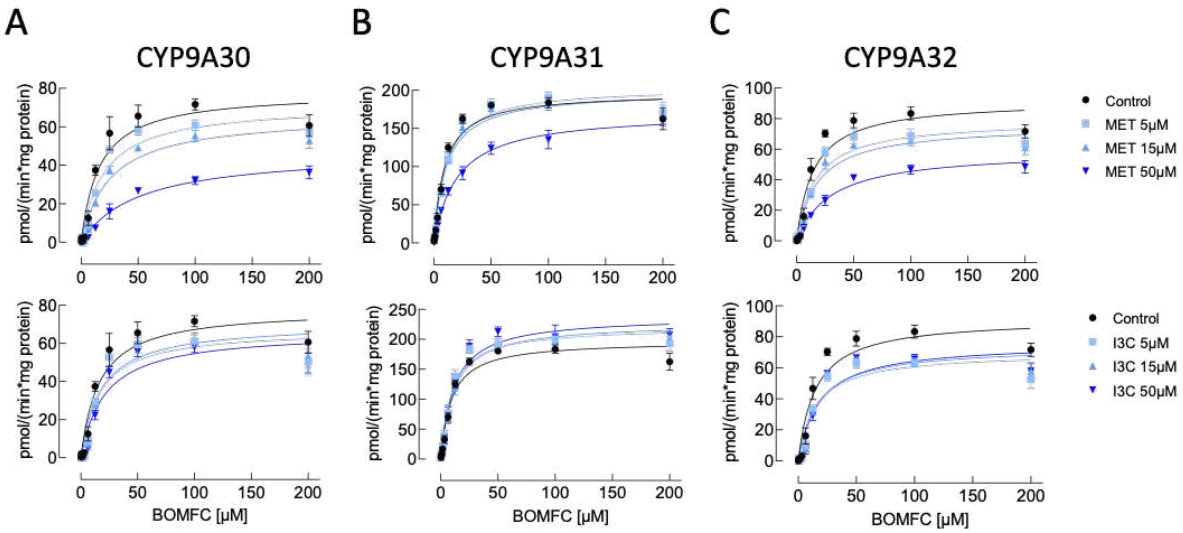

Figure 5. Steady-state kinetics of 7-hydroxy-4-(trifluoromethyl)coumarin (HC) formation using BOMFC as a substrate by recombinantly expressed *Spodoptera frugiperda* (A) CYP9A30, (B) CYP9A31 and (C) CYP9A32 in the presence of different concentrations of either methoprene (MET) or indole-3-carbinol (I3C).

Résumé

La légionnaire d'automne, *Spodoptera frugiperda* (Lepidoptera: Noctuidae), est un ravageur polyphage qui se nourrit de nombreuses plantes hôtes, dont des cultures importantes comme le maïs, le riz et le sorgho. Ce ravageur est responsable chaque année de milliards de dollars de pertes agricoles et n'a envahi que récemment l'hémisphère oriental, dont l'Asie. La lutte contre cet insecte se base principalement sur l'utilisation d'insecticides ce qui a entrainé l'apparition de résistance à de nombreuses classes chimiques d'insecticides. *S. frugiperda* a développé des mécanismes sophistiqués d'adaptation pour éliminer les composés toxiques (toxines de plantes ou insecticides) comme la surexpression et la duplication de gènes d'enzymes de détoxication. Souvent exprimées à un niveau basal, ces enzymes sont induites quand l'insecte est exposé à un xénobiotique. Si ces dernières sont bien connues chez plusieurs insectes ravageurs, les facteurs de transcription impliqués dans le contrôle de leur expression restent largement inexplorés. Le but de ma thèse a été de déterminer le rôle du facteur de transcription Cap'n'collar isoforme C (CncC) et musculoaponeurotic fibrosarcoma (Maf) dans l'adaptation de *S. frugiperda* aux xénobiotiques en utilisant le modèle cellulaire Sf9. J'ai montré que CncC et plusieurs gènes de détoxication sont induits par l'indole 3-carbinol (I3C), un glucosynolate présent dans les Brassicaceae comme le chou et le brocoli, et le méthoprène (Mtp), un insecticide qui imite l'hormone juvénile (JH). J'ai montré que la surexpression transitoire de CncC en cellules Sf9 est suivie d'une surexpression de certains de ces mêmes gènes de détoxication. Afin de caractériser le rôle des facteurs de transcription dans cette réponse j'ai établi deux types de lignées cellulaires transformées de manière stable. Le premier surexprime (OE) CncC, Maf ou les deux gènes et le second a été muté pour CncC (Knock-Out, KO) en utilisant la technique du CRISPR/Cas9. J'ai réalisé des tests de viabilité (MTT) et utilisé des sondes moléculaires en High Content Screening (HCS) pour tester si la modification de la voie de CncC:Maf affectait la capacité des cellules à faire face au stress toxique. Les lignées OE étaient plus tolérantes à l'I3C et au Mtp que le contrôle, tandis que les lignées KO étaient plus sensibles à ces composés. Les activités d'enzymes de détoxication, les carboxylesterases (CE) et les glutathion S-transférases (GST), à l'égard de substrats modèles étaient accrues dans les lignées OE, alors qu'elles étaient diminuées dans les lignées KO. Des études récentes ont montré que l'activation de la voie de CncC:Maf est médiée par la production d'espèces réactives de l'oxygène (ROS) lors d'un stress toxique. J'ai donc mesuré la production de ROS dans les cellules Sf9 traitées avec l'I3C et le Mtp. Les deux composés ont déclenché des pulses de ROS bien qu'à des niveaux limités dans les lignées OE, contrairement aux lignées KO pour lesquelles les niveaux de ROS étaient plus importants. L'utilisation d'un antioxydant a annulé les pulses de ROS et restauré la tolérance des cellules KO à l'I3C et au Mtp. Enfin, j'ai comparé les gènes différentiellement exprimés dans les lignées OE et KO lors une analyse transcriptomique (RNA-seq). Ceci m'a permis d'identifier les gènes potentiellement contrôlés par CncC et Maf, la plupart d'entre eux étant des gènes de détoxication dont le rôle dans la résistance aux insecticides et la métabolisation de composés de plantes a été démontrée dans plusieurs études. En conclusion, je présente ici de nouvelles données suggérant que la voie de signalisation CncC:Maf joue un rôle central dans l'adaptation des FAW aux composés environnementaux toxiques et aux insecticides. Ces connaissances aident à mieux comprendre les voies d'expression des gènes de détoxication et peuvent être utiles à la conception de nouveaux moyens de lutte contre les insectes en interférant avec ces voies et l'expression des gènes de détoxication.

Mots clés : Cap'n'collar isoform C (CncC), détoxication, résistance, adaptation aux plantes, régulation génétique